Displacement Mechanics and Stability of Foamy Oil during Secondary Recovery of Heavy Oil Using Methane and Air

by

Enoc Jeremias Teodoro Basilio Meza

A thesis submitted in partial fulfillment of the requirements for the degree of

Master of Science

In

Petroleum Engineering

Department of Civil and Environmental Engineering
University of Alberta

Abstract

Heavy oil and extra-heavy oil (natural bitumen and oil sands) resources represent 70% of the global petroleum reserves and are mostly found in shallow reservoirs with thin pay zones formed by unconsolidated sands. Thermal recovery methods are recognized for being the most efficient; yet, these methods face environmental challenges due to the high emissions of carbon dioxide generated by high energy demands, leading to high operational costs. Therefore, non-thermal recovery methods have attracted special attention from both industry and academia.

Foamy oil is the terminology commonly accepted to describe an atypical behavior associated with heavy oil flow formed as a response to pressure depletion. The cyclic solvent injection (CSI) technology is a solvent-based non-thermal process that has gained interest and is considered as an effective technique for increasing the recovery factor either as a follow-up process to the cold heavy oil production with sand (CHOPS) or for thin heavy oil reservoirs. Notwithstanding that many experimental investigations on foamy oil flow were carried out, theoretical foundations of its performance are still not convincing enough, and the mechanisms for the dynamic processes and stability continue to not be fully understood.

In order to develop a mechanistic understanding of foamy oil flow in a porous medium, laboratory experiments under two different well arrangement scenarios were considered, single-well and multi-well injection schemes, using methane and air as the injection gasses. Single-well CSI scheme injection experiments were performed in order to understand, in a more representative manner, the foamy oil generation by injecting gas externally to post-CHOPS reservoirs. The multi-

well CSI scheme was considered to be applied in thin heavy oil reservoirs, and post-CHOPS reservoirs. For both arrangements, different injection strategies were performed, based on alternating gas injection and simultaneous gas injection. It was observed that on a single-well injection scheme, injecting a mixture of air and methane simultaneously can help to obtain larger recovery factors per cycle than when using methane alone. On a multi-well injection scheme, it has been observed that an alternating gas injection strategy has a better performance than the simultaneous injection. Using air has been observed to save methane usage up to 26% and 51% in single-well and multi-well injection schemes, respectively.

Furthermore, in order to study the efficiency of using methane, air, and their mixture to generate stable foamy oils, observational experiments were performed by means of macroscopic (naked eye) and microscopic visualization which was interpreted through foamy oil stability parameters such as time of foamability and collapse, number of gas bubbles, gas bubbles distribution, and maximum bubble size. Using a mixture of air and methane has been observed not only to expand the volume of oil by 2.5 (volume expansion caused by methane has been found to be as high as 3.0) but also to delay the defoaming process.

Acknowledgments

First and foremost, I would like to thank God for lighting my way through life, reminding me that He is always by my side, and knowing that: "*I am able to do all things through the one who strengthens me*". I would also like to thank my parents, Teodoro Basilio and Eladia Meza, and to my closest relatives for their infinite love and support.

I would like to express my deepest gratitude to my supervisor, Dr. Tayfun Babadagli, for his guidance and advice during my research period. His experience, patience, and generosity have made a huge contribution to the realization of this thesis. This research was conducted under Dr. Babadagli's NSERC Industrial Research Chair in Unconventional Oil Recovery (industrial partners are Petroleum Development Oman, Total E&P Recherché Développement, SiGNa Oilfield Canada, Husky Energy, Suncor Energy, Saudi Aramco, Devon, APEX Eng., BASF) and an NSERC Discovery Grant (No: RES0011227). I gratefully acknowledge these supports.

The realization of this thesis would have not been possible without the help and support of the laboratory technicians of the Enhanced Oil & Gas Recovery and Reservoir Characterization (EOGRRC) Research Group. I would like to express my sincere gratitude to MSc. Mihaela Istratescu, for his kind and selfless support when performing my laboratory experiments and for always providing everything to accomplish my experimental goals. I want to thank MSc. Linxing Lin for his assistance and support. I want to thank Lindsey Gauthier for her hard work on the review of this thesis and every submitted paper.

I want to thank my good friends Randy Pratama, Ilyas Al-Kindi, Fritjof Bruns and Martin Wang for sharing this important journey with me, and for their time spent in our endless technical discussions.

My deepest gratitude will always be to all the professors and scholars from the School of Petroleum and Natural Gas Engineering at the Universidad Nacional de Ingenieria (UNI) in Peru. I also acknowledge the financial support from ProUNI, sponsored by Southern Peru Copper Corporation.

Table of Contents

List of Tables

List of Figures

Chapter 1

Introduction

Heavy oil is an unconventional petroleum resource classified as conventional heavy oil when the crude viscosity is under 1,000 cP and an API gravity under 21° but higher than 10°, and as unconventional heavy oil when the crude viscosity is at least 1,000 cP and the API gravity is less than 10°. Heavy oils are mostly formed by biodegradation (i.e. metabolism of lighter hydrocarbons to produce methane and enrich heavy hydrocarbons) and found in shallow reservoirs, formed by unconsolidated sands (Faergestad, 2016). Heavy oils are hydrocarbons with low fractions of volatile compounds with low molecular weights and relatively high proportions of high molecular weight compounds of lower volatility. The low mobility of these type of oils is associated to their high viscosities due to a complex assortment of different molecular and chemical compounds such as paraffin and asphaltenes with high melting points and high pour points (Banerjee, 2012; Huc, 2010). The recovery of this type of hydrocarbon resources is insofar much more difficult when compared to oil recovery from conventional petroleum reservoirs (Speight, 2016). Figure 1.1 shows the global petroleum reserves distribution, insofar reported as 1.665 trillion barrels (Central Intelligence Agency, 2017), from which unconventional petroleum resources represent 70% of the global petroleum reserves, and from this percentage, 15% represents heavy oil reserves, mostly located in Venezuela and Canada (Faergestad, 2016).

The properties and fluid flow behavior of conventional crude oil are very different when compared to heavy oil. The difference in the chemical composition of each type of fluid is the main reason for a variation in properties (Speight, 2014), principally viscosity and pour point. Due to its high viscosity, heavy oil recovery requires different recovery techniques than those designed for conventional crude oil recovery, since they do not generally address the problems associated with the production of heavy oil. Figure 1.2 presents the current heavy oil depletion technologies, from which the current commercial technologies are blue colored. The main technologies for heavy oil recovery can be divided into cold production and thermal enhanced oil recovery (EOR).

Thermal enhanced oil recovery is recognized for being the most efficient and generally reaching recovery factors of 60% of the original oil in place (OOIP), or even as high as 70–80% in some favorable reservoirs (Sheng, 2013). The current commercial technology for thermal recovery includes steam drive, cyclic steam stimulation (CSS) and steam-assisted gravity drainage (SAGD). Notwithstanding their high technical efficiency, these methods face environmental challenges due to the high emission of carbon dioxide due to its high energy demands along with

cost-efficiency challenges because of the high-cost of heat supply, posttreatment and maintenance (Zhao et al., 2014). These considerations are more severe in heavy oil reservoirs with thin pay zones, e.g. heavy oil deposits in Western Canada (Srivastava et al., 1999), due to high water usage and a severe heat loss throughout the overburden and underburden (Chakma and Jha, 1992).

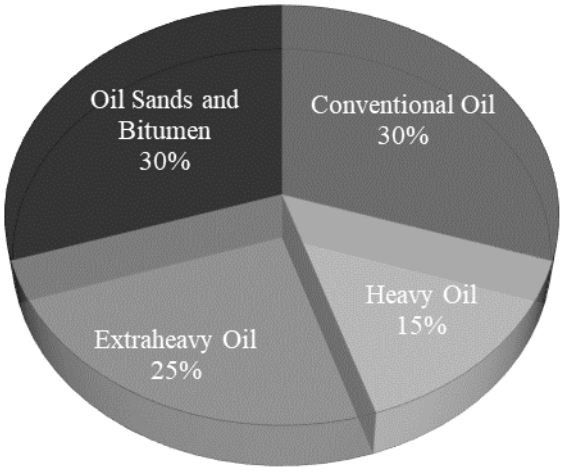

Figure 1.1—Global oil resources (Faergestad, 2016).

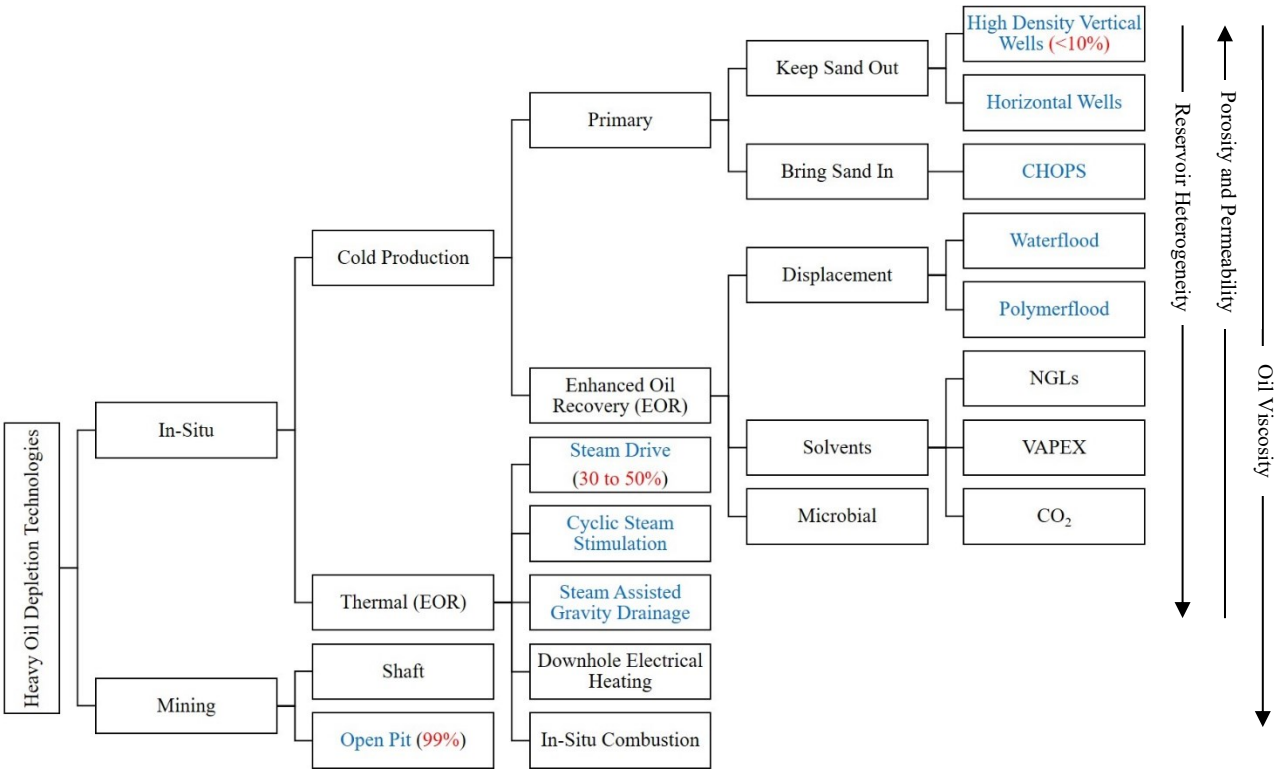

Figure 1.2—Heavy oil recovery spectrum (Pospisil, 2011)

The non-thermal production of heavy oil without sand is known as cold production. Current cold production commercial technologies include primary production, where recovery factors are poor ranging from 5% to 10% (Bret-Rouzaut and Favennec, 2011), and cold heavy oil production with sand (CHOPS) in which sand is deliberately produced along with oil, water, and gas leaving behind cavity-like spaces with high porosity and permeability, also known as wormholes. This process has been observed to enhance the oil rate and improve remarkably the productivity over conventional primary production and reaching recoveries from 12% to 25% of the OOIP (Speight, 2016; Warner, 2007). Displacement techniques such as waterflooding and polymer flooding are also currently used as cold production processes. However, the latter may not be as effective due to the high viscosity of the heavy oil that causes an unfavorable mobility ratio in any displacement process (Speight, 2016). Therefore solvent-based non-thermal recovery methods such as vapor extraction (VAPEX) and cyclic solvent injection (CSI) have attracted special attention from industry and academia.

Cyclic solvent injection has a great potential to enhance the final heavy oil recovery since CSI can perform successfully in thin heavy oil reservoirs after cold production, and has emerged as an effective follow-up process to post-CHOP reservoirs, in which the existence of high-permeability wormholes increase not only the area of contact between the injected gas and the heavy oil but also the overall productivity (Du et al., 2015). Thus, a comprehensive understanding of CSI process in this type of reservoirs is paramount to recover the vast residual heavy oil resources remaining underground.

1.1 Statement of the Problem

Primary depletion of a solution-gas-drive reservoir relies entirely on the forces present in the reservoir, such as the expansion of the fluids present in the reservoir when pressure declines. Generally, the performance of a solution-gas-drive reservoir present relatively rapid pressure decline; low initial producing gas-oil ratio (GOR) increasing over time to a much higher GOR; (3) declining oil production rate; and finally achieving a relatively low oil recovery, which declines with increasing oil viscosity (Sheng et al., 1999). For heavy oil reservoirs, the expected solution gas drive recovery factor is typically lower than 5% (Sheng and Maini, 1996). However some heavy oil reservoirs in Venezuela, China, Albania, Oman, and West Canada under primary production (Smith 1988; Chen and Maini 2005; Maini and Busahmin 2010; Zhou et al. 2017) have

exhibited an unusual behavior like low producing gas-oil ratio (GOR), good pressure maintenance and high primary production recovery (Maini et al. 1993; Albartamani et al. 1999; Bora et al. 2000; Turta et al. 2003) when compared to a conventional solution gas drive reservoir performance. The produced heavy oil was observed to contain high gas-volume-fraction trapped and having the form of an oily continuous foam (Sheng et al. 1997), which gave rise to the widely used term "foamy oil" (Maini 2001) to identify this type of produced oils. Foamy oil mechanism has also been observed as a flow-enhancement when producing reservoirs under a CHOPS process (Warner, 2007).

Foamy oil is formed as a response to a pressure depletion process (Sheng et al. 1995, 1997, 1999). The dynamics and stability of foamy oil, as pressure drops, is determined by four main stages: (1) Bubble nucleation, since gas gets trapped due to capillary forces in the oil because of its high viscosity; (2) bubble growth, as pressure drops the tiny gas bubbles trapped in the heavy oil start growing, increasing the effective compressibility of the oil; (3) bubble trapping – mobilization, which enables the oil to advance more easily in the direction of the gas flow, eventually reaching (4) bubble disengagement and coalescence/breakup (Kraus et al. 1993). Maini and Busahmin (2010) stated that these bubbles dynamic processes occur simultaneously.

Foamy oil stability is still not entirely understood but it has been observed to be affected by some fluid properties like oil viscosity and dissolved gas ratio; rock properties like absolute permeability; and by operating parameters such as saturation pressure, pressure depletion decline rate, dissolved gas composition, and time. Despite the great advances in the description and understanding the foamy oil stability, there are still uninvestigated techniques to delay the dynamic process of bubble coalesce and ameliorate the life of the stable foam.

The production stage mechanism in a CSI process, where the heavy oil is recovered under the solution gas drive mechanism can be comparable, to some extent, to the foamy oil mechanism, i.e. pressure depletion of methane-saturated heavy oil. Despite the high gas-oil mobility ratio that may considerably lessen the effectiveness of this mechanism (Jamaloei et al. 2013; Jiang et al. 2014), CSI has many more advantages for thin reservoirs when compared to other solvent-based non-thermal recovery methods (Sun et al. 2016). Therefore, CSI is considered an effective technique for increasing the recovery factor whether as a follow-up process to the CHOPS or for thin heavy oil reservoirs (Dong et al. 2006; Du et al. 2015; Jia et al. 2015).

Previous studies have focused on the understanding of foamy oil flow mechanics under primary production by performing pressure depletion experiments on a live-oil-saturated sandpack and seeking for the potential application of using methane (Zhang et al. 1999; Maini, 2003; Ostos and Maini, 2005; Goodarzi and Kantzas, 2008; Li et al., 2012; Liu et al., 2016; Zhou et al., 2016; Abusahmin et al. 2017; Soh and Babadagli 2017), propane (Shayegi et al. 1996; Ivory et al. 2010; Bjorndalen et al. 2012; Qazvini Firouz and Torabi 2014), carbon dioxide (Shi and Kantzas 2008; Or et al. 2014; Zhou et al. 2018), and their mixtures (Soh et al. 2016; Rangriz Shokri and Babadagli 2017; Soh and Babadagli 2017; Soh et al. 2018) as CSI solvents. Among these solvents, methane has been observed to give better foaming characteristics as well as being more advantageous due to its larger availability and economic efficiency (Sun et al. 2015). Yet, studies on foamy oil generated by an external gas drive, i.e. injecting methane to a dead-oil-saturated sandpack, are very limited (Shi and Kantzas, 2008; Qazvini Firouz and Torabi, 2012; Soh and Babadagli, 2017).

A full understanding of the performance of foamy oil generated by an external gas drive and cost-effective approaches for improving the foamy oil stability like using co-injection gasses and trying new injection schemes and strategies are required to make the CSI process more efficient.

1.2 Aims and objectives

The present study aims to understand the flow mechanics of the methane-based foamy oil and the effects of using air as a co-injection gas to improve the foamy oil stability, and hence final heavy oil recovery. Furthermore, the effects of different injection approaches—single-well injection and multi-well injection schemes—and different injection strategies—alternating gas injection and simultaneous gas mixture injection—are evaluated regarding their ability to better mobilize the oil and improve the final heavy oil recovery. The general objectives of this research are listed below:

- Designing reservoir-representing laboratory setups and establish procedures to better analyze and describe the behavior of foamy oil flow in a porous medium.
- Visualizing the dynamics of gas bubbles in a high viscosity oil, namely, bubble nucleation, bubble growth, and bubble coalescence and breakup through macroscopic (naked eye) and microscopic observations at laboratory conditions.

- Quantifying the efficiency of different injection approaches and strategies based on local pressure gradients and final heavy oil recovery. Cyclic sandpack flooding experiments are carried on in order to measure the effects of each type of injection.
- Studying the efficiency of using three different gasses (i.e. methane, air, and a mixture of air and methane at a volume ratio of 1) to generate stable foamy oils. Macroscopic (naked eye) and microscopic visualization should lead to the interpretation of foamy oil stability parameters such as time of foamability and collapse, number of gas bubbles, gas bubbles distribution and maximum size.
- Quantifying, at laboratory conditions, the potential amount of methane that can be saved up when using air as a foamy oil ameliorative.

1.3 Structure of the Thesis

The present paper-based thesis is divided into five chapters. Chapter 2 is based on one paper previously presented at a technical conference, and its subsequent modification which is currently under review in a research journal. Chapter 3 consist of a paper submitted to a research journal and it is currently under review for its posterior publication. Chapter 4 consists of a paper that has been accepted for presentation at a technical conference.

Chapter 1. This chapter introduces the reader into the general knowledge of heavy oil, describing at a high level what heavy oil is, the globally available amount of this type of resources, and the current technology applied for its recovery. It also contains a general description of the foamy oil phenomenon observed when producing heavy oil fields. The statement of the problem and the main objectives of this research project are also outlined in this chapter.

Chapter 2. Dead-oil sand pack experiments were performed to represent a multi-well injection scheme in a thin pay zone heavy oil reservoir. Four tests of a five-cycle-CSI process were carried out following different injection strategies. Air was used as a co-injection gas not only to reduce the amount of methane usage but to improve the stability of the generated foamy oil.

Chapter 3. An extensive review of the mechanics of the methane-based foamy oil is presented in this chapter. Furthermore, this chapter gathers all the main observations made by previous authors

when performing live-oil and dead-oil sandpack experiments with methane and comes up with trends to identify the main parameters affecting the stability of foamy oil.

Chapter 4. Foamy oil stability is analyzed after recombining heavy oil with methane, air, and their mixture. Observational experiments were carried out by means of macroscopic (naked eye) and microscopic visualization which was interpreted through foamy oil stability parameters such as time of foamability and collapse, the number of gas bubbles, gas bubbles distribution, and maximum bubble size. Furthermore, sandpack experiments are performed following a different injection scheme. Results were compared with our previous studies.

Chapter 5. Presents the general conclusions achieved in this study along with suggestions for future work and improvements related to the understanding of the mechanics of foamy oil and its potential application as an enhanced oil recovery technique.

Chapter 2

Feasibility Study of Air for Improved Foam Stability and Cost-Effective Enhanced Heavy Oil Recovery

This chapter of the thesis is a revised and modified version of the published conference paper SPE 193761, presented at the SPE International Heavy Oil Conference and Exhibition, held in Kuwait City, Kuwait on 10-12 December 2018 and soon thereafter submitted to the journal *SPE Reservoir Evaluation and Engineering* and it is currently under review.

2.1 Preface

Foamy oil flow is commonly encountered in heavy oil production from homogeneous or heterogeneous (after cold heavy oil production with sands—CHOPS) reservoirs. This can be due to a drive mechanism in the primary production (depletion of methane saturated heavy oil) and secondary stage (gas injection after primary production). In the primary stage, among other important parameters, the pressure depletion rate has been reported to be the most critical characteristic to control this type of flow. In the secondary stage, gas amount and type (sole injection of methane, carbon dioxide, propane, or a combination of these), and application conditions (soaking time on cyclic solvent injection durations, depletion rate) are critical.

The cornerstone of the foamy oil behavior relies on its stability, which depends on parameters such as oil viscosity, temperature, dissolved gas ratio, pressure decline rate, and dissolved gas (solvent) composition. Although the process has been investigated and analyzed for different parameters in the literature, the optimal conditions for an effective and more economical process (mainly foamy oil stability) has not been thoroughly understood, especially for secondary recovery conditions.

In this study, air has been used as an ameliorative to improve foamy oil stability. Four pressure depletion tests were performed, each of them consisting of five consecutive cycles. Each pressure depletion test included eight independent pressure recordings obtained from pressure transducers distributed along the sandpack holder for 48 hours. In order to reach the optimal conditions of the applications, three different pressure depletion rates were tested at 0.23 psi, 0.51 psi/min, 1.53 psi/min, together with air as an ameliorative for foamy oil stability. We observed that increasing pressure depletion rates increased the formation of foamy oil, however, when pressure depletion rates were too high, negative effects on the final oil recovery factor were observed. We also observed that injecting air into the sandpack caused an increase in the heavy oil viscosity, and the subsequent injection of methane as a solvent became more effective in generating more stable foamy oil, which resulted in obtaining a higher oil recovery factor. This novel approach is expected to improve the understanding and use of foamy oil mechanics as well as to achieve higher foamy oil stability aiming to increase the final heavy oil recovery factor.

Keywords: Foamy Oil Stability, Air Injection, Heavy Oil, Viscosity Alteration

2.2 Introduction

Heavy oil reservoirs contain hydrocarbons with low fractions of volatile compounds and high proportions of high molecular weight compounds such as paraffin and asphaltenes. These reservoirs are characterized as having very viscous oils with very low mobility (Speight 2016). An anomalous fluid flow behavior has been observed in reservoirs in Venezuela, China, Albania, Oman, and Western Canada, of which have been produced under primary production with a solution gas drive mechanism (Chen and Maini 2005; Maini and Busahmin 2010; Smith 1988; Zhou *et al*. 2018). This atypical behavior involves low producing gas-oil ratios (GOR), good pressure maintenance, and a prominent primary production recovery (Albartamani *et al*. 1999; Kumar and Pooladi-Darvish 2002; Maini *et al*. 1993) when compared with conventional solution gas drive performance.

Foamy oil is the terminology commonly accepted to describe the aforementioned performance associated with heavy oil flow behavior (Maini, 2001) formed as a response to the pressure depletion process (Sheng *et al*. 1995, 1997, 1999). The properties of foamy oil relate to four main stages: (1) Bubble nucleation, since gas gets trapped due to capillary forces in the oil because of its high viscosity; (2) bubble growth, as pressure drops the tiny gas bubbles trapped in the heavy oil start growing, increasing the effective compressibility of the oil; (3) bubble trapping – mobilization, which enables the oil to advance more easily in the direction of the gas flow, eventually reaching (4) bubble disengagement and coalescence/breakup (Kraus *et al*. 1993). It is noteworthy to mention that all of the aforementioned bubble dynamics occur simultaneously (Maini and Busahmin 2010). Foamy oil stability is still not thoroughly understood but is acknowledged to depend on saturation pressure, oil viscosity, temperature, dissolved gas ratio, pressure decline rate, dissolved gas (solvent) composition, and time. The understanding of foamy oil stability has been thoroughly studied and has been greatly improved over time, though there are still some unresolved issues.

Among the non-thermal methods for enhanced heavy oil recovery, the CSI process is considered an effective technique for increasing the recovery factor (RF) either as a follow-up process to the cold heavy oil production with sand (CHOPS) or for thin heavy oil reservoirs (Dong *et al*. 2006; Du *et al*. 2015; Jamaloei *et al*. 2013). In this regard, this study broaches the in situ generation of foamy oil and its respective stability and flow performance in a CSI process. It has

been studied by running four pressure depletion tests on a sandpack initially saturated with dead heavy oil. Methane was used as the main solvent, and air as an ameliorative for the foamy oil stability. The physics behind the flow behavior of the generated foamy oil due to the depletion rate and type of solvent/mixture used has been studied by means of pressure profiles, oil and gas recovery factors, differential pressures, and pressure gradients. This study focuses on the physics of the CSI process when air is injected with methane to improve heavy-oil displacement.

Effects of Air in Heavy Oil. Mayorquin-Ruiz and Babadagli (2016) observed that heavy oil viscosity increases when exposed to air due to a low-temperature oxidation (LTO) process. Oxidation reactions for heavy oils depend on SARA compositions, hydrocarbon (H/C) ratios and specific oxidation paths (Li *et al*. 2017). Many reaction products are produced as a result of hydrocarbon oxidation as shown below (Burger 1972):

Oxidation to a carboxylic acid:

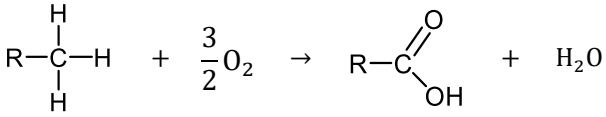

(1)

Oxidation to aldehyde:

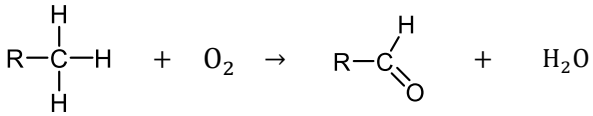

(2)

Oxidation to ketone:

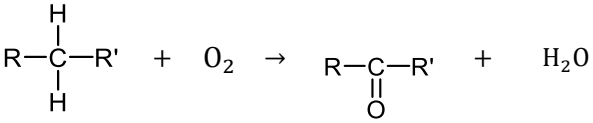

(3)

Oxidation to alcohol:

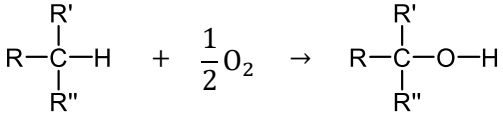

(4)

Oxidation to hydroperoxide:

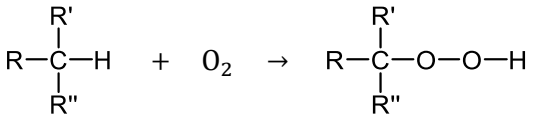

(5)

It has been observed in the laboratory that LTO has some effects on the hydrocarbon composition. After a SARA analysis on oxidized Athabasca bitumen and fresh Athabasca bitumen before oxidation, Babu and Cormack (1984) observed that the percentage of saturates remained unaffected, aromatics percentage decreased (aromatics were transformed to resins and resins were transformed to asphaltenes), and asphaltenes percentage increased. Furthermore, during the oxidation process, they observed the resin composition increased and decreased subsequently throughout the process. Similarly, Niu *et al*. (2011) studied the LTO reaction process by conducting a SARA analysis on light and heavy oil samples both before and after the LTO reaction. They observed that LTO is more prone to occurrence in heavy oils rather than light oil compounds. Furthermore, they conducted air flooding (dynamic oxidation) experiments using a slim tube on four pure oil compounds and components (i.e. n-hexadecane, paraffin, anthracene, and asphaltenes), of which were chosen to represent each SARA pseudo-component in order to investigate their reactivity in the LTO reactions. Based on the results, they concluded that saturate and aromatic contents decreased and asphaltene and resin content increased. Many studies on the physical and chemical effects of LTO on crude oil have been carried out and agree that LTO has limited control on the process for light oil samples, but the opposite occurs for heavy oils, in which viscosity and density change drastically (Fassihi *et al*. 1990; Khansari 2014; Mamora 1995). This increase in oil viscosity through LTO reactions will enable more stable foamy oil, and therefore, air is suggested to be used in the CSI application (Soh and Babadagli 2017, 2018). This study focuses on the physics of the CSI process when air is injected with methane to improve heavy-oil displacement.

2.3 Materials and Methodology

Pressure depletion tests performed in sandpacks (porous media) were conducted under pseudo-steady state conditions in the laboratory in order to investigate the drawdown pressure effects in the in-situ generation of foamy oil for an effective heavy oil solution gas drive recovery. All of the

pressure depletion tests were performed at room temperature and at a stable pressure depletion rate.

Experimental Materials

The dead heavy oil (free of gas at atmospheric pressure) sample of 13.2 API gravity used in this study was obtained from Eastern Alberta, Canada. Dead oil viscosity, measured with a rotational viscometer (DV – II + Pro, Brookfield Engineering Inc., USA), and density of 27,400 mPa•s and 0.9755 kg/m3, in the order of precedence, were both measured at atmospheric pressure and at a temperature of 21°C. Dead oil compositions and the results of saturates, aromatics, resins, and asphaltenes (SARA) analysis are shown in Tables 2.1 and 2.2, respectively. Table 2.3 lists the sandpack physical properties used for every pressure depletion test. Methane (99.97% pure), used as a solvent, and air (21% oxygen and 79% nitrogen) were both purchased from Praxair Canada Inc. and were used to generate the foamy oil systems. Nitrogen (provided by Praxair Canada Inc.) was used as a pressure testing gas with a purity of 99.99%. Silica sand with a grain size between 250 – 500 μm was used to pack the porous medium. Deionized water (silica content < 0.1 ppm), used for measuring the sandpack properties, was purchased from ACROS Organics, Fisher Scientific Canada Inc.

Experimental Apparatus

The schematic diagram of the experimental equipment is shown in Figure 2.1. Four systems can be identified in the setup:

1. An injection system consisting of a syringe pump (500 D, Teledyne ISCO Inc., USA) and a floating piston fluid accumulator (1000 ml, JEFRI – Donald Baker Robinson, Canada).
2. A sandpack system consisting of a 150 cm (59 in) long and 5 cm (2 in) internal diameter stainless steel sandpack holder containing two fluid distribution caps located at the inlet and at the outlet ports. The sandpack holder is evenly equipped with 7 pressure transducers (PX309 – 005A5V, OMEGA Engineering Inc., Canada) with an accuracy of ±0.25% FS (Full Scale) and numbered in an ascendant order from the injection port to the production port (P1, P2, P3, P4, P5, P6, and P7), 2 rugged pipe plug thermocouple probes (TC-K-NPT, OMEGA Engineering Inc., Canada) numbered in ascendant order (T1 and T2) located at the injection port and at the production end, respectively, 1 transition junction style

thermocouple probe (TJ36, OMEGA Engineering Inc., Canada) named T3, a data acquisition (DAQ) device (cDAQ – 9171, National Instruments Corporation, USA), and a DAQ computer.

3. A pressure depletion control system consisting of a back pressure regulator – BPR (EB1ZF1 – SS316, EquiliBAR, USA) with a pressure transducer (P8) and a syringe pump.
4. A produced oil and gas collector system consisting of a borosilicate glass cylinder (500 ml, Fisher Scientific Inc., Canada), an electronic balance (BL – 4100S, Setra Systems Inc., USA) with an accuracy of ±0.01 g, and a mass flow controller (M – 100SCCM – D/5M, Alicat Scientific Inc., USA) with an accuracy of 0.2% FS.

Table 2.1—Compositional analysis of the dead heavy oil.

Component	wt%	Component	wt%	Component	wt%	Component	wt%	Component	wt%
C_1	0.00	C_{16}	0.20	C_{39}	0.00	C_{62}	0.00	C_{85}	1.39
C_2	0.00	C_{17}	0.14	C_{40}	0.00	C_{63}	0.00	C_{86}	3.00
C_2H_4	0.00	C_{18}	0.12	C_{41}	0.00	C_{64}	2.24	C_{87}	1.37
C_3	0.00	C_{19}	0.12	C_{42}	0.50	C_{65}	0.00	C_{88}	2.55
C_3H_6	0.00	C_{20}	0.09	C_{43}	0.00	C_{66}	0.00	C_{89}	2.30
i – C_4	0.00	C_{21}	0.37	C_{44}	0.00	C_{67}	0.00	C_{90}	0.87
n – C_4	0.00	C_{22}	0.09	C_{45}	0.00	C_{68}	0.00	C_{91}	2.91
Other C_4	0.00	C_{23}	0.37	C_{46}	0.61	C_{69}	0.00	C_{92}	2.28
i – C_5	0.00	C_{24}	0.07	C_{47}	0.00	C_{70}	0.00	C_{93}	3.44
n – C_5	0.00	C_{25}	0.11	C_{48}	0.00	C_{71}	0.00	C_{94}	8.90
Other C_5	0.00	C_{26}	0.08	C_{49}	0.00	C_{72}	0.00	C_{95}	0.00
i – C_5	0.00	C_{27}	0.09	C_{50}	0.75	C_{73}	0.00	C_{96}	6.50
n – C_5	0.00	C_{28}	0.00	C_{51}	0.00	C_{74}	0.00	C_{97}	0.00
Other C_6	0.00	C_{29}	0.16	C_{52}	0.00	C_{75}	0.00	C_{98}	4.97
C_7	0.05	C_{30}	0.09	C_{53}	0.00	C_{76}	0.00	C_{99}	4.27
C_8	2.22	C_{31}	0.00	C_{54}	0.97	C_{77}	0.00	C_{100}	0.00
C_9	0.11	C_{32}	0.17	C_{55}	0.00	C_{78}	0.00	C_{110}	21.33
C_{10}	0.18	C_{33}	0.00	C_{56}	0.00	C_{79}	5.04	C_{120}	10.30
C_{11}	0.39	C_{34}	0.00	C_{57}	0.00	C_{80}	0.00	$C_{120}+$	0.08
C_{12}	0.36	C_{35}	0.28	C_{58}	0.00	C_{81}	1.68		
C_{13}	0.00	C_{36}	0.00	C_{59}	1.64	C_{82}	2.17	Total	100.00
C_{14}	0.47	C_{37}	0.00	C_{60}	0.00	C_{83}	0.00		
C_{15}	0.37	C_{38}	0.31	C_{61}	0.00	C_{84}	1.24		

Table 2.2—SARA analysis results.

Property	Measured %
Saturates	37.03
Aromatics	15.68
Resins	32.16
Asphaltenes	14.25

Table 2.3—Sandpack physical properties for each test.

Test	Porosity (%)	Permeability (Darcy)	Pore volume (cm^3)
Test #1	43.32	9.96	1275.85
Test #2	43.14	9.32	1270.68
Test #3	43.61	10.25	1284.44
Test #4	43.10	9.31	1269.54

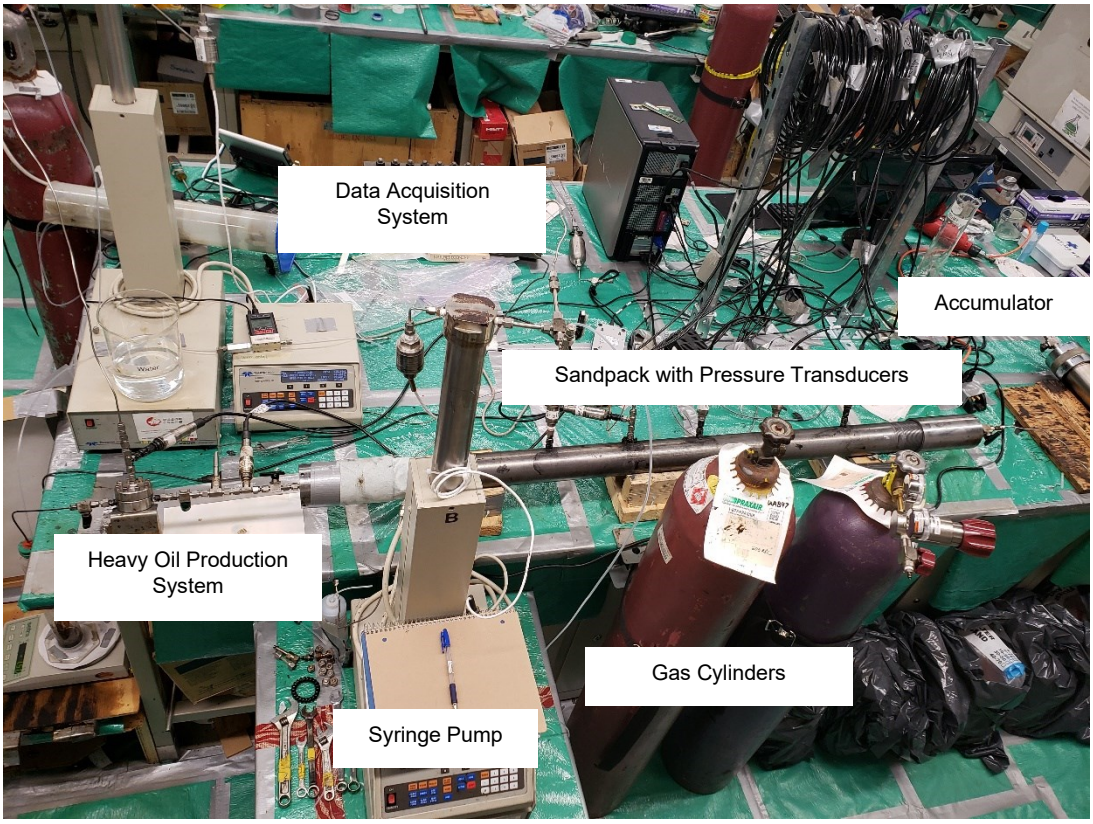

Figure 2.1—Schematic of the experimental setup.

Experimental Procedure

The experimental procedure comprises of a model preparation (cleaning and leakage testing) for each test, which in turn consists of five consecutive cycles with each cycle consisting of three stages: (1) injection stage, (2) soaking stage, and (3) production stage. The flowchart summarizing the experimental procedure is depicted in Figure 2.2. Sandpack model preparation comprises six steps:

1. The sand was wet packed in the sandpack holder while being slightly vibrated and vacuumed for 24 hours to reduce moisture content.
2. A leakage test was performed in the packed sand by pressurizing the sandpack holder with nitrogen gas up to 1.5 times the test pressure. The sandpack system was deemed to be free of leakage if the applied pressure did not change drastically for at least one day.
3. The sandpack was vacuumed for another 24 hours to evacuate all of the nitrogen and to prevent the dead zones effect.
4. Deionized water was imbibed into the vacuumed sandpack. The volume of water soaked up by the porous media was measured in order to calculate both the pore volume (PV) and the porosity of the porous medium.
5. A syringe pump was used to inject water into the sandpack under seven different flow rates to measure the permeability by exercising Darcy's law, which states that the ratios between the flow rates and the pressure differences between the two ends of the sandpack are constant. Under different flow rates, different permeabilities were obtained and, consequently, the average permeability was considered as the absolute permeability.
6. Dead oil was flooded into the sandpack, displacing the deionized water, at a constant low flow rate (0.2 cc/min) to allow for better oil distribution in the pore space. Approximately 2 PV of dead oil was used to displace the deionized water until no traces of water were observed in the oil collected in the production end.

The procedure for each cycle consisted mainly of three stages:

1. During the injection stage, the BPR pressure was established at 50% higher than the injection pressure. The solvent and/or gas was injected at a high flowrate (150 cc/min) until a pressure of 550 psi was reached in the sandpack holder.
2. During the soaking stage, all valves linked to the sandpack holder were closed and soaked for a period of at least 48 hours to allow the system pressure to stabilize, since gas dissolution causes a system pressure drop. If the pressure in the system was not stabilized, an extra day of soaking was applied repetitively until a considerable system pressure drop was no longer observed.

3. The production stage started by programming the BPR pressure (set to 20% higher than the injection pressure) to decrease linearly with time. The BPR was controlled by the

water-filled syringe pump, of which regulated the outlet (upstream) pressure by opening only as much as necessary to restrain the desired pressure at the inlet. The transient pressure data generated for the pressure depletion process were dynamically monitored and recorded by the pressure transducers. The produced foamy oil was collected in the cylinder, where its weight was permanently controlled and recorded by the electric balance. The volume of the produced gas was constantly measured and recorded by the gas flow meter. All of the data acquired through the electronic devices were transformed and sent to the data acquisition computer. This stage was considered to be finished when the BPR pressure reached atmospheric pressure.

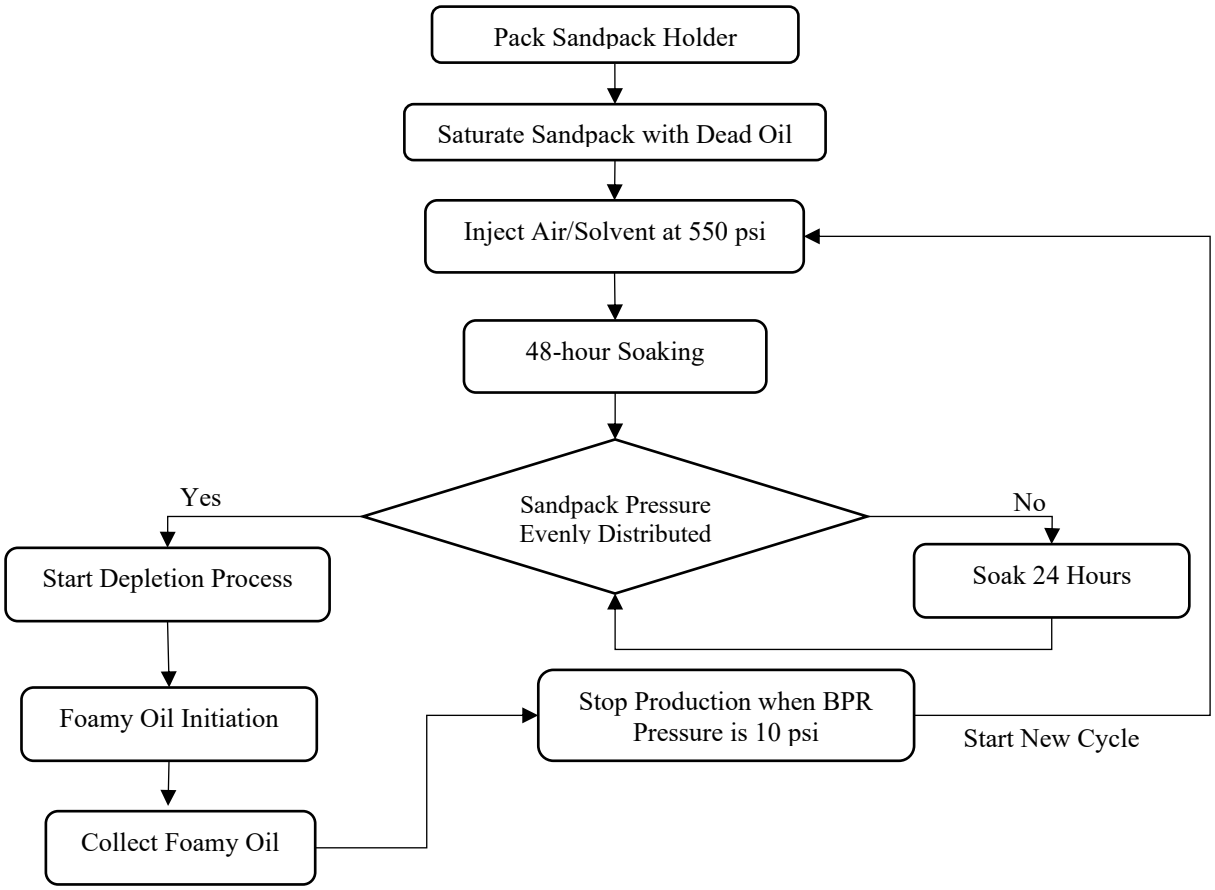

Figure 2.2—Flowchart of the experimental procedure.

2.4 Experimental Results

Many authors agree that increasing the pressure depletion rate leads to higher oil recovery factors (Abusahmin *et al*. 2017; Maini 2003), however, this may not be the case when pressure depletion rates are too high. In our previous studies (Soh and Babadagli 2018), by performing sandpack depletion tests under a CSI process for different pressure depletion rates (0.23 psi/min, 0.51 psi/min, and 1.53 psi/min), we observed that at an intermediate pressure depletion rate (i.e. 0.51 psi/min), a maximum oil RF was achieved (see Figure 2.3). Our intermediate pressure depletion rate of 0.51 psi/min is the one used for the present study.

The feasibility of utilizing methane and air in the CSI process for enhancing heavy oil recovery by the *in-situ* generation of foamy oil and the subsequent analysis of foamy oil flow was studied by performing 20 cycles of sandpack pressure depletion at a rate of 0.51 psi/min in four tests. With the objective of studying the foamy oil flow mechanism, the collected experimental data will be analyzed through production performance indicators such as oil and gas recovery factors (RF), cumulative gas-oil ratios (cGOR), as well as pressure profiles, pressure gradients, and pressure differentials.

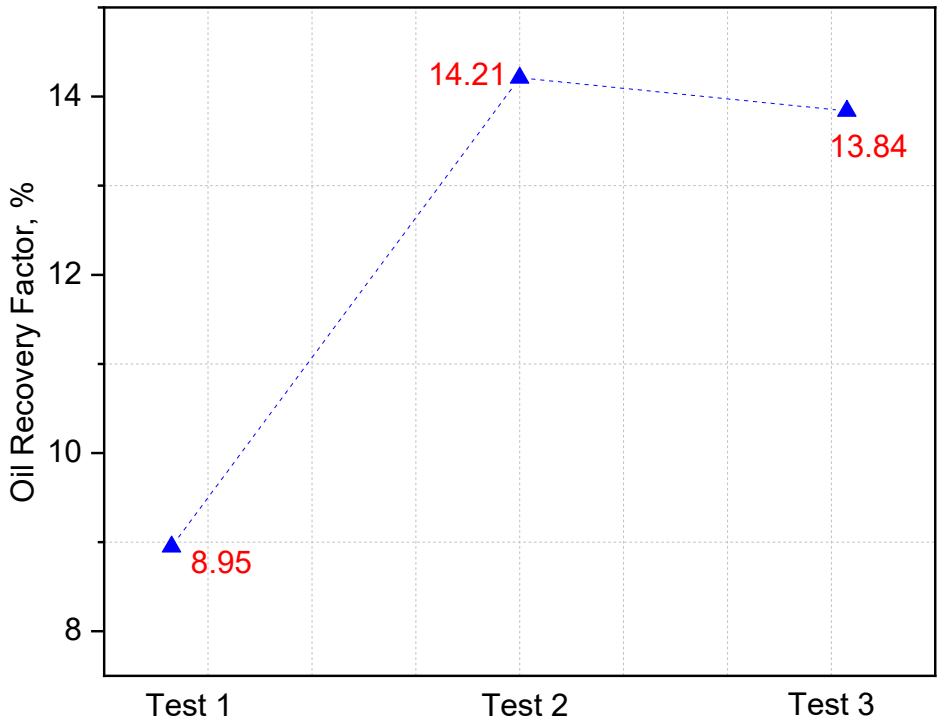

Figure 2.3—Oil RF vs. pressure depletion rates (Soh and Babadagli 2018).

The CSI process consists of three main consecutive stages: (1) injection stage; (2) soaking stage; and (3) production stage. During the injection stage, right after the solvent has been injected into the sandpack, it causes a surge in pressure. Once the solvent is injected into the sandpack, the soaking stage takes place and the diffusion process starts causing a pressure drop in the sandpack resulting in oil viscosity reduction, oil swelling, and reduction of the interfacial tension (IFT) between the solvent and the heavy oil (Das and Butler 1998; Luo *et al*. 2007; Maini and Busahmin 2010). The soaking stage is considered to be finished when a considerable pressure drop in the sandpack is no longer observed. During the production stage, the pressure drop in the sandpack is the main producing force, thus causing the formation and flow of foamy oil, in which three principal dynamic processes of the evolution of gas bubbles occur simultaneously: bubble nucleation and bubble growth, bubble trapping/mobilization, and bubble disengagement and coalescence/breakup (Maini and Busahmin 2010). Due to the dynamics of bubble behavior, heavy oil recovery is enhanced significantly.

The initial oil saturation (Soi) and initial water saturation (Swi) for each test, total number of pore volumes (PV) of gas injected (Vgas) at a pressure of 600 psi per cycle, the average pressure in the sandpack after the soaking stage (Psoak), the cumulative gas-oil ratio (cGOR), heavy oil RF per cycle, total heavy oil RF, gas RF per cycle, and the total Gas RF are presented below in Table 2.4. It is worth noting that the most significant contribution to the ultimate heavy oil recovery factor for each test was made in the first three cycles. Furthermore, as observed in Figures 2.4 and 2.5, the oil saturation close to the injection port is noticeably higher at the end of each test, whereas cleaner sand is observed close to the producing port. This insinuates that in some measure, the location of the heavy oil affects the final recovery and that during the first cycle the heavy oil close to the production port is primarily produced.

Figure 2.4—Remaining heavy oil saturation at the injection port.

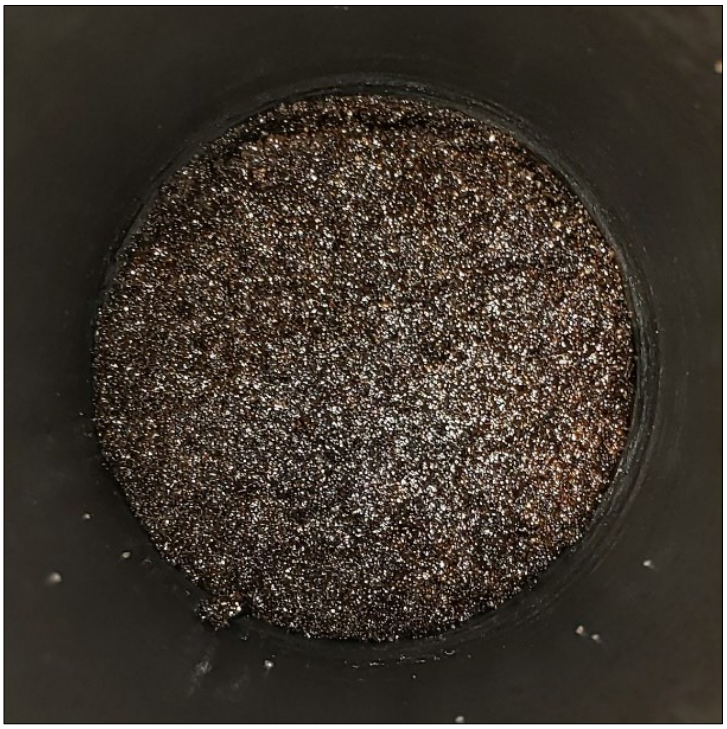

Figure 2.5—Remaining heavy oil saturation at the production port.

Table 2.4—Summary of details and results of experiments.

Test	Cycle	Gas Composition	V_{gas} (PV)	P_{soak} (psi)	cGOR (Scm^3/cm^3)	Oil RF (%)	Total Oil RF (%)	Gas RF/Cycle (%)	Total Gas RF (%)
Test #1	Cycle 1	100% Methane	0.11	532	0.02	3.36	26.45	0.01	61.62
S_{oi} = 87.77%	Cycle 2	100% Methane	0.13	571	21.02	8.48		29.48	
S_{wi} = 12.23%	Cycle 3	100% Methane	0.08	505	47.67	14.14		170.72	
	Cycle 4	50% Air – 50% Methane	0.31	538	2179.70	0.42		61.82	
	Cycle 5	50% Air – 50% Methane	0.29	542	18123.23	0.05		68.59	
Test #2	Cycle 1	50% Air – 50% Methane	0.16	551	52.06	2.37	23.49	14.93	46.29
S_{oi} = 88.04%	Cycle 2	50% Air – 50% Methane	0.08	563	23.08	7.60		45.93	
S_{wi} = 11.96%	Cycle 3	50% Air – 50% Methane	0.24	566	68.54	6.88		38.29	
	Cycle 4	50% Air – 50% Methane	0.28	546	218.45	2.94		45.94	
	Cycle 5	100% Methane	0.23	549	241.22	3.71		78.00	
Test #3	Cycle 1	100% Air	0.02	554	20.90	4.48	28.29	79.90	69.10
S_{oi} = 86.95%	Cycle 2	100% Methane	0.10	564	15.41	8.95		85.53	
S_{wi} = 13.05%	Cycle 3	100% Air	0.12	546	48.00	8.77		67.68	
	Cycle 4	100% Methane	0.28	573	347.96	3.58		86.47	
	Cycle 5	30% Methane after 70% Air	0.27	587	368.70	2.51		67.39	
Test #4	Cycle 1	100% Methane	0.01	567	0.00	2.70	27.30	0.00	71.79
S_{oi} = 87.43%	Cycle 2	100% Methane	0.08	562	26.29	10.81		66.69	
S_{wi} = 12.57%	Cycle 3	100% Air	0.15	556	60.86	7.57		61.37	
	Cycle 4	100% Methane	0.27	539	200.93	5.41		79.22	
	Cycle 5	100% Air	0.23	551	1075.96	0.81		73.75	

Test #1

Methane is considered to be advantageous when compared to other solvents due not only to its larger availability and economic efficiency but also because it has been observed to give favorable foaming characteristics (Sun *et al*. 2015). The objective of Test #1 was to study the foamy oil flow behavior in a porous media for a dead heavy oil-methane system under a CSI process in three consecutive cycles, followed by two cycles using a gas composition of 50% methane and 50% air in order to observe the effect of air in the foaming formation process. Figs. 2.6a-e display the pressure profiles, heavy oil RF, and gas RF curves for the sandpack pressure depletion process in Test #1. The average pressure in the sandpack for this test was 538 psi, and the pressure in the producing end was reduced from 600 psi to 10 psi at a constant rate of 0.51 psi/min.

At the beginning of every cycle and at the end of the soaking period, the pressure displayed in every port was similar. Ideally, if no excess gas was injected into the sandpack, and a reasonable amount of soaking time was given to the system, free gas should not be present; meaning that said free gas diffused into the heavy oil thus forming a single-phase system. At the very beginning of the depletion process, the oil has very small compressibility, since the bubbles will neither start

nucleating (size of bubbles is negligible) nor growing until the pressure in the sandpack is higher than the pressure in the producing end. As a consequence of this, during this period, the pressure depletion rate will be the same along the sandpack.

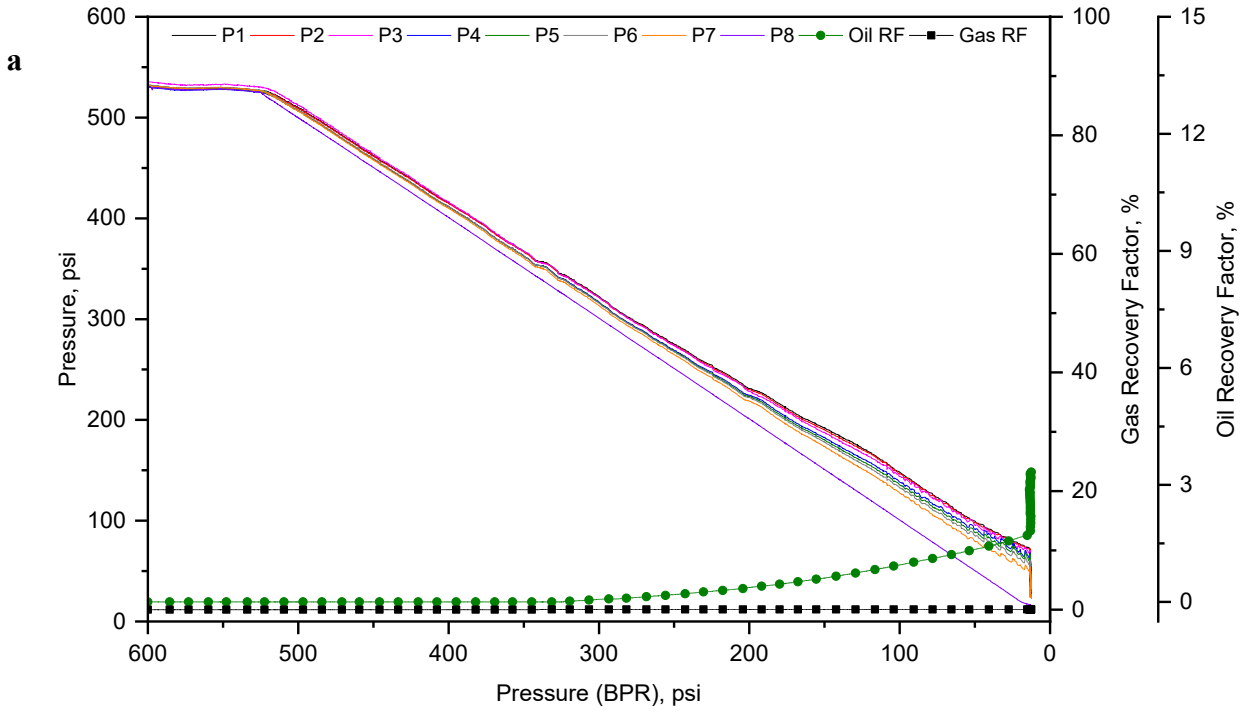

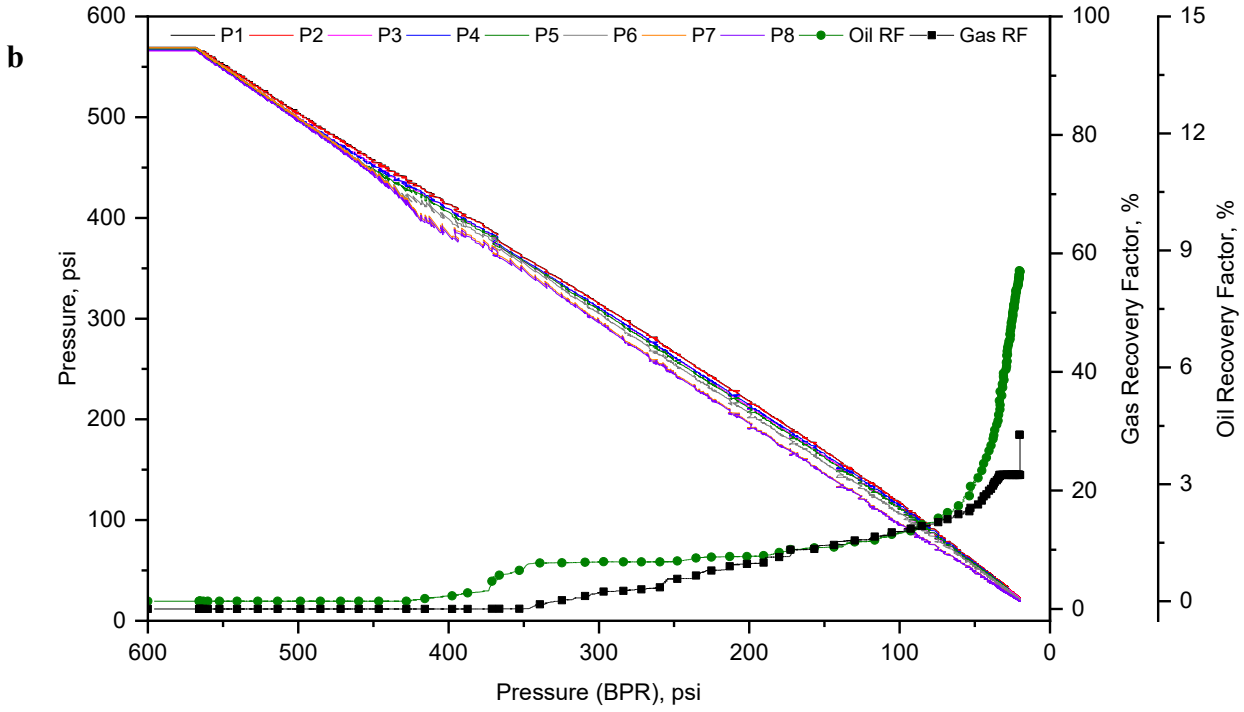

c

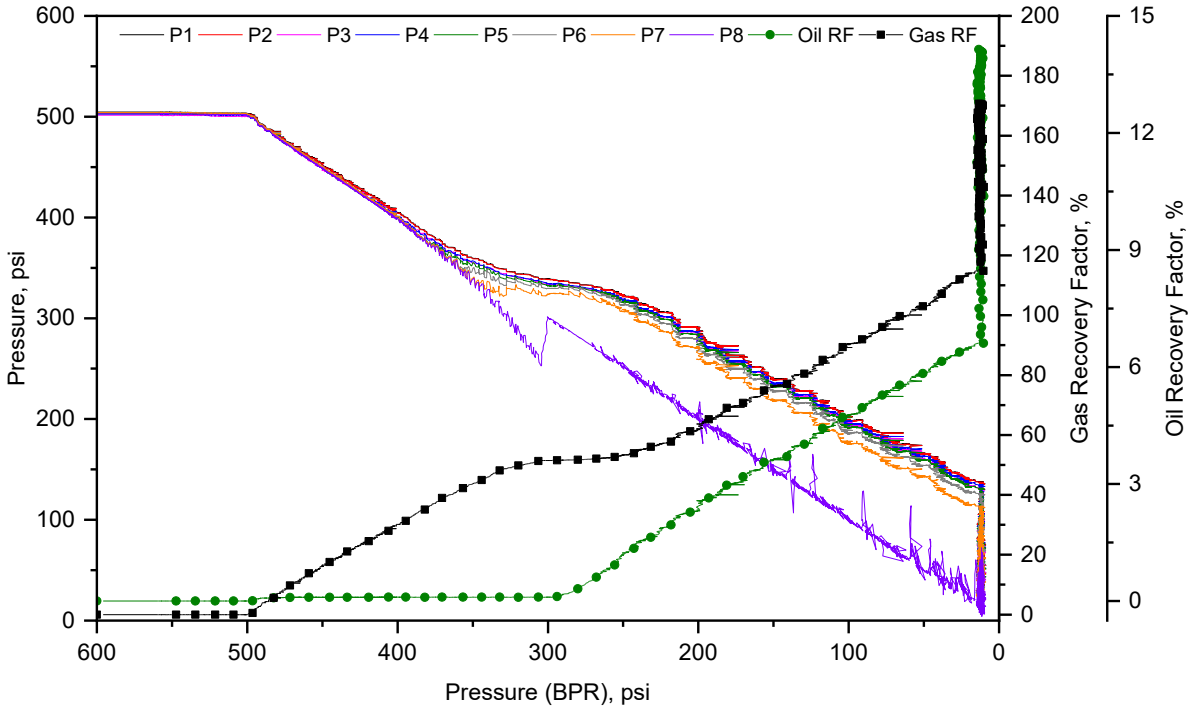
P1
P2
P3
P4
P5
P6
P7
P8
Oil RF
Gas RF
Pressure, psi
Gas Recovery Factor, %
Oil Recovery Factor, %
Pressure (BPR), psi

d

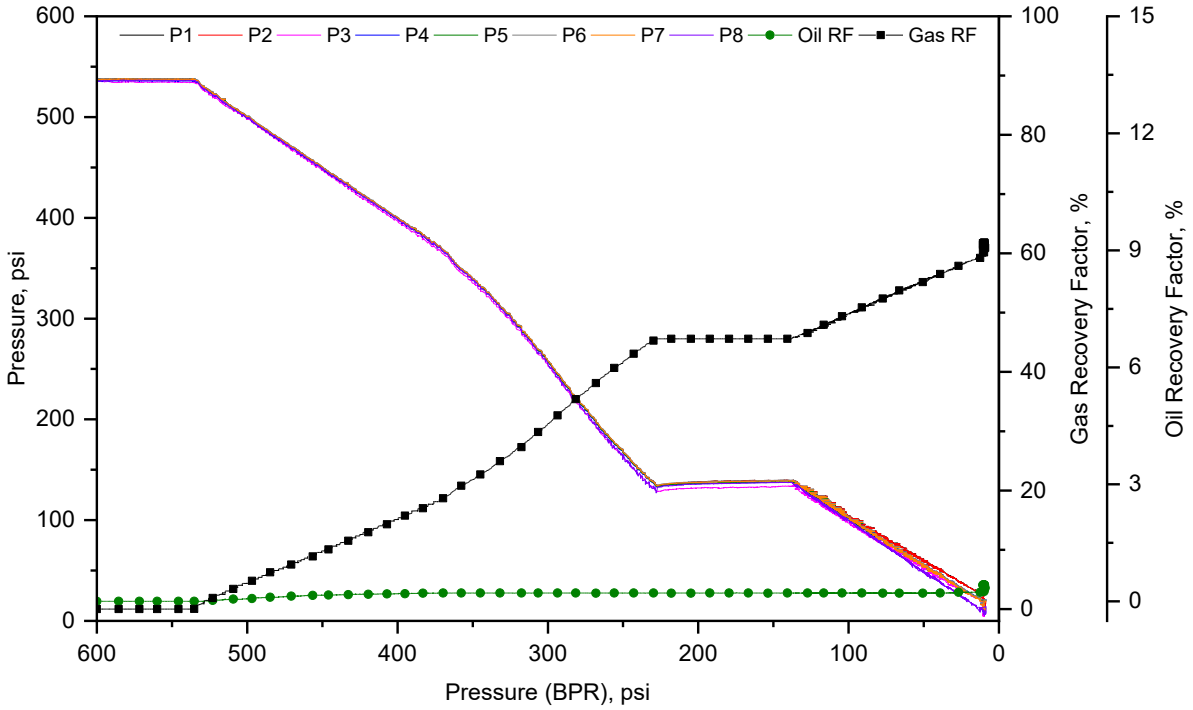
P1
P2
P3
P4
P5
P6
P7
P8
Oil RF
Gas RF
Pressure, psi
Gas Recovery Factor, %
Oil Recovery Factor, %
Pressure (BPR), psi

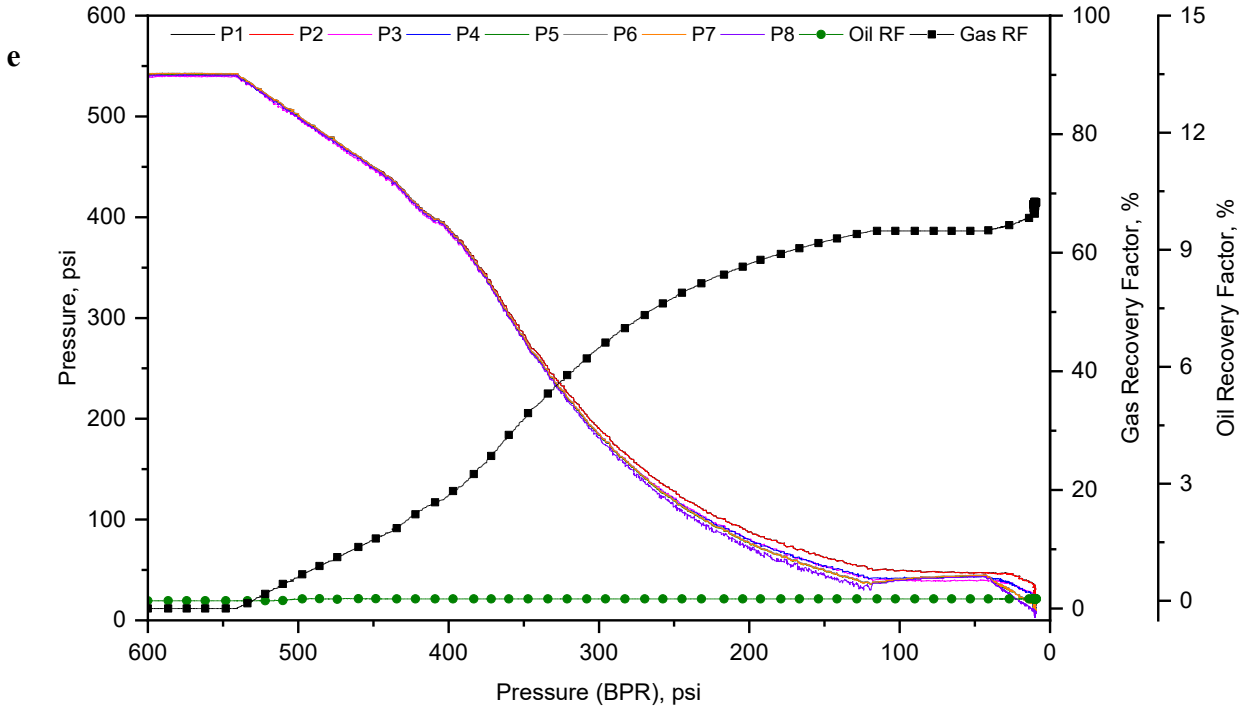

Figure 2.6—Pressure profiles for cycles 1 – 5 (a-e) for Test #1.

Once the pressure in the BPR reaches the existing pressure in the sandpack, four main stages of bubble dynamics can be observed as explained before: (1) very small bubbles start nucleating and being trapped by the heavy oil capillary forces originated by its high viscosity, and as pressure drops, (2) the compressibility of the oil starts increasing due to an increase in bubble sizes reducing the heavy oil density; (3) the trapped bubbles not only maintain the pressure in the system but also start mobilizing the oil in the direction of the gas flow (higher to lower pressure) due to the pressure differentials (ΔP1 to ΔP7), which are defined as the difference between the pressure at specific points in time in the sandpack (i.e. the pressure gauges location identified as P1 to P8 in Fig. 2.1, and the pressure at the producing end – BPR); and (4) when the pressure differentials reach their highest value, bubble disengagement and coalescence/breakup start occurring in the system, forming a continuous gas phase and reducing the foamy oil mechanism efficiency. Pressure gradients (Pg1 to Pg7) describe the difference in pressure between two consecutive points in time per unit length; these points were selected as the location of the pressure transducers.

In the first cycle, the sandpack is fully saturated with dead oil, meaning only a small amount of gas can be diffused into the heavy oil, of which is trapped by the capillary forces occurring in the oil (Zhou *et al*. 2018). As the amount of methane injected is relatively low and has a good diffusion capability into oil, low-pressure differentials are generated (see Figs. 2.7a-e). The reason behind these differentials being that the nucleated bubbles are very small and remain trapped in the heavy oil, and as pressure drops, the oil starts expanding and small amounts of low compressibility oil start producing (see Fig. 2.8) with a negligible amount of produced gas. Fig. 2.6a depicts a smooth depletion process with no abrupt changes in the slope of pressure profiles with almost no gas production and Fig. 2.7a shows higher pressure differentials only in locations just close to the producing end. As the cycles continue, sufficient space was created for the gas to start diffusing effectively if an appropriate soaking period is provided.

Kumar and Pooladi-Darvish (2002) point out that at early stages the size of the bubbles is too small and can be neglected; nonetheless, it is at this stage that gas supersaturation is starting, and along with oil production, it eventually reaches bubble nucleation. This phenomenon can be observed in the pressure profiles when the pressure recordings in the pressure gauges start deviating from the pressure in the producing end. As production continues, the size of the bubbles trapped by the oil capillary forces increases, giving way to the formation of foamy oil. The high viscosity of the oil causes a slow growth of the bubbles, retarding coalescence dramatically, improving this way the stability of the foamy oil (Wang et al. 2009). In the first three cycles, as the pressure in the producing end is continuously decreasing, the pressure differentials grow almost synchronously before bubble nucleation and growth occur, however, once this dynamic stage is reached, the organized pressure response is disturbed since the pressure is being maintained in areas where bubbles are being trapped, growing and mobilizing at the same time. This dynamic process is the main characteristic of the formation of foamy oil, collected at the producing end (Fig. 2.9), that allows higher oil recoveries. It is worth mentioning that the higher the generated pressure differentials, meaning a higher number of bubbles trapped in the heavy oil, the higher the final oil recovery factor. The bubble dynamics between two specific points (e.g. P1 to P2 or P2 to P3, etc.) in the sandpack can be understood by looking at the pressure gradient curves shown in Figs. 2.10a-e. It should be mentioned that the first points in the sandpack where bubble nucleation starts and the highest pressure gradient occurs are between the pressure ports P7 and P8 (P8 is located very close to the BPR, which is the device controlling the constant pressure depletion). As

pressure continues decreasing, the pressure propagates towards all pressure gauges ending in the injection port. The originating pressure gradients occur along the sandpack holder starting on Pg7 and finishing on Pg1. Taking a closer look at Fig. 2.10, on average, for the first three cycles, Pg5 registers the second largest pressure gradients, after Pg7. This is an important observation as it indicates that bubble nucleation and subsequent foamy oil formation is mainly happening in the middle of the sandpack holder then leading to the production end, of which can be observed in the final amount of oil recovered. Figs. 2.11a-e show the cGOR for every cycle in Test #1. It is noteworthy that the cumulative gas oil ratio increases with every cycle. For the three first cycles, the cGOR, increases at a reasonable pace, however, for cycles four and five the values are too high. These high values are mainly due to gas slippage and channeling since less oil is present in the sandpack making it difficult for the gas to diffuse into the heavy oil. Additionally, since the composition of the injected gas in the last two cycles is air and methane, the air moves directly towards the producing end whereas some methane is still getting trapped in the heavy oil, of which can be seen in the gas recovery factor of ~60% for both cycles.

a

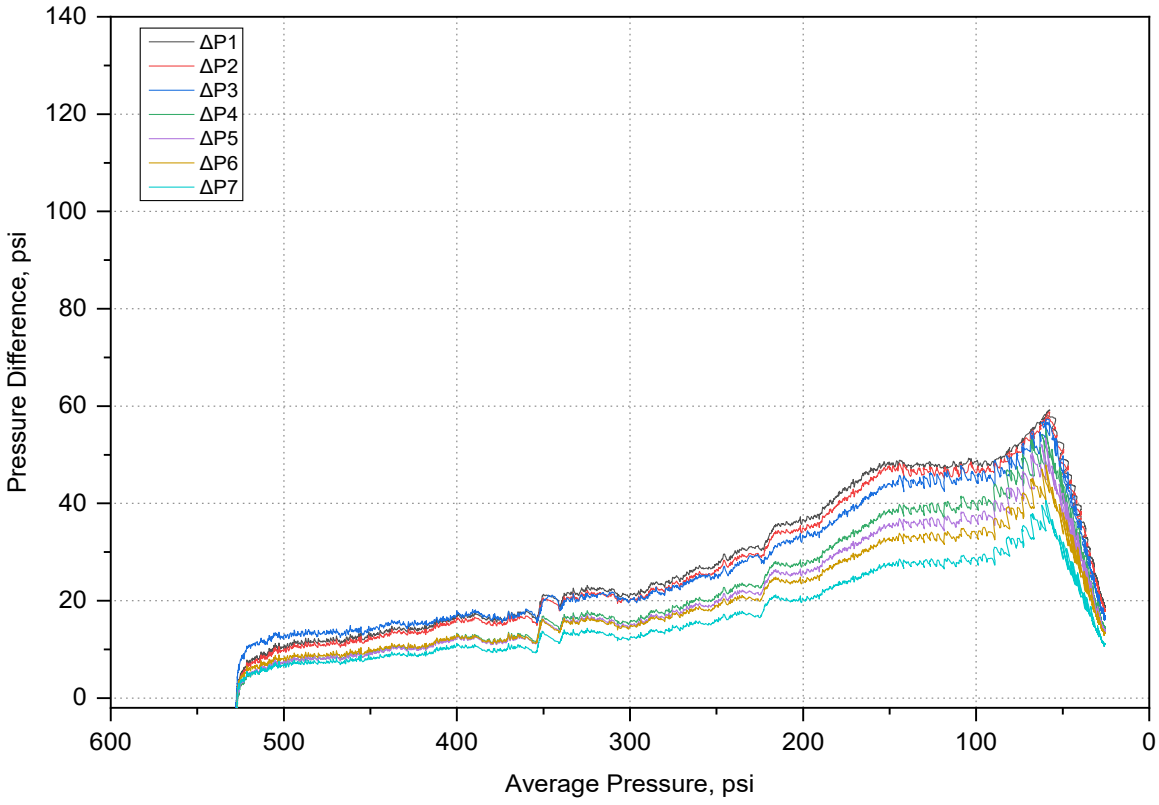

b

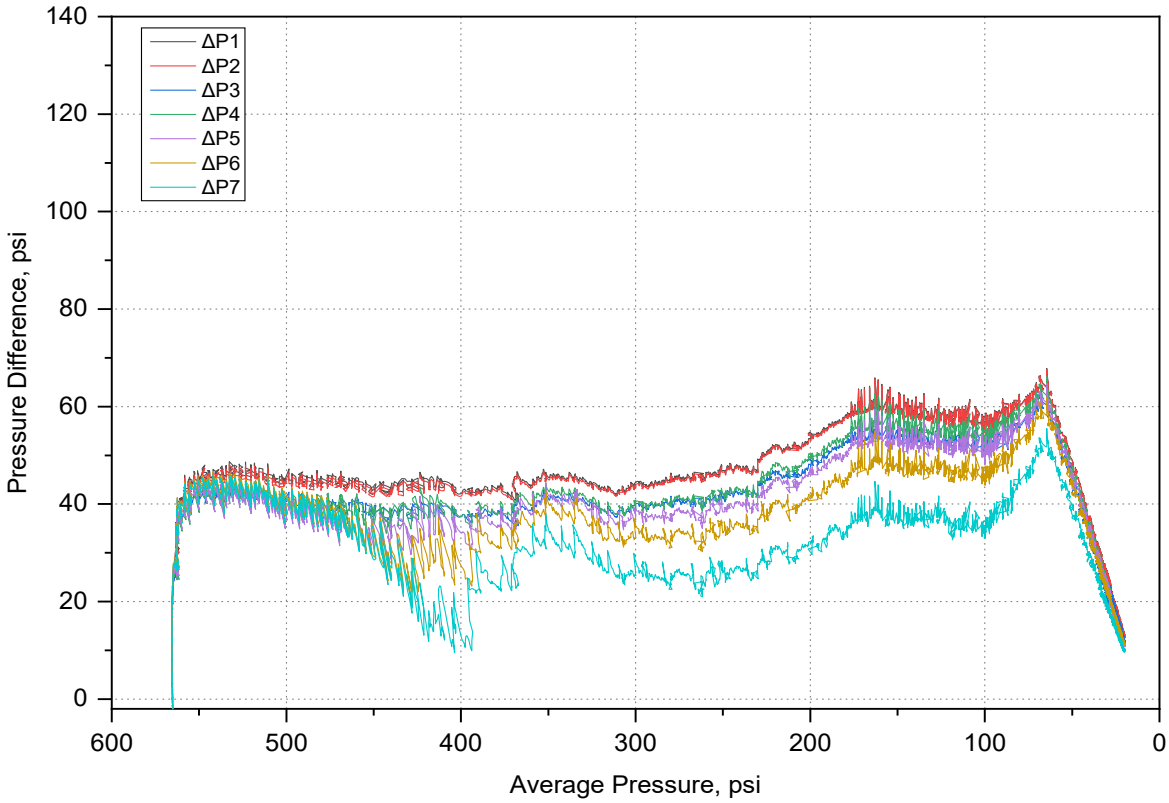
ΔP1
ΔP2
ΔP3
ΔP4
ΔP5
ΔP6
ΔP7
Pressure Difference, psi
Average Pressure, psi
140
120
100
80
60
40
20
0
600
500
400
300
200
100
0

c

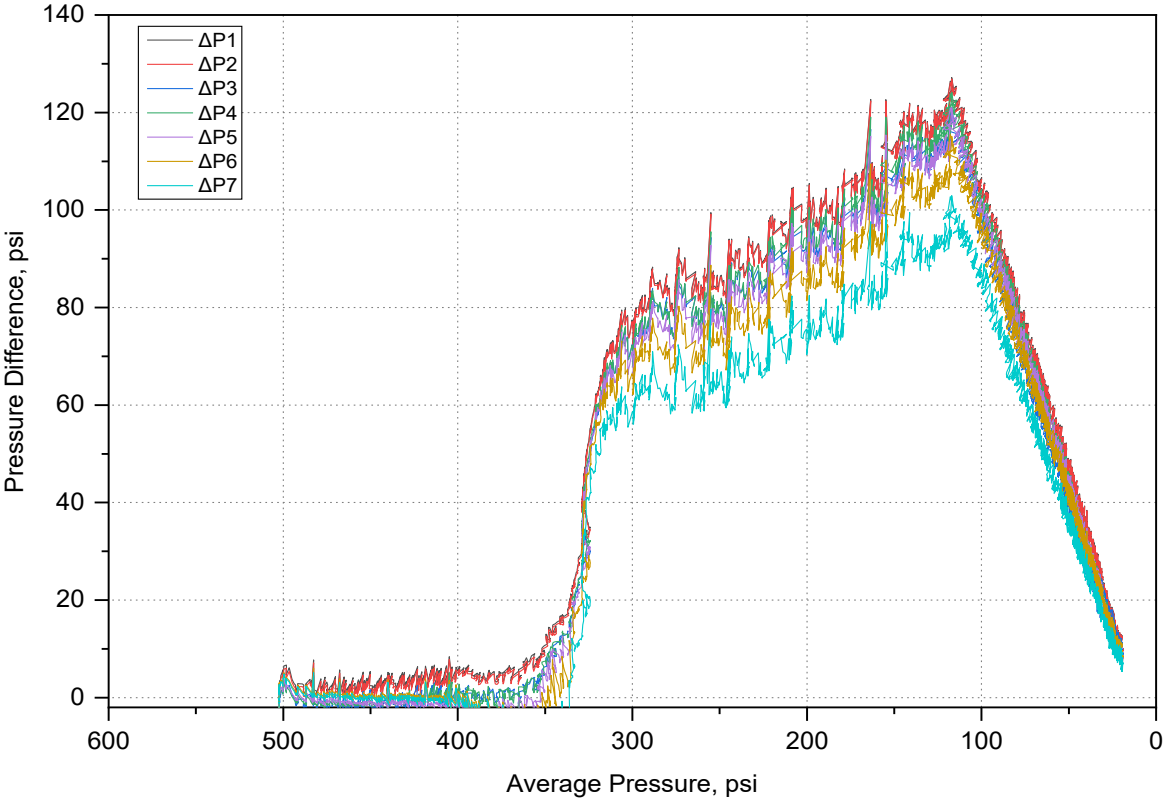
ΔP1
ΔP2
ΔP3
ΔP4
ΔP5
ΔP6
ΔP7
Pressure Difference, psi
Average Pressure, psi
140
120
100
80
60
40
20
0
600
500
400
300
200
100
0

d

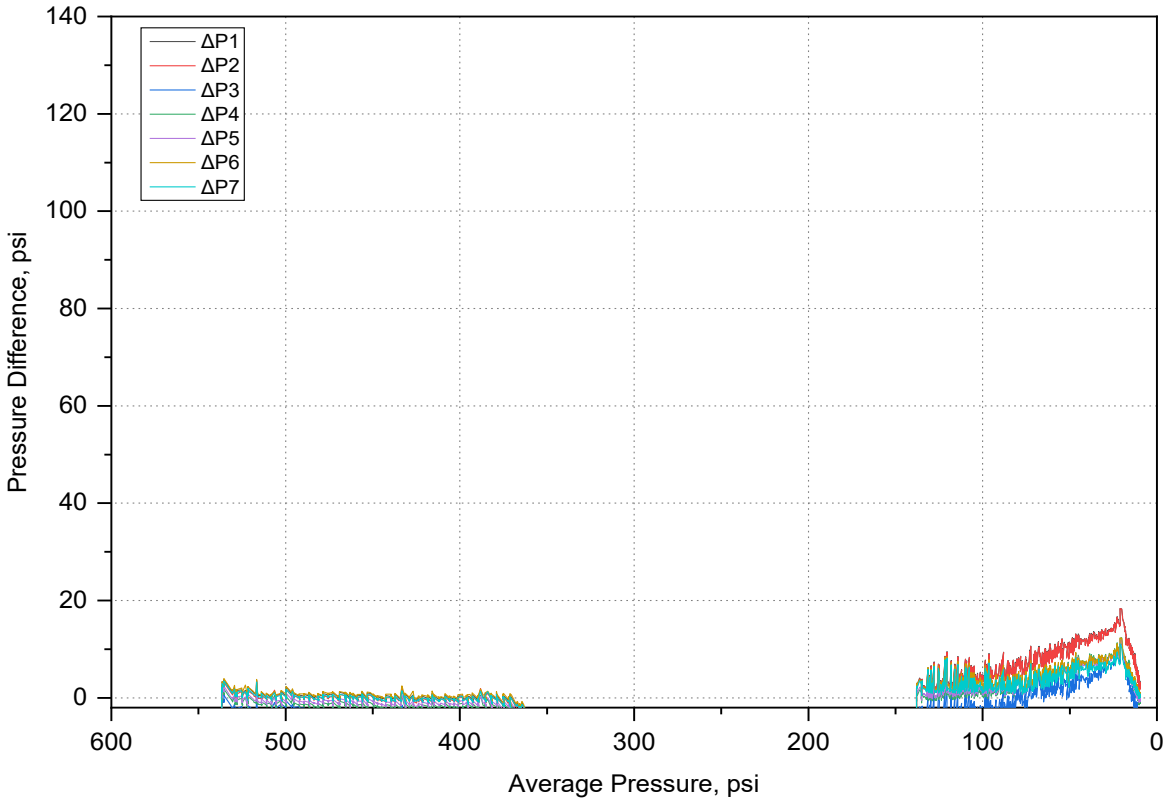

e

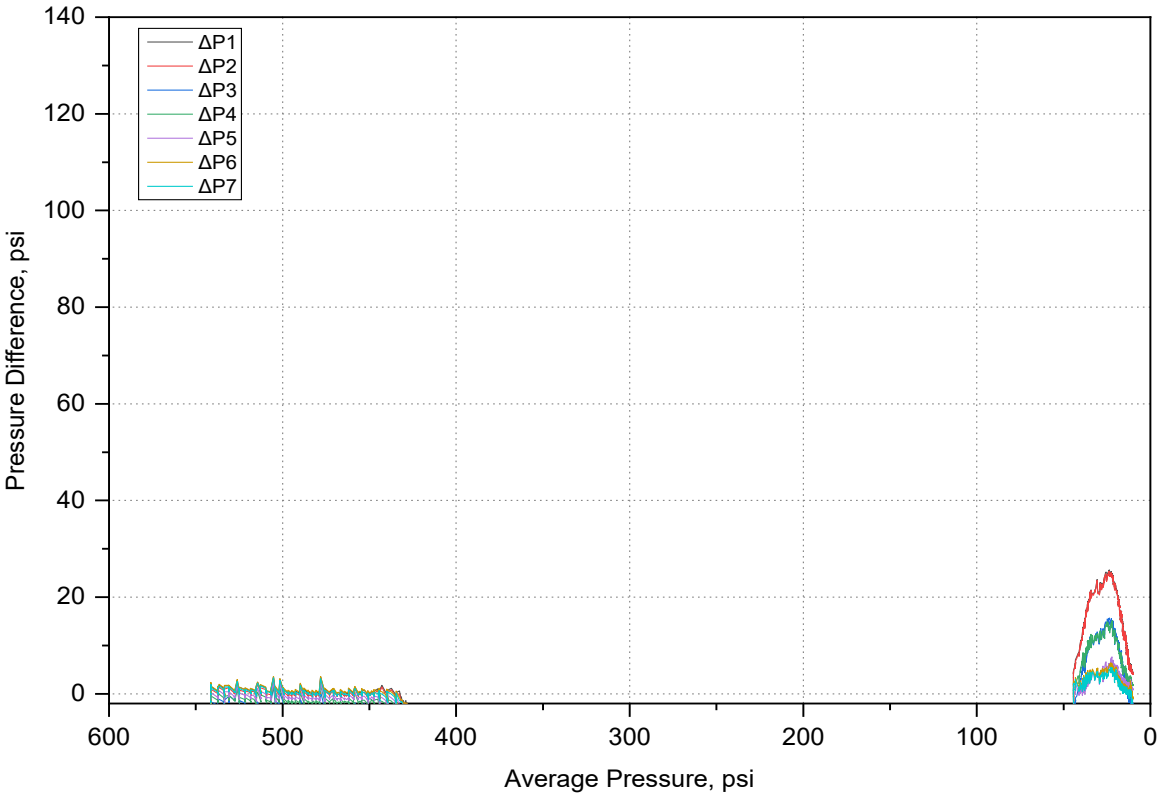

Figure 2.7—Pressure differentials for cycles 1 – 5 (a-e) for Test #1.

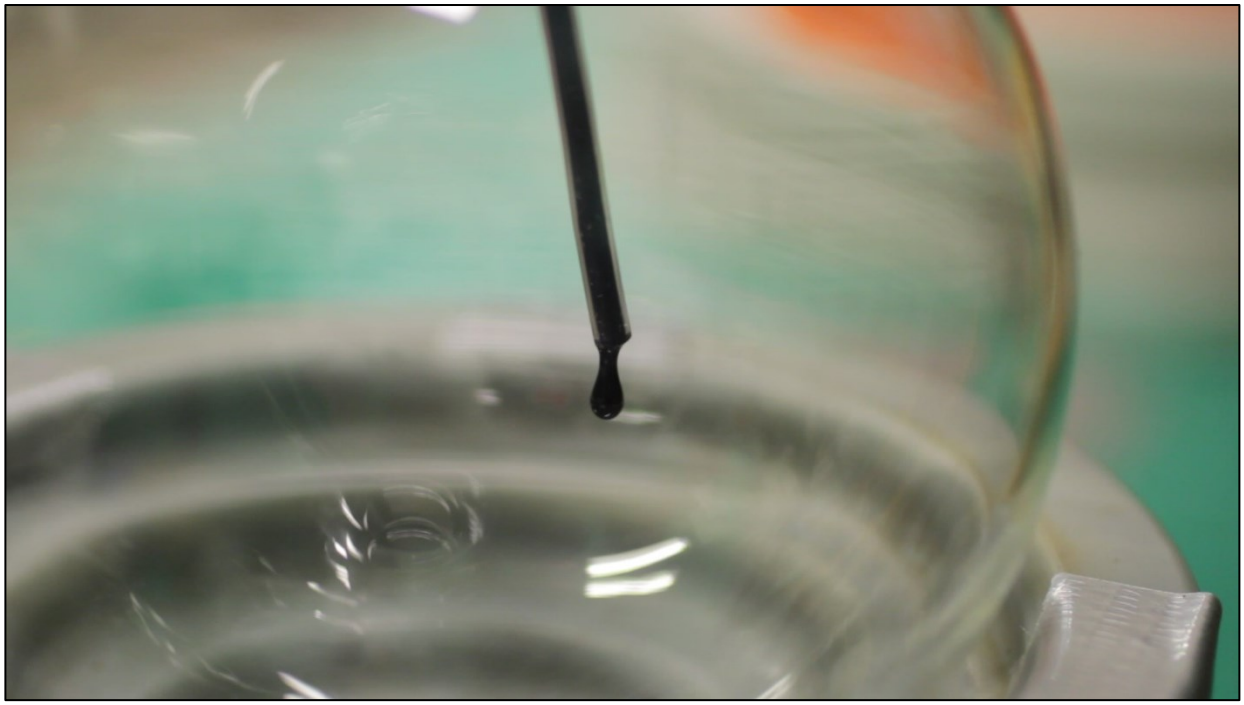

Figure 2.8—Low compressibility produced oil.

Figure 2.9—Foamy oil collected at the production end.

a

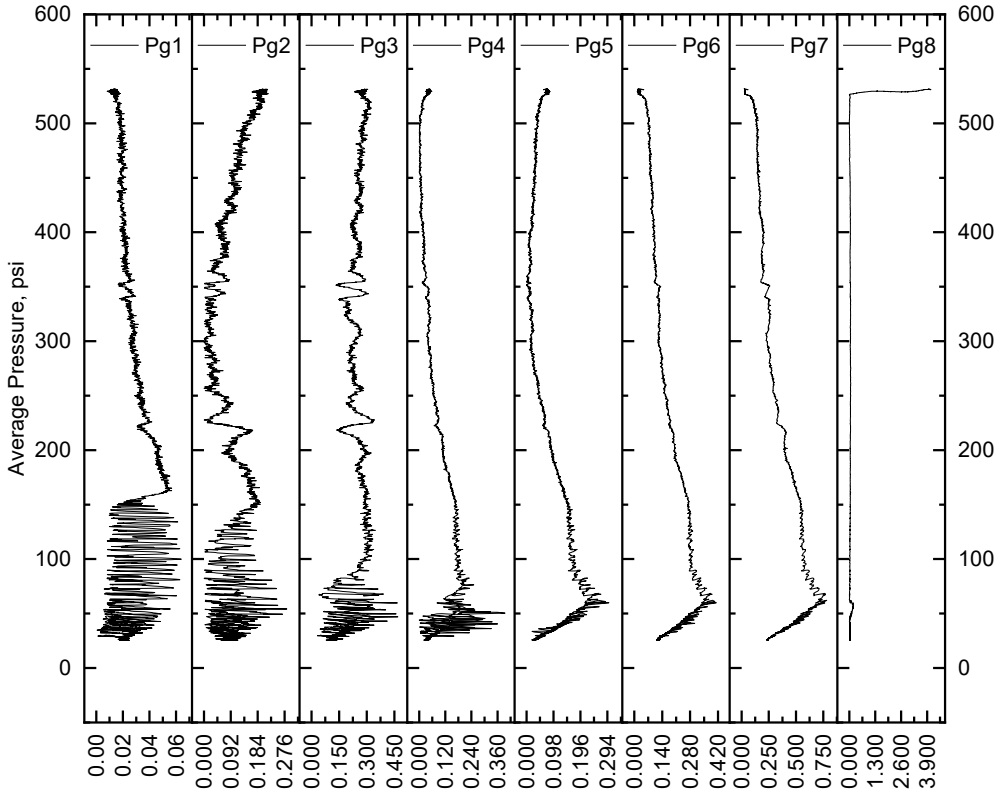
Pg1
Pg2
Pg3
Pg4
Pg5
Pg6
Pg7
Pg8
Average Pressure, psi
0
100
200
300
400
500
600
0.00
0.02
0.04
0.06
0.000
0.092
0.184
0.276
0.000
0.150
0.300
0.450
0.000
0.120
0.240
0.360
0.000
0.098
0.196
0.294
0.000
0.140
0.280
0.420
0.000
0.250
0.500
0.750
0.000
1.300
2.600
3.900

b

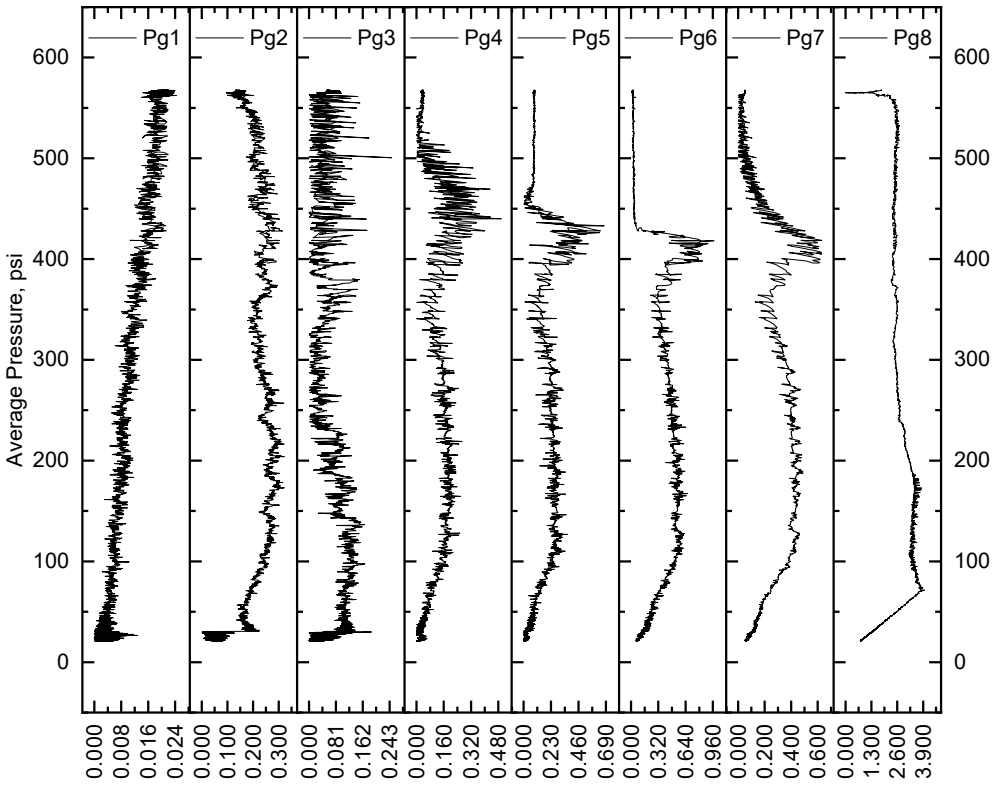
Pg1
Pg2
Pg3
Pg4
Pg5
Pg6
Pg7
Pg8
Average Pressure, psi
0
100
200
300
400
500
600
0.000
0.008
0.016
0.024
0.000
0.100
0.200
0.300
0.000
0.081
0.162
0.243
0.000
0.160
0.320
0.480
0.000
0.230
0.460
0.690
0.000
0.320
0.640
0.960
0.000
0.200
0.400
0.600
0.000
1.300
2.600
3.900

c

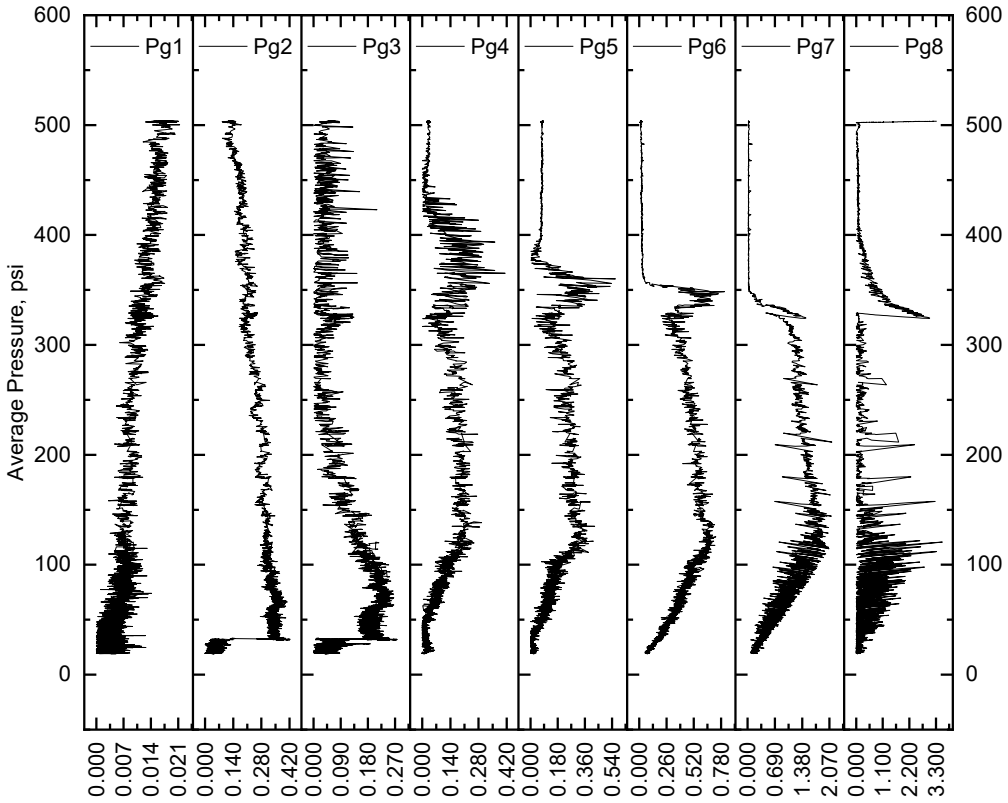
Pg1
Pg2
Pg3
Pg4
Pg5
Pg6
Pg7
Pg8
Average Pressure, psi
0
100
200
300
400
500
600
0.000 0.007 0.014 0.021
0.000 0.140 0.280 0.420
0.000 0.090 0.180 0.270
0.000 0.140 0.280 0.420
0.000 0.180 0.360 0.540
0.000 0.260 0.520 0.780
0.000 0.690 1.380 2.070
0.000 1.100 2.200 3.300

d

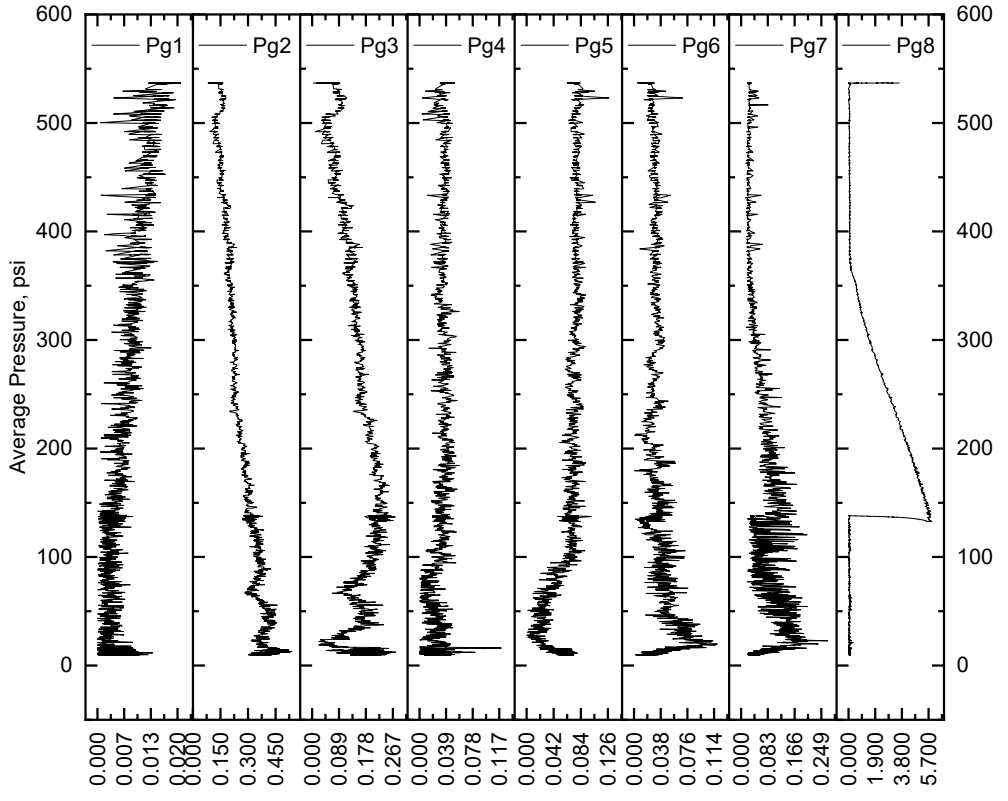
Pg1
Pg2
Pg3
Pg4
Pg5
Pg6
Pg7
Pg8
Average Pressure, psi
0
100
200
300
400
500
600
0.000 0.007 0.013 0.020
0.000 0.150 0.300 0.450
0.000 0.089 0.178 0.267
0.000 0.039 0.078 0.117
0.000 0.042 0.084 0.126
0.000 0.038 0.076 0.114
0.000 0.083 0.166 0.249
0.000 1.900 3.800 5.700

e

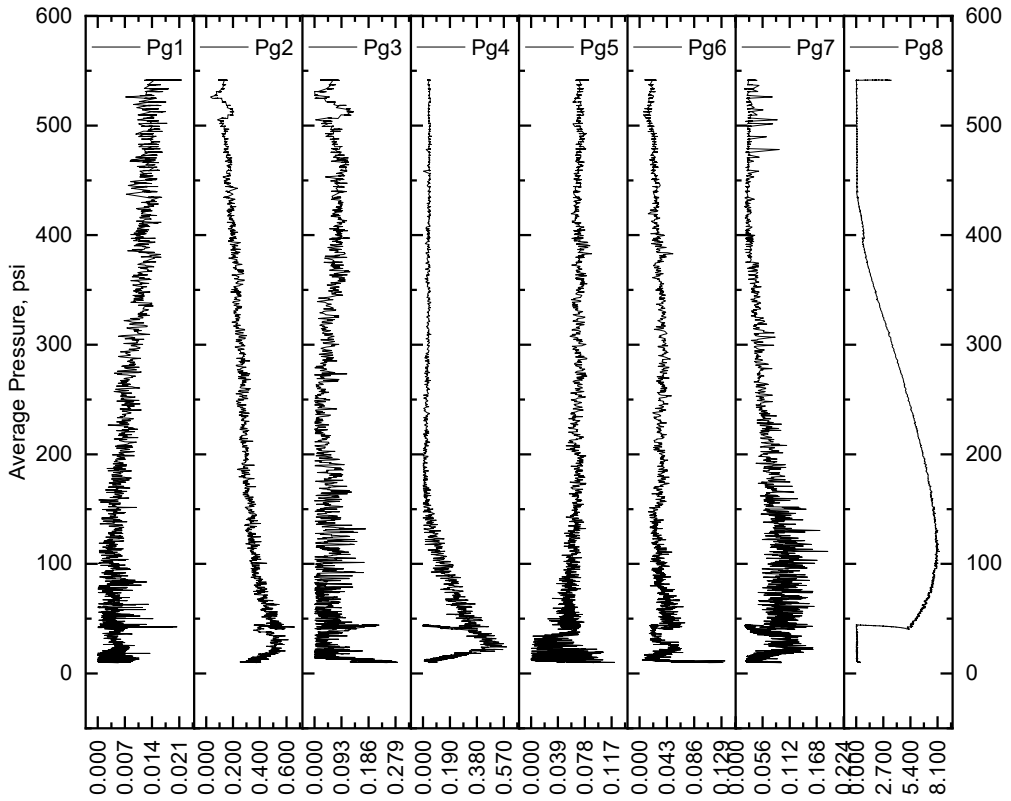

Figure 2.10—Pressure gradients for cycles 1 – 5 (a-e) for Test #1.

a

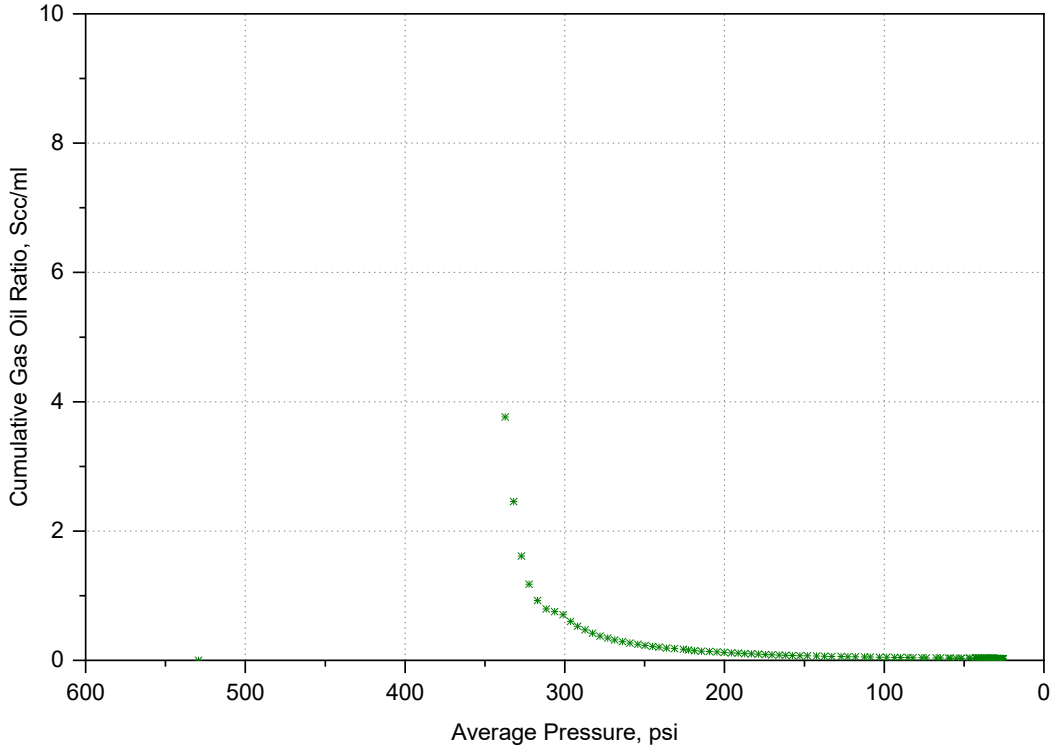

b

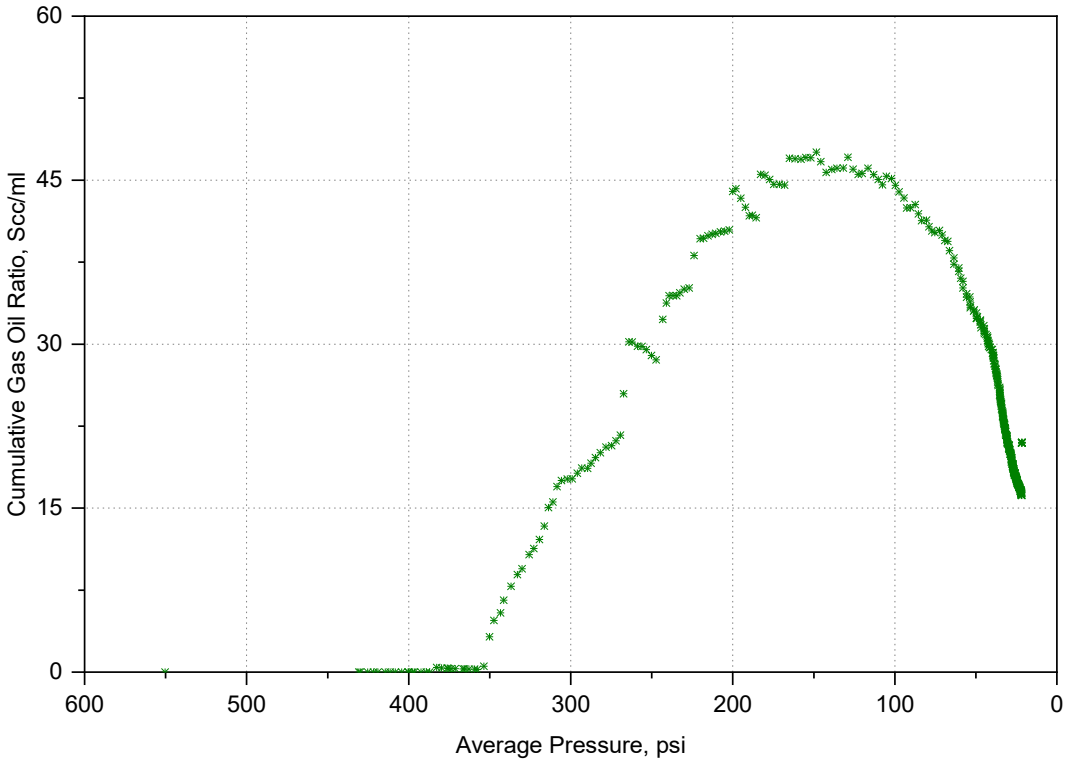
60
45
30
15
0
Cumulative Gas Oil Ratio, Scc/ml
600
500
400
300
200
100
0
Average Pressure, psi

c

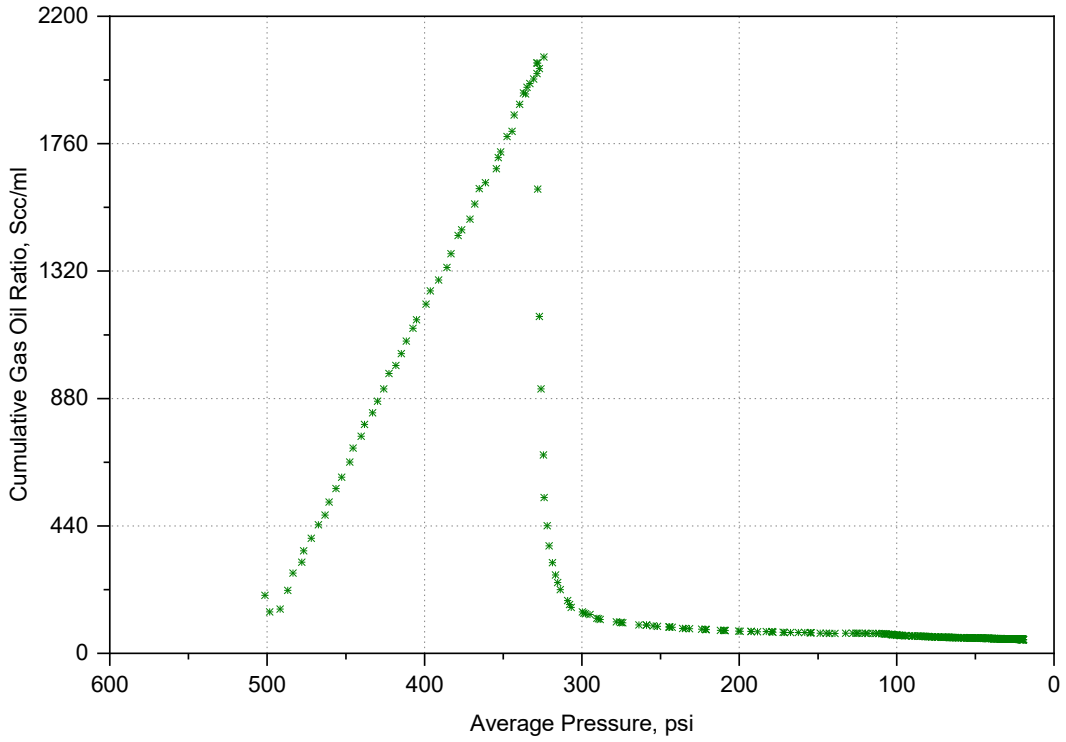
2200
1760
1320
880
440
0
Cumulative Gas Oil Ratio, Scc/ml
600
500
400
300
200
100
0
Average Pressure, psi

d

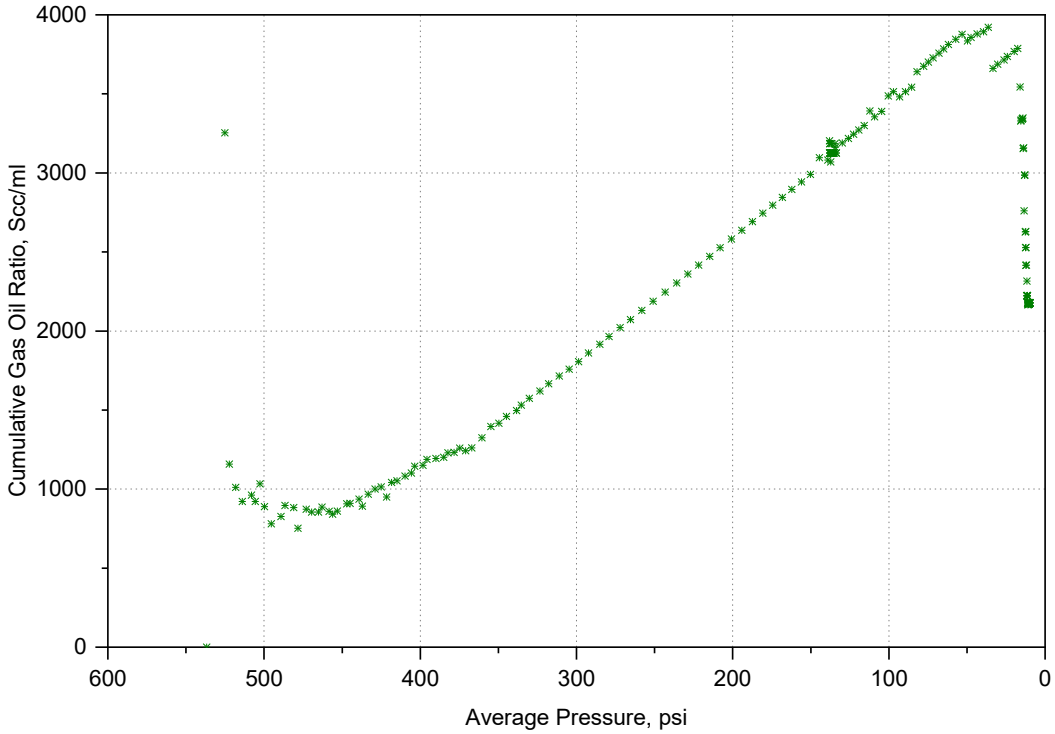

e

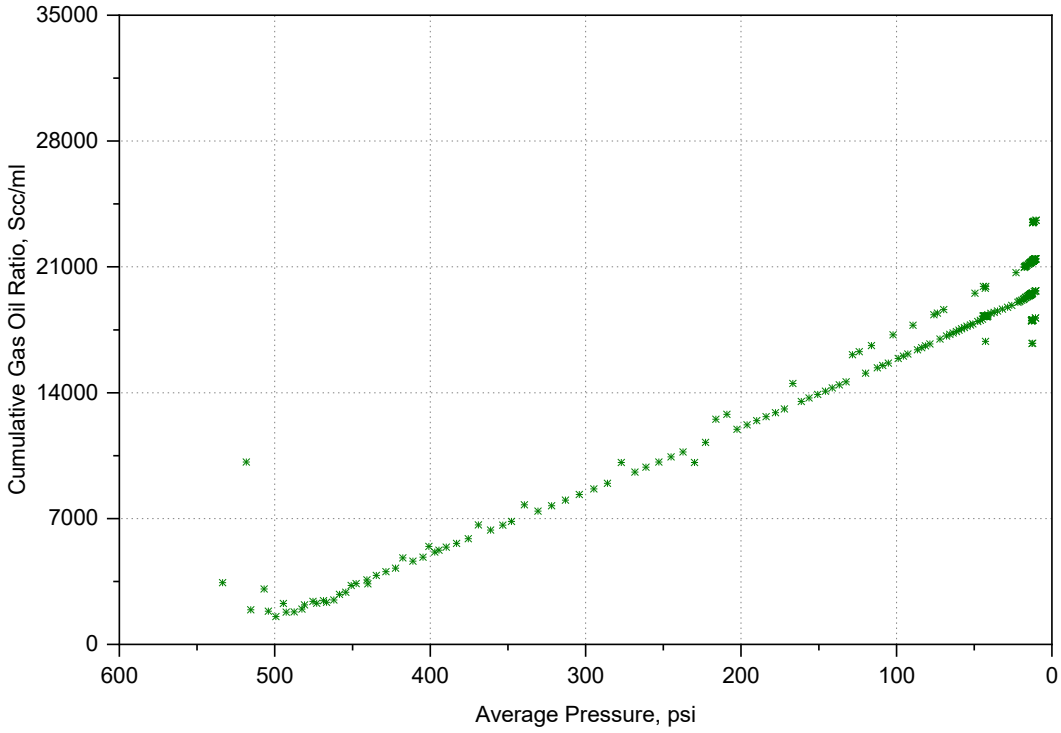

Figure 2.11—Cumulative gas-oil ratios for cycle 1 – 5 (a-e) for Test #1.

Test #2

The main objective of Test #2 was to evaluate the feasibility of utilizing an even mixture of methane and air as the injection gas. In order to do so, the bubble dynamics of the second and third cycles have been analyzed. The main expectation of performing this test was to obtain a higher amount of bubbles trapped in the heavy oil. To create this scenario, the viscosity of the heavy oil was increased (due to the low oxidation process) so that methane would diffuse and be trapped more efficiently in the oil. Experimental results show that this is the case when the lowest ultimate recovery factors have been observed, i.e. the less efficient injection strategy. In the second cycle, Fig. 2.12a shows an early and continuous production of gas, with no presence of heavy oil production as pressure is constantly decreased. As can be seen, oil production starts at a pressure of 300 psi, further confirmed by the cumulative gas oil ratio results, which is basically until the pressure in the system reaches around 300 psi. However, at this stage, stable foamy oil is formed as indicated by good pressure maintenance (Figs. 2.13 and 2.14). Naturally, once the foamy oil is driven out of the sandpack, the pressure difference in the system increases due to the enlargement of the trapped bubbles.

In the third cycle, the amount of early gas produced was much higher. A higher amount of gas had been injected, but also the gas found a path for channeling, resulting in leftover gas that did not diffuse into the oil flowing directly to the producing end, of which is due to the high mobility ratio. Fig. 2.15b indicates that the main driving energy comes from the bubbles trapped in the previous cycle, where only 38% gas recovery factor has been obtained.

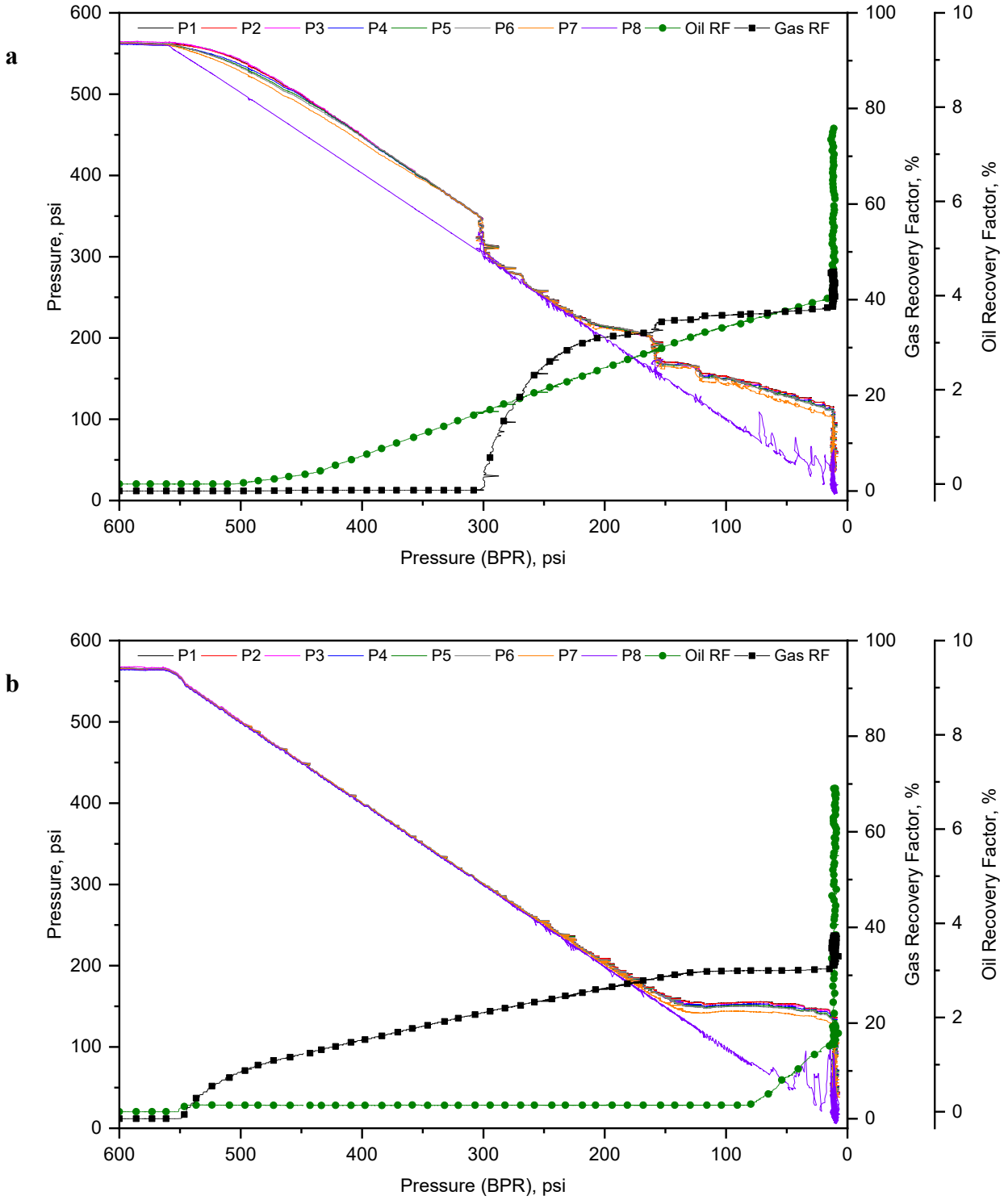

Figure 2.12—Pressure profiles for (a) Cycle 2, and (b) Cycle 3 for Test #2.

a

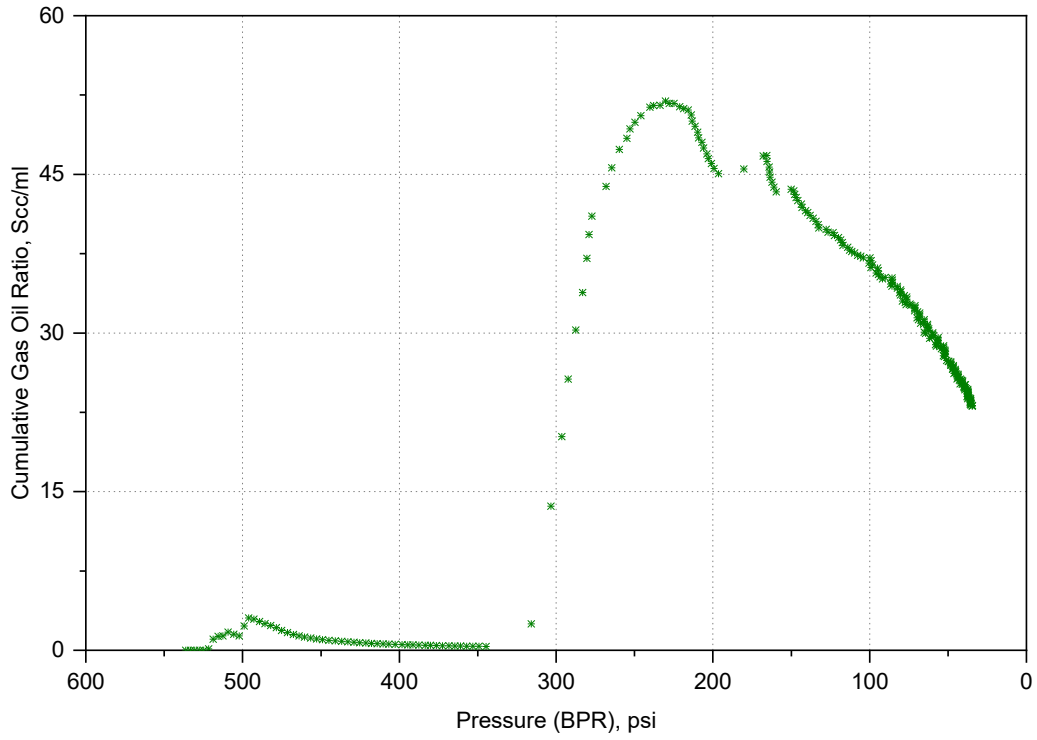

b

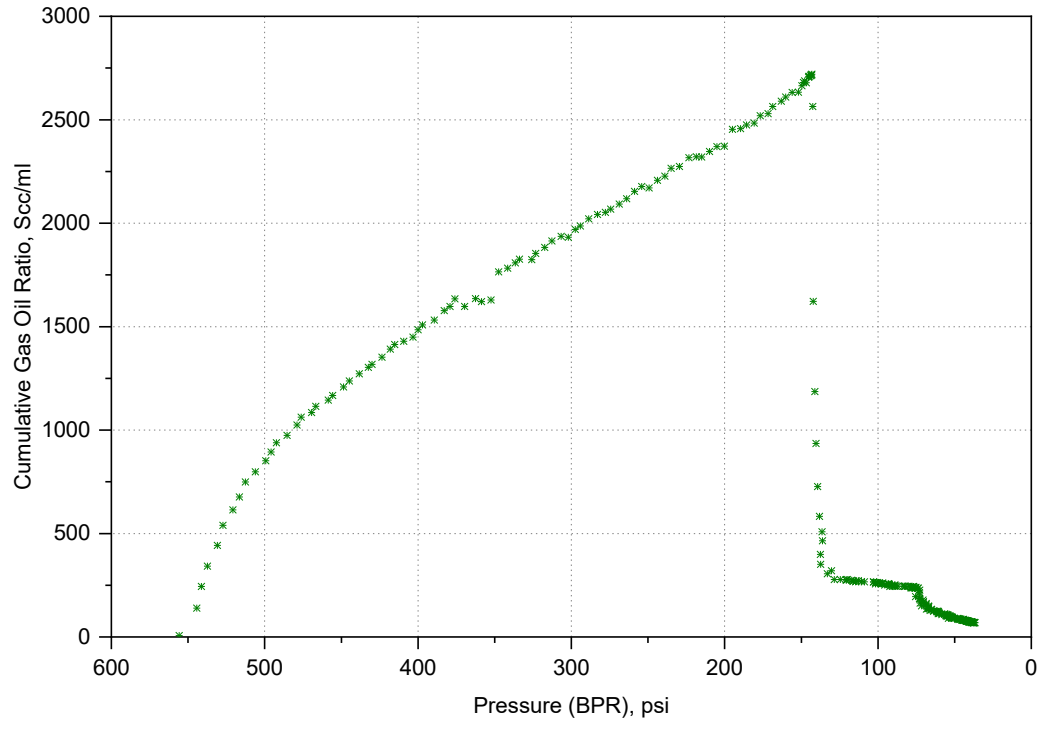

Figure 2.13—Pressure profiles for (a) Cycle 2, and (b) Cycle 3 for Test #2.

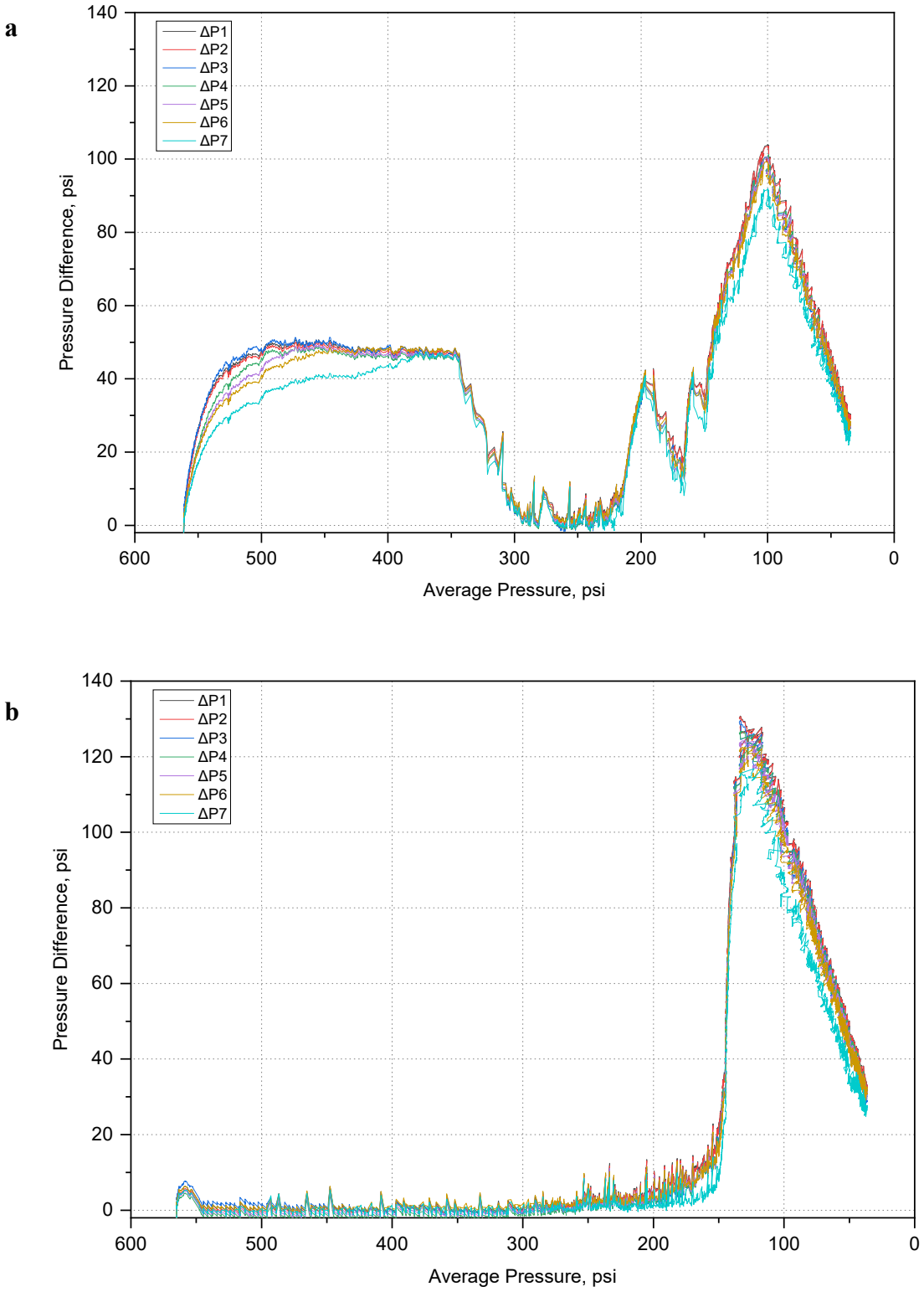

Figure 2.14—Pressure profiles for (a) Cycle 3, and (b) Cycle 4 for Test #4.

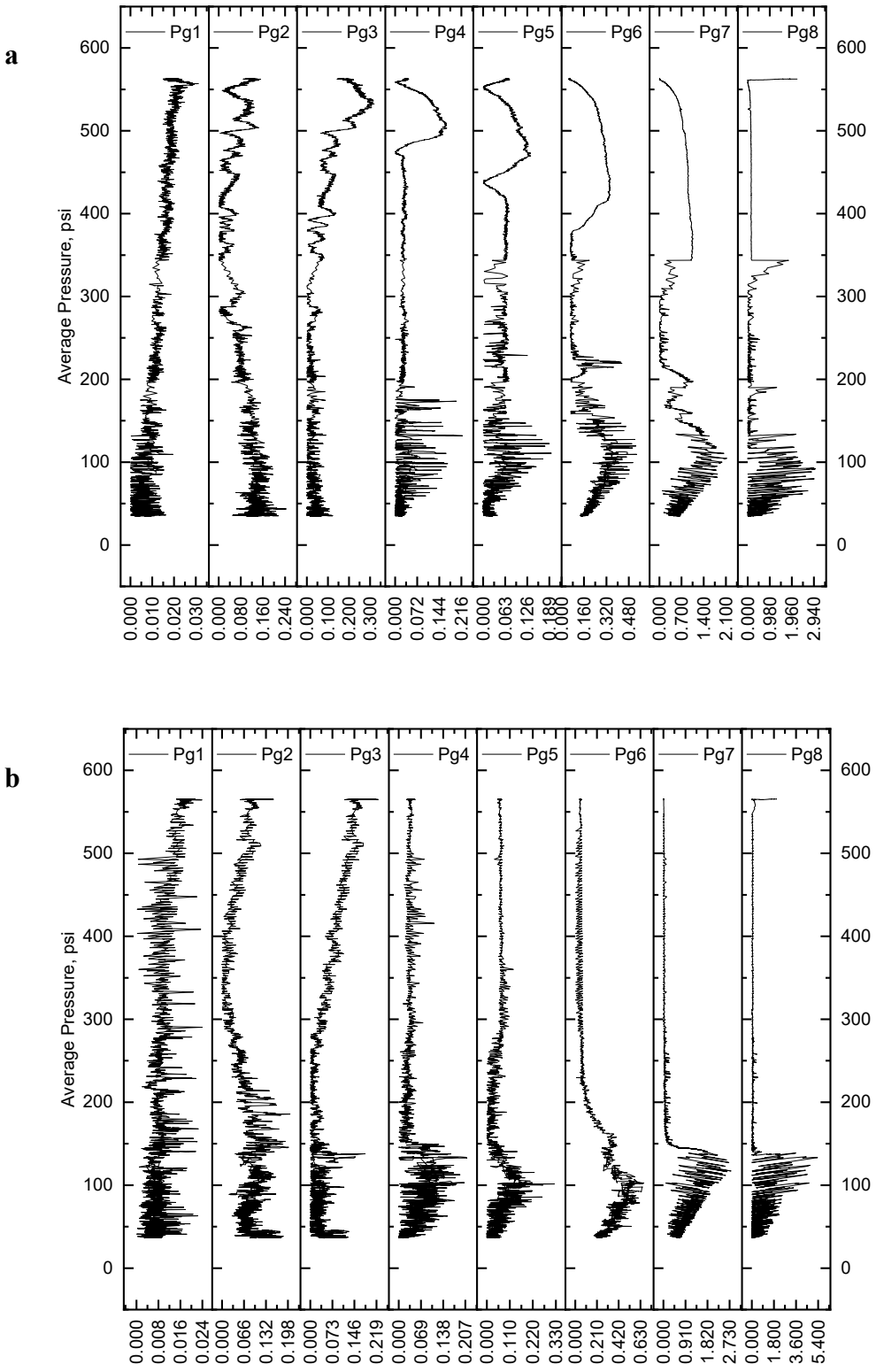

Figure 2.15—Pressure profiles for (a) Cycle 3, and (b) Cycle 4 for Test #4.

Test #3

In order to study injection strategies in the CSI process using air, Test #3 was conducted by alternating the injection gas. The strategy started with air and was followed by methane until five cycles were completed. After, air was injected again, but the main objective of Test #3 was to investigate the effect of methane injection after an air injection phase. The stage where foamy oil forms is very clear in Fig. 2.16; the pressure profiles for the second cycle (methane-based) exhibit a slope deviation, and in the third cycle (air-based), the average sandpack pressure is being reduced along with the pressure in the BPR. Besides early gas production for both cycles (observed in Fig. 2.17), it is important to analyze the pressure differentials (see Fig. 2.18) and pressure gradients (see Fig. 2.19) generated when decreasing the pressure at the producing port. After an air injection cycle, it can be observed that the foaming process starts at a pressure of 400 psi and the pressure is maintained until the end of the producing stage. Not only are high-pressure differentials observed, but also a very high-pressure gradient is generated from the middle of the sandpack to the producing end.

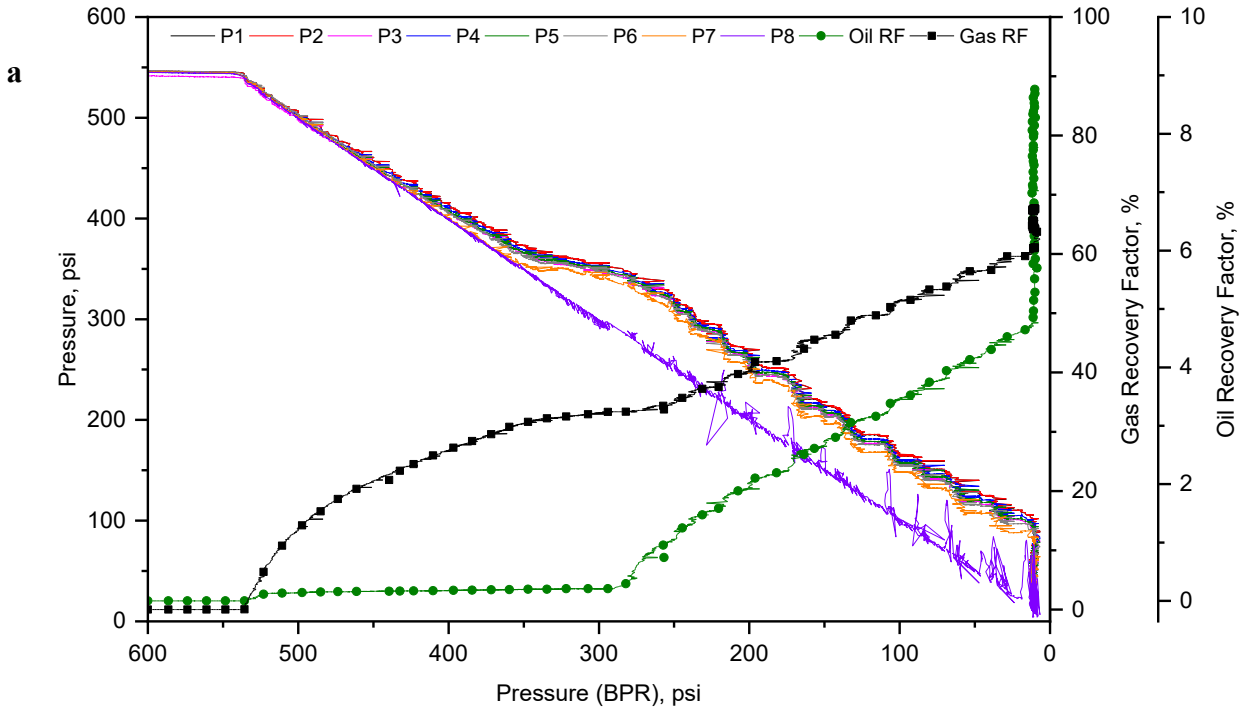

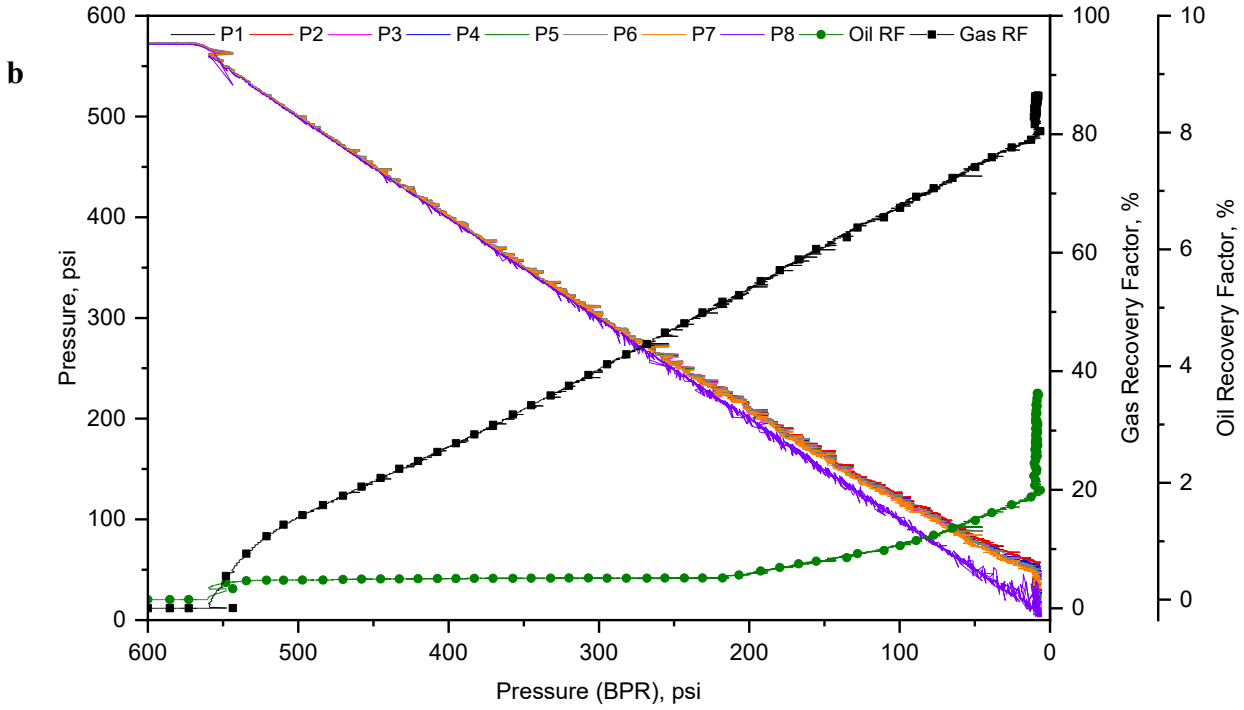

Figure 2.16—Pressure profiles for (a) Cycle 2, and (b) Cycle 3 for Test #3.

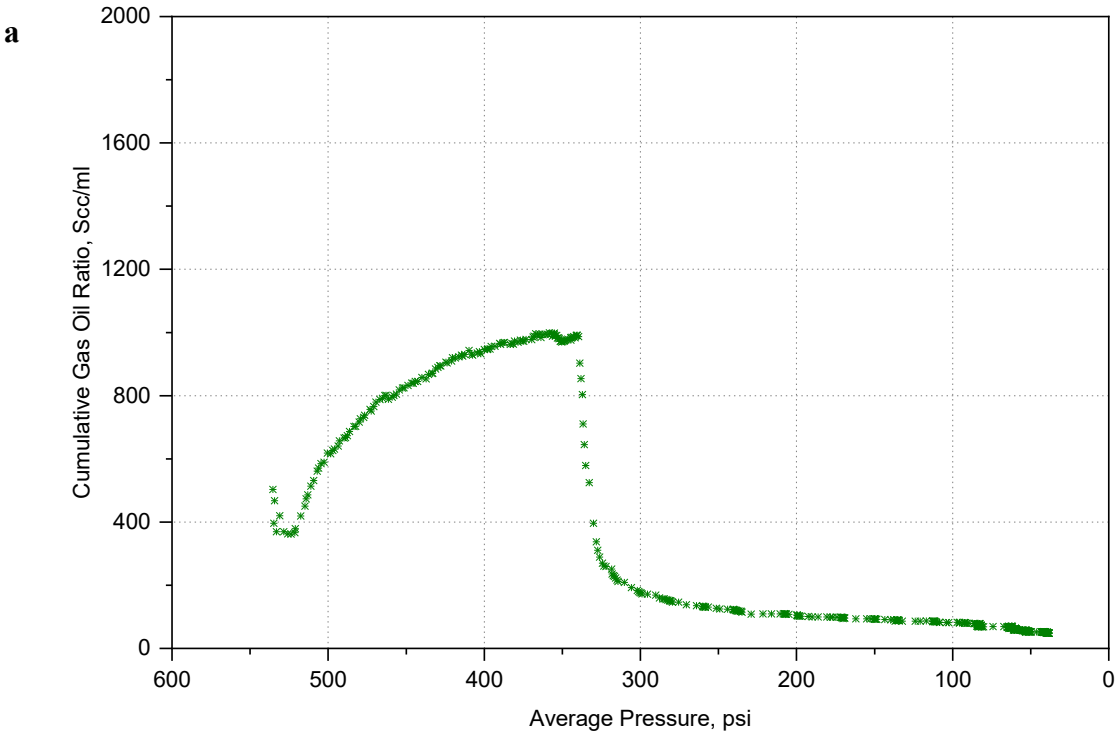

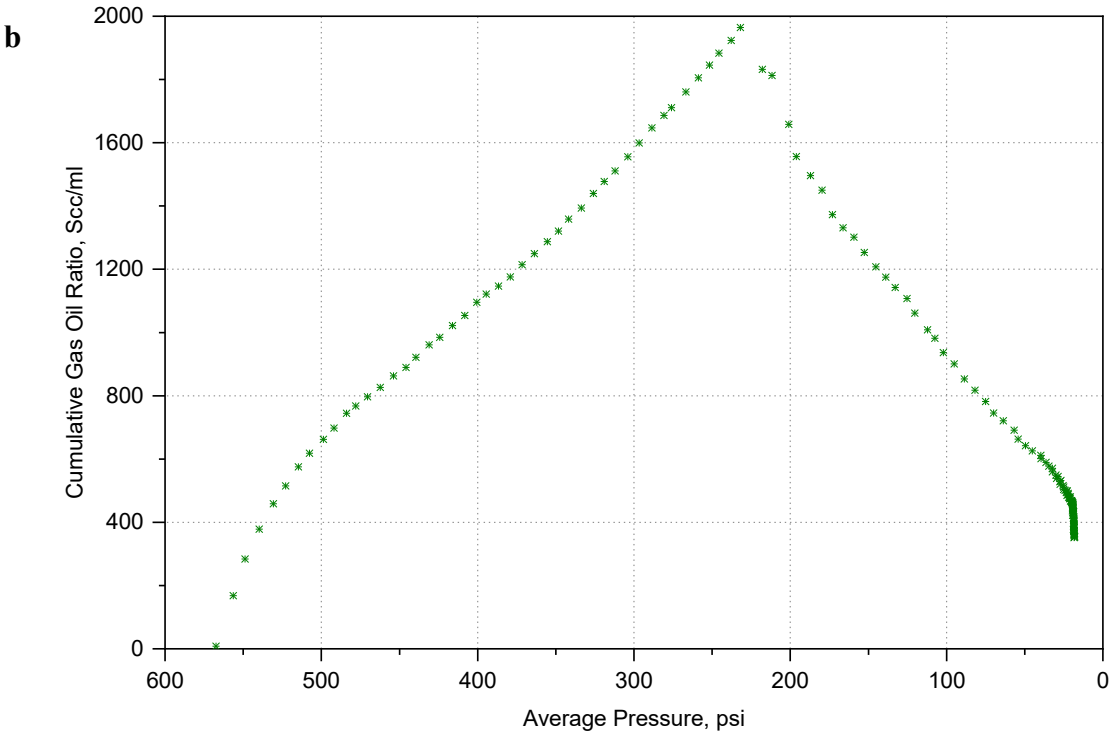

Figure 2.17—Cumulative gas-oil ratios for (a) Cycle 2, and (b) Cycle 3 for Test #3.

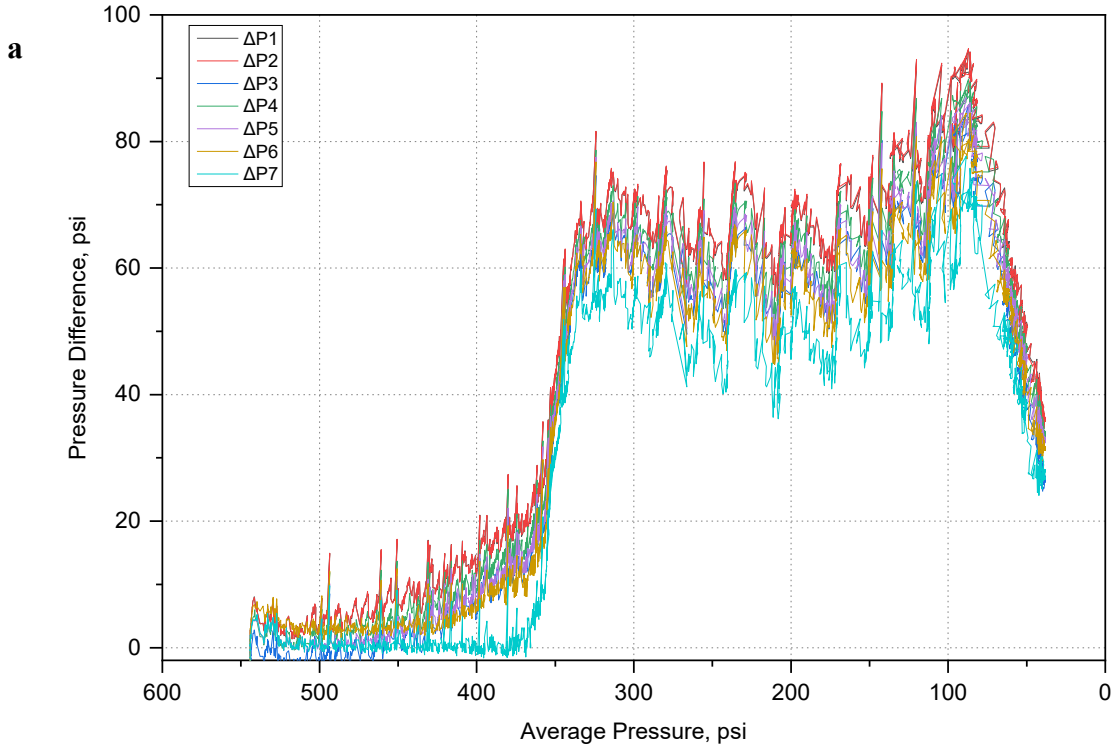

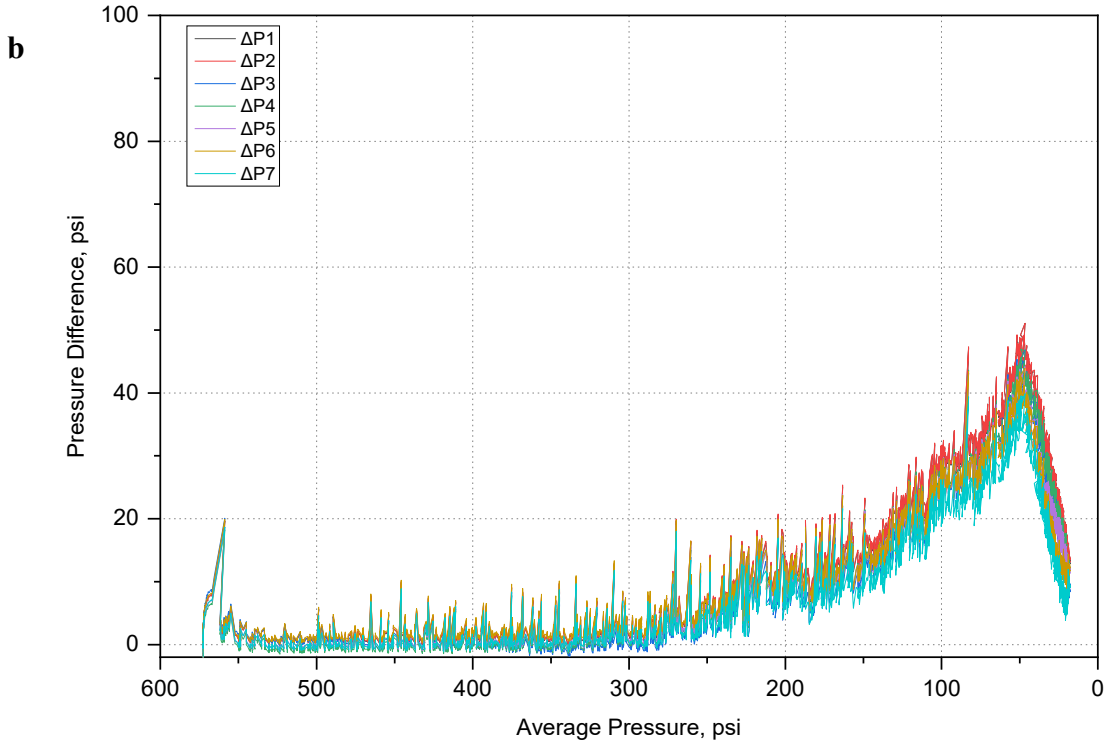

Figure 2.18—Pressure differentials for (a) Cycle 2, and (b) Cycle 3 for Test #3.

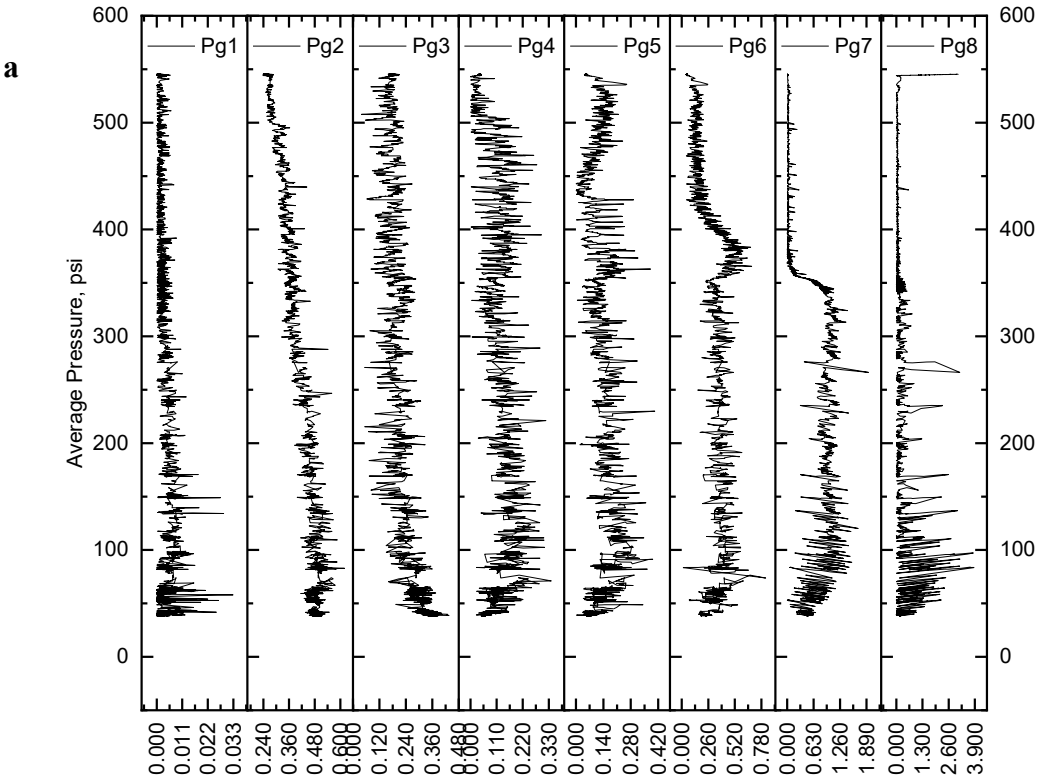

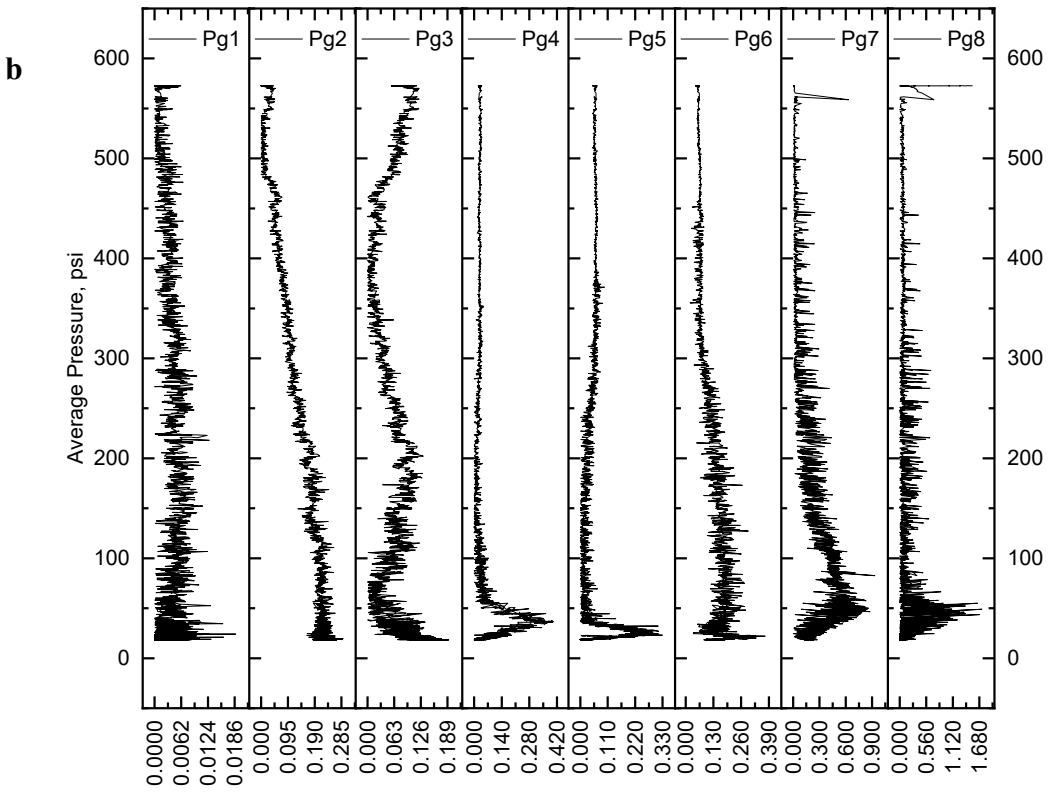

Figure 2.19—Pressure gradients for (a) Cycle 2, and (b) Cycle 3 for Test #3.

Re-pressurizing the system in Cycle 3 by injecting air leads to recovering the remaining foamy oil formed in the previous cycle. Fig. 2.16b shows an early production of gas accompanied by oil production, which starts increasing when a pressure of 200 psi has been reached in the sandpack. This last remaining energy in the sandpack will create the necessary pressure drawdown to promote the flow of the previous formed foamy oil, thus creating pressure maintenance close to the production end and allowing a final recovery factor of 8.77% for this cycle.

Test #4

The main objective of Test #4 was to investigate the effect of the injection technique. Opposed to Test #3, the process was started by injecting methane into the sandpack. Two initial cycles of consecutive methane injection were performed in this test, with the objective of allowing the system formation of foamy oil, as explained before likely to happen in the second cycle. This phenomenon happens after a higher diffusion area has been achieved by producing some oil out of the system during the first cycle. Figs. 2.20a-b show the Test #4 pressure profiles for Cycle 3 and Cycle 4, respectively. Both clearly show that free gas phase and channeling exists, a result of

free gas finding its way out of the system once the pressure in the BPR reaches the average sandpack pressure, thus leading to a fast a linear pressure drop in the system causing high initial cGOR, as seen in Figs. 2.21a-b.

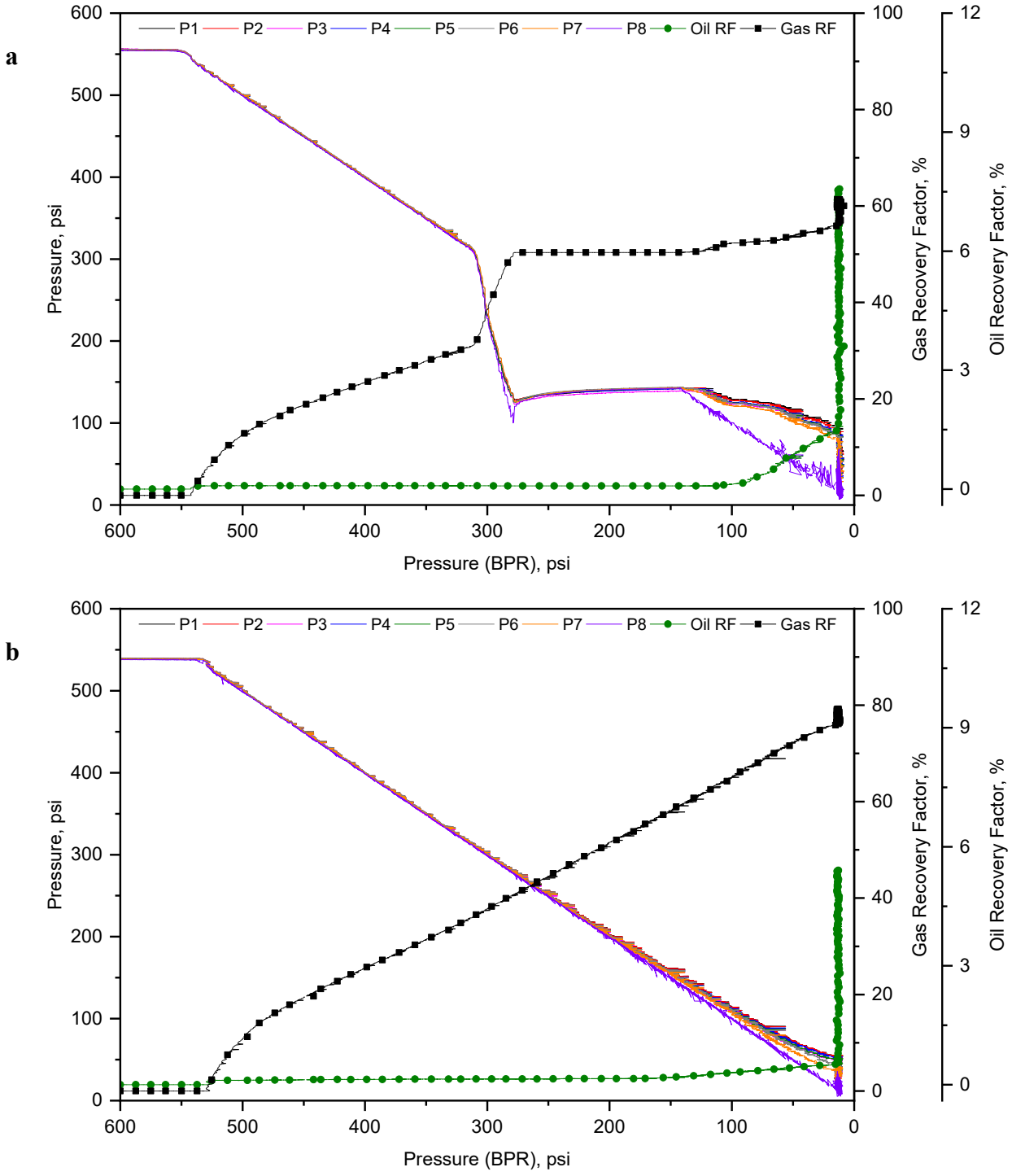

Figure 2.20—Pressure profiles for (a) Cycle 3, and (b) Cycle 4 for Test #4.

During the pressure depletion process in the third cycle, the average pressure in the sandpack is slightly higher than the one in the producing end, generating small pressure differentials that lead to negligible oil production; however, neither efficiently enough for mobilizing the heavy oil nor effective enough for causing bubble nucleation. Although, when the pressure in the system reaches from 300 psi to 150 psi, the foamy oil flow mechanism starts taking place. This can be observed through Figs. 2.22a-b where negative pressure differentials (the pressure in the system is lower than the one in the BPR) and high-pressure gradients (see Figs. 2.23a-b) are formed. During this period of bubble nucleation and growth, good pressure maintenance can be observed in the pressure profile, due to foamy oil flow within the sandpack. Once the pressure in the system has reached 150 psi, foamy oil starts being produced and causing higher pressure differentials. During this process, the cGOR decreases as more oil start being pulled out of the sandpack.

In the entire depletion process during the fourth cycle, the average pressure in the sandpack is slightly higher than the pressure in the producing end, and the oil is mainly driven out due to the initial pressurization of the system and the remaining gas is trapped from the previous cycle.

a

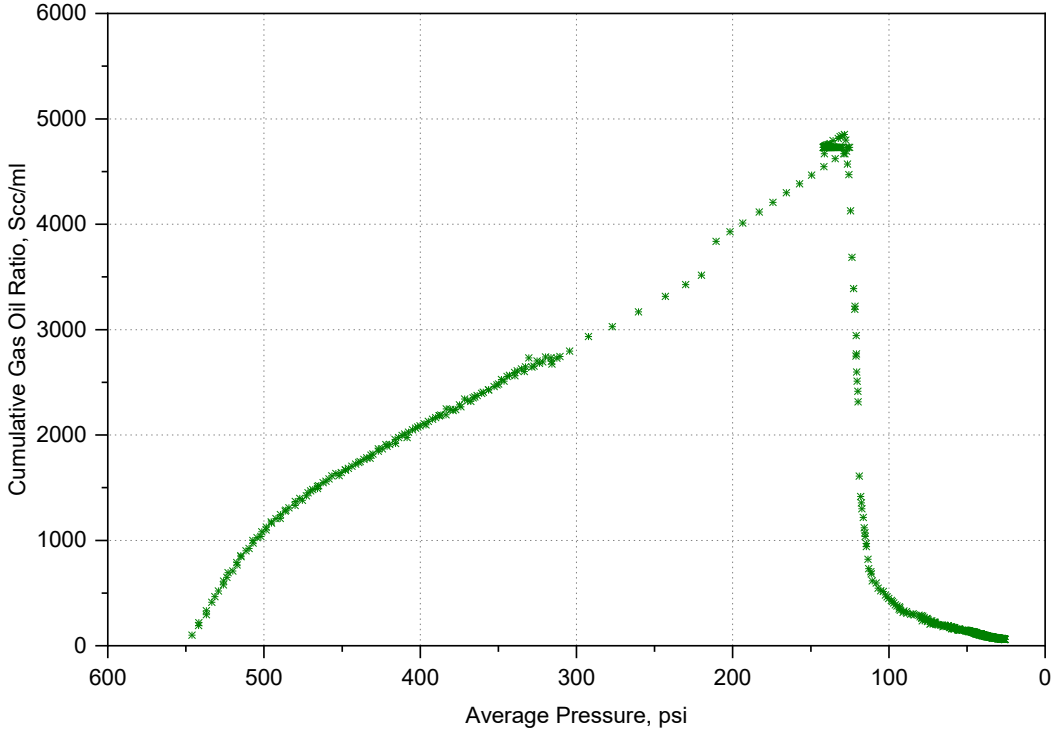

b

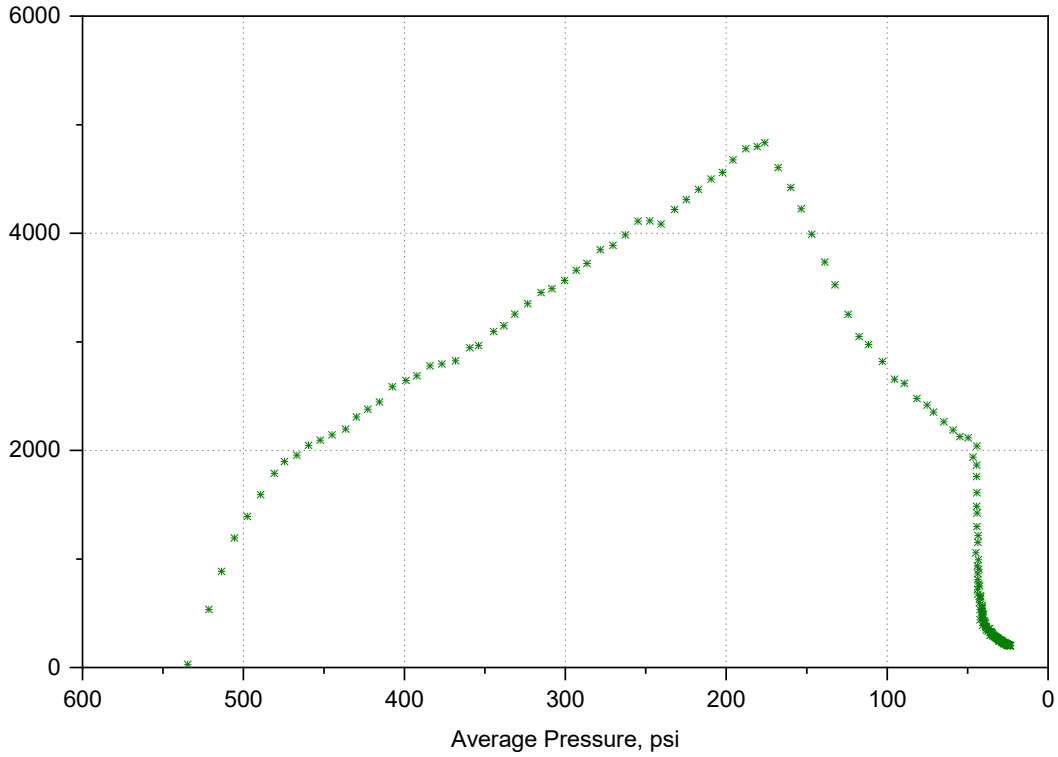

Figure 2.21—Pressure profiles for (a) Cycle 3, and (b) Cycle 4 for Test #4.

a

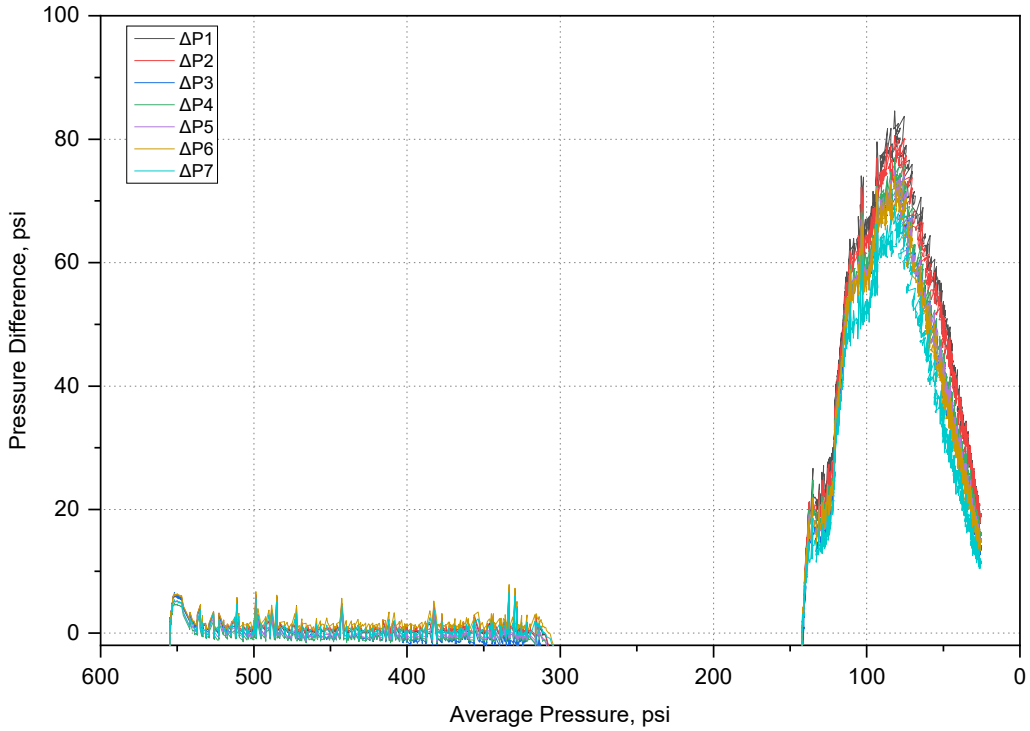

b

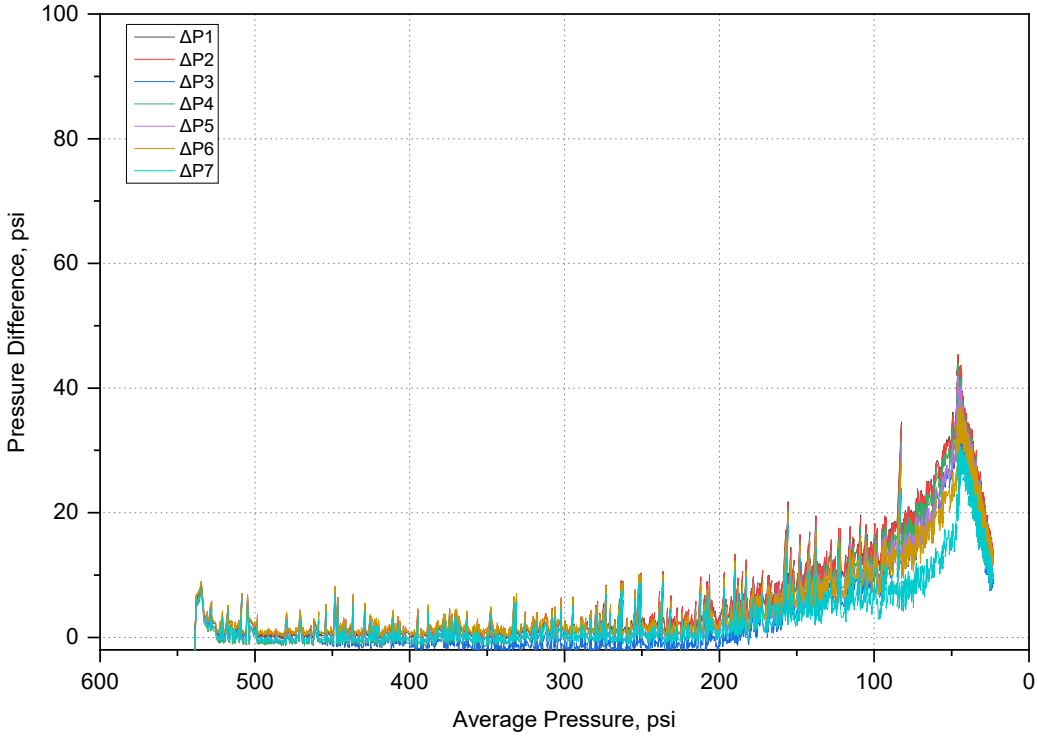

Figure 2.22—Pressure profiles for (a) Cycle 3, and (b) Cycle 4 for Test #4.

a

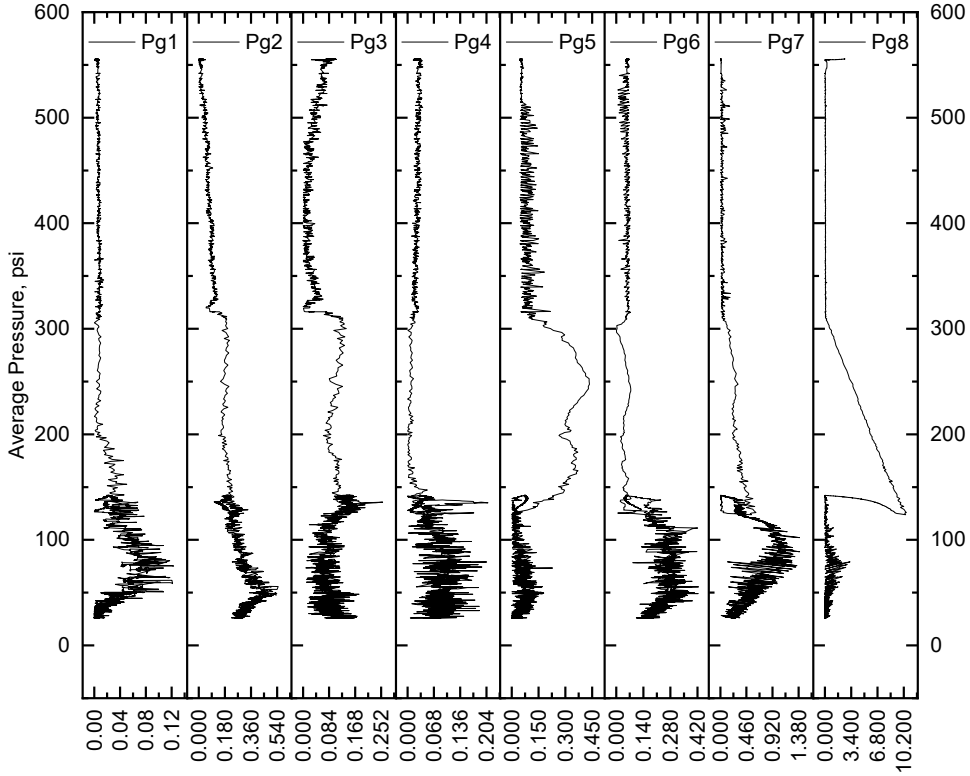

b

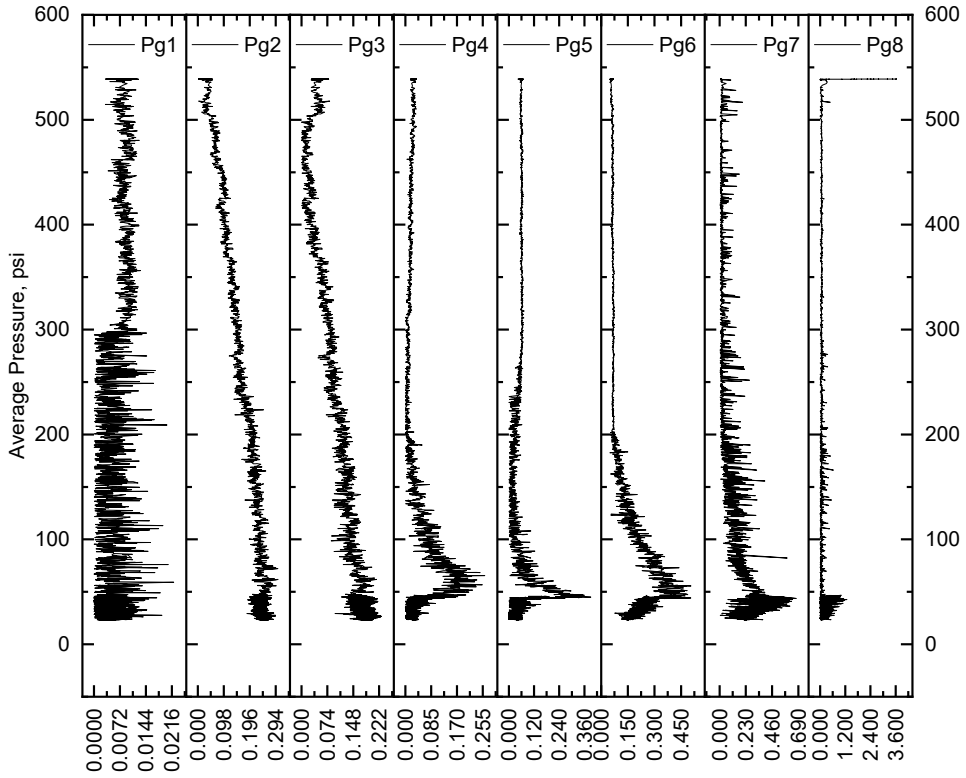

Figure 2.23—Pressure profiles for (a) Cycle 3, and (b) Cycle 4 for Test #4.

2.5 Discussion

Fig. 2.24 depicts the final heavy oil recovery factor in each test compared with the ratio of the total air/methane injected in each test. Under different gas compositions and injection strategies, the results show that with an alternating injection strategy, starting with either air or methane (Test #3 and Test #4), higher ultimate recovery factors are obtained and the highest ratios of air/methane are utilized. This strategy affects positively to the cost-effectiveness of the process, i.e. the amount of solvent used has been dramatically reduced. Two main effects of using air in the processes can be remarked, (1) air helps to pressurize the system, generating the same pressure drawdown with a smaller quantity of solvent and (2) air tends to increase the heavy oil viscosity due to low temperature oxidation, facilitating the formation of foamy oil and enhancing its flow through the porous medium, leading to a higher recovery factor by enhancing the foamy oil stability.

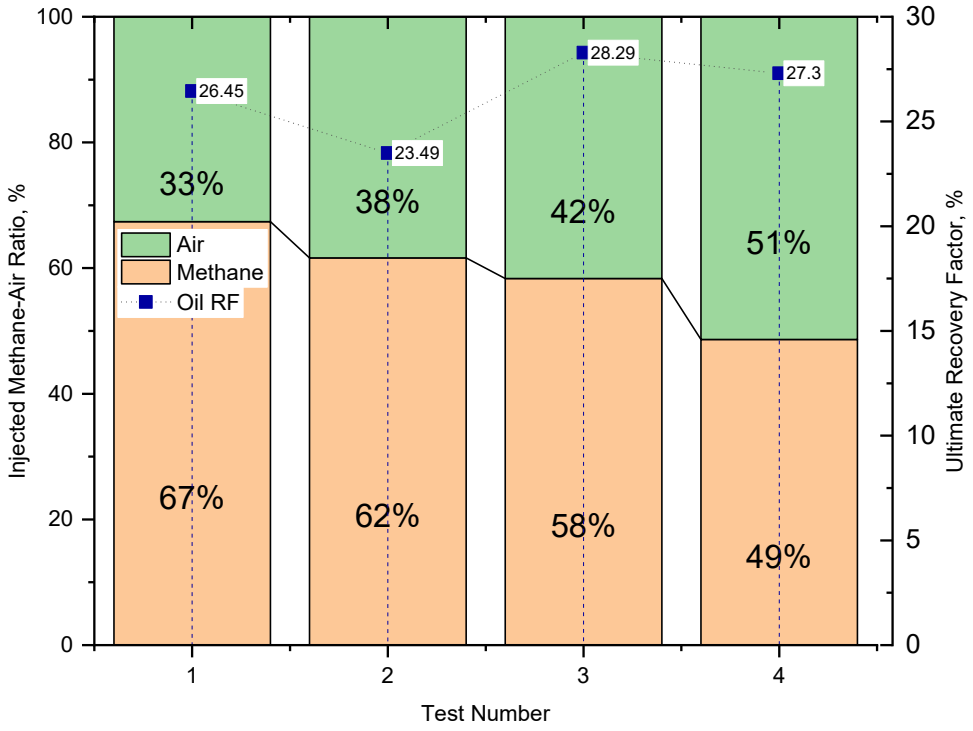

Figure 2.24—Injected methane-air ratio and ultimate recovery factor for each test.

Fig. 2.25 shows the gas utilization for every test. In this study, gas utilization is defined as the stock tank barrel of oil obtained for every thousand standard cubic feet. Experimental results indicate that on average, the first, second, and third cycles had a gas utilization of 515.35 STB/MSCF, 371.47 STB/MSCF, and 325.04 STB/MSCF in the order of precedence. This utilization not only confirms what we explained before—that the most efficient cycles are the first three—but also shows that recoveries as high as 1030 STB/MSCF can be obtained under this technique, making the process both highly cost-effective and suitable for the current low oil price environment. Nevertheless, the upscaling stage for these experiments is not covered in this paper and will be a subject for further studies.

Fig. 2.26 shows the trend for the cumulative gas-oil ratios as the number of cycles is increased. Experimental results indicate a low cGOR for the first three cycles, but when the fourth and fifth cycles are carried out, the cGOR increases steeply. As explained before, getting a higher cGOR does not exactly lead to obtaining a higher heavy oil recovery factor; mainly, it occurs due to gas channeling and slippage in the sandpack holder. Since the amount of gas injected into the sandpack is higher than the void space in the reservoir, low sweep efficiency occurs due to the high mobility ratio and low-pressure maintenance.

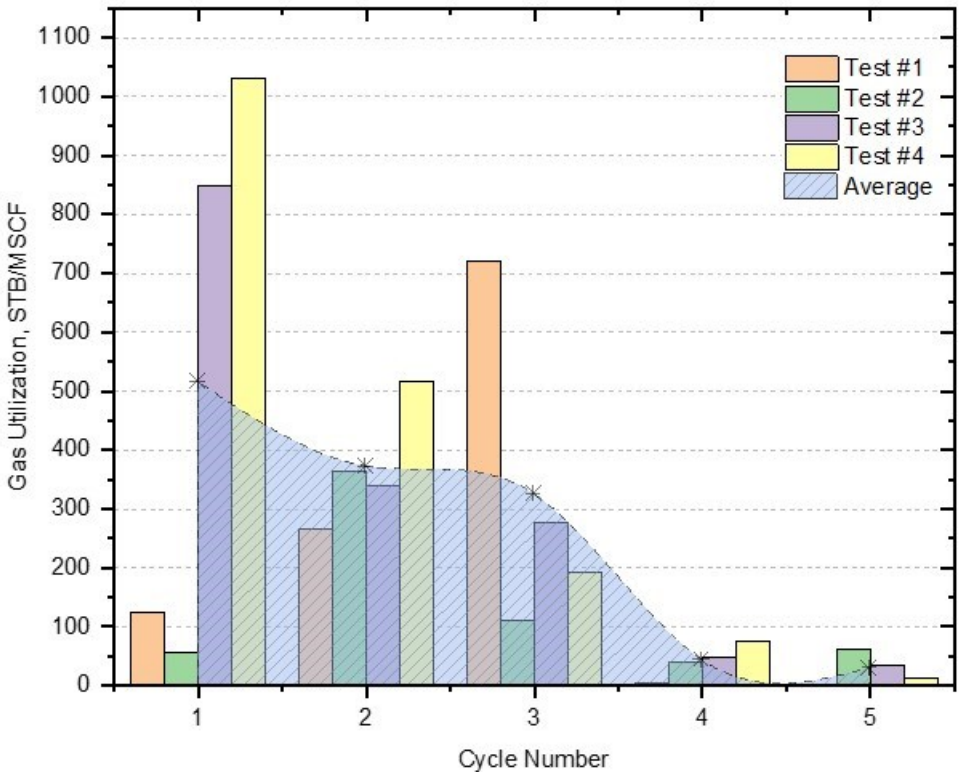

Figure 2.25—Gas utilization for each test.

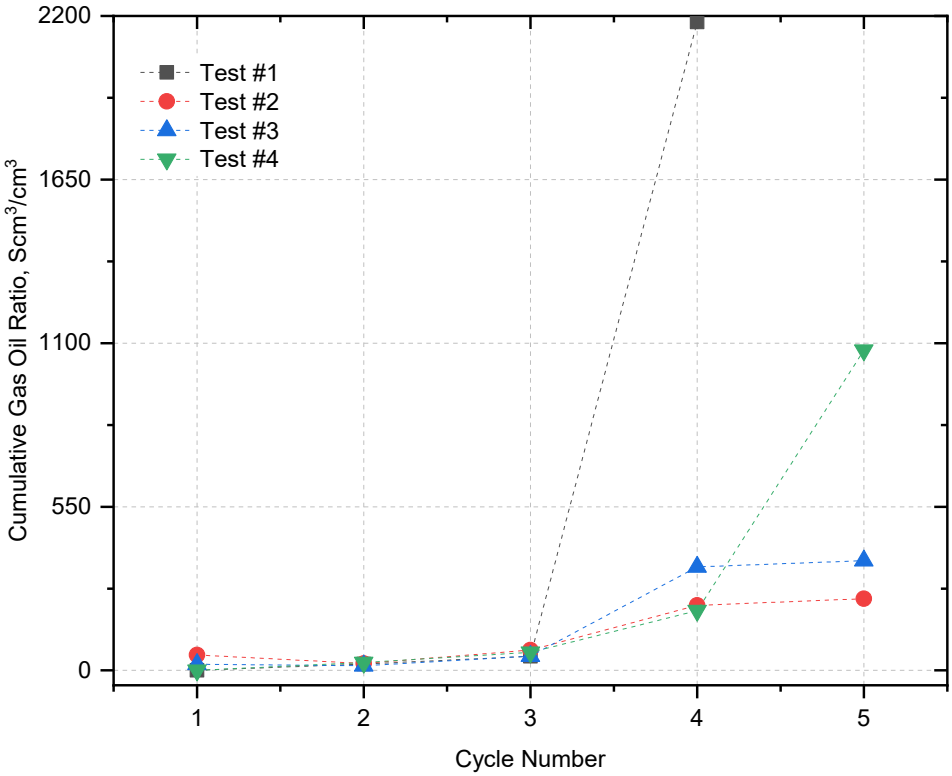

Figure 2.26—Cumulative production gas-oil ratio for each cycle and test.

To obtain a better understanding of the production performance, the heavy oil recovery factor for every cycle in each test and the trend of heavy oil recovery as the number of cycles is increased are analyzed. The average recovery factor per cycle number depicted in Fig. 2.27a, showing that the main contribution to the ultimate recovery factor in every test is made by the second and third cycles. As explained before, in the first cycle the sandpack is entirely saturated by dead heavy oil, making the diffusion process difficult (thereby making the foamy oil formation difficult). This difficulty is due to the small amounts of gas injected and the small diffusion areas; thus, the main mechanism of heavy oil production is the expansion of the injected gas due to the pressure drawdown. However, most of this gas remains trapped due to the high viscosity of the oil, particularly if the gas used is methane, due to its good diffusivity in heavy oil. This can be confirmed by the very low cGOR and the small gas recovery factors obtained for the first cycle in all tests. The trend for the cumulative heavy oil recovery factor indicates that still increasing the number of cycles will lead to a higher ultimate recovery factor, however the incremental production after the third cycle is very small, as observed in Fig. 2.27b.

a

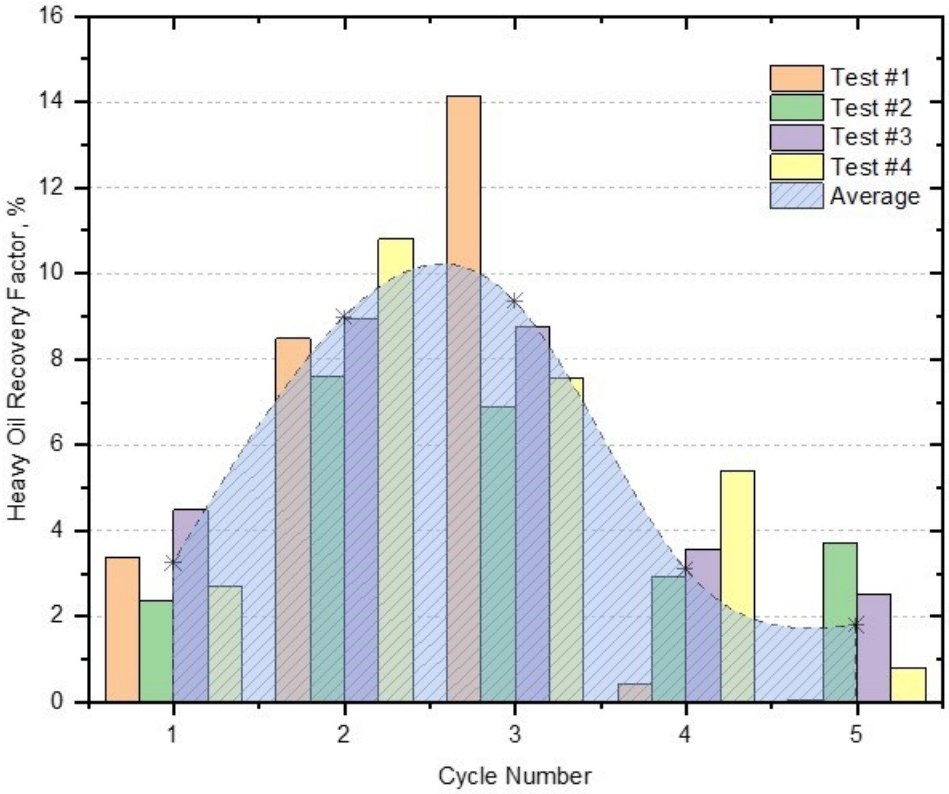

b

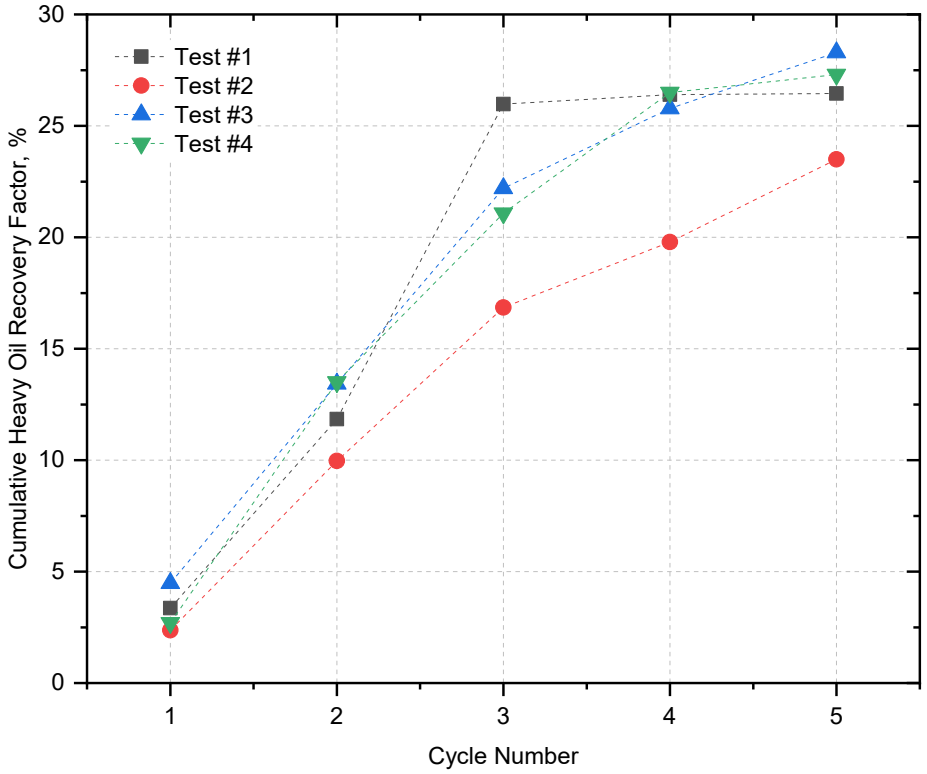

Figure 2.27—(a) Oil recovery factors and (b) cumulative oil recovery factors for Tests 1-4.

2.6 Conclusions

In this study, four tests of a five-cycle-CSI process were performed using a long sandpack saturated with dead heavy oil, with the objective of analyzing the effect of gas composition, number of cycles, and the feasibility of using air as an ameliorative of the foamy oil stability. The following conclusions can be drawn from this research:

1. The viscosity of heavy oil facilitates the formation of foamy oil and air was observed to assist in this matter. The quantity of solvent used in the CSI process was reduced to make the entire process cost-effective. In other words, the use of air significantly reduced the quantity of solvent used since it not only helped increase the heavy oil viscosity and consequently improved foamy oil stability, but it also pressurized the system, generating the same amount of pressure drawdown with a smaller quantity of solvent.

2. Ultimate heavy oil recovery factors as high as 28.29% along with gas recovery factors as high as 69.10% have been obtained, thus indicating the suitability of the methane-air based CSI processes as an enhanced oil recovery technique.
3. The main contribution to ultimate heavy oil recovery factors is made in the first three cycles. In all tests, the last two cycles showed low recovery factors, very high cumulative gas-oil ratios, and fast depletion of the sandpack average pressure.
4. The highest recovery factor was obtained when alternating between air and methane as injection gasses, with three being the optimum number of cycles.
5. Using air with methane (by alternate injection) can reduce the cost of the process maintaining the recoveries obtained by pure methane. This efficiency improvement is obtained by starting the process with air or methane. If more cycles are targeted, starting with methane (Test #4) could be more advantageous in the long run.

Chapter 3

Mechanics of Foamy Oil during Primary and Secondary Recovery of Heavy Oil: A Comprehensive Review

This chapter of the thesis is a revised version of the research paper submitted to the journal *SPE Reservoir Evaluation and Engineering*.

3.1 Preface

Foamy oil flow is commonly encountered in heavy oil production from homogeneous or heterogeneous (after cold heavy oil production with sands—CHOPS) reservoirs. This can be a drive mechanism in the primary production (depletion of naturally methane saturated heavy oil) and secondary stage (gas—primarily methane—injection after primary production). In the former, among other important parameters, pressure depletion rate has been reported to be the most critical parameter to control the process. In the latter, type and amount of the gas (also described as "solvent") and application conditions such as soaking time durations and depletion rates are critical. The cornerstone of the foamy oil behavior relies on its stability, which depends on parameters such as oil viscosity, temperature, dissolved gas ratio, pressure decline rate, and dissolved gas (solvent) composition. Although the process has been investigated and analyzed for different parameters in the literature, the optimal conditions for an efficient process (mainly foamy oil stability) has not been thoroughly understood, especially for the secondary recovery conditions. In this paper, internal and external gas drive mechanisms for foamy performance are reviewed in detail. The optimal conditions of the applications (gas type, amount and combination, injection schemes, and sequences), were compiled and listed for different primary production and secondary recovery stages. Combination of methane with other gases was also discussed to accelerate the process and reduce cost in an effort to improve efficiency. It is reported that combining methane injection with air as a secondary recovery method can save up to 51% of solvent gas.

Keywords: Cyclic Solvent Injection, Foamy Oil Mechanisms, Methane Injection, Core Flooding of Heavy-Oil, Cold Production

3.2 Introduction

Heavy oils are hydrocarbons with low fractions of volatile compounds with low molecular weights and relatively high proportions of high molecular weight compounds of lower volatility. Heavy oil is an unconventional resource classified as conventional heavy oil when the crude viscosity is under 1,000 cP and an API gravity under 21° but higher than 10°, and as unconventional heavy oil when the crude viscosity is at least 1,000 cP and the API gravity is less than 10°. The low mobility of these type of oils is associated with their high viscosities due to a complex assortment of different molecular and chemical compounds such as paraffins and asphaltenes with high melting points and high pour points (Huc 2010; Banerjee 2012; Speight 2016). For heavy oil reservoirs having a thin pay zone (Srivastava et al. 1999) like the ones in Western Canada, thermal methods such as Steam Assisted Gravity Drainage (SAGD) (Denney 1997; Singhal et al. 1998), Cyclic Steam Stimulation (CSS) (Donnelly 2000; Bybee 2008) and Steam Flooding (Hama et al. 2014) do not result in an effective nor economical application due to the high water usage and the severe heat loss. Therefore solvent-based non-thermal recovery methods (Ali 1976) including methods like Vapor Extraction (VAPEX) (Butler and Mokrys 1991; Torabi et al. 2012), Cyclic Solvent Injection (CSI) (Ivory et al. 2010; Torabi et al. 2012) and the huff 'n' puff (HnP) process (Sayegh and Maini 1984; Issever et al. 1993; Alzahrani et al. 2014) were observed to be the most applicable techniques and have attracted special attention from industry and academia.

Numerous unconventional heavy oil reservoirs in Venezuela, China, Albania, Oman, and West Canada under primary production (Smith 1988; Chen and Maini 2005; Maini and Busahmin 2010a; Zhou et al. 2017) showed an unusual behavior like low producing gas-oil ratio (GOR), conversely to the GOR's predicted by conventional black-oil-model simulators (Kraus et al. 1993), good pressure maintenance and high primary production recovery (Maini et al. 1993; Albartamani et al. 1999; Bora et al. 2000; Kumar and Pooladi-Darvish 2002; Turta et al. 2003; Chen and Maini 2005; Li et al. 2012; Chen et al. 2015; Sun et al. 2015). High gas volume fraction was retained in these produced oils, having the form of an oily continuous foam (Sheng et al. 1997). This foaminess observed in samples collected at the wellhead when depleting unconventional heavy oil reservoirs under a solution gas drive mechanism has given rise to the widely used term "foamy oil" (Maini 2001).

Foamy oil flow is commonly encountered in heavy oil production from homogeneous or heterogeneous (after Cold Heavy Oil Production with Sands—CHOPS) reservoirs. To some extent, this driving mechanism in the primary production (i.e. depletion of methane saturated heavy oil) is comparable to the production stage of a CSI process, where the heavy oil is recovered under the solution gas drive mechanism, however, one main issue is that this mechanism is affected by the high gas-oil mobility ratio, which significantly lessens its effectiveness (Jamaloei et al. 2013; Jiang et al. 2014), but, even so, CSI has many more advantages for thin reservoirs when compared to other solvent-based non-thermal recovery methods (Sun et al. 2016). Therefore, CSI is considered an effective technique for increasing the recovery factor (RF) whether as a follow-up process to the CHOPS or for thin heavy oil reservoirs (Dong et al. 2006; Du et al. 2015; Jia et al. 2015).

Previous experimental tests were performed at a laboratory scale for studying the CSI process by using methane (Shayegi et al. 1996; Dong et al. 2006; Qazvini Firouz and Torabi 2012, 2014; Sun et al. 2015; Busahmin et al. 2017; Zhou et al. 2017), propane (Shayegi et al. 1996; Ivory et al. 2010; Bjorndalen et al. 2012; Qazvini Firouz and Torabi 2014), carbon dioxide (Shi and Kantzas 2008; Or et al. 2014; Zhou et al. 2018), and their mixtures (Soh et al. 2016; Rangriz Shokri and Babadagli 2017; Soh and Babadagli 2017; Soh et al. 2018; Basilio and Babadagli 2019) as injection solvents. Among these solvents, methane has been observed to give better foaming characteristics as well as being more advantageous due to its larger availability and economic efficiency (Sun et al. 2015).

3.3 Mechanics of Heavy Oil Displacement by Methane

Cyclic Solvent Injection Process

The CSI process is considered to be an effective follow-up process to CHOPS and it is a very well-known technique for improved oil recovery, consisting of three consecutive stages: (1) the injection stage, (2) the soaking stage and (3) the production stage (Jha 1986; Sheng 2013; Temizel et al. 2017). Generally, light hydrocarbons (e.g. methane and propane) and carbon dioxide are used as injection solvents. The injection stage is the briefest stage, in which the solvent is injected at a very high rate, causing an increment in the pressure of the heavy oil reservoir. The soaking stage is very crucial as it is the stage in which the processes contributing to recovery such as oil swelling

take place. During the production stage, the pressure in the reservoir is released, causing the non-dissolved solvent to be produced as gas phase, resulting in high cumulative gas-oil ratios. The pressure drop in the reservoir is the main producing force causing the foamy oil to be taken out. The heavy oil recovery mechanisms in a CSI process are mainly oil viscosity reduction, surface tension reduction, oil swelling, and foamy oil formation (Das and Butler 1998; Luo et al. 2007; Maini and Busahmin 2010b). The latter being the focus of the present study.

Two main fluid zones in the porous medium with different properties can be differentiated in a CSI process, i.e. gas zone or solvent chamber and the heavy oil zone. The gas zone is mainly dominated by free gas-oil flow, while the heavy oil zone is dominated by the foamy oil flow (Hong et al. 2017). Emphasis should be given to the diffusion coefficient prediction since it is due to this parameter that the injected gas is able to dissolve into the heavy oil by molecular diffusion and enhance the oil recovery.

Foamy Oil Flow

The anomalous behavior observed in many heavy oil reservoirs under primary depletion around the world, where higher recovery factors were obtained when compared to conventional solution gas drive reservoir, was attributed to the foamy oil phenomenon (Wenlong *et al*. 2008). The foamy crude oil is mainly formed as a response to a pressure depletion process (Smith 1988; Sheng *et al*. 1995). The foamy solution gas drive compared to the solution gas drive presents higher recovery factors (5-25%), low gas-oil ratios (GOR), high oil production rate, and gas flows as tiny bubbles dispersed in oil appears as pressure drops. Consequently, researchers suggested that reservoir flow mobility could be improved in the wellbore vicinity when a pressure gradient is established (Sheng *et al*. 1999). Foamy oil generation is mainly based on the behavior of gas, stated in Table 3.1, at any given time in a heavy oil reservoir, as explained by Maini (1996).

Conventional hydrocarbon reservoirs only have a bubble point. However, in foamy hydrocarbon reservoirs, in addition to the bubble point, some authors suggested the existence of a pseudo-bubble point as the pressure point where the gas phase becomes a continuous phase. When these foamy oil reservoirs reach the bubble point, the gas exsolution process commences and gas starts forming a gas-in-oil dispersion due to the nucleation of tiny bubbles which get trapped for a quite extended period of time in the oil due to its high viscosity (Kraus *et al*. 1993; Chen and Maini

2005; Liu *et al*. 2016) improving the oil phase mobility. The bubbles' nature maintains the energy in the reservoir and displaces the surrounding oil to advance in the direction flow. This phenomenon greatly reduces heavy oil viscosity (Hongfu *et al*. 2002) and increases the effective compressibility of the oil phase (Kraus *et al*. 1993). The gas will remain entrained in the foamy oil until the reservoir pressure drops to the pseudo-bubble point (Kraus *et al*. 1993). Hence, foamy oil properties are mainly related to three principal dynamic processes of the evolution of gas bubbles during the flow of foamy oil: (1) bubble nucleation, (2) bubble growth, (3) bubble trapping—mobilization, and (4) bubble disengagement and coalescence/breakup, which occur simultaneously (Maini and Busahmin 2010b). Figure 3.1 shows a general gas evolution process in heavy oil: (1) Pressure P1 is greater than or equal to the gas saturation pressure; (2) as pressure decreases to P2, i.e. bubble point pressure, tiny bubbles start nucleating in the system and remain trapped due to the high viscosity; (3) P3, is not a specific pressure point but a range of pressures between the bubble point and the pseudo-bubble point where gas bubbles grow due to mechanical expansion, this phase is very important since during this period gas bubbles will maintain the reservoir pressure, and start mobilizing the oil in the direction of flow, and where the foamy oil mechanism has its largest efficiency; and (4) as pressure further decreases, pseudo-bubble point is reached, and gas bubbles coalesce at a high rate, breaking up and giving place to the free gas phase formation, it is when the foamy oil mechanism *per se*, has finished.

Despite the numerous field observations, the specific parameters affecting foamy oil stability is still not thoroughly understood, but it is known it depends on pressure, local pressure gradients, and time. For instance, in some non-aqueous foams created by pressure dropping, the froths initially formed are stable until they are stretched too far by additional evacuation, upon which they collapse (Brady and Ross 1944).

The understanding of foamy oil stability is being extensively studied, and it has greatly improved over time. Among many authors, Sheng *et al*. (1995), Akin and Kovscek (2002), Tang *et al*. (2006), Adil and Maini (2007), Wong and Maini (2007), Ivory *et al*. (2010), Li *et al*. (2012), Liu *et al*. (2016), and Abusahmin *et al*. (2017) performed laboratory experiments to study foamy oil stability and the influence of different parameters as well as the relationship with porous media on recovery factors by performing pressure depletion tests on foamy oil flow using a sandpack system. They agreed and demonstrated through experimental observations that foamy oil stability is positively

affected by higher oil viscosities, asphaltenes content, larger amounts of dissolved gas, high-pressure depletion rates, significant initial GOR, and larger initial oil volume.

Table 3.1—Gas behavior in foamy Oil (Maini 1996).

Phase	Behavior
(1) Dissolved gas	Thermodynamically, part of the liquid phase
(2) Dispersed gas	Thermodynamically, separate phase
	Hydrodynamically, part of the liquid phase
(3) Free gas	Flows independently (certain gas still remains trapped)

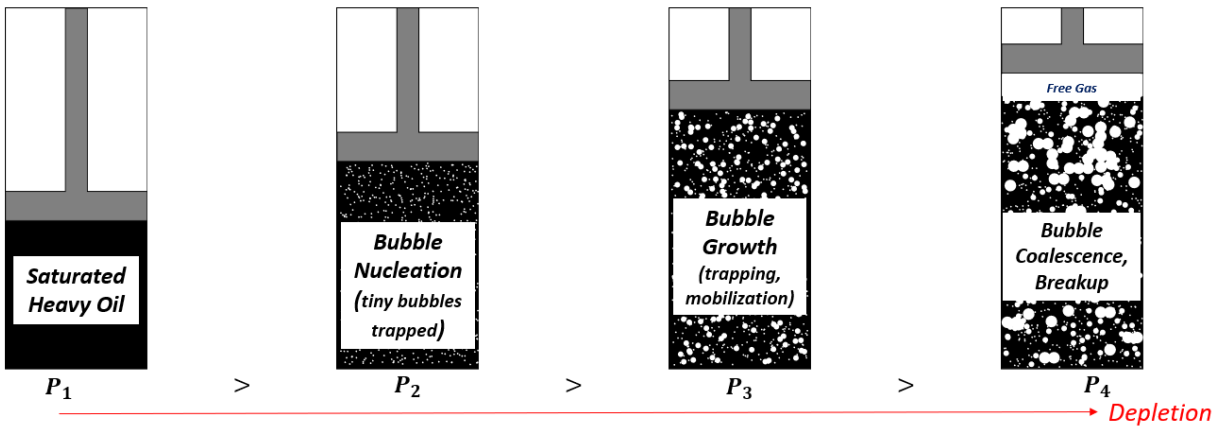

Figure 3.1—Bubble dynamics during foamy oil formation.

Effect of Temperature

Zhang *et al*. (1999) studied the effect of temperature on the stability of foamy oil. They run one-dimensional sand-pack depletion experiments at several different temperatures ranging from 22°C to 175°C. Isothermal depletion tests showed that the highest recovery factor is obtained at an intermediate temperature, 70°C for these tests. Hence, leading to the idea that higher temperatures will affect negatively to the positive effects of higher oil viscosities.

Effect of Oil Viscosity

Foamy oil stability decreases with the reduction of oil viscosity (Sheng 1997) since it affects the gas coalescence dynamics. At early stages, coalescence occurs due to the bubble growth mainly caused by the exsolution of the dissolved gas, as high oil viscosity dwindles bubble growth by slowing down the gas diffusion. At later stages, bubble growth and thereafter coalescence is

pressure-driven, governed by expansion and oil drainage, as high oil viscosity diminishes the rate of oil drainage and consequently bubbles coalescence (Maini 1996; Bora *et al*. 2000; Arora and Kovscek 2003; George *et al*. 2005; Peng *et al*. 2009).

Effect of Pressure Depletion Rate

The effect of pressure depletion rate has been extendedly studied and it is widely agreed that a greater depletion rate is beneficial to improve the effect of foamy oil, since higher depletion rates induce large pressure gradients, increasing the capillary number which results in a more frequent bubble generation and breakup reducing the probability of bubble coalescence and the formation of a continuous gas phase (Ostos and Maini 2005). Zhou *et al*. (2016) showed the existence of a critical pressure depletion rate in a methane-based foamy oil, at which maximum recovery factor can be achieved, indicating that when pressure depletion rate is too high, larger bubbles are formed blocking the oil production and reducing ultimate recovery.

Effect of Heavy Oil Chemistry

Asphaltene is essentially composed of polynuclear aromatic ring layers associated with numerous alkyl chains and functional groups (Yen *et al*. 1961), suspended colloidally in crude oil, then forming a colloidal system (Wang *et al*. 2009). Greater interfacial stability has been observed when the solution asphaltene content was higher (Peng *et al*. 2009), since asphaltenes adsorb at the gas-oil interface, protecting bubbles from coalescence (Claridge 1994). Many scholars postulated that asphaltene, that appears to expedite bubble nucleation, lessen critical supersaturation and control bubble coalescence, does not contribute significantly to the stabilization of the gas bubbles that evolve during the heavy oil solution gas drive process, thus not remarkably improving the foamy oil performance (Bora *et al*. 2000; Adil and Maini 2007). However, it was also pointed out that the positive effect of higher depletion rates is different in crude oils containing asphaltenes from those with no asphaltenes (Adil and Maini 2007) since the acid and base groups present on asphaltene appear to form an interlinked network structure (Peng *et al*. 2009).

Diffusion Coefficient

Diffusivity is a transport phenomenon needed to compute the rate of mass transfer of a species as a result of its molecular diffusion into a medium (Bird *et al*. 1924), and it is an imperative consideration in several oil recovery processes since it is a very important parameter for

determining the amount of gas diffusing into oil in gas injection projects. It is expected to control the promptness of the process in view of the fact that the rate of solvent absorption depends on the diffusion coefficient (Das and Butler 1996; Riazi 1996; Riazi 2005), resulting in viscosity reduction and oil swelling, hence, improving the heavy oil recovery. According to Das and Butler (1996), unrealistic results can be reached if diffusivity is neglected since it is a strong function of solvent concentration.

Methane CSI process is a pressure-driven mechanism involving the nucleation of bubbles in oil, and as the pressure falls below the bubble point pressure, the growth of gas bubbles cause the oil to be driven out of the pores mainly due to mass diffusion, interfacial tension (IFT), oil viscosity, and solubility parameters (Li and Yortsos 1995; Zhang *et al*. 2000; Kumar and Pooladi-Darvish 2001; George *et al*. 2005). The rate of diffusion of the dissolved gas from the gas-oil interface into the body of the liquid phase controls the rate of dissolution of methane in a quiescent body of hydrocarbon (Pomeroy *et al*. 1933; Bertram and Lacey 1935; Reamer *et al*. 1956). Upreti *et al*. (2007) concluded that precise diffusion data for solvent-heavy oil systems are necessary to determine the volume and flow rate of gas needed for a gas injection project. It will also define the amount of heavy oil reserves that would undergo viscosity reduction, the time required by the reserves to become less viscous and more mobile as desired, and finally, the rate of live oil production from the reservoir.

The measurement of gas diffusion coefficients in heavy oils has been addressed by many authors (Riazi 1996; Zhang *et al*. 2000), in which they proposed different experimental methods. Ordinarily, direct and indirect methods were used for measuring the diffusion coefficients in hydrocarbon systems (Riazi 1996; Upreti and Mehrotra 2002; Sheikha *et al*. 2005; Zhou *et al*. 2018). The direct method includes those tests where the experimental system is disturbed. In this method, samples of the fluid are taken at various times and are evaluated by compositional analyses to measure the concentration distribution of gas in the heavy oil phase, followed by a mathematical mass transfer model, however, experimental errors may take place in these tests (Sigmund 1976; Nguyen and Farouq Ali 1998). The indirect method includes non-intrusive tests, where the change in some properties of the gas-heavy oil system such as the volume of gas dissolved, the motion of the gas-heavy oil interface, and the decrease in pressure of the system (pressure decay method) are measured and related to the composition of the heavy oil (Grogan *et al*. 1988; Do and Pinczewski

1993; Zhang *et al*. 2000; Jamialahmadi *et al*. 2006). Furthermore, novel techniques such as the measurement of the self-diffusion coefficients by using Nuclear Magnetic Resonance (NMR), followed by the use of correlations to find the binary diffusion coefficients (Hirasaki *et al*. 2003), and the dynamic pendant drop volume analysis (DPDVA) (Wen and Kantzas 2005; Tharanivasan *et al*. 2006) were recently proposed.

Many researchers studied the diffusion coefficient of a heavy oil-methane system (see Table 3.2) and its relationship with pressure, temperature, gas concentration, and solvent and oil composition (Riazi and Whitson 1993). For instance, Jamialahmadi *et al*. (2006) measured the diffusion coefficient of methane in liquid hydrocarbons over an extensive range of pressures and temperatures and found that diffusivity tended to increase with pressure and temperature (Upreti and Mehrotra 2002; Jamialahmadi *et al*. 2006).

Table 3.2—Experimental diffusion coefficients of heavy oil-methane systems.

Proposed by	Oil Sample	Gravity (°API)	T (°C)	μ_o (mPa.s)	Test Method	Boundary Condition	P (MPa)	Diffusion Coefficient ($D \times 10^{-9}$ m^2/s)
Zhang *et al*. (2000)	Intevep	-	21	5000	Pressure decay	Equilibrium	3.471	8.6
Hepler *et al*. (1989)	Athabasca	-	50	8360	-	Quasi-equilibrium	5.0	0.4 – 0.75
Upreti and Mehrotra (2002)	Athabasca	9.1	25 75 90 25 50 75	821000 @25°C	Pressure decay	Equilibrium	4.0 8.0	0.0810 0.2932 0.4315 0.0582 0.1518 0.4315
Creux *et al*. (2005)[a]	Heavy Oil	14.83	48	3904	Constant pressure	Equilibrium	4.0	0.158
Yang and Gu (2006)	Lloydminster	11.72	23.9	23000 @°23.9	DPDVA	-	6.0 – 14.0	0.12 – 0.19
Tharanivasan *et al*. (2004)	Heavy Oil	-	21		Pressure decay	Equilibrium, quasi-equilibrium, non-equilibrium	3.42	16.0 – 16.5
Tharanivasan *et al*. (2006)	Lloydminster	11.72	23.9	20267 @°23.9	Pressure decay	Equilibrium, quasi-equilibrium, non-equilibrium	4.9 – 5.0	0.21 – 0.22
Faruk and Maurice (2002)	Intevep	-	21	5000	Pressure decay	Non-equilibrium	3.471	0.22
Faruk and Maurice (2003)	Intevep	-	21	5000	Pressure decay	Non-equilibrium	3.42	0.5
Jamialahmadi *et al*. (2006)	Iranian Heavy Oil	-	50	-	Pressure decay	-	3.5	9.8

[a] A mixture of 90% methane and 10% carbon dioxide has been used in this study

3.4 Experimental Studies

The flow of oil and gas in a porous medium can be understood with laboratory studies, which are essential prior to the application (e.g. pilot tests) of any enhanced oil recovery technique in a heavy oil field. Sandpack pressure depletion tests have been widely used with the purpose of understanding the flow and formation of foamy oil in porous reservoirs, since experimental conditions such as pressure depletion rate, temperature, length of the porous medium, oil viscosity, oil specific gravity, and injection pressure can be precisely controlled and real-time data can be effectively recorded. A commonly used experimental setup for studying foamy oil flow in the laboratory comprises the use of an injection system, sandpack (porous medium), pressure transducers, pressure depletion rate controller, data acquisition system, collection vessel, and a gas flow controller as shown in Figure 3.2.

Pressure depletion tests were performed by previous authors in order to characterize the foamy oil flow. Reservoir (porosity, permeability, oil saturation) and fluid (viscosity, specific gravity) properties of a lab-scale representation of a heavy oil reservoir under a solution gas drive mechanism, i.e. primary depletion, and, external gas drive mechanism, i.e. CSI process, are shown in Table 3.3 and Table 3.4. The laboratory operating parameters; namely, the number of cycles, injection pressure, soaking time, and pressure depletion rates were reported along with the final heavy oil recovery factors.

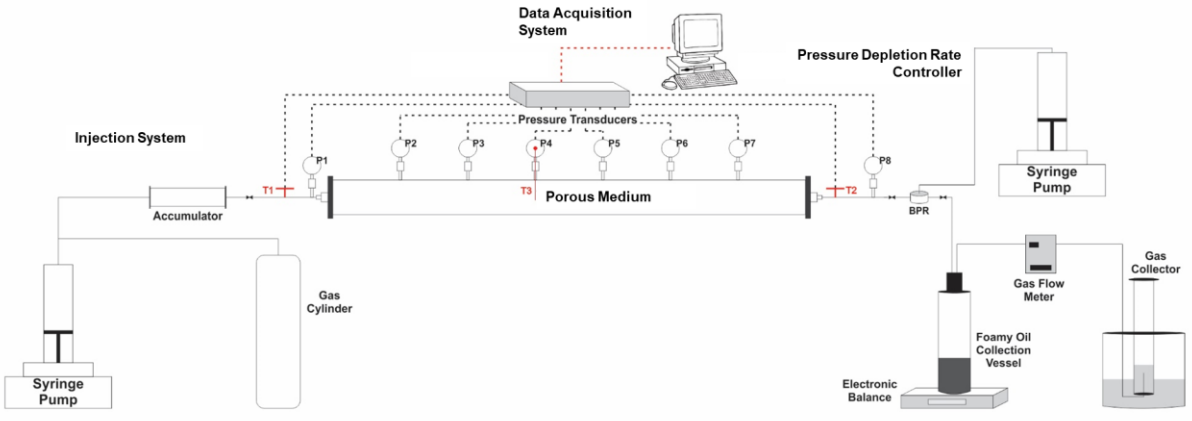

Figure 3.2—General Experimental Setup for Foamy Oil Experimental Studies.

Table 3.3—Sandpack depletion tests performed with live heavy/mineral oil – methane systems.

Proposed by	T (°C)	$\mu_{dead\ oil}$ (cp)	$\mu_{live\ oil}$ (cp)	Gravity API°	Size (L x D, cm x cm)	S_o (%)	K (D)	Φ (%)	P_{sat} (psi)	Initial GOR (cc/ml)	Δp/Δt (psi/min)	RF (%)
Zhang *et al*. (1999)	22	104,000	16,506	-	50 x 3.81	93.70	*Silica Sand* 3.1	38	600	12.7	0.3 ~ 0.5	20.14
			16,506						600	12.7	0.05 ~ 0.07	17.82
	70		319						550	12.3	0.3 ~ 0.5	29.10
			319						550	12.3	0.05 ~ 0.07	21.08
	122		36						550	11.7	0.3 ~ 0.5	26.82
			36						550	11.7	0.05 ~ 0.07	17.49
	175		9.7						600	11.1	0.3 ~ 0.5	17.17
			9.7						600	11.1	0.05 ~ 0.07	12.72
Maini (2003)	-	-	-	-	100 x 4.5	90.00	*Silica Sand* 4.5	34.7	500	-	0.379	23.60
											0.024	10.30
Ostos and Maini (2005)	21	*Mineral Oil* 1,945	-	-	200 x 5.3	92.00	*Ottawa Sand* 24.19	36.28	500	9.49	0.041	13.20
												20.79
												20.31
											0.081	18.33
												19.61
												22.81
											0.327	26.03
												25.77
												26.43
Goodarzi and Kantzas (2008)	23	10,695	4,837	12.64	1860 x 1.9	90.79	*Silica Sand* 1.93	36.4	1137	13.94	0.347	10.20
		10,711	5,688		1820 x 1.9	92.40	*Glass Beads* 11.81	37.8	1075	13.87	0.342	22.20
Li *et al*. (2012)[a]	54	6,151	28,040	-	120 x 2.5	89.3	*Silica Sand* 1.575	38.9	943	18.0	1.102	11.60
						91.3	7.361	40.6		18.0	1.102	21.50
						91.5	16.356	42.7		18.0	1.088	24.80
Liu *et al*. (2016)	50.5	25,460	21,825	10.57	80 x 5	97	*Quartz Sand* 5.877	38.8	1015	19.7	0.483	28.10
			22,130							17.8		25.80
			22,484							13.2		22.40
			22,876							10.4		20.30
		20,180	16,680	14.23						19.7		26.30
		14,132	11,879	18.71						19.7		24.70
		9,602	7,439	21.14						19.7		22.40
Zhou *et al*. (2016)	21	2,200	1562	15.24	100 x 3.8	96.72	*Glass Beads* 6.18	36.17	290	6.62	0.067	14.06
						97.18	6.03	36.15			0.141	20.12
						96.20	6.24	35.66			0.247	22.13
						97.41	5.93	35.98			0.583	12.11
			592			96.74	6.14	36.34	392	25.30	0.125	9.09
						97.89	6.08	36.08			0.267	15.61
						96.93	6.20	35.83			0.576	21.80
						96.99	6.32	36.59			0.966	20.44
Abusahmin *et al*. (2017)	23	*Mineral Oil* 1,876	1,080	26.42	200 x 6.4	92.00	*Silica Sand* 24	34	500	9.1	0.406	26.10
											0.247	23.90
											0.086	13.70
											0.021	13.10
		Crude Oil 2,608	1,300	19.68						11.0	0.350	26.00
											0.230	25.30
											0.048	22.00
											0.023	16.00
Soh and Babadagli (2017)	21	*Crude Oil* 17,500	-	10.71	150 x 5.0	90.50	*Silica Sand* 4.33	34.46	500	-	0.23	8.95
						93.00		36.74			0.51	14.21
						92.00		38.13			1.53	13.84

In order to understand the mechanics of foamy oil flow in the primary recovery of heavy oil, and the factors that affect its performance, live oil pressure depletion tests were carried out. Previous researchers paid heed to main operating parameters such as pressure depletion rates, liquid system characteristics like heavy oil viscosity, temperature, and gas-oil ratio, and porous medium characteristics, namely permeability. The main physical phenomenon to be understood in the flow of foamy oil is supersaturation, caused by pressure reduction, leading to the nucleation of gas bubbles (Sheng *et al*. 1999). Gas supersaturation occurs when an excessive amount of gas is dissolved in a liquid system, exceeding that at the equilibrium pressure and temperature.

Zhang *et al*. (1999) utilized a sample of cold lake heavy oil to study the effects of temperature on foamy oil behavior. They designed eight sets of experiments grouped into fast depletion and slow depletion tests as shown in Table 3.3. As observed in Figure 3.3, at isothermic conditions, they found out that higher depletion rates represent higher recovery factors. The latter was later confirmed by Li *et al*. (2012), who utilized a heavy oil sample from the Orinoco Belt and a mixture of 87% methane and 13% carbon dioxide as the gas solvent. However, it is noteworthy that the highest recovery factors were obtained at intermediate temperatures, concluding that an optimum operating temperature exists that is determined by the heavy oil chemistry. Maini (2003) carried out slow and fast pressure depletion experiments, confirming that pressure depletion rates have an important effect on final heavy oil recovery, decreasing with the decreasing pressure depletion rate. During the same test, he also tried switching from fast pressure depletion rates to slow depletion rates and vice versa. He found out that for both cases, final recovery was not positively affected, which means that additional final recoveries were not achieved. Ostos and Maini (2005) investigated the effects of capillary and gravitational forces during foamy oil flow at different depletion rates, by placing the sandpack in three different orientations, horizontal, vertical with the producing end at the top, and vertical with the producing end at the bottom. Results are shown in Figure 3.4. For all three sandpack orientations, it can be seen that the average capillary number is directly proportional to the pressure depletion rate, being the one with the producing end at the top the one reaching the highest capillary number. The influence of the gravitational forces on the final oil recovery can be divided into three according to the sandpack orientations. It is evident that the effects of gravitational forces are high when the sandpack is vertically placed, and low when the sandpack is horizontally placed. According to the experimental results, at high capillary numbers, the effect of gravitational forces are quasi-negligible, whereas at low capillary

numbers the effects become more pronounced, being the horizontal orientation (lowest gravitational forces interference) the one achieving the lowest final recoveries. It is noteworthy that for both highest pressure depletion rates, the highest recovery factor is achieved against the gravity force. Goodarzi and Kantzas (2008) focused on studying the effects of absolute permeability on the foamy oil dynamics and final heavy oil recovery. In addition, they paid attention to the effects of the length difference in sandpack experiments. They observed that higher oil recovery factors are obtained in higher-permeability systems, explaining that higher permeabilities lead to higher supersaturation and higher critical gas saturations, affecting positively the pressure distribution and bubble nucleation which is eventually translated in a higher final oil recovery, confirming the findings of Sarma and Maini (1992) and Li *et al*. (2012) as shown in Figure 3.5. They also described the foamy oil mechanism as a localized phenomenon that occurs at different locations and at different times. Liu *et al*. (2016) performed an outstanding work by analyzing the effect of solution GOR and viscosity of heavy oil in a series of experiments in order to study their effect on the final heavy oil recovery. They used a Venezuelan heavy oil sample and mixed it with different mass fractions of kerosene to modify the oil viscosity. The general trends they observed for both cases were that final heavy oil recovery increases as solution GOR and viscosity are higher as depicted in Figure 3.6. In an attempt to study the effects of saturation pressure on the performance of foamy oil flow, Abusahmin *et al*. (2017) performed two live oil experiments, prepared at 300 psi and 500 psi and depleted at 0.264 psi/min and 0.247 psi/min, respectively. They obtained similar recovery factors, 23.8%, and 23.9%, in both tests in a 1.5-day-depletion-process. The main differences between both processes were the earlier and higher gas production rates at 500 psi, i.e. higher GORs, and higher and earlier oil production rates at a pressure of 300 psi. The effect of pressure depletion rate on the foamy oil flow performance has been found to have a significant effect on the final recovery of heavy oil. Among many authors, the effects of the pressure depletion rate on the primary depletion process of heavy oil formations under foamy oil flow conditions and using pure methane as the main dissolved gas have been studied by Maini (2003), Liu *et al*. (2016), Zhou *et al*. (2016), Abusahmin *et al*. (2017), and Soh *et al*. (2018). Furthermore, Ostos and Maini (2005) and Abusahmin *et al*. (2017) utilized mineral oil with the same purpose. As a forward-looking vision to enhance the final oil recovery after a primary depletion process, Li *et al*. (2012) and Zhou *et al*. (2016) focused on studying the effect of using different solvents (methane, mixtures of methane-propane, and mixtures of methane-

carbon dioxide) on foamy oil flow under different pressure depletion rates to be used in CSI projects to enhance the final heavy oil recovery. Even when the studies have been conducted under different conditions, using heavy crude oil or heavy mineral oil, methane or even the mixture of methane with other solvents, the results on their experimental studies agree that decreasing the pressure depletion rate leads to a reduced foamy oil flow performance, which will eventually drive to obtain a lower recovery of heavy oil. The final recovery factors are in direct proportion to the pressure depletion rates, as shown in Figure 3.7 and Figure 3.8. However, Zhou *et al*. (2016) found the existence of a critical pressure depletion rate at which a maximum recovery factor can be achieved. This finding was later confirmed by Soh *et al*. (2018). It is noteworthy that the experimental conditions such as sandpack length and diameter; packing material, i.e. sand and glass beads; live oil saturation pressure; and the used pressure depletion rates were different, yet they found a critical depletion rate which was different for each research group. These findings suggest that the effect of depletion rates are different for each type of oil and solvent used.

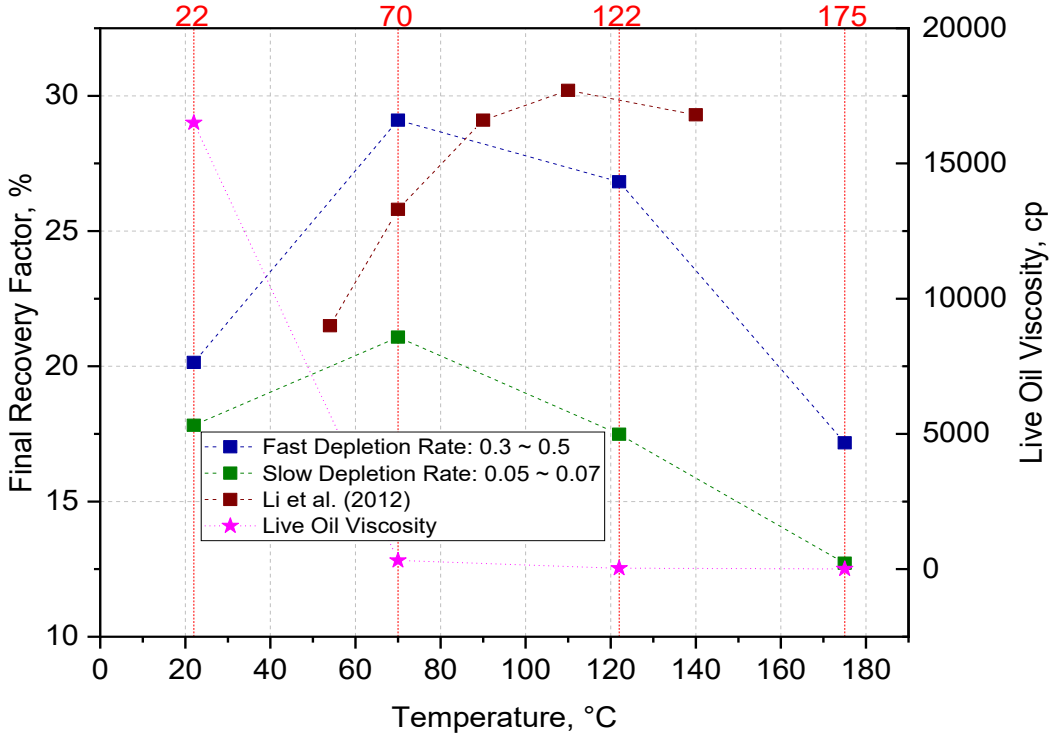

Figure 3.3—Effect of temperature on the final oil RF and the viscosity of live oil (Zhang, 1999; Li *et al*. 2012).

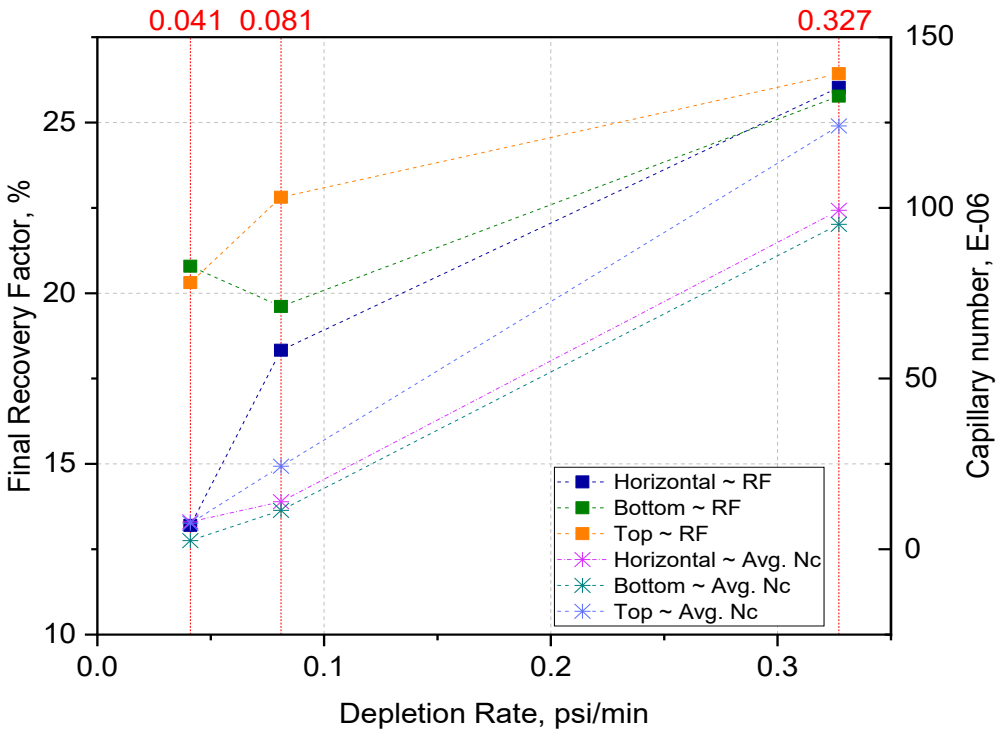

Figure 3.4—Effect of gravity on heavy oil recovery at different depletion rates (Ostos and Maini 2005)

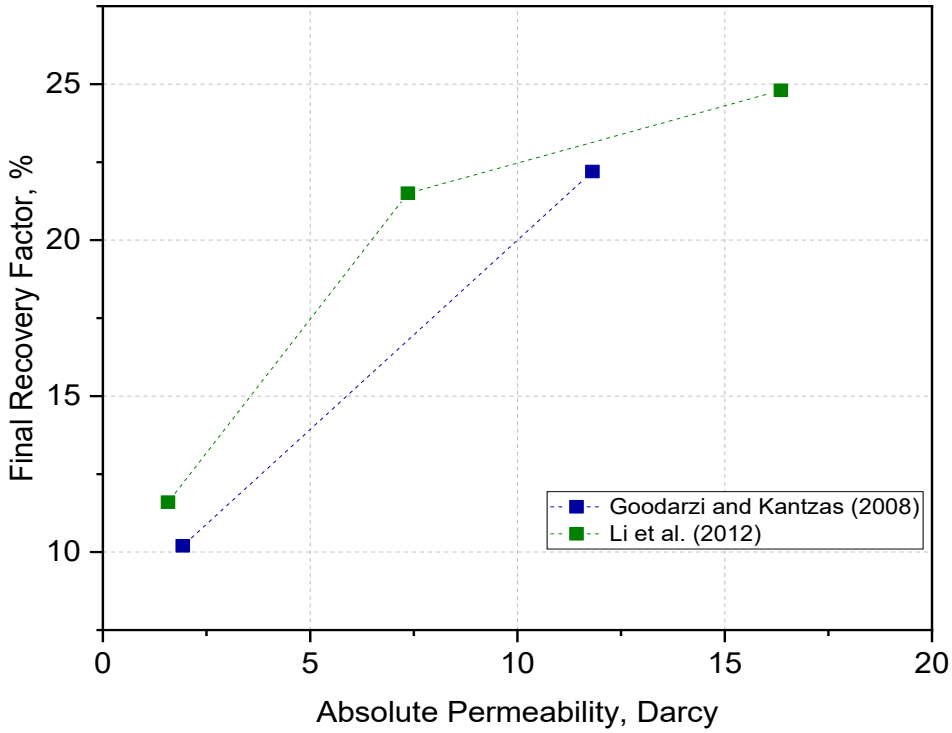

Figure 3.5—Effect of absolute permeability on final oil recovery (Goodarzi and Kantzas 2008; Li *et al*. 2012).

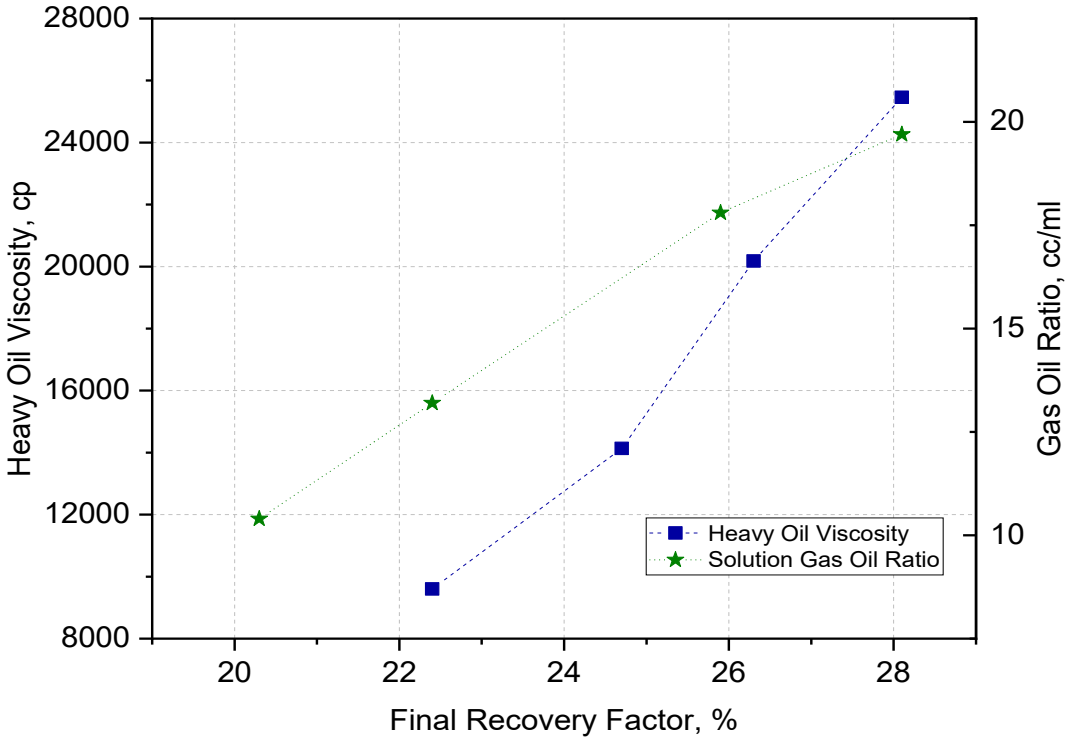

Figure 3.6—Effect of heavy oil viscosity and solution gas-oil ratio on oil recovery (Liu *et al*. 2016)

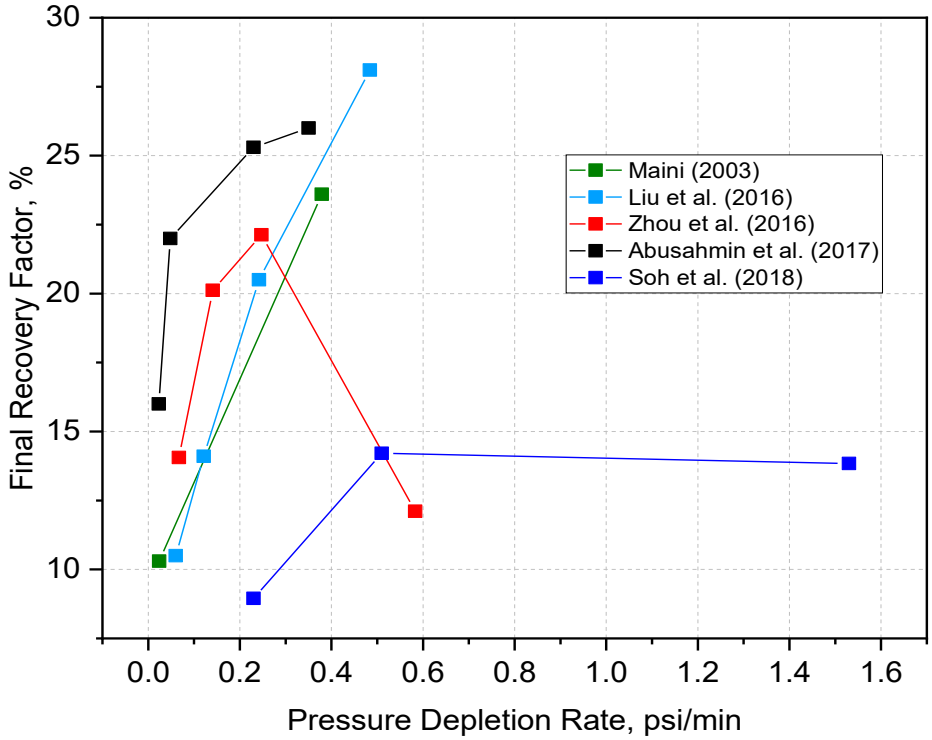

Figure 3.7—Effect of pressure depletion rate on final heavy crude oil recovery (Maini 2003; Liu *et al*. 2016; Zhou *et al*. 2016; Abusahmin *et al*. 2017; Soh *et al*. 2018).

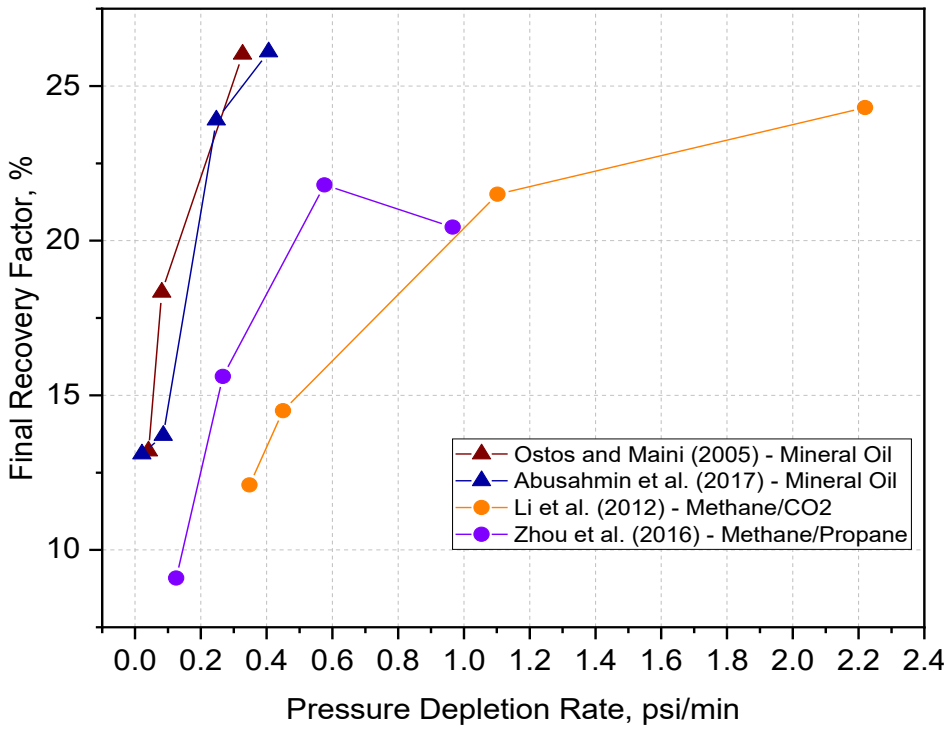

Figure 3.8—Effect of pressure depletion rate on final heavy mineral oil recovery (Ostos and Maini 2005; Li *et al*. 2012; Zhou *et al*. 2016; Abusahmin *et al*. 2017).

With the objective of studying the mechanisms of the in situ generation of gas-in-oil dispersion and the mechanisms that allow its flow for a CSI process applied after primary heavy oil recovery, Shi and Kantzas (2008), Qazvini Firouz and Torabi (2012), Soh and Babadagli (2017) and Basilio and Babadagli (2019) performed long core experiments packed with sand and glass beads, which were initially saturated with dead oil. Experimental details such as the number of tests, laboratory conditions, oil characteristics, porous media description, number of cycles, injection pressure, depletion rates used, and the resulting final oil recovery are shown in Table 3.4. The general experimental procedure for each cycle was reported as follows: (1) inject solvent into the gas-free heavy oil at a pre-defined operating pressure; (2) allow solvent diffusion, giving it a specific soaking time or awaiting until system equilibrium is achieved; (3) depressurize system at a specific depletion rate until the system achieves a predesignated pressure.

Shi and Kantzas (2008) performed two after-primary-depletion experiments using methane as the injection solvent. They used two porous media with different permeabilities, the less permeable medium was packed with sand and used for Test 1, and the more permeable medium

was packed with glass beads and used for Test 2. They observed that there is a noticeable difference in saturation time and production performance between the two of them due to the difference in permeability. A 10-times shorter stabilizing time has been observed in Test 2. Also, they noted that at the farthest position from the producing end, Test 1 lessened to half of the initial pressure after three days, whereas for Test 2 it took 35 days. Even though the final recovery factors are close to each other (see Figure 3.9), these results highlight the importance of a high-permeability porous medium in soaking time and production performance in a CSI process. Qazvini Firouz and Torabi (2012) performed four one-day-soaking-period experiments under different injection pressures, finding that higher injection pressures bring about higher cumulative recovery factors. Although pore volumes of methane injected were not reported, it is clear that higher operating pressures are due to higher volumes of solvent injected. Maximum heavy oil recovery factors were approximately 8%, 11.5%, and 12.5% at operating pressures of 500 psi, 750 psi, and 1000 psi, in the order of precedence. The highest recovery factors were achieved during the third and the fourth cycles, as depicted in Figure 3.9. Between those three operating pressures, there is no remarkable difference to conclude that higher saturation pressures lead toward higher recovery factors in an economic-efficient way. The same was also observed in live oil experiments, as above-mentioned. Hence, special attention should be given to the soaking time, since a better solvent diffusion process will occur if enough time is given to the system.

Besides using methane as the only solvent, Soh and Babadagli (2017) and Basilio and Babadagli (2019) utilized air as a co-injection gas. Their results are presented in Figure 3.10. In addition to its low cost, air was mainly used to pressurize the heavy-oil-saturated-sandpack as well as to increase the heavy oil viscosity due to a low-temperature oxidation process (Mayorquin-Ruiz and Babadagli 2016b; Basilio and Babadagli 2018) and, therefore improving the foam quality when injected with/before methane, since a higher oil viscosity enables a higher resistance to the flow of gas bubbles in the oil phase, making the foamy oil system more stable (Sheng *et al*. 1997) and leading to a higher oil recovery. Soh and Babadagli (2017) carried out two tests (Test 1 and Test 2), of three consecutive cycles. Test 1 consisted of injecting air in the first cycle, and methane in the second and third cycles. Test 2 consisted of the injection a mixture of air and methane in a gas composition ratio of one. They used two pressure depletion rates, performing the depletion process of each cycle in two stages: (1) a depletion rate of 0.51 psi/min from 500 to 190 psi; and (2) a depletion rate of 0.23 psi/min from 190 to 70 psi. Basilio and Babadagli (2019) performed

four pressure depletion tests, considering five consecutive cycles for each test. They made an effort to reduce the use of methane by using a different assortment of air-methane mixtures for each test, which composition and main results are listed in Table 3.5. They used operating pressures around 550 psi, allowing enough soaking time for the system to spontaneously reach the equilibrium. At a depletion pressure of 0.51 psi/min and recovery factors as high as 28.29% have been achieved in an alternating (methane-air) injection strategy.

Table 3.4—Sandpack depletion tests performed with dead heavy oil and methane.

Proposed by	Test	T (°C)	μ_o (cp)	Gravity API°	Size (L x D, cm)	S_o (%)	K (D)	Φ (%)	Number of Cycles	P_{inj} (psi)	$P_{cut-off}$ (psi)	T_{soak} (day)	Δp/Δt (psi/min)	Total RF (%)
Shi and Kantzas (2008)	1	23	10,695	12.64	1860 x 1.9	90.79	*Silica Sand* 1.93	36.4	1	890.53	30	1.25	0.339	4.80
	2		10,711		1820 x 1.9	92.40	*Glass Beads* 11.81	37.8		932.59		0.125		5.20
(Qazvini Firouz and Torabi, 2012)	1	28	1,423	15.84	30.48 x 5.1	88.89	*Berea Core* 1.8	24	5	250.00	40	1	-	0.0
	2					88.89			8	500.00				38.0
	3					87.41			9	750.00				45.0
	4					87.41			9	1000.00				50.0
(Soh and Babadagli, 2017)	1	25.0	27,400	17.45	150 x 5.0	9.5	*Silica Sand* 1.41	34.46	3	500	70	2 ~ 3	0.51 ~ 0.23	36.21
	2					8.0	2.51	38.13	3	500	70	2 ~ 3		23.74
Basilio and Babadagli (2019)	1	21.0	27,400	13.55	150 x 5.0	87.77	*Silica Sand* 9.96	43.32	5	537.60	30	4	0.51	26.45
	2					88.04	9.32	43.14	5	555.00	30	5		23.49
	3					86.95	10.25	43.61	5	564.80	30	5		28.29
	4					87.43	9.31	43.10	5	555.00	30	4		27.30

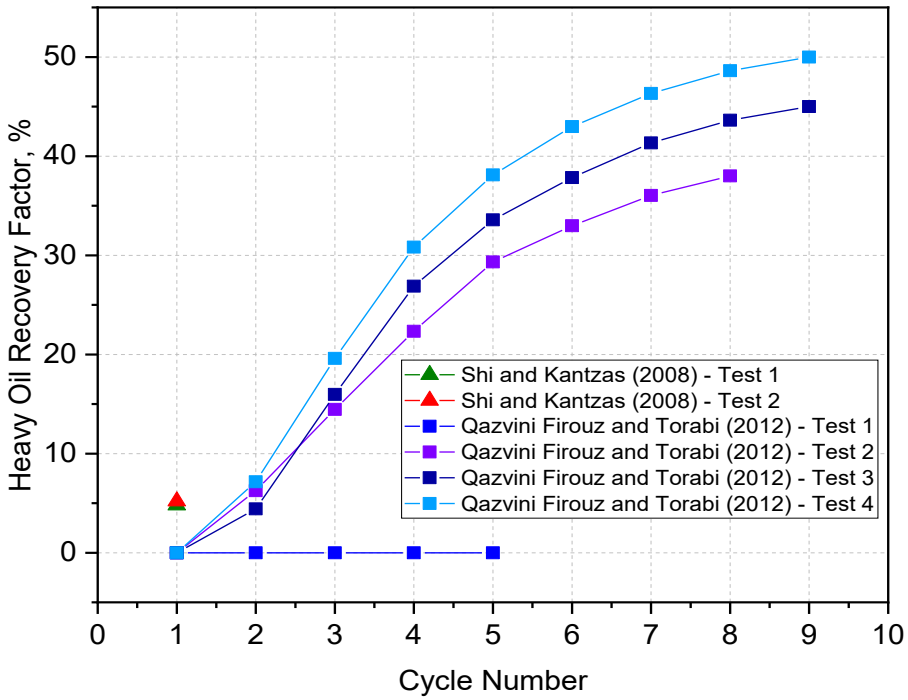

Figure 3.9—Effect of Pressure Depletion Rate on Final Heavy Oil Recovery (Shi and Kantzas 2008; Qazvini Firouz and Torabi 2012).

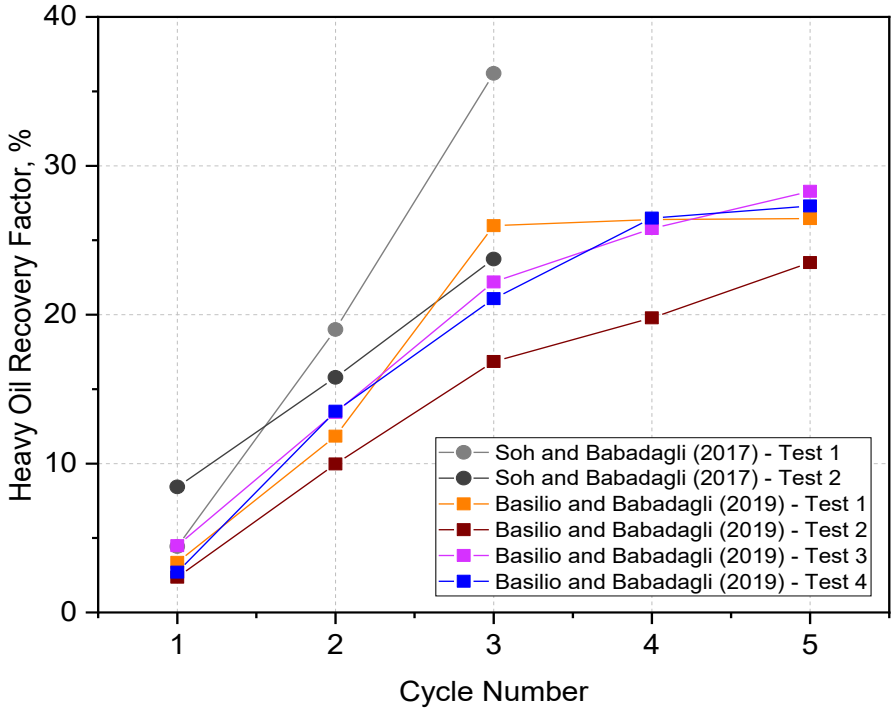

Figure 3.10—Effect of pressure depletion rate on final heavy oil recovery (Soh and Babadagli 2017; Basilio and Babadagli 2019).

Table 3.5—Summary of experimental details and Results from Basilio and Babadagli (2019).

Test	Cycle	Gas Composition	V_{gas} (PV)	P_{soak} (psi)	cGOR (Scm^3/cm^3)	Oil RF (%)	Total Oil RF (%)	Gas RF/Cycle (%)	Total Gas RF (%)
Test 1	Cycle 1	100% Methane	0.11	532	0.02	3.36	26.45	0.01	61.62
	Cycle 2	100% Methane	0.13	571	21.02	8.48		29.48	
	Cycle 3	100% Methane	0.08	505	47.67	14.14		170.72	
	Cycle 4	50% Air – 50% Methane	0.31	538	2179.70	0.42		61.82	
	Cycle 5	50% Air – 50% Methane	0.29	542	18123.23	0.05		68.59	
Test 2	Cycle 1	50% Air – 50% Methane	0.16	551	52.06	2.37	23.49	14.93	46.29
	Cycle 2	50% Air – 50% Methane	0.08	563	23.08	7.60		45.93	
	Cycle 3	50% Air – 50% Methane	0.24	566	68.54	6.88		38.29	
	Cycle 4	50% Air – 50% Methane	0.28	546	218.45	2.94		45.94	
	Cycle 5	100% Methane	0.23	549	241.22	3.71		78.00	
Test 3	Cycle 1	100% Air	0.02	554	20.90	4.48	28.29	79.90	69.10
	Cycle 2	100% Methane	0.10	564	15.41	8.95		85.53	
	Cycle 3	100% Air	0.12	546	48.00	8.77		67.68	
	Cycle 4	100% Methane	0.28	573	347.96	3.58		86.47	
	Cycle 5	30% Methane after 70% Air	0.27	587	368.70	2.51		67.39	
Test 4	Cycle 1	100% Methane	0.01	567	0.00	2.70	27.30	0.00	71.79
	Cycle 2	100% Methane	0.08	562	26.29	10.81		66.69	
	Cycle 3	100% Air	0.15	556	60.86	7.57		61.37	
	Cycle 4	100% Methane	0.27	539	200.93	5.41		79.22	
	Cycle 5	100% Air	0.23	551	1075.96	0.81		73.75	

3.5 General Discussion

Notwithstanding, many different experimental schemes were tested and detailed investigations on foamy oil flow were carried out, theoretical foundations of its performance are still not convincing enough, and the mechanisms for the dynamic processes continue to be not fully understood. However, the effects of certain operating parameters affecting the final recovery of high viscous oils, and a general description of the dynamic process can be dragged from experimental observations of foamy oil flow in porous media using methane as the main solvent.

In contrast to a conventional solution gas drive in which the final recovery factor decreases as the oil viscosity increases, heavy oil reservoirs exhibit an anomalous behavior in such a way that higher the viscosity, the higher the recovery. As noted earlier, experiments performed under foamy oil flow conditions showed a direct proportion between heavy oil viscosity and the final heavy oil recovery factor. Hence, a valid explanation is that as the reservoir is being depleted, the tiny bubbles present in the foamy oil gain mass as the solvent is diffusing into the oil, also, the compressibility of the solvent causes a mechanical expansion, in which viscosity opposes to the bubble growth (Huber *et al*. 2013). This opposition to growth will restrain the eventual coalescence of bubbles, trapping them and making the foam more stable which results in a better reservoir energy maintenance, improving the final oil recovery. Contrary to this behavior, in low-viscosity oils, the lack of heavy components does not help to the bubble trapping process, resulting in an unstable and not very efficient foamy oil performance (Sheng *et al*. 1999; Zhou *et al*. 2016; Abusahmin *et al*. 2017).

It is also clear that temperature plays an important role in the heavy oil recovery factor since it is inversely proportional to the oil viscosity. As explained before, differently from a conventional solution gas drive, higher oil viscosities, i.e. lower reservoir temperatures, are beneficial for a foamy solution gas drive. Nevertheless, even when at lower reservoir temperatures, which can be understood as higher oil viscosities, the fraction of dispersed gas in the oil is higher and the reservoir energy better maintained, meaning the resistance to flow is higher. On the other hand, higher temperatures not only will dramatically reduce heavy oil viscosity and diminish the resistance to flow but also debilitate the ability of heavy oil to capture and restrain the solution gas, affecting negatively the foamy oil phenomenon benefits. This might explain why higher final oil recoveries have been obtained at intermediate temperatures (Zhang *et al*. 1999; Liu *et al*. 2016).

According to Darcy's law and models used for conventional solution gas drive, the absolute permeability and oil flow rate are directly proportional but the final oil recovery factor does not seem to be affected. However, experimental results showed that in heavy oil reservoirs under foamy oil flow condition, higher permeabilities allow the formation of higher local pressure gradients and the recovery of higher quantities of heavy oil. This observation is very important as it develops the potential application of in-situ generated foamy oil recovery in a CSI process as a post-CHOPS technique, where high-permeability wormholes are generated after the cold production process. However, the effect of the absolute permeability of some rock-fluid properties still remains unanswered, since the effect of bubbles on relative permeability values still remain unquantified (Sheng *et al*. 1999; Zhou 2015).

It has been observed that the final heavy oil recovery increases as pressure depletion rate is higher. This is perhaps the most important parameter since the heavy oil recovery efficiency under a foamy oil flow performance relies on the exsolution of dissolved gas. As pressure continuously decreases, a large number of tiny bubbles nucleate, controlled by the level of gas supersaturation, and get eventually trapped in the oil due to its high viscosity. Then, these gas nuclei start migrating within the oil, displacing it in the direction of flow. Simultaneously, gas bubbles grow as a result of the ongoing pressure drop, followed by gas bubble break up and coalescence leading eventually to form a continuous gas phase, which is when foamy oil flow ends. Experimental results indicated that the foamy oil performance is more efficient at high depletion rates, whereas at low depletion rates the production behavior is close to a conventional solution gas drive. Even at high-pressure depletion rates, the pressure drawdown in the reservoir is low, but the existence of induction zones in which tiny bubbles are generated as a response of local pressure gradients control the generation of foamy oil.

Figure 3.11 shows a schematic of the porous medium where foamy oil flow takes place. As bubbles continue growing due to pressure drop, pore throats will be blocked generating even higher local pressure gradients, which is able to cause bubbles deformation and overcome the resistance to flow. This dynamic process of blocking pore throats is responsible for maintaining the reservoir energy. It is noteworthy that the leftmost part of the picture has still bubbles nucleating and following the already known bubble dynamics since lower pressure gradients are

generated in that area. It means that for a specific porous medium there are different local pressures that behave like different bulk heavy oil-gas systems.

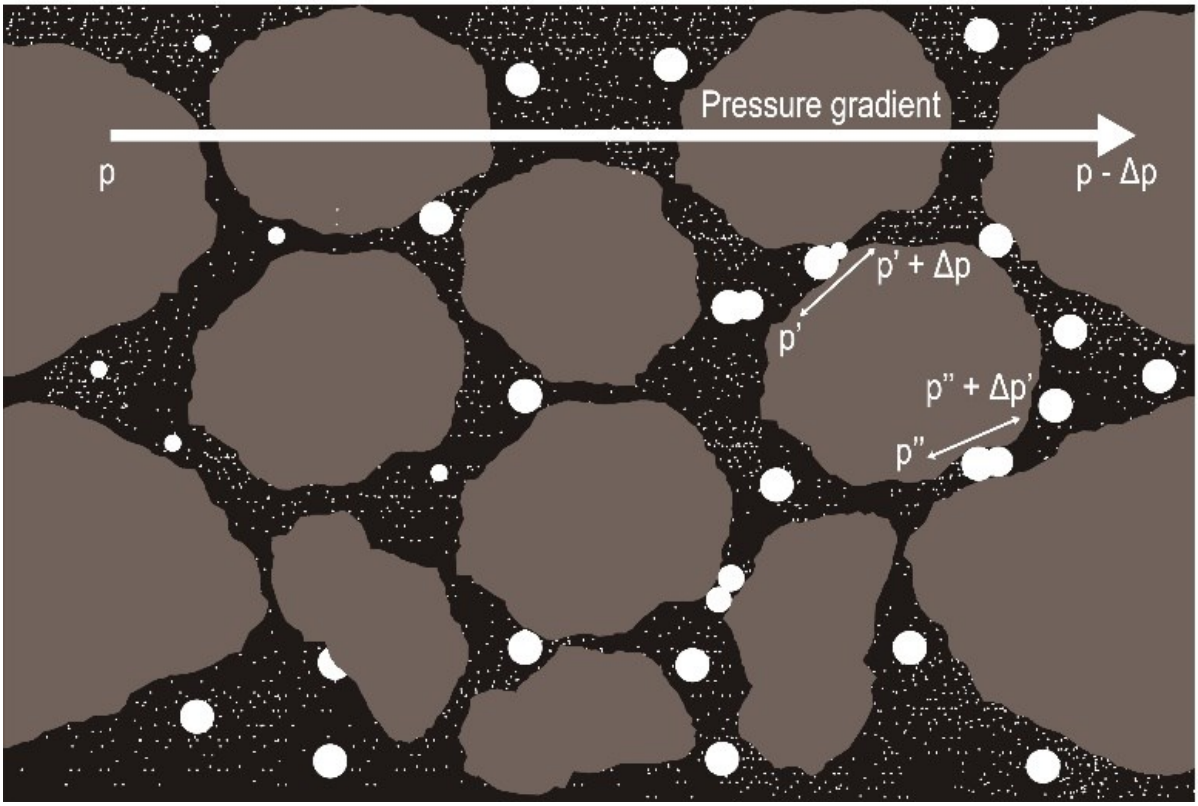

Figure 3.11—Pore throat blockage by gas bubbles showing local pressure gradients.

It has been shown before that capillary number, Nc, (**Equation 3.1**) has a linear relationship with the pressure depletion rates:

Equation 1—Relationship between viscous and capillary forces.

$$\mathbf{N_c} = \frac{\textbf{viscous forces}}{\textbf{capillary forces}} = \frac{\boldsymbol{\upsilon\mu}}{\boldsymbol{\sigma}} = \left(\frac{\mathbf{k}}{\boldsymbol{\sigma}}\right)\left(\frac{\mathbf{dP}}{\mathbf{dx}}\right)$$

where υ is Darcy's velocity; μ is the oil viscosity; k is the absolute permeability; σ is the oil interfacial tension, and (dP/dx) is the pressure gradient. Considering the fact that capillary number is related to the ultimate recovery of oil, the local pore-scale capillary numbers should be studied in detail for foamy oil systems (Sheng *et al*. 1999; Warner 2007).

The foamy oil behavior observed during primary production in a heavy oil reservoir under solution gas drive can be synthetically generated by external gas drive, i.e. injecting solvent gasses

into the reservoir. This is, in a sense, a secondary recovery attempt and, as discussed earlier, the generation of local pressure gradients is crucial in generating the foamy oil performance during this process. Basilio and Babadagli (2019) performed foamy oil experiments to study a cost-effective external gas drive, of which results are presented in Table 3.5. The local pressure gradients for Test 1 (five cycles) are presented in Figure 3.12. Pressure gradients were calculated as the differential pressure of two consecutive pressure ports, divided by the length between them. The vertical axis represents the average pressure (psi) in the sandpack, and the horizontal axis represents the length of the sandpack divided into seven sections. Referring to Figure 3.2, in which pressure ports are located along the sandpack, P1 represents the farthest pressure transducer location from the producing end, and P8 represents the closest pressure transducer location from the producing end. The pressure gradient between the pressure ports P1 and P2 is named Pg1, the pressure gradient between the pressure ports P2 and P3 is named Pg2, and so on and so forth. It is necessary to clarify that Pg8 is, in fact, a pressure gradient in the tubing, and not in the porous medium, therefore their values are high. During Cycle 1, the sandpack is fully saturated with dead oil, then, there was not enough space for the gas to be able to diffuse and low-pressure gradients were observed, with a maximum of 0.78 psi/cm in Pg7, making foamy oil process inefficient, and as a consequence, low compressibility oil is produced.

On the other hand, in Cycles 2 and 3, different behaviors of pressure gradients can be observed at different locations. It is important to notice that as pressure drops, these both cycles keep a plateau of pressure gradients, helping to mobilize the oil more efficiently and as a consequence, high recovery factors were achieved in these cycles. Fig. 3.14 shows the produced heavy oil, and its foaminess is evident. Cycles 4 and 5 exhibit almost null pressure gradients. It is important to notice that the highest values of pressure gradients are located close to the injection port, which means that even though the gas bubbles are trapped in that section of the sandpack, the number of bubbles seems to be less than the previous cycles generating gradients not sufficient enough to mobilize the oil efficiently. Also, this was observed as a faster pressure depletion process when compared with other cycles, i.e. there was not good pressure maintenance, and a lower recovery factor was obtained.

a

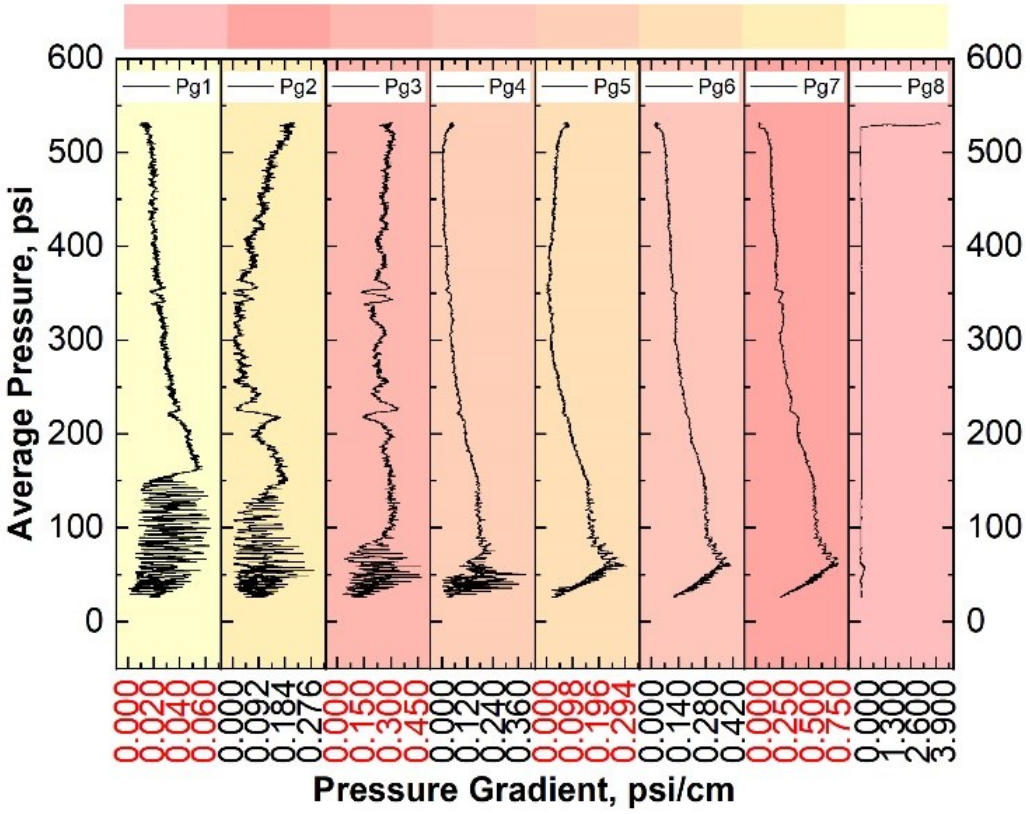
Pg1
Pg2
Pg3
Pg4
Pg5
Pg6
Pg7
Pg8
Average Pressure, psi
0
100
200
300
400
500
600
Pressure Gradient, psi/cm

b

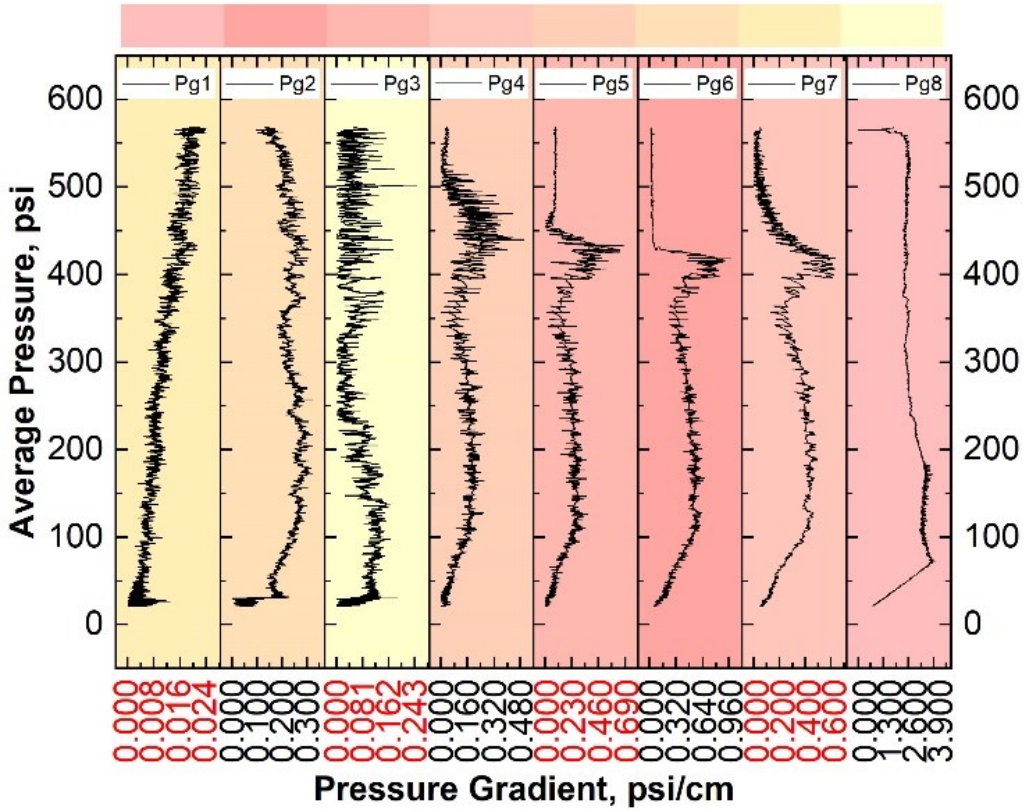
Pg1
Pg2
Pg3
Pg4
Pg5
Pg6
Pg7
Pg8
Average Pressure, psi
0
100
200
300
400
500
600
Pressure Gradient, psi/cm

c

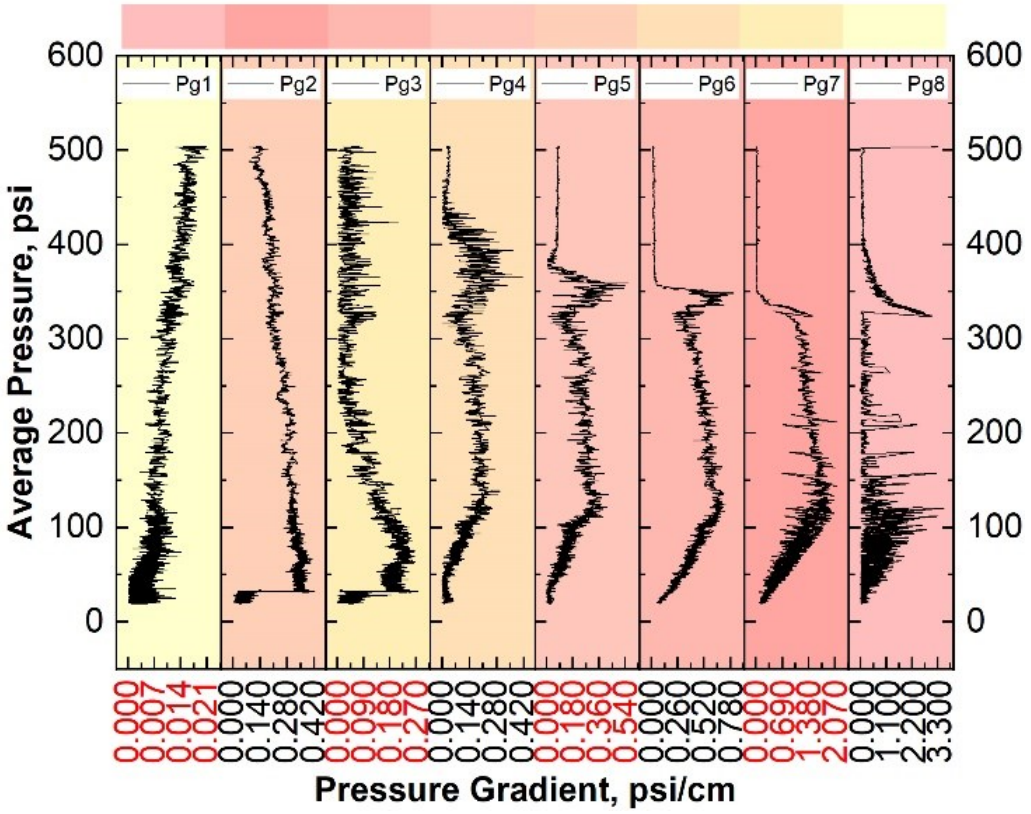
Pg1
Pg2
Pg3
Pg4
Pg5
Pg6
Pg7
Pg8
Average Pressure, psi
0
100
200
300
400
500
600
Pressure Gradient, psi/cm

d

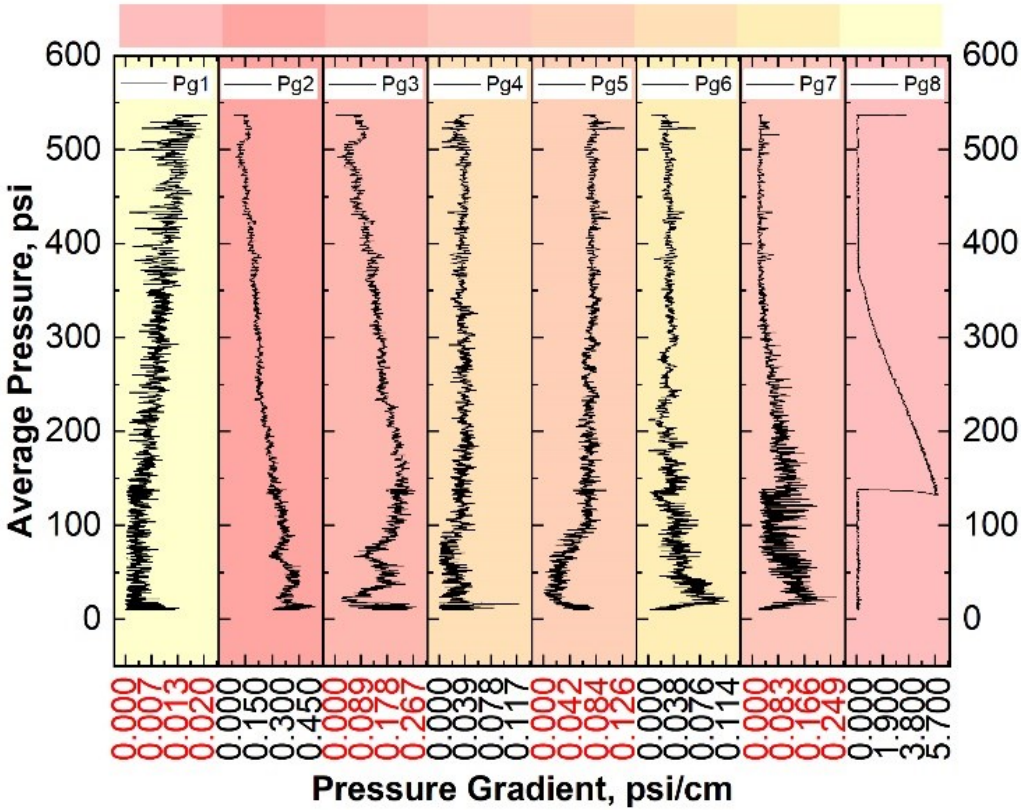
Pg1
Pg2
Pg3
Pg4
Pg5
Pg6
Pg7
Pg8
Average Pressure, psi
0
100
200
300
400
500
600
Pressure Gradient, psi/cm

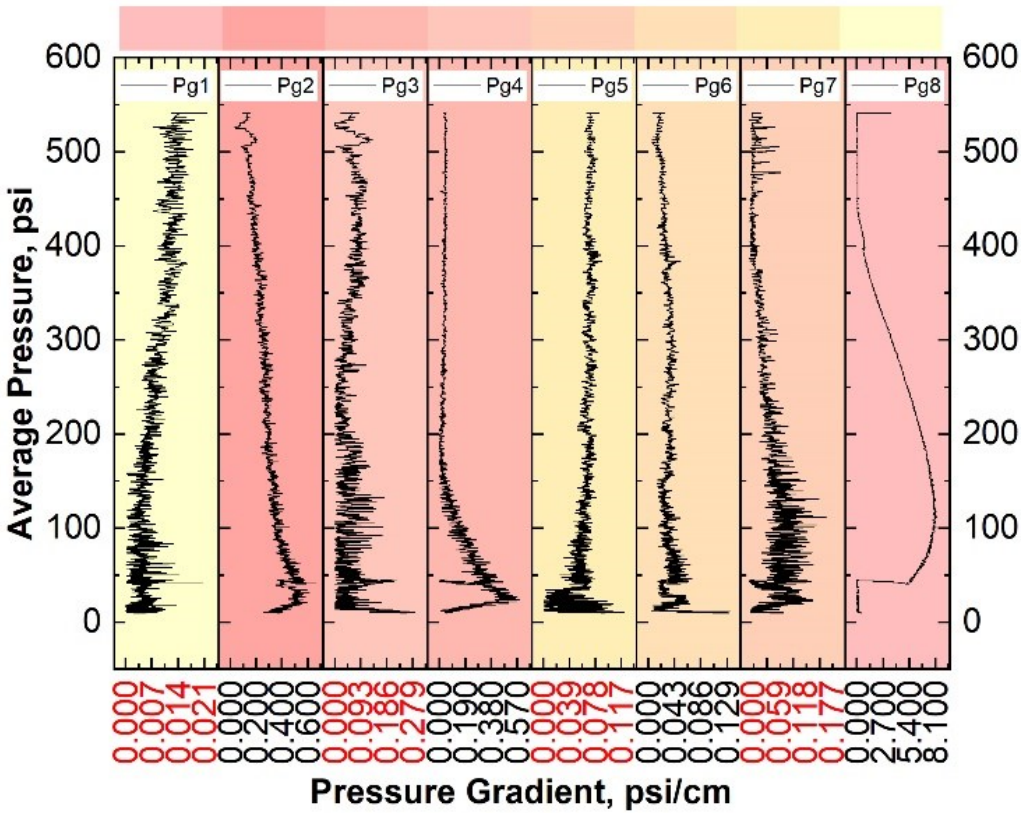

Figure 3.12—Pressure gradients for each cycle for Test 1, X-axes are expressed in psi/cm.

The local pressure gradients for Cycle 3 and Cycle 4 in Test 4 are presented in Figure 3.15. The injection of pure air in Cycle 3 was done in order to increase the sandpack pressure and confirm the hypothesis that a more stable foamy oil is achieved with higher oil viscosities, reached through low-temperature oxidation with air. After a methane injection, the objective of pressurizing the system was achieved, and the recovery factor resulted in 7.57%. It is noteworthy that from the previous Cycle 2 only 66.69% of methane was recovered, with the rest still trapped in the heavy oil. Hence, the main production mechanism was foamy oil flow, pushed with the front of air toward the producing end. Pressure gradients in Cycle 4 have a rising tendency. The bubble dynamic behavior, which unlike the fourth cycles from the other tests, was still maintained, and close to the producing end. Even when the smallest PV of gas was injected, compared to the other tests, yet the highest recovery factor was obtained when compared to the other tests. It is clear the bump indicating the highest pressure gradient was located by the end of the sandpack, similarly to Cycles 2 and 3 from Test 1.

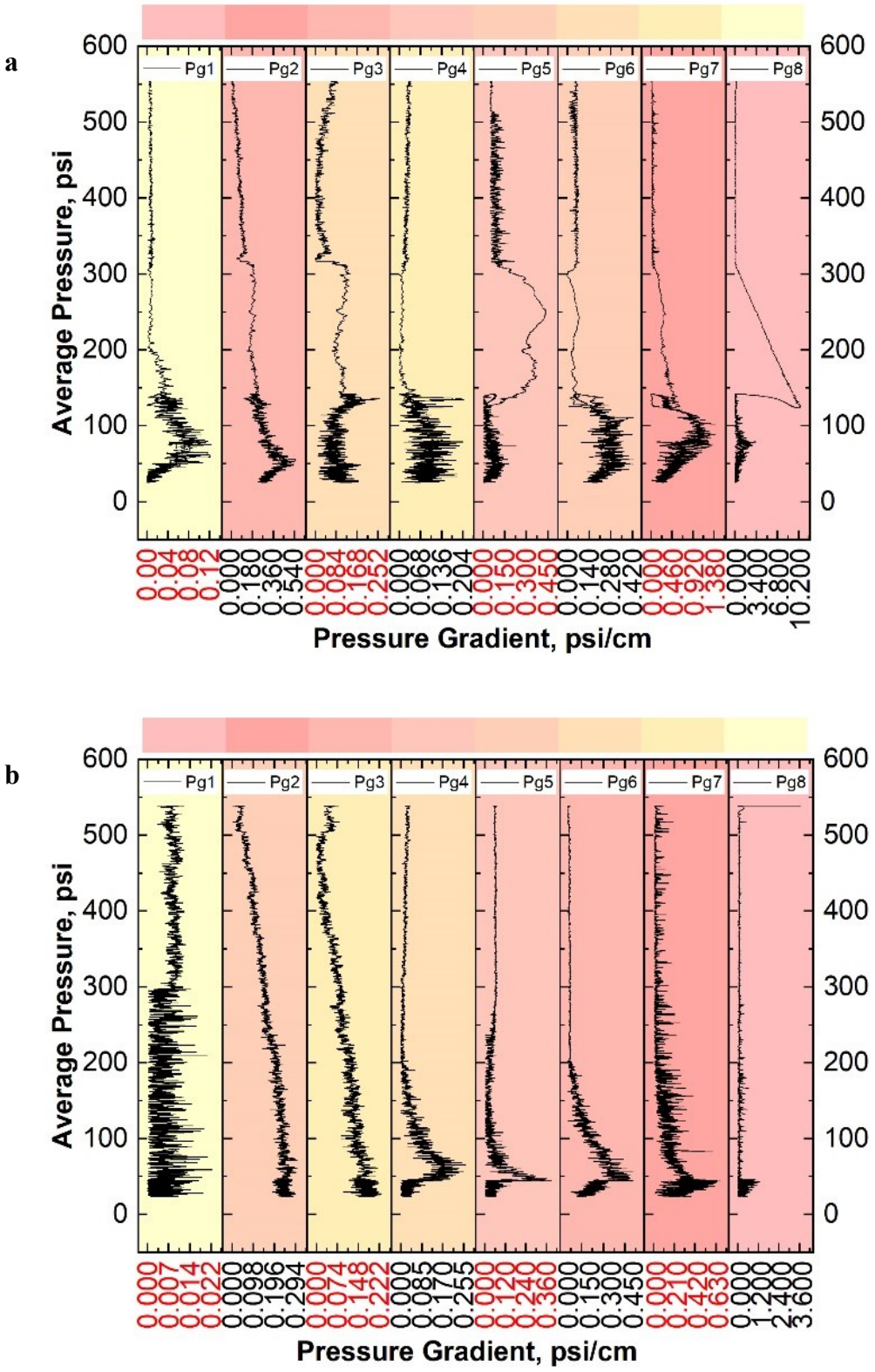

Figure 3.13—Pressure profiles for (a) Cycle 3, and (b) Cycle 4 for Test #4.

3.6 Economics of the In-Situ Formed Foamy Oil

Enhanced oil recovery projects in heavy oil reservoirs can be more expensive than in conventional ones, thus, there is a need to make the process successful at the smallest possible cost. Solvent-based recovery techniques for heavy oil recovery are considered an economical alternative to thermal methods in thin and shallow reservoirs due to its advantageous availability and economic efficiency. A very detailed economic analysis of a solvent injection EOR process was presented by Zekri and Jerbi (2002). They conducted sensitivity analyses for oil prices, capital expenditures, operating expenditures, tax rates, royalty rates, and inflation. They stated that the economics of these kinds of projects will be positively impacted with higher oil prices, upgraded EOR technology, lower cost for gas injection, and solvent gas recycling and reutilization.

Sun *et al*. (2016) observed a significant improvement on foamy oil formation effectiveness and stability, resulting in a higher final heavy oil recovery, by using methane as a gas drive energy provider and a foaming agent that promotes the in situ formation of foamy oil and improves its stability. Aiming to lower the cost for solvent usage and improve the efficiency of heavy oil recovery, Basilio and Babadagli (2019) performed laboratory experiments for in-situ formed foamy oil recovery. They used methane as the solvent gas and air as a foaming ameliorative in three different ways: (1) using pure methane; (2) using a mixture of air-methane in a gas composition ratio of 1:1; (3) alternating injection of methane and air in five consecutive cycles. They found out that using alternating methane-air injection strategy is better than the sole injection of methane, resulting in higher recovery factors with less use of solvents. This is technically due to the positive effect of air on the stability of foamy oil by increasing oil viscosity to certain extent if injected before methane. From a financial perspective, they reported that using air and solvent can save up to 51% in solvent usage, and it is conceivable that this technique can succeed because it would be economically beneficial.

3.6 Conclusions

From the live oil (primary recovery) and dead oil (secondary recovery) foamy oil flow experiments available in the literature, three conclusions can be pointed out. First, post-CHOPS reservoirs are suitable candidates for a CSI process, since the high permeability facilitates the diffusion of solvent and allows the in situ generation of foamy oil. Although the general trend and the effects of certain

operating parameters have been studied, a comprehensive mathematical and physical description that allows the prediction of the foamy oil behavior is still lacking, hence a considerable effort is required to obtain a clear definition. Second, soaking time and injection pressure during secondary recovery are two operating parameters that should not be taken separately as the pre-defined operating injection pressure will allow establishing the critical supersaturation pressure, and the soaking time will allow the solvent to distribute itself throughout the surface area of the heavy oil. However, depending on the project objectives, an optimum injection pressure based on the mole fractions of solvents needed for the volume of the dead oil should be defined. Third, according to the heavy oil composition, laboratory experiments and upscaling studies should be performed in order to find the right operating parameters such as pressure depletion rate and solvent injection strategy. Experimental tests with an Albertan heavy oil showed that a sequentially alternating injection strategy of air – methane and reducing the pressure of the porous medium at an "intermediate" depletion rate, led to obtaining high recovery factors with less than 50% solvent usage. The successful implementation of the CSI recovery process will depend on the strategy for making the process as inexpensive as possible requiring cautiously tailored experimental studies for pilot projects.

Chapter 4

Cost Reduction of Cyclic Solvent Injection Using Air in Heavy Oil Reservoirs: An Experimental Analysis to Determine Optimal Application Conditions

This chapter of the thesis is a revised version of the research paper submitted to the journal *SPE Reservoir Evaluation and Engineering*.

4.1 Preface

Primary recovery of heavy oil is characteristically ineffective due to low energy. Further production enhancement requires rigorous and expensive methods such as steam injection, solvent injection, or waterflooding with the help of chemicals. Methane and carbon dioxide are commonly used solvents in CSI (cyclic solvent injection) applications to energize the heavy oil deposits (making it foamy and increasing reservoir pressure) in thin, low permeability reservoirs, and after CHOPS (cold heavy oil production with sand); however, the high-cost yields an inefficient process. We propose a new approach to reduce the associated cost by using air to pressurize the reservoir and improve the foaminess process since we observed in our previous studies (Soh and Babadagli 2018, Basilio and Babadagli, 2018) that air causes an increment on heavy oil viscosity by almost 50%. This process reduces the cost as the amount of methane injected is curtailed, but the process needs to be optimized by determining the optimal application conditions by maximizing final heavy oil recovery.

To study the use of air for a technical and economic improvement of CSI with methane, pressure depletion tests were performed at a pressure depletion rate of -0.51 psi/min in a cylindrical sandpack, placed in a 150 cm long and 5 cm diameter sandpack holder supplied with eight evenly distributed pressure transducers and three thermocouples. The process consisted of three main stages: (1) injection, (2) soaking, and (3) production. Production profiles (pressure at every port, pressure differences, and pressure gradient) and saturation distributions were studied to determine the conditions yielding the best sweep and the highest oil and gas recovery factor with minimal use of gas injected. Different injection/production schemes (alternate or co-injection of an air-methane pair and different injector-producer alignments), depletion rates, and soaking times were tested to determine the conditions to maximize the recovery factor. Furthermore, observational experiments at a macroscopic and microscopic scale after the PVT tests were performed by recombining the heavy oil sample with sole air, sole methane, and a mixture of air and methane at a volume ratio of 1.

Using a mixture of air and methane not only expanded the volume of oil (gas bubbles trapped into the oil) by 2.5 but also delayed the defoaming process at both macroscopic and microscopic scales. Numerous tiny gas bubbles were initially observed, which kept its size and number for more time than the methane case, which is an indication of restraining fast bubble

growth and subsequent coalescence. The best injection strategy for a single-well injection scheme was the simultaneous injection of air and methane on a soaking period of 2–3 days, whereas for a multi-well injection scheme an alternating injection strategy on a soaking period of 4–5 days offered the best performance. Cumulative oil and gas recovery factors were as high as 27.46% and 76.68%, respectively, when air was accompanied by methane. Using air as a foamy oil ameliorative was observed to save up to 26% on methane use in single-well injection schemes and up to 51% on multi-well injection schemes.

Keywords: Optimization of Cold Heavy Oil Production, Co-Injection of Air and Methane, Foamy Oil, Cyclic Solvent Injection, Foamy Oil Sandpack Experiments.

4.2 Introduction

Despite the general understanding of heavy oil flow in a porous medium, in which a recovery factor of no more than 4–5% of the original oil in place is expected, some heavy oil reservoirs presented an anomalous behavior during primary recovery. This behavior included better-than-expected production rates, low produced gas-oil ratios, good pressure maintenance, and high recovery factors (Bora et al. 2000; Maini 1996). This unusual driving mechanism is known as the foamy oil flow and has been observed in many heavy oil reservoirs in Venezuela, China, Oman, Kuwait, USA (Alaska), and Canada (Chen and Maini 2005; Maini et al. 2010; Smith 1988). Foamy oil behavior mechanics is still not fully understood, and its generation and flow are currently under study. The in situ generation of foamy oil has been a subject of study by many scholars since foamy oil flow has been observed to provide better performance than the one forecasted by conventional simulators (Kumar and Pooladi-Darvish 2002; Sun et al. 2017). Foamy oil flow occurs mainly due to the exsolution process of dissolved gas, as consequence of induced pressure depletion. As pressure starts declining, size-negligible bubbles start nucleating, which grow in time as pressure declines mainly by expansion and diffusion (Bondino et al. 2009). These bubbles remain trapped due to viscous and capillary forces present in the oil high viscosity. Bubble trapping is one of the most important physical characteristics of foamy oil flow, since it will assist in maintaining the reservoir pressure and facilitate the high viscous oil flow in the direction of the gas flow (Maini et al. 2010), i.e. in the direction of the pressure drop, at a velocity greater than predicted for conventional flow theories. Further pressure reduction will lead to a bubble coalescence/break up and eventually ending in a single gas-phase formation, which is when the foamy oil mechanism per se has ended (Firoozabadi 2001; Sheng 2013). Foamy oil flow has been studied extensively in the laboratory by sandpack experiments since it allows control of the rate of pressure depletion and the real-time monitoring of the pressure distribution along the sandpack (Joseph 2002). Previous researchers focused on targeted parameters in order to understand their effects in the foamy oil flow performance. Li et al. (2012) and Zhang et al. (1999) studied the effect of reservoir temperature and found the existence of an intermediate temperature that depends on the viscous oil chemistry, at which a maximum recovery can be obtained. Ostos and Maini (2005) analyzed the effects of gravitational forces and reported that the highest heavy oil recovery was achieved when producing the viscous oil against the gravity force. Goodarzi and Kantzas (2008), Li et al.

(2012) and Sarma and Maini (1992) investigated the effects of absolute permeability and concluded that the final oil recovery is directly proportional to the absolute permeability since a better nucleation process occurs due to a higher contact area between the oil and the solvent. Liu et al. (2016) studied the effects of heavy oil viscosity and initial solution gas-oil ratio and concluded that a higher viscosity and a higher initial gas-oil-ratio affect the foamy oil performance positively, i.e. a higher recovery factor. Abusahmin et al. (2017) analyzed the effects of the saturation pressure and observed that even though the production performance was different, i.e. different production and gas rates, similar final heavy oil recovery factors were obtained. One of the most important parameters in foamy oil flow performance and extensively studied was the pressure depletion rate (Maini 2003; Ostos 2003; Li et al. 2012; Rangriz Shokri and Babadagli 2014; Liu et al. 2016; Abusahmin et al. 2017). Despite the difference in experimental arrangements (i.e. depletion rates, experimental temperatures, initial gas-oil-ratios, sandpack dimensions, initial oil saturation), and the difference in heavy oils used (i.e. heavy oil viscosity and specific gravity), they agreed that the dynamic process of bubble nucleation, growing and coalescence was more efficient at higher depletion rates also leading to higher recovery factors. Soh et al. (2018) and Zhou et al. (2016) reported the existence of a critical depletion rate, at which the highest recovery factor can be obtained, in both cases these critical depletion rates were different, suggesting that the value of a critical depletion rate is specific for every experimental condition. The characteristic of these previous experiments is that they were performed to understand mainly the primary recovery mechanism of foamy oil, meaning they saturated the sandpack with oil recombined with methane, and carried out a depletion process. In order to investigate the performance of foamy oil flow as an enhanced recovery method, Qazvini Firouz and Torabi (2012), Shi and Kantzas (2008), and Soh et al. (2018) externally injected solvent (gas) into an initially dead-oil-saturated sand pack and after a period of soaking time, they carried out the pressure depletion process. The main characteristic of this type of experiment was the cyclical methodology that reached up to nine cycles per experiment giving final recovery factors as high as 50%. To the best of our knowledge, only these few experiments were performed in order to investigate the feasibility of using methane injection as a solvent-based enhanced oil recovery technique and understand the performance of externally-generated foamy oil. Thus, more extensive experimental tests focusing on injection strategies, soaking times and experimental arrangements are needed for a better understanding of the process and its applicability in a cost-efficient way.

In our previous studies (Basilio and Babadagli 2018, 2019a, 2019b), we performed foamy oil experiments in a horizontally placed dead-oil-saturated sandpack, provided with an injection end and a producing end, being each of them located in both ends of the sandpack assembly. The experimental process consisted of three main stages: (1) gas solvent was injected by one side, (2) soaking time was allowed for the system pressure to stabilize, and (3) foamy oil was recovered on the other side. In this paper, a new configuration of the sandpack assembly is proposed, changing the common experimental scheme followed before by previous researchers (Shi and Kantzas 2008; Qazvini Firouz and Torabi 2012; Soh et al. 2018) when performing dead oil sandpack experiments. As explained before, methane was injected by the producing end into a sandpack horizontally placed and initially saturated with dead oil, only allowing a unidirectional distribution of the injected gas solvent. As an attempt of testing a more reservoir-like cyclic solvent injection (CSI) performance, the injection and production port was placed in the middle of the sandpack holder, allowing the gas to diffuse in different directions as it occurs in a real reservoir. With this configuration, the effects of wormholes in an after-CHOPS reservoir were observed to be beneficial for a CSI process, since the wormholes increase the area of contact between the solvent and the heavy oil, allowing a faster solvent diffusion and also improving the flow of the foamy oil toward the producer well (Du et al. 2015). The objective of placing this port in the middle of the sandpack was taking advantage of the smooth inner surface of the sandpack holder, which behaves as a high-permeability medium, acting as the wormholes observed in a post-CHOPS reservoir. It was observed that higher permeabilities allow a better foamy oil performance (Goodarzi and Kantzas 2008; Li et al. 2012).

The novelty of the present work is the use of air as an ameliorative for the stability of the methane foamy oil, with the objective of making the process cost-efficient, by minimizing the amount of methane injected into the reservoir. Furthermore, in order to understand the foamy oil flow in a more realistic injection strategy and under different injection schemes, then a new experimental scheme for a better understanding during the injection, soaking and producing stages was proposed. The results were also compared with another type of injection configuration and conditions and suggestions were made in order to achieve the most efficient and optimal operation conditions for practical applications.

4.3 Materials and Methods

The defoaming process of the foamy oil was analyzed by performing core scale experimental runs and also visual investigations at the macroscopic and microscopic scale. In these tests, foamy oil was generated by the nucleation of bubbles after depressurization of a gas saturated heavy crude oil. Fig. 4.1 shows the experimental setup used for these experiments. A high-pressure high-temperature stainless steel aging cell with an internal volume of 500 ml, with a maximum working pressure of 1800 psi at standard temperature, and a maximum working pressure of 1050 psi at 260°C, was utilized for this test. The general experimental procedure was carried out as follows:

1. A sample of 125 ml of dead crude heavy oil was poured into the cell and then pressurized at 500 psi with the desired solvent gas (methane, air, and a mixture of them).
2. After allowing suitable soaking time, i.e. it was stopped when no drastic changes in pressure were observed, the cell was placed in a lab stand and connected to a configuration of a needle valve and a coiled tube via a ball valve.
3. A sample of 20 ml was taken out of the cell and poured into a 150 ml-graduated Pyrex glass cylinder for the macroscopic observation. For the microscopic observation, a thin film of foamy oil was created by pouring two drops of foamy oil between two microscope slides, with a scale of 2200 µm length and 1467 µm width. These samples were the result of a depressurization process carried out by opening the ball valve, of which the main function was to prevent or limit the flow of gas/solvent mixture. Once it reached to the needle valve, it was opened gradually to avoid a drastic pressure drop. The objective of using tubing with a coiled geometry was to improve the bubble size distribution and stabilize the foam flow by avoiding a dramatic pressure drop since the coiled geometry helps to reduce the kinetic energy, and as a consequence reduces the impact energy (Blázquez et al. 2016).
4. The evolution of both microscopic and macroscopic observations was recorded with a high-resolution camera and a digital microscope, respectively.

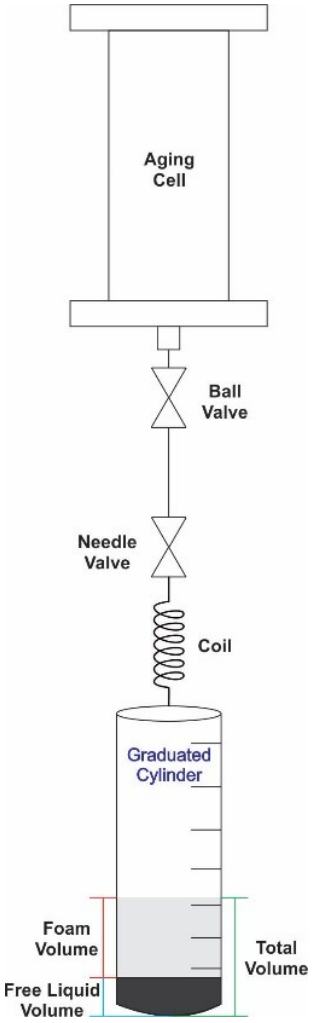

Figure 4.1—Experimental setup for the observational experiments

Furthermore, sandpack experiments utilizing a different approach then our previous studies were performed. The experimental setup utilized for these experiments is presented in Fig. 4.2, and it can be divided into three systems:

1. The injection system consists of a gas cylinder attached to a syringe pump, which is used to inject the solvent, methane, and air, at a pressure of 550 psi into a sand pack.
2. Sandpack porous medium was prepared using 250–500 μm grain size silica sand. The sandpack is located in a sandpack holder of 150 cm length and 5 cm diameter, which contains six pressure transducers to study the pressure evolution dynamics, and three thermocouples to monitor the temperature in the system. The pressure transducers and

thermocouple send electric signals (voltages) to a data acquisition device connected to a data acquisition computer, which after a cautious calibration convert the electric signals into pressure (psi) data.

3. The production system contains a back-pressure-regulator (BPR) attached to a syringe pump to control the pressure depletion process. Also, a seventh pressure transducer is located before the BPR to control the pressure in the tubing. The syringe pump coupled to the BPR is programmed to linearly reduce the producing pressure from 600 psi to 10 psi at a rate of 0.51 psi/min. It also contains a collection vessel located on top of an electronic balance, in order to monitor the foamy oil production over time. A gas flow meter is connected to the vessel to control the flow of gas and cumulative gas production. Sandpack preparation, properties measurement, and specification for every piece of equipment used in this type of experiment were detailed in our previous publication (Basilio and Babadagli 2018).

The sample of dead heavy oil used in the present study, for both types of experiments, was obtained from a reservoir in Eastern Alberta, Canada. The compositional analysis and the results of saturates, aromatics, resins, and asphaltenes (SARA) analysis, where the high mass percentage of heavy hydrocarbon compounds is evident, are shown in Fig. 4.3. One of the most important characteristics of the present study was the given soaking time for the solvent to diffuse effectively. During this stage, for both experiments, the entire system was shut-in and the evolution of the system pressure was monitored with pressure transducers. An initial soaking period of 48 hours was allowed, and taking into consideration the pressure drop due to gas dissolution, extra 24 h soaking-time was allowed cyclically, if necessary, until a maximum of ± 3 psi pressure change was observed.

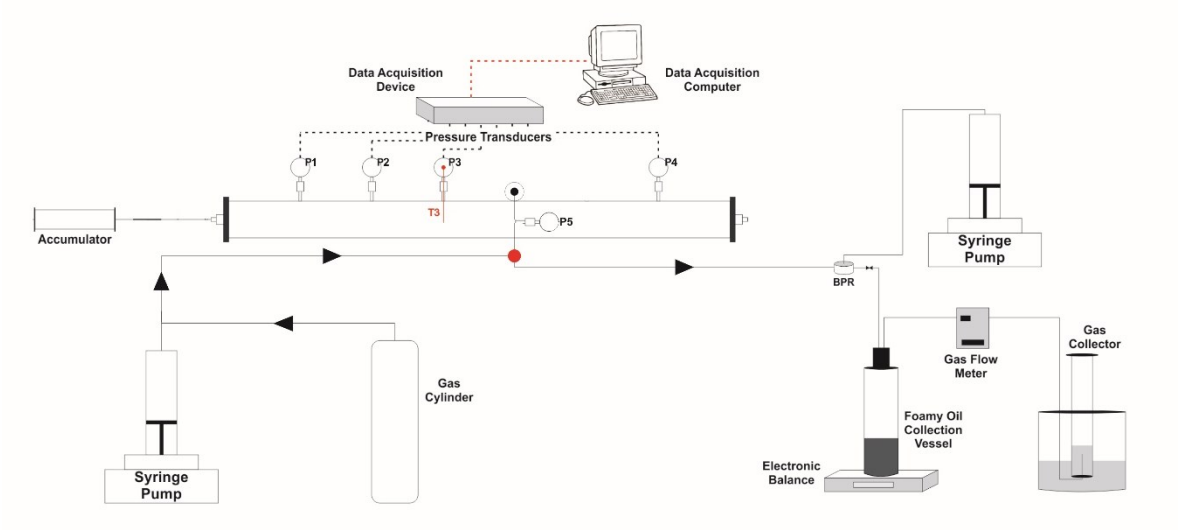

Figure 4.2—Experimental equipment used in all tests.

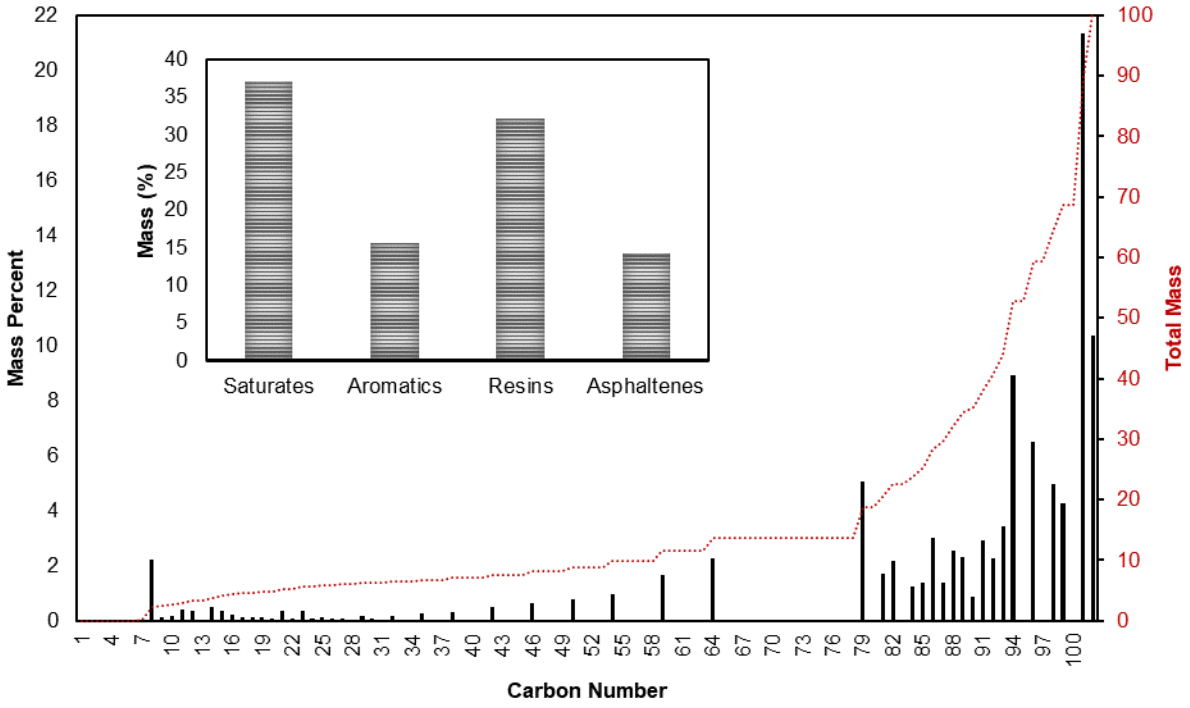

Figure 4.3—Compositional analysis and SARA analysis results of the dead heavy oil.

4.4 Experimental Results

Two different types of experiments were carried out, (1) observation cell experiments and (2) sandpack experiments. For both experiments, the effects of methane and air in the foamy oil performance, i.e. foamy oil generation and stability, were studied.

Observational Experiments

The objective of these experiments was to observe how different are the dynamics of foamy oil and how gas bubbles behave during the exsolution process at both scales, macroscopic (naked eye) and microscopic, in three different experiments. Foamy oil was generated utilizing sole methane, sole air, and a gas mixture of methane and air with a volume ratio of 1:1.

Macroscopic experiments performed in this study were intended to understand the foamability and collapse of foamy oil occurring at atmospheric pressure with different gases. In this regard, after pouring the gas-in-oil dispersion sample into the graduated glass, the dynamic process of the explosive foaming (bubbling) was observed for 24 hours.

Microscopic observations started after pouring two drops of the gas-in-oil dispersion on the microscope slide, the thin film was observed under the microscope lens during 24 hours at laboratory conditions. The gas bubbles distribution in the film was analyzed by calculating the total area occupied by the gas bubbles and divided by the total area of the film on an hourly basis. Furthermore, in order to understand the dynamic process of bubble nucleation and growth, the number of bubbles present in the film was counted every hour without regard to the bubble size, since they occur simultaneously. Bubble coalescence was studied by calculating the area of the largest bubble present in the film every hour since smaller bubbles are continuously merging into bigger bubbles. It is understood that the foamy oil mechanism was ended when a vast number of bubbles gradually merged to form a continuous gas phase.

Effects of Methane

Methane was observed to yield good foaming characteristics since as a hydrocarbon gas, it has a good affinity with heavy oil to form stable foams based on the pressure and temperature of the system (Morrison 1996). In this study, a volume expansion, i.e. (foamy oil volume)/ (dead oil volume), of 3.0 was observed when generating a methane-based foamy oil. Hence, the question

remaining for this study is “can this foaming performance be improved in a cost-efficient way?” Fig. 4.4a shows the macroscopic view of a fresh sample (0 hours) of methane-in-oil dispersion, it can be observed to the naked eye, that a vast amount of bubbles start appearing on top of the sample. It can be presumed that a higher amount of gas diffused into the oil, and once the external pressure was reduced to atmospheric pressure, bubbles start migrating from a region with higher pressure to a lower pressure region, the dynamic process was observed during a 24-hour period. Fig. 4.5a presents the microscopic observation at a time of 0 hours. To the selected scale, 178 bubbles were observed, and approximately 10 of these bubbles had a bigger-than-average size. Understanding the size of bubbles is very important to comprehend the stability and performance of foamy oil. As it was widely explained, as pressure drops, size-negligible bubbles start appearing in the bulk-oil, which increases in size due to mechanical expansion and diffusion as pressure further decreases. These tiny bubbles are the ones giving the heavy oil the foam-like appearance and are the main cause of foamy oil flow efficiency. However, it is important to note that the stability of the foamy oil relies on the capacity to avoid fast-growing bubbles, so rapid break up and coalescence is avoided. Fig. 4.6 shows the evolution over time of the macroscopically observed foamy oil, in which bubbles are not only increasing in number but also in size, becoming more visible every hour. At 24 hours, bubble-free spots can be observed, indicating the total exsolution of gas in those spots. Fig. 4.7 displays the microscopic observation of the methane-based foamy oil. Even though methane offers good foaming characteristics, it can be observed that only after 1 hour, bubbles considerably increased in size, and reaching total coalescence (end of foamy oil mechanism) after 15 hours.

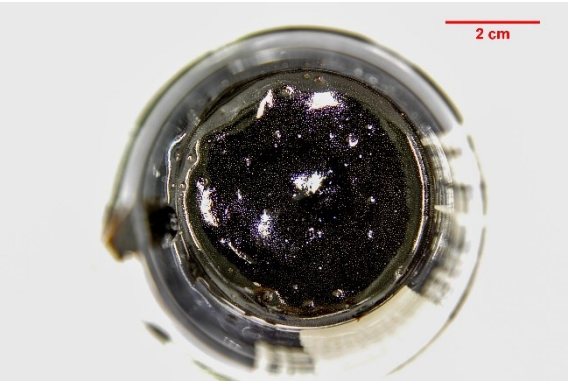

a. Methane based foamy oil

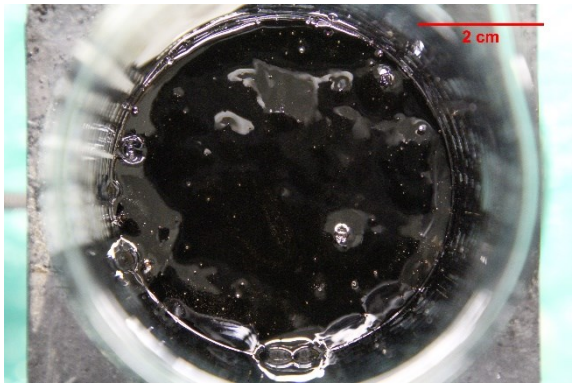

b. Air-based foamy oil

c. Foamy oil based on 50% methane – 50% air.

Figure 4.4—Macroscopic observation of the dynamics of foamy oil at t=0.

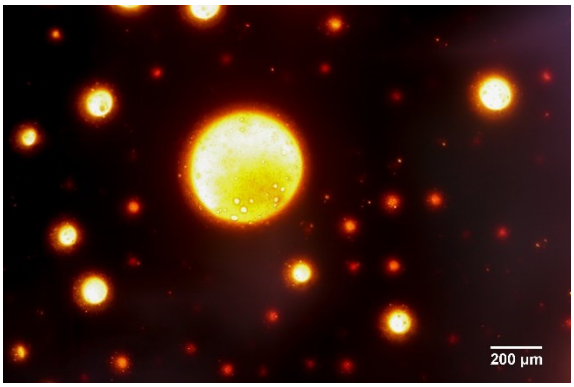

a. Methane based foamy oil

b. Air-based foamy oil

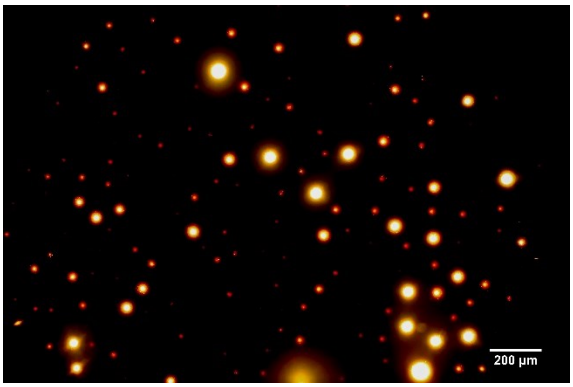

c. Foamy oil based on 50% methane – 50% air.

Figure 4.5—Microscopic observation of the dynamics of foamy oil at t=0.

Effects of Air

The main objective of using air is not the formation of foamy oil per se but to make the process more economical and efficient by reducing the use of solvent, i.e. obtaining similar results when using pure solvent, and improve the foaminess stabilization by increasing the heavy oil viscosity, as explained in our previous studies (Soh and Babadagli 2018; Basilio and Babadagli 2018). Different from methane, the volume expansion reached with air was observed to be 1.14, which demonstrates its poor foaming performance. Fig. 4.4b shows the macroscopic view of the air-heavy oil mixture at 0 hours, to the naked eye, it looks like a smooth surface with a few air bubbles on top. The low value of volume expansion is an indication that not only a small percentage of air was able to disperse into the oil but also that the number of bubbles generated by air was fewer than the ones generated with methane. Fig. 4.5b is a microscopic view of the air-based foamy oil—which differs from the methane foamy oil only—and a total of 24 bubbles can be observed at 0 hours. Fig. 4.8 shows the 24-hour macroscopic observation of air bubbles dynamics. Even though air has a poor foamability performance, the bubble sizes did not increase considerably as they did in the methane case, giving the heavy oil a long-lasting foamy-oil appearance. The microscopic observation of the bubble size evolution is presented in Fig. 4.9. Despite the lower number of bubbles when compared with methane, it is clear that the bubble breakup and coalescence occur at a slower rate (delayed), and even though bubbles continuously grow over time, after 24 hours total bubble coalescence was not observed.

t=1 h **t=4 h** **t=7 h**

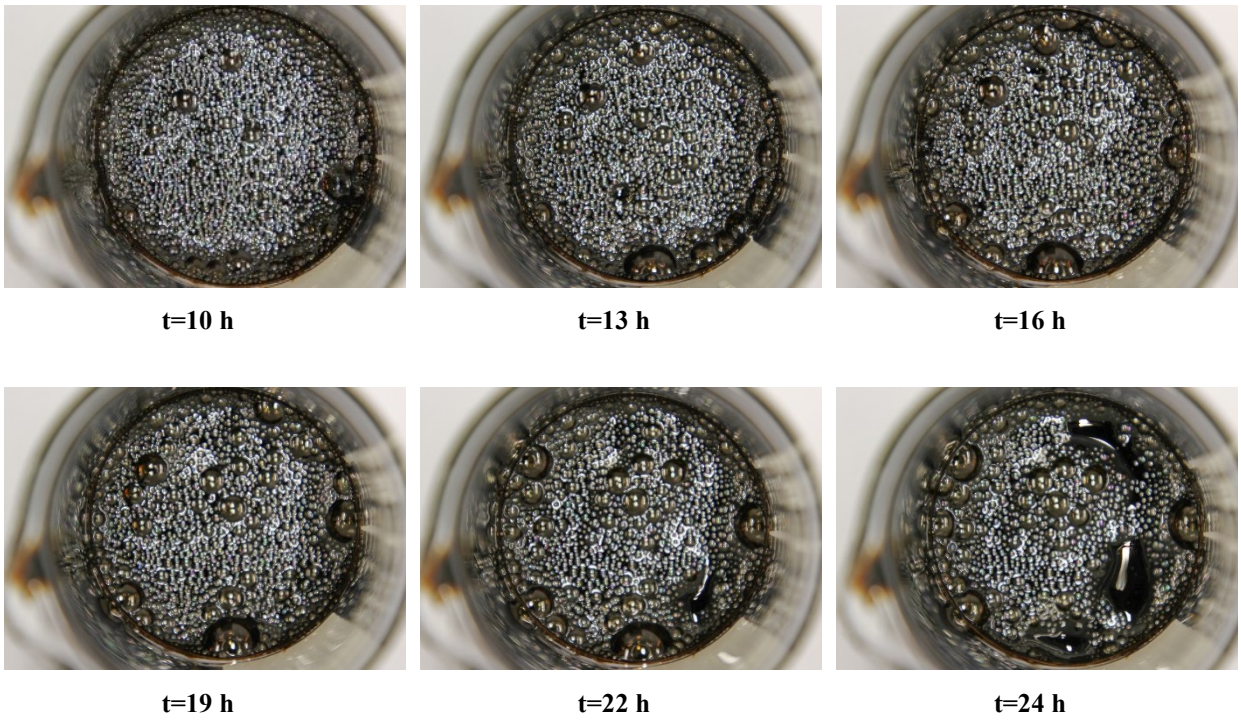

Figure 4.6—Macroscopic observation of methane-based foamy oil dynamics in 24 hours.

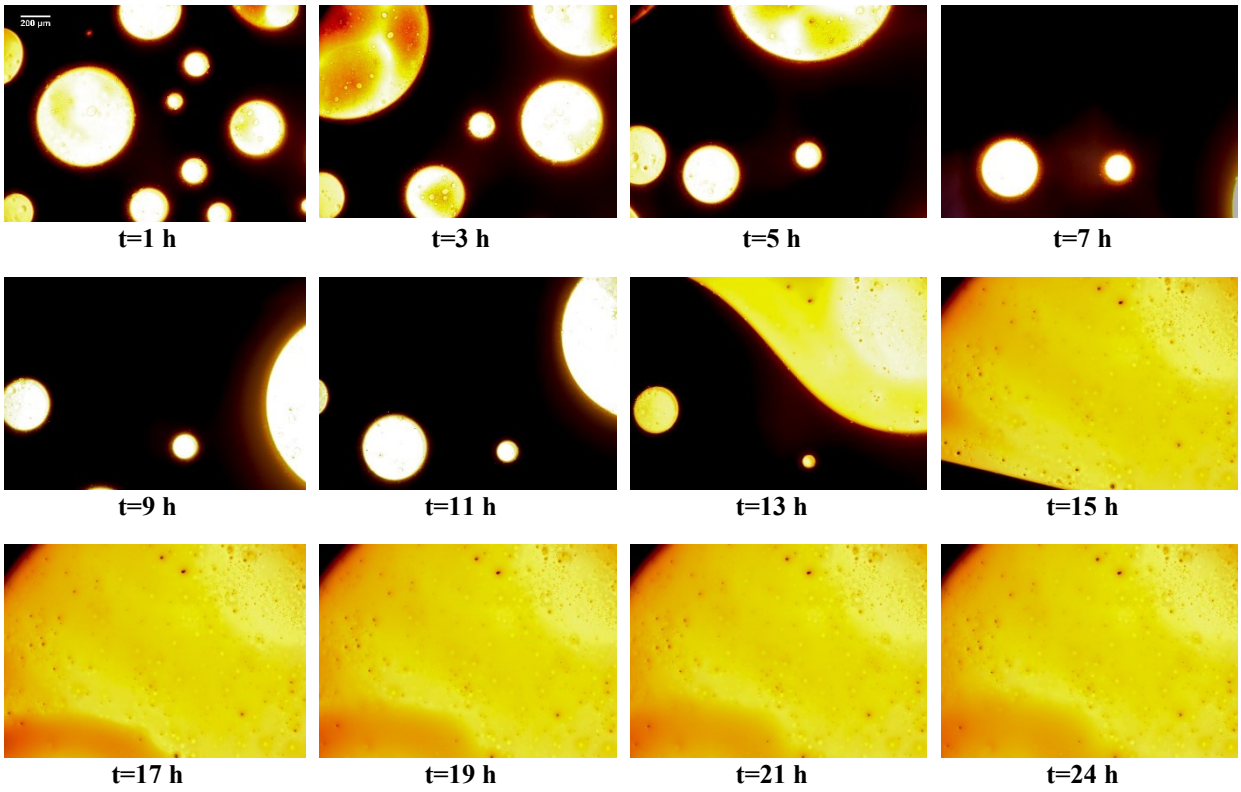

Figure 4.7—Microscopic observation of methane-based foamy oil dynamics in 24 hours.

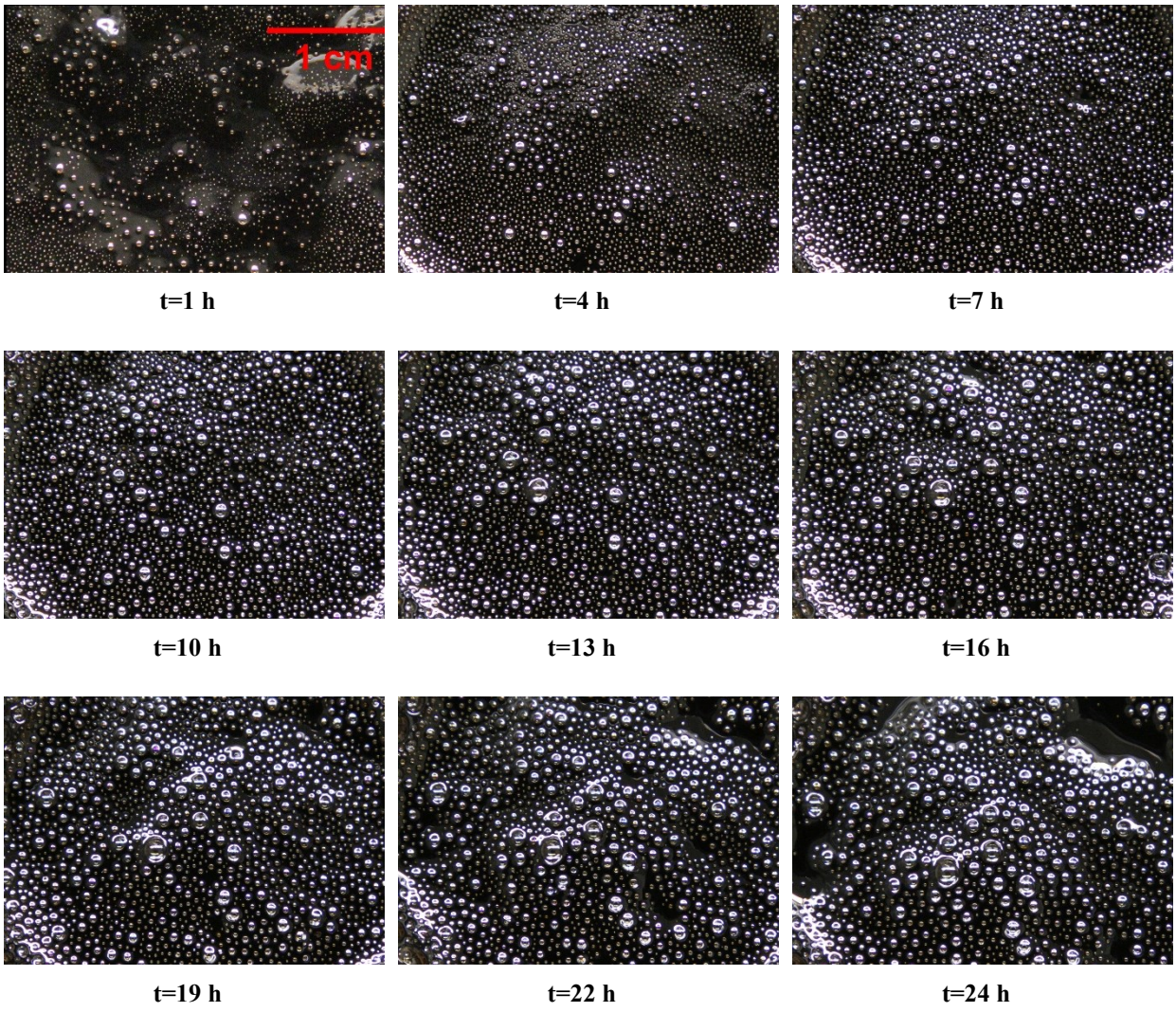

Figure 4.8—Macroscopic observation of air-based foamy oil dynamics in 24 hours.

Effects of air and methane mixture

The contemplation of delaying the coalescence process for the methane case was addressed by using air as a foaming ameliorative since air was observed to increase the viscosity of the heavy oil and delay the rapid growth of bubbles. Not too different from the methane case, using a mixture of 50% methane and 50% air resulted in a volume expansion of 2.5, indicating the good foamability characteristics of the mixture. Similar to the air case, to the naked eye, Fig. 4.4c shows the smooth surface, not foam-like appearance, present in the gas-in-oil dispersion at 0 hours. Microscopically, a vast number of bubbles are observed (371), having a smaller size than the methane-case bubbles (see Fig. 4.5c). The 24-hour observation of the sample poured into the glass cylinder is presented in Fig. 4.10, where the size of the observed bubbles is clearly smaller than the ones present in the

pure-methane foamy oil. However, after 24 hours, a bigger gas-free region than methane case is observed, suggesting that an optimum gas mixture should be explored. This will be the subject of further studies. The 24-hour microscopic observation is presented in Fig. 4.11. Conversely to the sole use of methane, bubble growth does not occur at a fast rate, and after 24 hours, complete coalesce (continuous gas phase) is still not observed. It confirms our previous hypothesis that air can help the foamy oil to be more stable, and greatly help in achieving not only a more efficient process but also reduce costs.

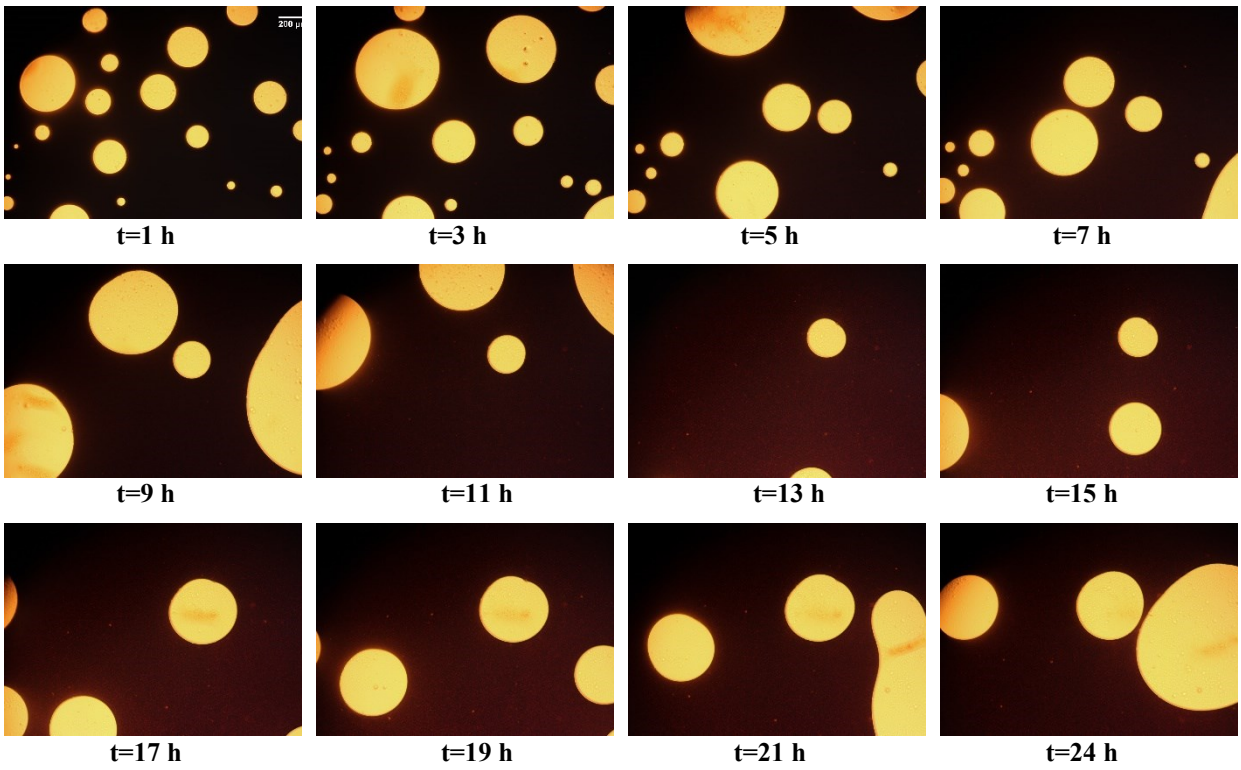

Figure 4.9—Microscopic observation of air-based foamy oil dynamics in 24 hours.

At a macroscopic scale, foamy oil stability can be understood by qualitative and quantitative evaluation of formability and collapse of foamy oil. In this study, the formability refers to the number of bubbles observed on the surface of the gas-in-oil dispersion. Fig. 4.12 shows the macroscopic gas bubble distribution, (total area occupied by gas bubbles) / (transversal area of the glass cylinder), for the foamy oil samples. As expected, methane shows the best foaming capacity, steeply increasing the number of bubbles over a 10-hour period, after this time, bubbles on the surface start collapsing, reducing the gas bubble distribution steadily. The collapse slope suggests that bubbles coalesce at a quasi-constant rate, with no agents to delay the bubble merging.

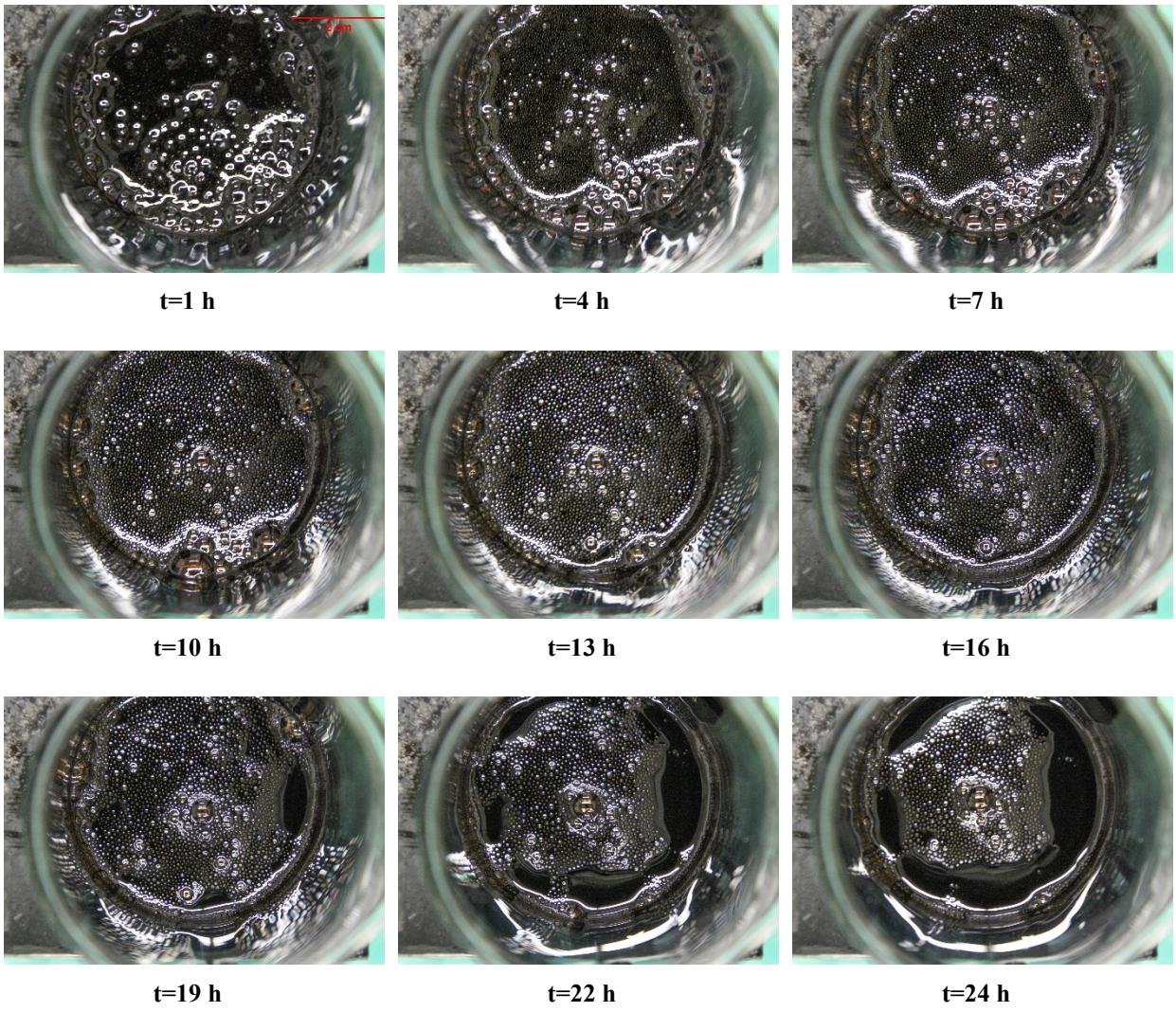

Figure 4.10—Macroscopic observation of the dynamics of foamy oil based on 50% methane – 50% air in 24 hours.

Conversely to methane, sole air shows poor foaming performance, starting the defoaming process only after 5 hours. However, an interesting observation is the very low reduction of gas bubbles distribution over time, keeping the gas bubble distribution almost constant in the next 19 hours. Two possible explanations can be dragged from this observation; (1) differently from methane, the quantity of air diffused into the oil was much less than for the methane case, resulting in a very poor volume expansion, and (2) even though the quantity of air diffused into the oil is much less, the collapsing process should have a similar trend as the methane case, however, the collapsing process (bubble nucleation, growth, and coalescence) seems to be slowed down,

resulting in a poor but stable foam. Since it was widely discussed that heavier viscosities result in more stable foams, this observation can be attributed to the increment in viscosity, as we previously observed and explained in our sandpack experiments the mechanism of air increasing heavy oil viscosity, confirming one of the hypotheses contemplated in our previous studies, which was considering air as an ameliorative for foamy oil stability. As expected, the foamability of the air and methane mixture is less efficient than using pure methane, reaching a peak of gas bubble distribution of 0.38 (compared to the 0.51 reached by methane). Nevertheless, at the atmospheric pressure, the defoaming process (collapse) was delayed for 3 extra hours, when compared with pure methane. Although the processes of bubble nucleation, growth and coalescence occur simultaneously, bubble coalescence can be greatly reduced if the mechanic expansion of the bubbles does not occur at a fast pace. This means the bigger the size of the bubble, the faster it will reach the surface and reach a higher gas bubble distribution in a shorter time. The collapse slope for the air-methane mixture is similar to the one observed for methane, with the exception of more erratic behavior, suggesting that tiny bubbles still remain trapped in the oil-bulk and will continue growing and driving the oil in the direction of flow.

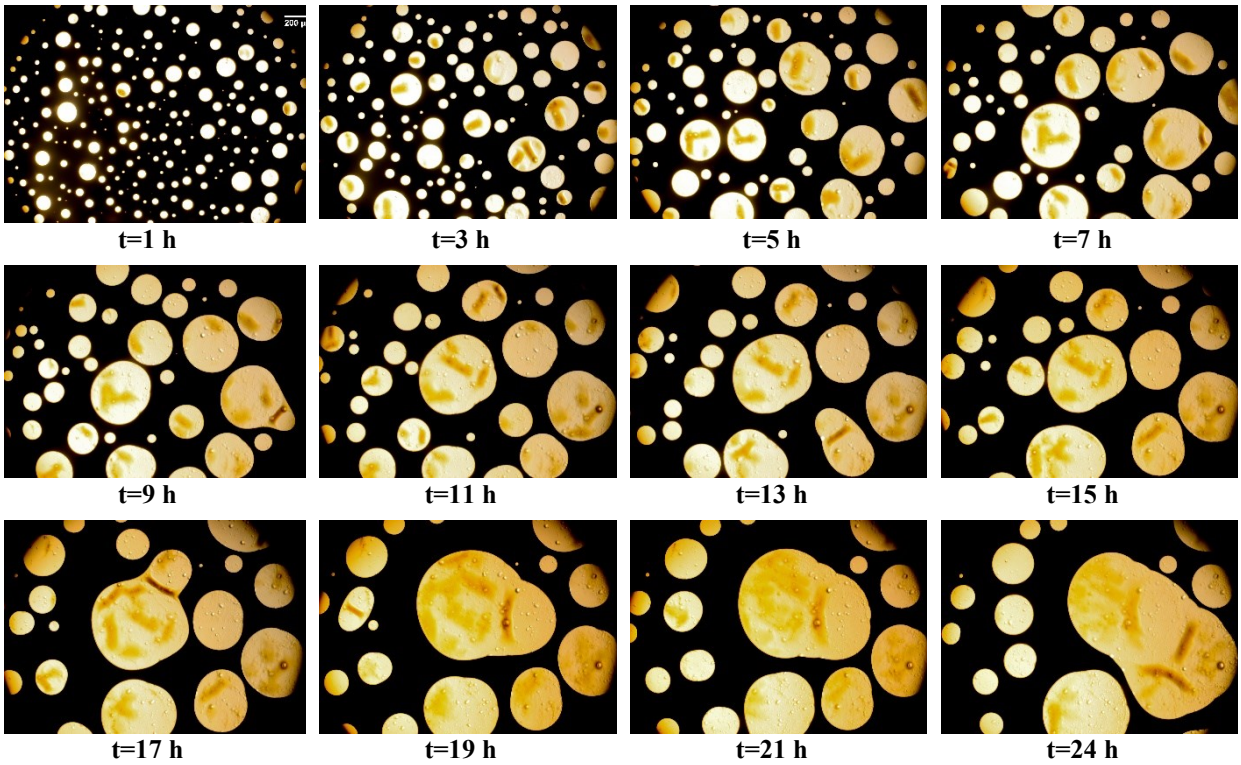

Figure 4.11—Microscopic observation of the dynamics of foamy oil based on 50% methane – 50% air in 24 hours.

Gas bubbles interaction was observed at a microscopic scale. Figs. 4.13–4.15 show the bubble dynamics at a microscopic scale in terms of the number of bubbles, gas bubble distribution, and maximum bubble size observed in a 24-hour period. As mentioned before, using methane alone leads to having good foaming characteristics, reaching a peak of 486 bubbles in 2 hours. However, since the viscous forces do not seem to be sufficient to restrain the bubble coalescence, the number of bubbles decreased drastically after 12 hours, and the gas bubble distribution nearly covering the entire microscope slide, after 16 hours. In other words, the foamy oil behavior ended after 16 hours, forming a continuous gas phase. This decrease is also confirmed by analyzing the maximum size of single bubbles, confirming that after 12 hours one single bubble occupies almost 100% of the area of the microscope slide. Once again, this observation confirms that coalescence (foam collapse) needs to be delayed in order to obtain a more stable foam.

It is also important to understand that the effectivity of the foamy oil mechanism relies on the number of bubbles trapped, and the time they can remain flowing without coalescing since these gas bubbles are the ones dragging the heavy oil in the direction of flow. The observation for the air-based foamy oil did not show a clear difference in the number of bubbles during the time of observation. Even though the number of bubbles was less than 50, this number remained quasi-stable, showing that neither nucleation (bubbles increment) nor coalescence (bubbles decrement) was as fast as the methane case. The low coalescence rate can be also observed in the gas bubble distribution curve, where only 32% of the microscope slide was occupied by the bubbles at the end of the observation. Also, the growth of bubbles seems to be restrained as well, since the maximum bubble size reached was 22% of the microscope slide, which is much less than the bubble size reached by methane. The main observation of using a mixture of 50% air and 50% methane was the tiny but numerous bubbles at the beginning of the observation (a total of 371 bubbles were observed at 0 hours). This number decreased drastically over time as a result of bubble coalescence. However, the gas bubble distribution was consistent indicating that there was no dramatic increment in bubble distribution in the 24-hour observation period. At the end of this observation, only a maximum of 53% of the microscope slide area was occupied by gas bubbles. Conversely to methane, this gas mixture showed much better stability in terms of delaying bubble growth and coalescence, with a maximum bubble size of 30% of the microscope slide.

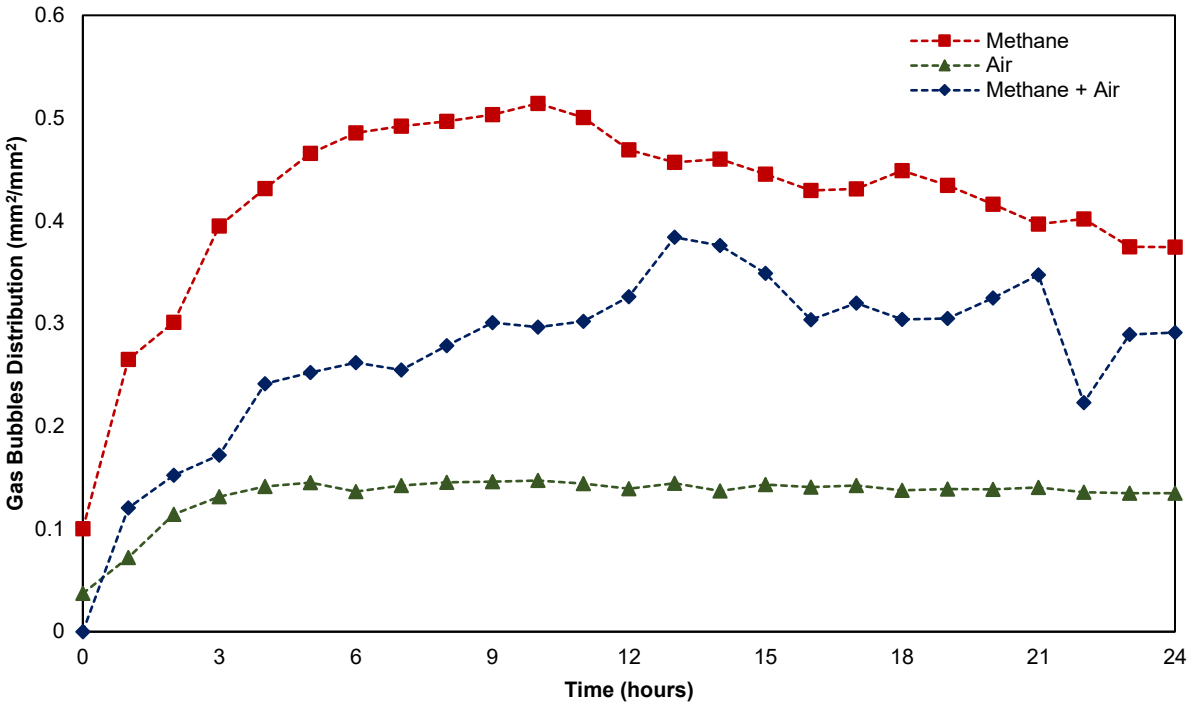

Figure 4.12—Foamability and collapse for foamy oil based on three different gasses at a macroscopic scale.

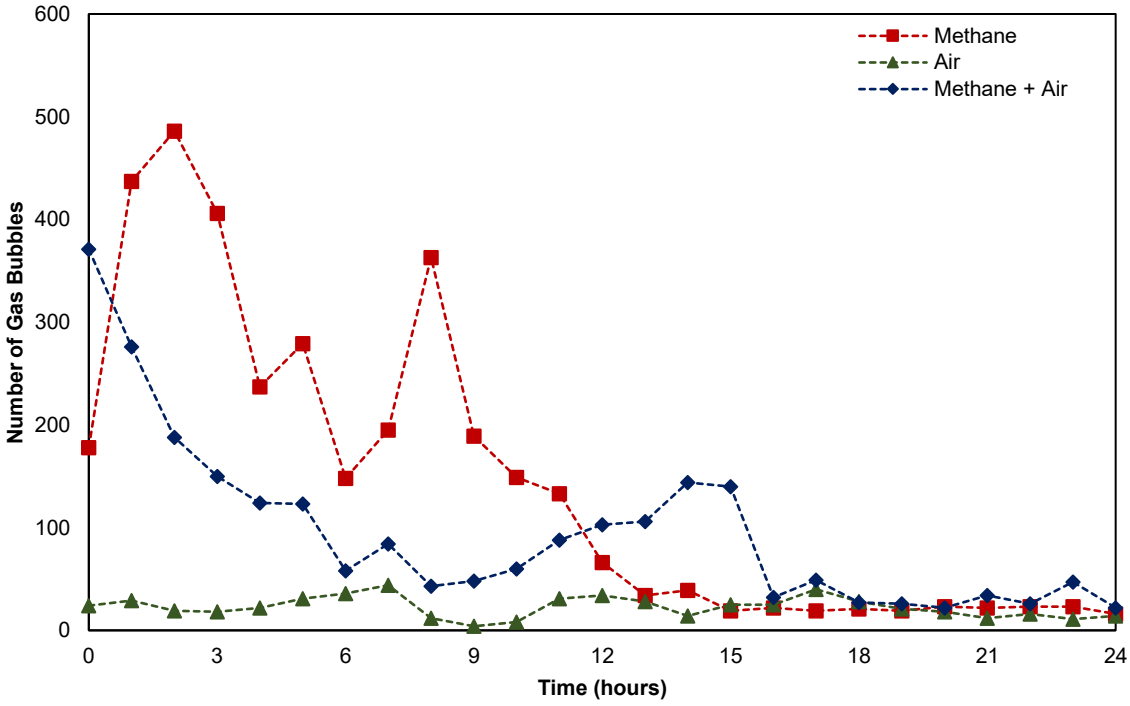

Figure 4.13—Number of gas bubbles observed for foamy oil based on three different gasses at a microscopic scale.

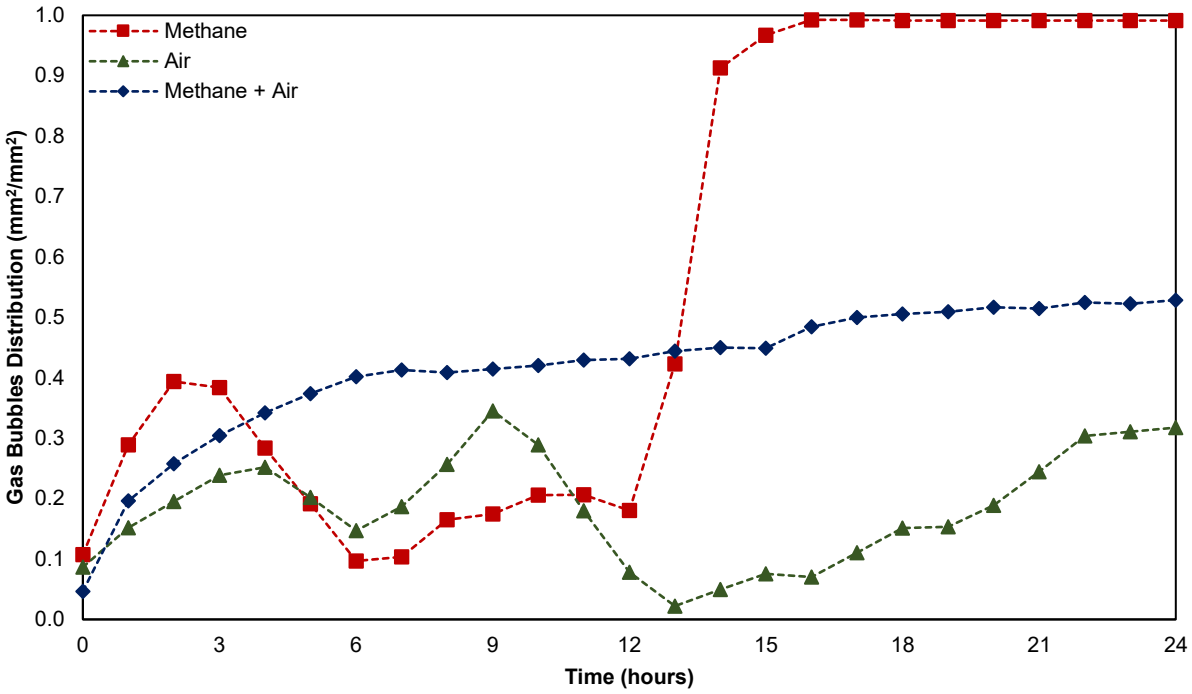

Figure 4.14—Gas bubbles distribution for foamy oil based on three different gasses at a microscopic scale.

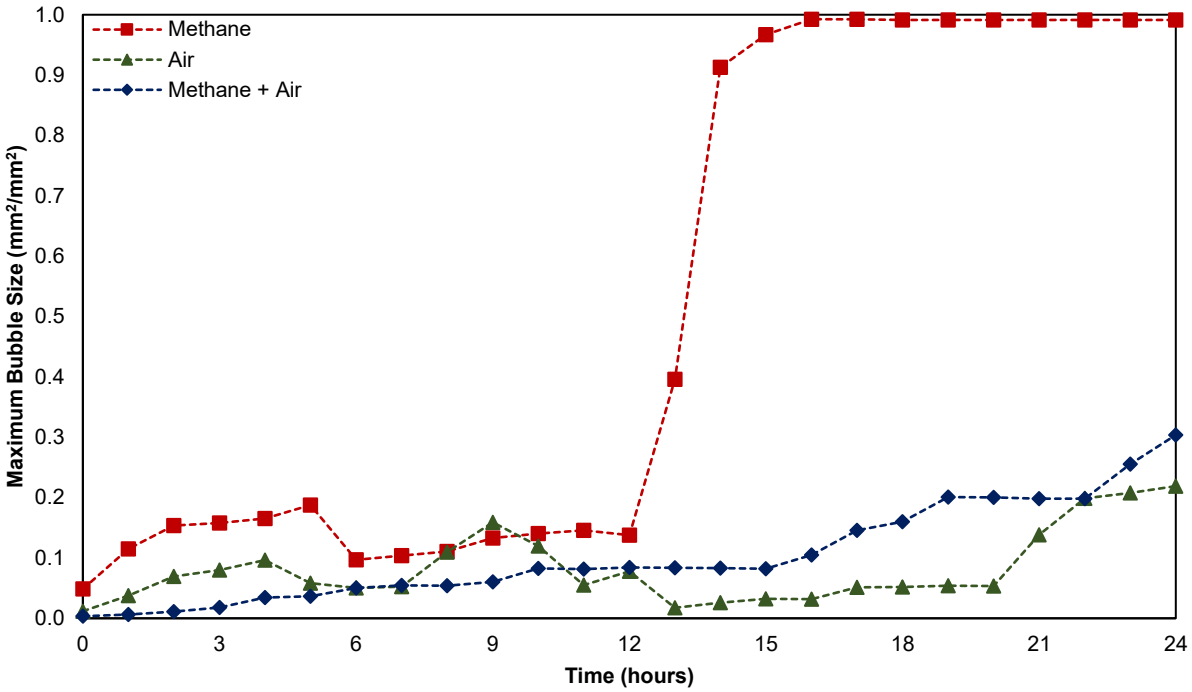

Figure 4.15—Maximum bubble size for foamy oil based on three different gasses at a microscopic scale.

Sandpack Experiments

Note that the objective of this study was to propose the most suitable injection strategy after a better understanding of the generation and stability of foamy oil. Therefore, three different sets of experiments were performed in order to understand the lab-scale foamy oil mechanism by injecting and producing the gas (solvent) through the same port. Table 1 describes the physical properties of the sandpack used for every test.

Test #1 was performed by injecting the gas horizontally from one end of the sandpack holder. Cycle 1 was performed using pure air, expecting to increase the heavy oil viscosity so that in Cycle 2 the injected methane could take advantage and generate a more stable foamy oil; however, both cycles resulted in very poor performance. Another cycle (Cycle 3) was performed using methane, expecting a better performance, but the outcome was still poor; therefore, only three cycles were performed for this test due to its poor performance.

Test #2 was run by injecting the gas in a horizontal (unidirectional) position. Cycle 1 was performed using methane, and since a poor performance was observed, methane injection was continued until Cycle 3. Because of the poor performance, which will be discussed below, the configuration of the setup was changed, placing the injection/production port in the middle of the sandpack holder. Thus, Cycles 4–6 were performed using methane, where a good performance was observed.

Test #3 was started using the new configuration shown in Fig. 4.3. Cycles 1 to 3 were performed with methane, and a similar performance for the three first cycles of Test#2 was observed. Cycle 4-6 were performed with the simultaneous injection of air and methane at a volume ratio of 1, expecting to improve the amount of heavy oil recovery because of the use of air, as previously explained.

Table 2 presents the results obtained for all tests. As part of a trial-and-error type experimentation, and because we observed from our previous experience that an alternating strategy resulting to be the most efficient, Test # 1 was started by injecting solely air to take advantage of viscosification of heavy oil for more stable foamization (as we previously discussed the increment of heavy oil viscosity to nearly 150% of its original value), prior to the injection of the gas solvent (methane). However, air did not only diffuse throughout the heavy oil but also

pushed the heavy oil away from the producing end. It was observed in the laboratory that after allowing a suitable soaking period (i.e. no major changes in pressure were observed), most of the gas remained "accumulated" in the tubing close to the injection port. Once the pressure in the backpressure regulator (BPR), reached less than 460 psi (initial injection pressure), the pressure in the sandpack was drastically reduced to 130 psi, resulting in a poor heavy oil recovery of 1.05% and a high gas recovery of 94.98%, indicating that most of the injected gas went out of the system. Cycles 2 and 3 were performed by using methane, and better results were not observed.

Table 4.1—Sandpack physical properties for each test.

Test	Porosity (%)	Permeability (D)	Pore volume (cm^3)
Test #1	42.96	9.84	1265.41
Test #2	40.15	10.08	1182.59
Test #3	41.72	9.15	1228.71

Test #2 was performed entirely with methane and served as a reference case for our further depletion tests when using air as a co-injection gas. The poor performance of injecting gas from one side of the sandpack holder suggested us to propose a more representative case when using a single injection/production port. In this regard, the location of the port was changed and placed in the middle of the sandpack. Positive results were observed after changing the location of the injection port, one of our hypothesis for explaining this better performance was based on the gas slippage effect due to the smoothness of the inner surface of the sandpack holder, behaving as high-permeability channels inside the sandpack and help in the gas diffusion process. This, in a sense, represents a reservoir with wormholes resulting in a post-CHOPS CSI.

It is noteworthy that the average soaking period for these tests was on average from 2–3 days. After performing the base case for this set of experiments, Test #3, was performed by using air as a co-injection gas. The main observation we can drag from this test was the poor performance in the first cycles. This can be attributed to the initial high saturation of heavy oil present in the sandpack since at the beginning of the test 86.84% of the pore volume is fully saturated with heavy oil leaving no space for the gas to diffuse effectively. As heavy oil was produced, more gas could be injected and a better foamy oil performance (heavy oil with a foamy aspect in the collection vessel) was observed. Cycle 4 exhibited the highest heavy oil recovery per cycle in this set of experiments, even higher than Cycle 4 from Test #2, which was entirely performed with methane.

4.5 Discussion and Suggestions

Thermal recovery methods such as steam injection and cyclic steam stimulation are the most widely applied enhanced oil recovery techniques in heavy oil reservoirs and have previously presented high recovery factors with good efficiency (Kumar 2006). However, in thin pay zone heavy oil reservoirs the result is less attractive, not only because of environmental impacts and energy balance considerations but because they do not result being cost-effective due to a severe heat loss (Chakma and Jha 1992) throughout the surrounding rock formations. These types of reservoirs are abundant in Canada (Srivastava et al. 1999) and need other options for EOR. High porosity unconsolidated sandstones heavy oil reservoirs straddling the Alberta-Saskatchewan border in Canada have been produced under cold heavy oil production with sand (CHOPS) technology, leaving behind an internal erosion as a form of a system of high-permeability channels due to the continuous production of the unconsolidated sand. This network of channels is known as wormholes (Chen 2006). Despite of the improved performance of CHOPS, when compared to a conventional cold heavy recovery, which achieves a maximum of 5% final recovery, they only presented final heavy oil recoveries of up to 20% of the original oil in place (OOIP), leaving behind a considerable amount of heavy oil, and a huge potential for the application of an enhanced oil recovery technique (Speight 2016) in these reservoirs.

The successful implementation of an enhanced oil recovery (EOR) technique can be complex and long-lasting, its application is related to the reduction of risks and uncertainties taking into consideration the economic feasibility of the project. For successfully implementing an EOR process, it is important to consider comprehensive screening criteria after selecting the candidate reservoir, so the most suitable EOR process can be determined. Once the EOR technique has been selected, and before performing pilot tests and the complete implementation along the reservoir, an extensive performance prediction and process design must be considered (Gharbi et al. 2012). The latter is considered to be the most important stage since not only the efficiency but also the associated costs of the project can be estimated. This stage includes performing comprehensive laboratory studies along with multi-scenario reservoir simulation studies. It is noteworthy that a good understanding of the selected EOR technique is the cornerstone for developing adequate reservoir simulation models (Vesna et al. 2014).

In this regard, we focused not only on the understanding of the foamy oil mechanism as an enhanced recovery technique (due to the beneficial characteristics such as pressure maintenance and the generation of local pressure gradients which helps to mobilize the oil toward the wellbore) but also its potential application in thin heavy oil reservoirs and post-CHOPS reservoirs. Our focus was also on the determination of the most suitable injection strategy by providing relevant experimental observations and supports to be also used as data in the field scale simulation studies. With these efforts, the outcome could be translated to a cost-reduction of the process.

In order to develop a mechanistic understanding of foamy oil flow in a porous medium, laboratory experiments under two different well arrangement scenarios were considered. Table 2 (Tests 2-3) shows the experimental results for a single-well arrangement, i.e. same port used for injection and production, and Table 3 (Tests 4-7) shows the results of our previous study performed for a multi-well injection scheme in a direct line drive arrangement, i.e. producer to injector ratio is equal to 1. Fig. 4.16 displays the amount of gas (PV) used for each test and Fig. 4.17 shows the final gas and oil recoveries.

Table 4.2—Summary of details and results of experiments based on a single-well CSI scheme.

Test	Cycle	Gas Composition	V_{gas} (PV)	P_{soak} (psi)	cGOR (Scm^3/cm^3)	Oil RF (%)	Total Oil RF (%)	Gas RF/Cycle (%)	Total Gas RF (%)
Test #1	Cycle 1	100% Air	0.01	460	105.89	1.05	4.32	94.98	85.26
S_{oi} = 86.85%	Cycle 2	100% Methane	0.04	485	61.35	2.44		76.56	
S_{wi} = 13.15%	Cycle 3	100% Methane	0.07	584	328.13	0.83		87.04	
Test #2	Cycle 1	100% Methane	0.02	500	4.00	1.55	26.11	8.74	67.42
S_{oi} = 87.44%	Cycle 2	100% Methane	0.03	512	42.49	2.23		67.07	
S_{wi} = 12.56%	Cycle 3	100% Methane	0.07	515	62.73	3.00		60.34	
	Cycle 4	100% Methane	0.09	565	37.35	6.78		63.22	
	Cycle 5	100% Methane	0.16	566	75.87	7.64		77.51	
	Cycle 6	100% Methane	0.23	560	150.98	4.91		67.95	
Test #3	Cycle 1	100% Methane	0.01	547	57.13	1.50	25.34	15.58	72.57
S_{oi} = 86.84%	Cycle 2	100% Methane	0.02	465	29.27	2.89		76.20	
S_{wi} = 13.16%	Cycle 3	100% Methane	0.04	533	33.71	4.77		85.24	
	Cycle 4	50% Air – 50% Methane	0.05	554	19.10	9.45		82.87	
	Cycle 5	50% Air – 50% Methane	0.08	559	52.12	4.83		64.20	
	Cycle 6	50% Air – 50% Methane	0.11	565	196.81	1.90		70.28	

Single-well CSI scheme injection experiments were performed in order to understand, in a more representative manner, the foamy oil generation by injecting gas externally to reservoirs previously produced under a CHOPS process. As previously explained, different experimental arrangements were performed in order to better represent the single-well CSI injection scheme and consider the existence of wormholes. It was discussed that for our laboratory conditions, the best

experimental arrangement was placing the injecting/producing port in the middle of the sandpack, since the smooth inner surface of the sandpack holder is not structured for fluid injection, the presence of the gas slippage phenomenon can be accounted to represent the extensive and high-permeability network of wormholes. This consideration was based on the large areal exposure of heavy oil to the injected gas when wormholes exist.

Table 4.3—Summary of previous experiments based on a multi-well CSI scheme (Basilio and Babadagli, 2019).

Test	Cycle	Gas Composition	V_{gas} (PV)	P_{soak} (psi)	cGOR (Scm^3/cm^3)	Oil RF (%)	Total Oil RF (%)	Gas RF/Cycle (%)	Total Gas RF (%)
Test #4	Cycle 1	100% Methane	0.11	532	0.02	3.36	26.45	0.01	61.62
S_{oi} = 87.77%	Cycle 2	100% Methane	0.13	571	21.02	8.48		29.48	
S_{wi} = 12.23%	Cycle 3	100% Methane	0.08	505	47.67	14.14		170.72	
	Cycle 4	50% Air – 50% Methane	0.31	538	2179.70	0.42		61.82	
	Cycle 5	50% Air – 50% Methane	0.29	542	18123.23	0.05		68.59	
Test #5	Cycle 1	50% Air – 50% Methane	0.16	551	52.06	2.37	23.49	14.93	46.29
S_{oi} = 88.04%	Cycle 2	50% Air – 50% Methane	0.08	563	23.08	7.60		45.93	
S_{wi} = 11.96%	Cycle 3	50% Air – 50% Methane	0.24	566	68.54	6.88		38.29	
	Cycle 4	50% Air – 50% Methane	0.28	546	218.45	2.94		45.94	
	Cycle 5	100% Methane	0.23	549	241.22	3.71		78.00	
Test #6	Cycle 1	100% Air	0.02	554	20.90	4.48	28.29	79.90	69.10
S_{oi} = 86.95%	Cycle 2	100% Methane	0.10	564	15.41	8.95		85.53	
S_{wi} = 13.05%	Cycle 3	100% Air	0.12	546	48.00	8.77		67.68	
	Cycle 4	100% Methane	0.28	573	347.96	3.58		86.47	
	Cycle 5	30% Methane after 70% Air	0.27	587	368.70	2.51		67.39	
Test #7	Cycle 1	100% Methane	0.01	567	0.00	2.70	27.30	0.00	71.79
S_{oi} = 87.43%	Cycle 2	100% Methane	0.08	562	26.29	10.81		66.69	
S_{wi} = 12.57%	Cycle 3	100% Air	0.15	556	60.86	7.57		61.37	
	Cycle 4	100% Methane	0.27	539	200.93	5.41		79.22	
	Cycle 5	100% Air	0.23	551	1075.96	0.81		73.75	

Test #2 was considered to be a base case since solely methane (which offers good foaming capabilities) had been used in six consecutive cycles. Total PV of methane used in this test was 0.6 at an average injection pressure of 536 psi. A total heavy oil recovery factor of 26.11% was achieved and a total of 67.42% of the injected gas during the six cycles was recovered, making the last three cycles the most efficient.

Test #3 was started with methane in three consecutive cycles, based on the previous experiment that higher recovery factors are achieved after the third cycle. Cycle 4-6 were selected to be performed with simultaneous injection of air and methane at a volume ratio of 1. Total PV of methane and air were 0.31 and 0.12, in the order of precedence. Cycle 4 resulted in the highest

recovery factor obtained in a single cycle, 9.45%, and the total heavy oil recovery factor was 25.34%, i.e. almost 40% of the cumulative production was obtained in a single cycle. The average injection pressure was 525 psi and the final gas recovery obtained was 7257%. On average, for all tests, soaking periods of 2 to 3 days were considered. As mentioned previously, the soaking period was considered to be finished when no drastic pressure changes were observed in the system for 24 hours, and producing times of 36 hours were observed for each cycle.

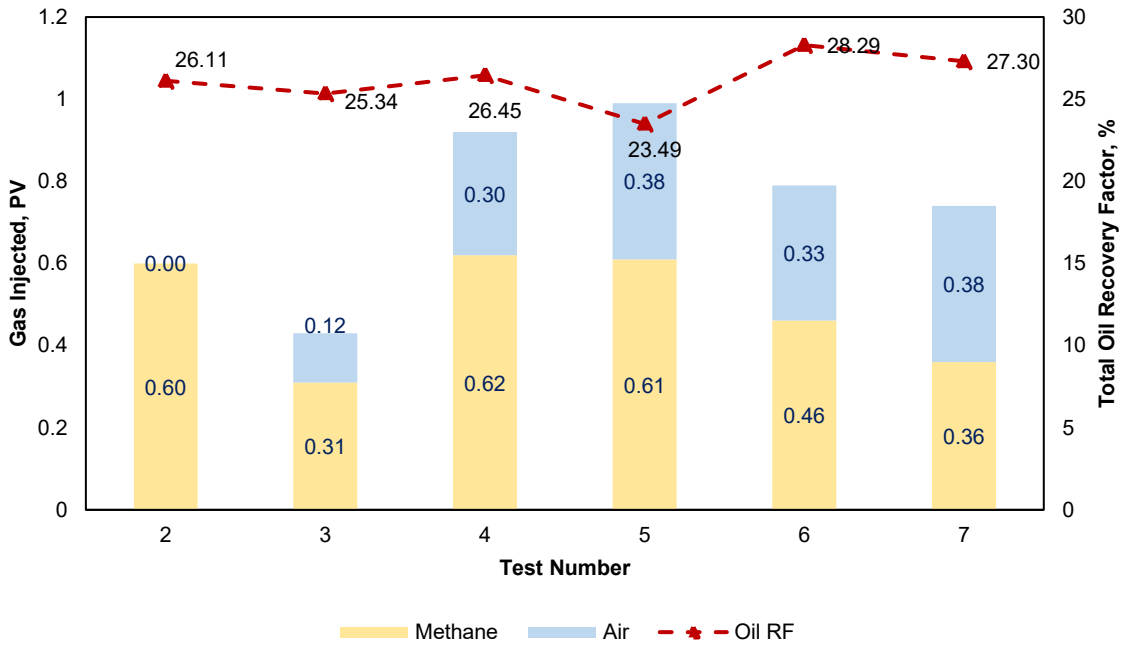

Figure 4.16—Injected gas PV for different injection strategies on single-well (2 and 3) and multi-well (4 to 7) CSI schemes.

Experiments performed under a multi-well CSI scheme were considered to be applied in thin heavy oil reservoirs, whether they had been previously produced by CHOPS technology or not. Different injection strategies were performed, based on five-cycle alternating gas injection (i.e. air injection followed by methane injection or vice versa) or simultaneous gas injection. Test #4 was considered as a base case, by injecting solely methane on three consecutive cycles, followed by two consecutive cycles of simultaneous injection of methane and air at a volume ratio of 1; all cycles were performed at an average injection pressure of 538 psi. Total PV of air and

methane injected in this test were 0.30 and 0.62, in the order of precedence. A total heavy oil recovery factor of 26.45% was achieved and 61.62% of the gas injected was recovered. The most efficient cycles were the ones when only methane was injected, suggesting the good performance of methane as an injection gas solvent due to its efficient diffusion into oil demonstrated by the final cGOR (0.02, 21.02, and 47.67 Scm3/cm3).

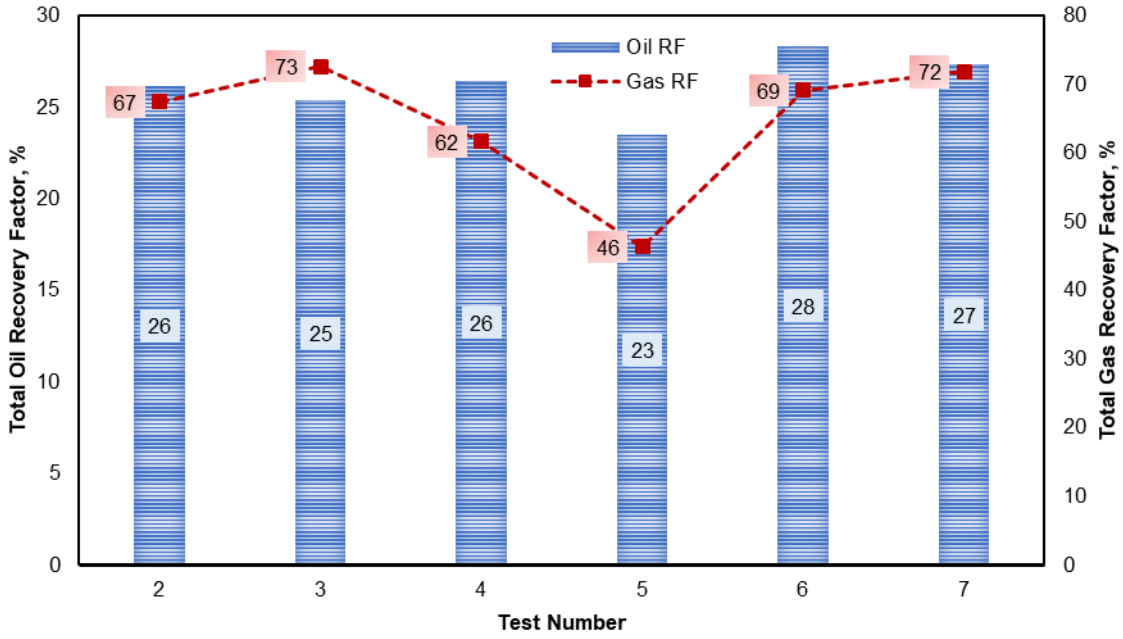

Figure 4.17—Final heavy oil and gas recoveries for different injection strategies on a single-well (2 and 3) and multi-well (4 to 7) CSI schemes.

Test #5 was run by simultaneously injecting methane and air at a volume ratio of 1 at an average injection pressure of 555 psi. The main objective was to reduce–as much as possible–the usage of methane; however, 0.38 PV of air and 0.61 PV of methane were used, meaning no drastic changes of methane usage were observed. Furthermore, a lesser performance was noticed when compared to the previous test, obtaining a final heavy oil recovery factor of 23.49%. A total gas recovery factor of 46.29%, along with final cGOR for the five cycles (maximum cGOR of 241.22 Scm3/cm3) suggest that a considerable amount of gas is still trapped in the reservoir producing good pressure maintenance, but not enough for dragging the oil toward the wellbore efficiently. Test #6 was performed under an alternating injection strategy. This test was started with air

injection in order to take advantage of two main characteristics: (1) producing heavy oil as a result of pressure drawdown, since air helps to pressurize the system, and (2) preparing most favorable conditions for the upcoming cycle when gas solvent, i.e. methane, is injected, since it was observed that air causes an increment on heavy oil viscosity, therefore, helping to form a more stable foamy oil. The average injection pressure for this system was 565 psi. In this test, the use of methane was reduced drastically, since a total of 0.46 PV of methane and 0.33 PV of air were used, achieving a heavy oil recovery factor of 28.229%, the highest recovery factor from all tests. Gas recovery factors of approximately 77% per cycle and a maximum cGOR of 368.70 Scm3/cm3 suggest not only the good pressure maintenance, present in all cycles but also the capacity of mobilizing the heavy oil toward the producing port. A similar performance was observed in Test #7, in which methane was initially injected in two consecutive cycles at an average pressure of 555 psi per cycle. Differently from the previous test, 0.00% of gas was recovered in the first cycle (79.90% was recovered in the previous test), generating only a 2.70% of heavy oil recovery. The advantage of the gas remaining trapped during the first and second cycle will cause a higher amount of oil being pushed toward the producing end when the sole air cycle begins, causing the need of less solvent usage. In this test, the lowest amount of gas was used, injecting only 0.36 PV of methane and 0.38 PV of air, and yet achieving a final heavy oil recovery factor of 27.30% and 71.79% of final gas recovery factor. On average, for all tests, soaking periods of 4 to 5 days were considered, as mentioned previously, the soaking period was considered to be finished when no drastic pressure changes were observed in the system (typically within 24 hours). The producing cycle was 48 hours in each cycle.

Figs. 4.18 – 4.21 present the performance of each cycle in term of heavy oil recovery factor and gas recovery factor for the aforementioned injection strategies, i.e. single-well (2 and 3) and multi-well (4 to 7) CSI schemes. It can be observed that for the single-well injection scheme, the best performance is obtained in cycles 4–6, whereas for a multi-well injection scheme the best performance is observed in cycles 1–3.

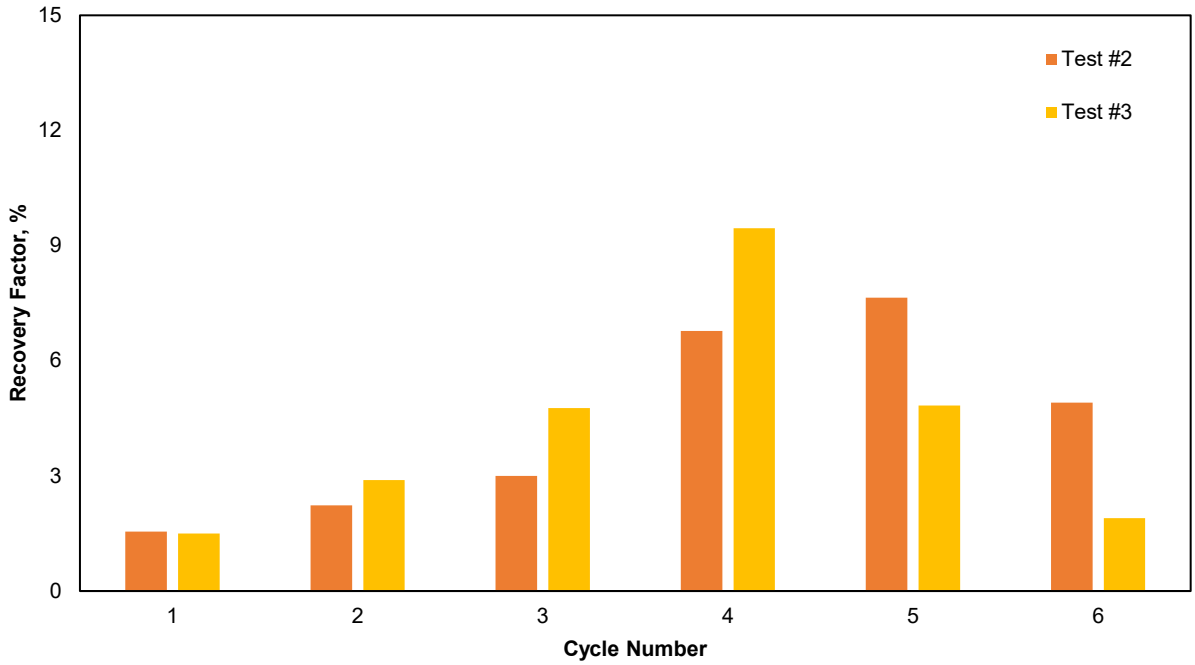

Figure 4.18—Heavy oil recovery factor based on a single-well injection scheme.

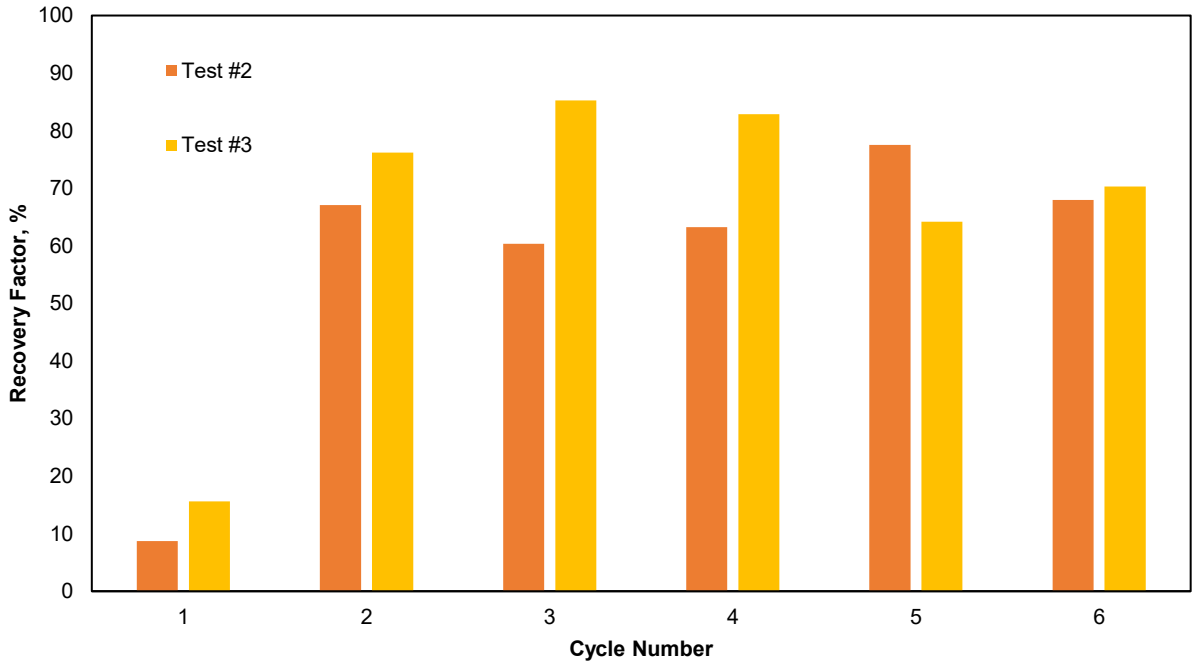

Figure 4.19—Gas recovery factor per cycle based on a single-well injection scheme.

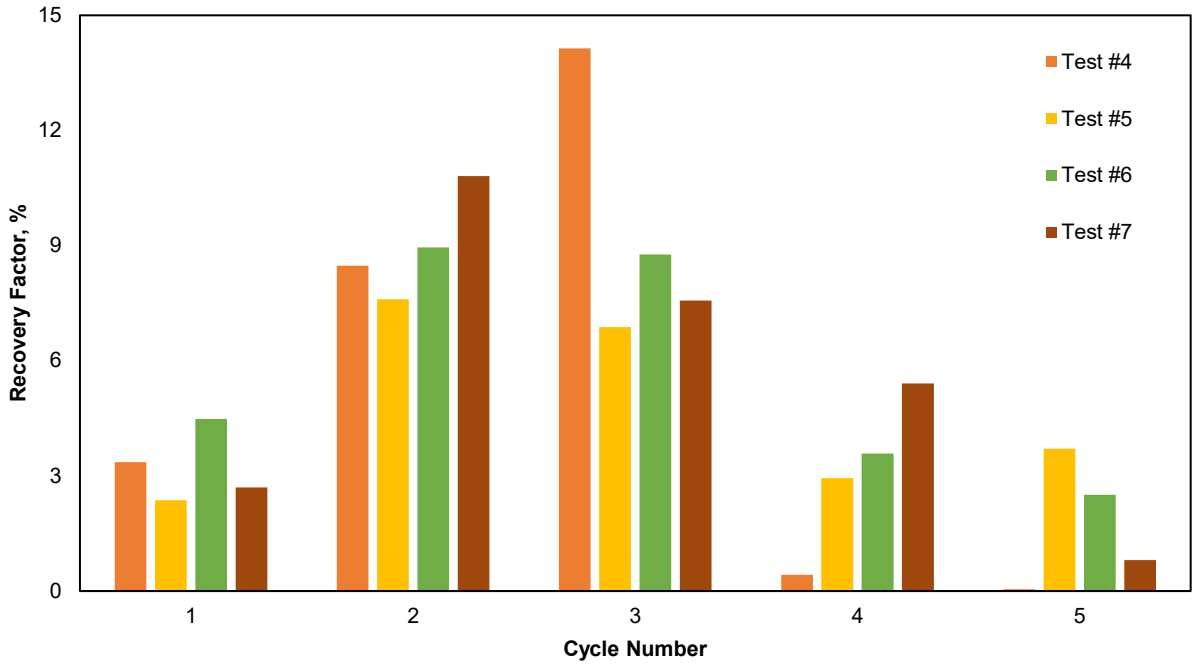

Figure 4.20—Heavy oil recovery factor per cycle based on a multi-well injection scheme.

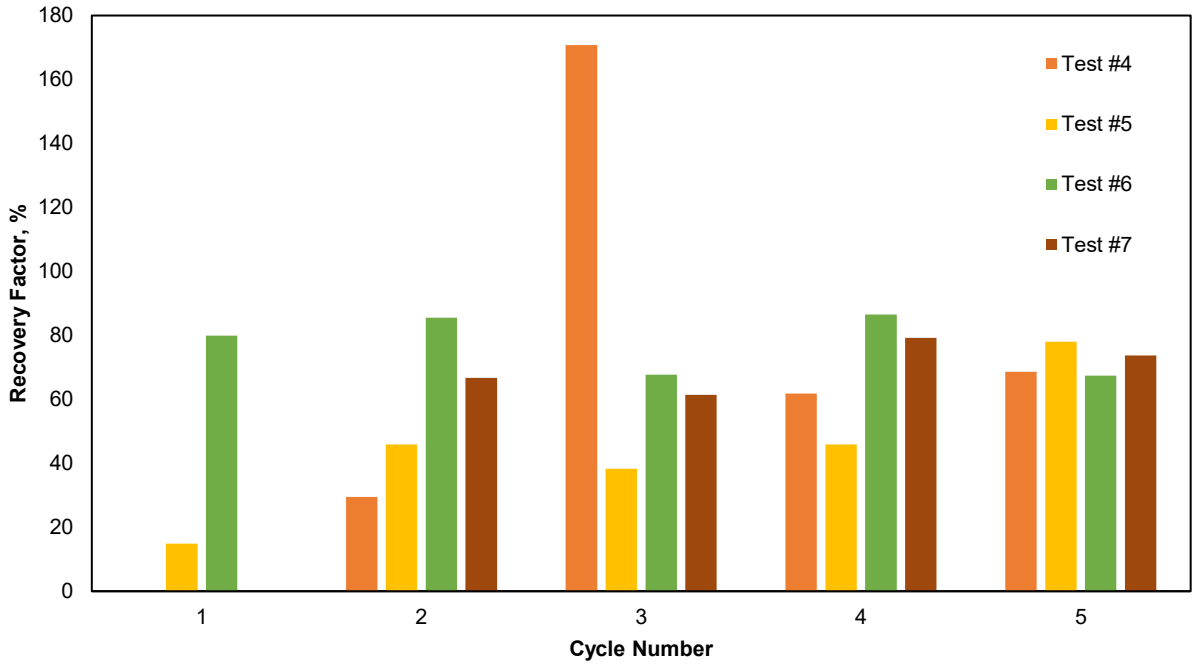

Figure 4.21—Gas recovery factor per cycle based on a multi-well injection scheme.

4.6 Conclusions and Remarks

Based on the sandpack and visual experiments performed using methane as the main solvent and air as foam stability ameliorative, the following conclusion can be drawn:

1. Air can be used as foam stability ameliorative as it increased heavy oil viscosity by almost 50%, and as observed in previous studies, foamy oil presents higher stability when viscosity is higher.
2. Methane is a good candidate for forming a good quality foam, with a volume expansion of 3. Despite its good foaming capabilities, it was observed that the defoaming process (bubbles grow, break up and coalescence) was faster than when mixed with air at a volume ratio of 1.
3. Air was also observed to have a very poor foaming performance, barely reaching 1.14 volume expansion. However, as previously observed, it is a good agent for increasing heavy oil viscosity and therefore increasing foamy oil stability when mixed with a gas solvent. Nevertheless, further studies should be performed to fully understand and characterize the negative contributions of using air a co-injection gas.
4. Using air as a co-injection gas delayed the defoaming process. Macroscopically, volume expansion of 2.5 was observed when mixed with methane. At a microscopic scale, different from using only methane as the solvent gas, initially generated (nucleate) a larger number of bubbles and to hold up the bubble growth, which in time helped to avoid the occurrence of fast bubble coalescence.
5. Two different injection (operation) approaches were considered in this study, i.e., single-well and multi-well injection schemes. Multi-well injection means, the gas was injected from the same well and the oil was produced from another well after a period of soaking by shutting the injection well. This was achieved by placing an injection port in one end of the sandpack holder and the other end port was used as a producer. This scheme was observed to be a good candidate for thin heavy oil reservoirs, whether they previously produced under a CHOPS technique or not. Single-well injection scheme was modeled by injecting the gas from the injection port and producing the oil from the same port, which was located in the middle of the sandpack holder. This approach improved gas distribution considering the smooth inner surface as high and interconnected permeability channels

surrounding the sandpack and helped improve the diffusion into oil. Hence, single-well injection schemes were observed to be good candidates for post-CHOPS applications, since the high-permeability channels present in these types of reservoirs expose a greater heavy oil surface area helping toward a more efficient gas diffusion process.

6. The injection strategies for single-well and multi-well injection schemes were observed to perform differently. Despite its capability of helping on improving foamy oil stability, air also helps to pressurize the system, since it does not diffuse into the oil efficiently. That is why starting with only air on a single-well scheme results in poorer performance since the oil surrounding the well is pushed further away and larger quantities of solvent and energy (higher pressure drawdowns) will be needed to bring the oil into the wellbore. We observed that injecting a mixture of air and methane (for this study a volume ratio of 1 was used) can help to obtain larger recovery factors per cycle than when using methane alone. Furthermore, an alternating injection strategy (sole air injection followed by sole methane injection or vice versa) was not found to be more efficient than the simultaneous injection of air and methane on a single-well injection scheme. On a multi-well injection scheme, even though the recovery factor might not be efficient, a single cycle can be performed by solely injecting air prior to the injection of methane, since besides helping on preparing more optimum conditions (higher heavy oil viscosity leading to higher foamy oil stability and performance) for the upcoming cycle when the gas solvent will be injected, it pressurizes the system and displaces the heavy oil toward the producing port. It was observed that for a multi-well injection scheme an alternating injection strategy has a better performance than the simultaneous injection of air and methane. Further research regarding volume injection ratios should be performed in order to find the optimum injection ratio.
7. Soaking periods for single-well injection schemes was observed to be on average from 2–3 days, which is less than the ones observed on multi-well injection schemes, being from 4–5 days on average. This was attributed to the difference on gas injection scheme, in the laboratory the single-well scheme takes advantage of the smooth inner surface of the sandpack holder (gas slippage effects) to easily distribute around the oil, where on a multi-well injection scheme, gas is injected to the middle of the sandpack (mixture of heavy oil and sand), making more difficult for the gas to be able to diffuse into the entire or most of the heavy oil present into the sandpack.

8. The pressure depletion ratio used in all tests was 0.51 psi/min, which was selected to be the best based on our previous laboratory experience. However, the use of different depletion rates for different gas composition should be a subject for further studies. Since each gas diffuses differently, depending on the volume ratio, generating a larger pressure drawdown in a shorter time (i.e. higher depletion rates), or generating a shorter pressure drawdown in a larger time (i.e. lower depletion rates) might generate different local pressure gradients behavior based on the gas composition which will affect the entire performance of the mechanics of foamy oil.
9. From an economic perspective, for a single well injection scheme, simultaneous injection of air and methane resulted on the most efficient strategy, helping to obtain larger recovery factors than when only methane was used and saving up to 67% of methane usage, whereas for a multi-well injection scheme alternating injection strategies of air and methane resulted not only in offering the most efficient performance (highest recovery factors) but also using a larger quantity of air, saving up to 51% on solvent usage.

Chapter 5

General Conclusions, Contributions and Future Work

5.1 General Conclusions and Contributions

Sandpack pressure depletion tests performed by previous scholars in order to understand the mechanics of methane-based foamy oil flow during the primary recovery of heavy oil. Even though the flow behavior is not entirely understood, foamy oil performance and stability are highly affected by some operating parameters. A foamy oil is considered stable when the dynamic behavior of bubble nucleation and growth occur efficiently, delaying the bubble coalescence and eventually forming a continuous gas phase, which in the end lead to obtaining higher heavy oil recovery factors. It was observed that higher values of absolute permeability, initial solution gas-oil ratio, heavy oil viscosity, average capillary number, and pressure depletion rates along with a low operating temperature, resulted in a better performance of foamy oil flow, translated in a higher final heavy oil recovery factor. It is noteworthy that optimum values (peaks) of operating temperature and pressure depletion rates were encountered and differed from each test. Furthermore, sandpack pressure depletion tests were also performed in order to understand the generation and behavior of a methane-based foamy oil by an external gas drive. It was observed that foamy oil flow performance and stability are positively affected by higher values of pressure depletion rate, heavy oil viscosity, and absolute permeability. The latter unlocks the potential application of externally generated foamy oil recovery with a CSI process as a post-CHOPS technique, where high-permeability wormholes are generated after the cold production process.

The successful implementation of the CSI recovery process on post-CHOPS and thin reservoirs depends on the strategy for making the process as inexpensive as possible requiring cautiously tailored and representative experimental studies. In this regard, besides using methane as the only solvent in sandpack experiments, air was used as a co-injection gas under different injection schemes and strategies. In addition to its low cost, air was mainly used to pressurize the system as well as to increase the heavy oil viscosity due to a low-temperature oxidation process and, therefore improving the foam quality when injected with/before methane. Furthermore, observational experiments were performed after recombining dead heavy oil with methane, air, and their mixture in order to study their efficiency on generating stable foamy oils. Observational experiments were performed by means of macroscopic (naked eye) and microscopic visualization which was interpreted through foamy oil stability parameters such as time of foamability and collapse, the number of gas bubbles, gas bubbles distribution, and maximum bubble size.

Based on the sandpack pack and visual experiments performed using methane as the main solvent and air as foam stability ameliorative, the following conclusions can be drawn:

1. Air has been observed to increase the viscosity of heavy oil by nearly 50% of its original value, unlocking the potential to be used foam stability ameliorative, since as observed in previous studies, foamy oil presents higher stability when viscosity is higher.
2. Methane has been observed to yield good foaming characteristics since as a hydrocarbon gas, it has a good affinity with heavy oil to form stable foams based on pressure and temperature of the system
3. Good volume expansion was observed when using methane for forming methane-based foamy oil, making it a good candidate for forming good quality foam. Despite its good foaming capabilities, it was observed that the defoaming process (bubbles grow, break up and coalescence) was faster than the one observed for the air and methane mixture.
4. Air was observed to have a very poor foaming performance. However as previously observed, it is a good agent for increasing heavy oil viscosity and therefore increasing foamy oil stability when mixed with a gas solvent.
5. Using air as a co-injection gas have been observed to delay the defoaming process. The initial generation (nucleation) of a large number of bubbles was observed and were kept for a longer time, holding up the bubble growth, which in time helped to avoid the occurrence of a fast bubble coalescence as it occurred with sole methane.
6. The injection strategies for single-well and multi-well injection schemes have been observed to perform differently. Despite its capability of helping on improving foamy oil stability, air also helped to pressurize the system, since it does not diffuse into the oil efficiently. That is why starting with only air on a single-well scheme, results in poorer performance, since the oil surrounding the well is pushed further away, and larger quantities of solvent and energy (higher pressure drawdowns) will be needed to bring the oil into the wellbore. We observed that injecting a mixture of air and methane (for this study a volume ratio of 1 have been used) can help to obtain larger recovery factors per cycle than when using methane alone. Furthermore, an alternating injection strategy (sole air injection followed by sole methane injection or vice versa) was not found to be more efficient than the simultaneous injection of air and methane on a single-well injection scheme. On a multi-well injection scheme, even though the recovery factor might not be

efficient, a single cycle can be performed by solely injecting air prior to the injection of methane, since besides helping on preparing more optimum conditions (higher heavy oil viscosity leading to higher foamy oil stability and performance) for the upcoming cycle when the gas solvent will be injected, it pressurizes the system and displaces the heavy oil toward the producing port. It has been observed that for a multi-well injection scheme an alternating injection strategy has a better performance than the simultaneous injection of air and methane. Further research regarding volume injection ratios should be performed in order to find the optimum injection ratio.

7. Soaking periods for single-well injection schemes have been observed to be on average from 2 – 3 days, which is less than the ones observed on multi-well injection schemes, being from 4 – 5 days on average.
8. In economic terms, air has shown to help to save considerable amounts of methane usage. In single well injection schemes, where the most efficient strategy was observed to be the simultaneous injection of air and methane, 26% of methane was replaced by air and resulted in higher recovery factors than when only methane was used. On the other hand, in multi-well injection schemes, where the most efficient strategy was observed to be the alternating injection methane and air, up to 51% of methane usage was saved by using air and achieving a much larger final heavy oil recovery factor when compared to similar experiments using only methane. Hence, it is conceivable that this technique can succeed because it would be economically beneficial.

5.2 Future Work

Many tests and experiments have been left for the future since they go beyond the scope of this research, but they are important to reduce uncertainties and conduct more representative experiments nonetheless. Future work concerns more comprehensive studies on specific aspects, mechanisms, and methodologies. Based on the challenges observed during the realization of this thesis, there is a need to perform more comprehensive work in the following aspects:

1. A predictive equation of state (EOS) for modeling the phase behavior of foamy oil is practically nonexistent. A representative EOS will help to obtain better results when performing numerical simulation studies.
2. The effects of the bubbles trapped into the oil on the relative permeability have not been addressed yet. Experimental work targeting this parameter will allow a better understating on the mechanics of foamy oil flow.
3. The negative effects of using air as a co-injection gas were not addressed in this research. Hence, further studies to fully understand and characterize these side effects are necessary.
4. Soaking time and injection pressure are mostly chosen based on field or laboratory experience. However, exploring the physics of the injection pressure along with soaking times, and considering the surrounding temperature, would lead not only to optimize the operating times but also operating costs.
5. The pressure depletion rate is an experienced-based parameter rather than physical-based. An equation for determining the optimum depletion rate based on the reservoir (permeability) and oil characteristics (composition, viscosity) is required to save experimental time and resources.
6. Upscaling studies are necessary to determine the viability and applicability of this type of EOR process, finding the most appropriate well arrangements and operating parameters such as pressure depletion rate and solvent injection strategy.

References

Chapter 1

Abusahmin, B.S., Karri, R.R., and Maini, B.B. 2017. Influence of Fluid and Operating Parameters on the Recovery Factors and Gas Oil Ratio in High Viscous Reservoirs under Foamy Solution Gas Drive. *Fuel* **197**: 497–517. https://doi.org/10.1016/j.fuel.2017.02.037

Albartamani, N.S., Ali, S.M.F., Lepski, B. et al. 1999. Investigation of Foamy Oil Phenomena in Heavy Oil Reservoirs. Presented at the SPE International Thermal Operations and Heavy Oil Symposium, Bakersfield, California, 17-19 March. https://doi.org/10.2118/54084-MS

Banerjee, D.K. 2012. *Oil sands, Heavy oil & Bitumen: From Recovery to Refinery*. Tulsa, OK. PenWell.

Bjorndalen, N., Jossy, W.E., and Alvarez, J.M. 2012. Foamy Oil Behaviour in Solvent Based Production Processes. Presented at the SPE Heavy Oil Conference, Calgary, Alberta, 12-14 June. https://doi.org/10.2118/157905-MS

Bora, R., Maini, B.B., and Chakma, A. 2000. Flow Visualization Studies of Solution Gas Drive Process in Heavy Oil Reservoirs with a Glass Micromodel. *SPE Reservoir Evaluation & Engineering* **3**(3): 224–229. https://doi.org/10.2118/64226-PA

Bret-Rouzaut, N., Favennec, J.-P., 2011. *Oil and Gas Exploration and Production: Reserves, costs, contracts*. Editions Technip.

Central Intelligence Agency, 2017. Crude oil - proved reserves — The World Factbook [WWW Document]. URL https://www.cia.gov/library/publications/the-world-factbook/fields/264.html (accessed 2.8.19).

Chakma, A. and Jha, K. N. 1992. Heavy-Oil Recovery from Thin Pay Zones by Electromagnetic Heating. SPE Annual Technical Conference and Exhibition, Washington, D.C., 4-7 October. SPE-24817-MS. https://doi.org/10.2118/24817-MS.

Chen, J.Z. and Maini, B. 2005. Numerical Simulation of Foamy Oil Depletion Tests. Presented at the Canadian International Petroleum Conference, Calgary, Alberta, 7-9 June. https://doi.org/10.2118/2005-073

Dong, M., Huang, S.-S.S., and Hutchence, K. 2006. Methane Pressure-Cycling Process with Horizontal Wells for Thin Heavy-Oil Reservoirs. *SPE Reservoir Evaluation & Engineering* **9**(02): 154–164. https://doi.org/10.2118/88500-PA

Du, Z., Zeng, F., and Chan, C. 2015. An Experimental Study of the Post-CHOPS Cyclic Solvent Injection Process. *Journal of Energy Resources Technology* **137**(4). https://doi.org/10.1115/1.4029972

Faergestad, I.M. 2016. The Defining Series: Heavy Oil. Schlumberger [WWW Document]. URL https://www.slb.com/resource-library/oilfield-review/defining-series/defining-heavy-oil (accessed 8.10.19).

Goodarzi, N.N. and Kantzas, A., 2008. Observations of Heavy Oil Primary Production Mechanisms from Long Core Depletion Experiments. *Journal of Canadian Petroleum Technology* **47**(4): 46–54. https://doi.org/10.2118/08-04-46

Huc, A.-Y. 2010. *Heavy Crude Oils - From Geology to Upgrading. An Overview*. Paris, France. Editions Technip.

Ivory, J., Chang, J., Coates, R., et al. 2010. Investigation of Cyclic Solvent Injection Process for Heavy Oil Recovery. *Journal of Canadian Petroleum Technology* **49**(9): 22–33. https://doi.org/10.2118/140662-PA

Jamaloei, B. Y., Dong, M., Yang, P. et al. 2013. Impact of Solvent Type and Injection Sequence on Enhanced Cyclic Solvent Process (ECSP) for Thin Heavy Oil Reservoirs. *Journal of Petroleum Science and Engineering* **110**: 169-183. https://doi.org/10.1016/J.PETROL.2013.08.028

Jia, X., Zeng, F., and Gu, Y. 2015. Gasflooding-Assisted Cyclic Solvent Injection (GA-CSI) for Enhancing Heavy Oil Recovery. *Fuel* **140**(15): 344–353. https://doi.org/10.1016/j.fuel.2014.09.066

Jiang, T., Zeng, F., Jia, X. et al. 2014. A New Solvent-Based Enhanced Heavy Oil Recovery Method: Cyclic Production with Continuous Solvent Injection. *Fuel* **115**: 426–433. https://doi.org/10.1016/J.FUEL.2013.07.043

Kraus, W.P., Mccaffrey, W.J., and Boyd, G.W. 1993. Pseudo-Bubble Point Model for Foamy Oils. Presented at the Annual Technical Conference, Calgary, Alberta, 9-12 May. https://doi.org/10.2118/93-45

Li, S., Li, Z., Lu, T. et al. 2012. Experimental Study on Foamy Oil Flow in Porous Media with Orinoco Belt Heavy Oil. *Energy & Fuels* **26**(10): 6332–6342. https://doi.org/10.1021/ef301268u

Liu, P., Li, W., Hao, M. et al. 2016. Quantitative Evaluation of Factors Affecting Foamy Oil Recovery in the Development of Heavy Hydrocarbon Reservoirs. *International Journal of Hydrogen Energy* **41**(35): 15624-15631. https://doi.org/10.1016/j.ijhydene.2016.04.031

Maini, B.B., Sarma, H.K., and George, A.E. 1993. Significance of Foamy-oil Behaviour in Primary Production of Heavy Oils. *Journal of Canadian Petroleum Technology* **32**(9). https://doi.org/10.2118/93-09-07

Maini, B.B. 2001. Foamy-Oil Flow. *Journal of Petroleum Technology* **53**(10): 54–64. https://doi.org/10.2118/68885-JPT

Maini, B.B. 2003. Effect of Depletion Rate on Performance of Solution Gas Drive in Heavy Oil Systems. Presented at the SPE Latin American and Caribbean Petroleum Engineering Conference, Port-of-Spain, Trinidad 27-30 April. https://doi.org/10.2118/81114-MS

Maini, B.B. and Busahmin, B. 2010. Foamy Oil Flow and its Role in Heavy Oil Production. *AIP Conference Proceedings* **1254**(2010): 103–108. https://doi.org/10.1063/1.3453794

Or, C., Sasaki, Y., Sugai, Y. et al. 2014. Numerical Simulation of CO2 Gas Microbubble of Foamy Oil. *Energy Procedia* **63**(2014): 7821–7829. https://doi.org/10.1016/j.egypro.2014.11.816

Ostos, A.N. and Maini, B.B. 2005. An Integrated Experimental Study of Foamy Oil Flow during Solution Gas Drive. *Journal of Canadian Petroleum Technology* **44**(4): 43–50. https://doi.org/10.2118/05-04-05

Pospisil, G., 2011. Heavy Oil Challenges & Opportunities - North Slope Alaska.

Qazvini Firouz, A. and Torabi, F. 2012. Feasibility Study of Solvent-Based Huff-n-Puff Method (Cyclic Solvent Injection) To Enhance Heavy Oil Recovery. Presented at the SPE Heavy Oil Conference, Calgary, Alberta, 12-14 June. https://doi.org/10.2118/157853-MS

Qazvini Firouz, A. and Torabi, F. 2014. Utilization of Carbon Dioxide and Methane in Huff-and-Puff Injection Scheme to Improve Heavy Oil Recovery. *Fuel* **117**: 966–973. https://doi.org/10.1016/j.fuel.2013.10.040

Rangriz Shokri, A. and Babadagli, T. 2017. Feasibility Assessment of Heavy-Oil Recovery by CO_2 Injection after Cold Production with Sands: Lab-to-Field Scale Modeling Considering Non-Equilibrium Foamy Oil Behavior. *Applied Energy* **205**: 615-625. https://doi.org/10.1016/j.apenergy.2017.08.029

Shayegi, S., Jin, Z., Schenewerk, P. et al. 1996. Improved Cyclic Stimulation Using Gas Mixtures. Presented at the SPE Annual Technical Conference and Exhibition, Denver, Colorado, 6-9 October. https://doi.org/10.2118/36687-MS

Sheng, J.J. 2013. *Enhanced Oil Recovery - Field Case Studies*. Lubbock, TX: Gulf Professional Publishing. https://doi.org/10.1016/C2010-0-67974-0

Sheng, J.J., Hayes, R.E., Maini, B.B. et al. 1995. A Proposed Dynamic Model for Foamy Oil Properties. Presented at the SPE International Heavy Oil Symposium, Calgary, Alberta, 19-21 June. https://doi.org/10.2118/30253-MS

Sheng, J.J., Maini, B.B., Hayes, R.E. et al. 1999. Critical Review of Foamy Oil Flow. *Transport in Porous Media* **35**(2): 157–187. https://doi.org/10.1023/A:1006575510872

Sheng, J. J. and Maini, B. B.: 1996, Foamy Oil Flow in Primary Production of Foamy Oil –A Literature Review. *The Petroleum Recovery Institute Report* 1995/96-7, pp. 2–10.

Sheng, J.J., Maini, B.B., Hayes, R.E. et al. 1997. Experimental Study of Foamy Oil Stability. *Journal of Canadian Petroleum Technology* **36**(4): 31–37. https://doi.org/10.2118/97-04-02

Shi, R. and Kantzas, A. 2008. Enhanced Heavy Oil Recovery on Depleted Long Core System by CH4 and CO2. Presented at the SPE International Thermal Operations and Heavy Oil Symposium, Calgary, Alberta, 20-23 October. https://doi.org/10.2118/117610-MS

Smith, G.E. 1988. Fluid Flow and Sand Production in Heavy-Oil Reservoirs under Solution-Gas Drive. *SPE Production Engineering* **3**(2): 169–180. https://doi.org/10.2118/15094-PA

Soh, Y. and Babadagli, T. 2017. Cost Effective EOR in Heavy-Oil Containing Sands by Gas Injection: Improvement of the Efficiency of Foamy Flow and Pressurization. Presented at the SPE/IATMI Asia Pacific Oil & Gas Conference and Exhibition, Jakarta, Indonesia, 17-19 October. https://doi.org/10.2118/186196-MS

Soh, Y., Rangriz-Shokri, A., and Babadagli, T. 2018. Optimization of Methane Use in Cyclic Solvent Injection for Heavy-Oil Recovery after Primary Production through Experimental and Numerical Studies. *Fuel* **214**: 457–470. https://doi.org/10.1016/j.fuel.2017.11.064

Soh, Y.J., Rangriz-shokri, A., and Babadagli, T. 2016. A New Modeling Approach to Optimize Methane-Propane Injection in a Field after CHOPS. Presented at the SPE Annual Technical Conference and Exhibition, Dubai, UAE, 26-28 September. https://doi.org/10.2118/181322-MS

Speight, J. 2014. *The Chemistry and Technology of Petroleum*, 5th Edition. Boca Raton, FL. Taylor & Francis Group.

Speight, J. 2016. *Introduction to Enhanced Recovery Methods for Heavy Oil and Tar Sands*, 2nd Edition. Cambridge, MA. Gulf Publishing Company. https://doi.org/https://doi.org/10.1016/C2014-0-01296-8

Srivastava, R.K., Huang, S.S., and Dong, M. 1999. Comparative Effectiveness of CO2, Produced Gas, and Flue Gas for Enhanced Heavy-Oil Recovery. *SPE Reservoir Evaluation & Engineering* **2**(3). https://doi.org/10.2118/56857-PA

Sun, X., Dong, M., Zhang, Y. et al. 2016. A New Foamy Oil-Assisted Methane Huff-N-Puff Method for Enhanced Heavy Oil Recovery in Thin Reservoirs. Presented at the SPE Canada Heavy Oil Technical Conference, Calgary, Alberta, 7-9 June. https://doi.org/10.2118/180742-MS

Sun, X., Dong, M., Zhang, Y. et al. 2015. Enhanced Heavy Oil Recovery in Thin Reservoirs Using Foamy Oil-Assisted Methane Huff-n-Puff Method. *Fuel* **159**: 962–973. https://doi.org/10.1016/j.fuel.2015.07.056

Turta, A.T., Maini, B.B., and Jackson, C. 2003. Mobility of Gas-in-Oil Dispersions in Enhanced Solution Gas Drive (Foamy Oil) Exploitation of Heavy Oil Reservoirs. *Journal of Canadian Petroleum Technology* **42**(3): 48–55. https://doi.org/10.2118/03-03-05

Warner, H.R. 2007. *Petroleum Engineering Handbook, Volume VI: Emerging and Peripheral Technologies*. Richardson, TX: Society of Petroleum Engineers.

Zhang, Y., Chakma, A., and Maini, B.B. 1999. Effects of Temperature on Foamy Oil Flow in Solution Gas-drive in Cold Lake Field. Presented at the SPE Annual Technical Meeting. https://doi.org/10.2118/99-41

Zhao D.W., Wang, J., Gates I.D. 2014. Thermal recovery strategies for thin heavy oil reservoirs. *Fuel* **117**: 431–441. https://doi.org/10.1016/j.fuel.2013.09.023

Zhou, X., Zeng, F., Zhang, L. et al. 2016. Foamy Oil Flow in Heavy Oil-Solvent Systems Tested by Pressure Depletion in a Sandpack. *Fuel* **171**: 210–223. https://doi.org/10.1016/j.fuel.2015.12.070

Zhou, X., Yuan, Q., Zeng, F. et al. 2017. Experimental Study on Foamy Oil Behaviour Using a Heavy Oil-Methane System in the Bulk Phase. *Journal of Petroleum Science and Engineering* **158**: 309-321. https://doi.org/10.1016/j.petrol.2017.07.070

Zhou, X., Yuan, Q., Peng, X. et al. 2018. A Critical Review of the CO2 Huff-N-Puff Process for Enhanced Heavy Oil Recovery. *Fuel* **215**: 813–824. https://doi.org/10.1016/j.fuel.2017.11.092

Chapter 2

Abusahmin, B.S., Karri, R.R., and Maini, B.B. 2017. Influence of Fluid and Operating Parameters on the Recovery Factors and Gas Oil Ratio in High Viscous Reservoirs under Foamy Solution Gas Drive. *Fuel* **197**: 497–517. https://doi.org/10.1016/j.fuel.2017.02.037

Albartamani, N.S., Ali, S.M.F., Lepski, B. et al. 1999. Investigation of Foamy Oil Phenomena in Heavy Oil Reservoirs. Presented at the SPE International Thermal Operations and Heavy Oil Symposium, Bakersfield, California, 17-19 March. https://doi.org/10.2118/54084-MS

Babu, D. R. and Cormack, D. E. 1984. Effect of Oxidation on the Viscosity of Athabasca Bitumen. The Canadian Journal of Chemical Engineering 62(4): 562–564. https://doi.org/10.1002/cjce.5450620417

Basilio, E. and Babadagli, T. 2018. Use of Air with Different Solvents Mixtures for Improved Foam Stability and Cost-Effective Heavy Oil Recovery. Presented at the SPE International Heavy Oil Conference and Exhibition, Kuwait City, Kuwait, 10-12 December. https://doi.org/10.2118/193761-MS

Burger, J. G. 1972. Chemical Aspects of In-Situ Combustion – Heat of Combustion and Kinetics. SPE J 12(5): 410–22. SPE-3599-PA. https://doi.org/10.2118/3599-PA

Chen, J.Z. and Maini, B. 2005. Numerical Simulation of Foamy Oil Depletion Tests. Presented at the Canadian International Petroleum Conference, Calgary, Alberta, 7-9 June. https://doi.org/10.2118/2005-073

Das, S.K. and Butler, R.M. 1998. Mechanism of the Vapor Extraction Process for Heavy Oil and Bitumen. *Journal of Petroleum Science and Engineering* **21**(1–2): 43-59. https://doi.org/10.1016/S0920-4105(98)00002-3

Dong, M., Huang, S.-S.S., and Hutchence, K. 2006. Methane Pressure-Cycling Process with Horizontal Wells for Thin Heavy-Oil Reservoirs. *SPE Reservoir Evaluation & Engineering* **9**(02): 154–164. https://doi.org/10.2118/88500-PA

Du, Z., Zeng, F., and Chan, C. 2015. An Experimental Study of the Post-CHOPS Cyclic Solvent Injection Process. *Journal of Energy Resources Technology* **137**(4). https://doi.org/10.1115/1.4029972

Fassihi, M. R., Meyers, K. O., and Baslle P. F. 1990. Low-Temperature Oxidation of Viscous Crude Oils. *SPE Res Eng* **5**(4): 609–16. SPE-15648-PA. https://doi.org/10.2118/15648-PA

Jamaloei, B. Y., Dong, M., Yang, P. et al. 2013. Impact of Solvent Type and Injection Sequence on Enhanced Cyclic Solvent Process (ECSP) for Thin Heavy Oil Reservoirs. *Journal of Petroleum Science and Engineering* **110**: 169-183. https://doi.org/10.1016/J.PETROL.2013.08.028

Khansari, Z. 2014. *Low Temperature Oxidation of Heavy Crude Oil: Experimental Study and Reaction Modeling*. PhD thesis, University of Calgary, Calgary, Alberta (January 2014).

Kraus, W.P., Mccaffrey, W.J., and Boyd, G.W. 1993. Pseudo-Bubble Point Model for Foamy Oils. Presented at the Annual Technical Conference, Calgary, Alberta, 9-12 May. https://doi.org/10.2118/93-45

Kumar, R. and Pooladi-Darvish, M. 2002. Solution-Gas Drive in Heavy Oil: Field Prediction and Sensitivity Studies Using Low Gas Relative Permeability. *Journal of Canadian Petroleum Technology* **41**(3): 26–32. https://doi.org/10.2118/02-03-01

Li, Y., Chen, Y., Pu, W. et al. 2017. Low Temperature Oxidation Characteristics Analysis of Ultra-Heavy Oil by Thermal Methods. *Journal of Industrial and Engineering Chemistry* **48**: 249–58. https://doi.org/10.1016/j.jiec.2017.01.017

Luo, P., Yang, C., Tharanivasan, A.K. et al. 2007. In Situ Upgrading of Heavy Oil in a Solvent-Based Heavy Oil Recovery Process. *Journal of Canadian Petroleum Technology* **46**(9). https://doi.org/10.2118/07-09-03

Maini, B., Sarma, H. K., and George, A. E. 1993. Significance of Foamy-Oil Behavior in Primary Production of Heavy Oils. *J Can Pet Technol* **32**(9). PETSOC-93-09-07. https://doi.org/10.2118/93-09-07

Maini, B.B. 2001. Foamy-Oil Flow. *Journal of Petroleum Technology* **53**(10): 54–64. https://doi.org/10.2118/68885-JPT

Maini, B.B. 2003. Effect of Depletion Rate on Performance of Solution Gas Drive in Heavy Oil Systems. Presented at the SPE Latin American and Caribbean Petroleum Engineering Conference, Port-of-Spain, Trinidad 27-30 April. https://doi.org/10.2118/81114-MS

Maini, B.B. and Busahmin, B. 2010. Foamy Oil Flow and its Role in Heavy Oil Production. *AIP Conference Proceedings* **1254**(2010): 103–108. https://doi.org/10.1063/1.3453794

Mamora, D. D. 1995. New Findings in Low-Temperature Oxidation of Crude Oil. SPE Asia Pacific Oil and Gas Conference, Kuala Lumpur, Malaysia, 20–22 March. SPE-29324-MS. https://doi.org/10.2118/29324-MS

Mayorquin-Ruiz, J. and Babadagli, T. 2016a. Optimal Design of Low-Temperature Air Injection with Propane for Efficient Recovery of Heavy Oil in Deep Naturally Fractured Reservoirs: Experimental and Numerical Approach. *Energy & Fuels* **30**(4): 2662–2673. https://doi.org/10.1021/acs.energyfuels.5b02864

Mayorquin-Ruiz, J. and Babadagli, T. 2016b. Low Temperature Air Injection with Solvents in Heavy-Oil Containing Naturally Fractured Reservoirs: Effects of Matrix/Fracture Properties and Temperature on Recovery. *Fuel* **179**: 376–390. https://doi.org/10.1016/j.fuel.2016.03.079

Niu, B., Ren, S., Liu, Y. et al. 2011. Low-Temperature Oxidation of Oil Components in an Air Injection Process for Improved Oil Recovery. *Energy & Fuels* **25**(10): 4299–4304. https://doi.org/10.1021/ef200891u

Sheng, J.J., Hayes, R.E., Maini, B.B. et al. 1995. A Proposed Dynamic Model for Foamy Oil Properties. Presented at the SPE International Heavy Oil Symposium, Calgary, Alberta, 19-21 June. https://doi.org/10.2118/30253-MS

Sheng, J.J., Maini, B.B., Hayes, R.E. et al. 1999. Critical Review of Foamy Oil Flow. *Transport in Porous Media* **35**(2): 157–187. https://doi.org/10.1023/A:1006575510872

Sheng, J.J., Maini, B.B., Hayes, R.E. et al. 1997. Experimental Study of Foamy Oil Stability. *Journal of Canadian Petroleum Technology* **36**(4): 31–37. https://doi.org/10.2118/97-04-02

Smith, G.E. 1988. Fluid Flow and Sand Production in Heavy-Oil Reservoirs under Solution-Gas Drive. *SPE Production Engineering* **3**(2): 169–180. https://doi.org/10.2118/15094-PA

Soh, Y. and Babadagli, T. 2017. Cost Effective EOR in Heavy-Oil Containing Sands by Gas Injection: Improvement of the Efficiency of Foamy Flow and Pressurization. Presented at the SPE/IATMI Asia Pacific Oil & Gas Conference and Exhibition, Jakarta, Indonesia, 17-19 October. https://doi.org/10.2118/186196-MS

Soh, Y. and Babadagli, T. 2018. Use of Air to Improve the Efficiency of Foamy Flow and Reservoir Pressurization in Heavy Oil Recovery. *J. Petr. Sci. and Eng.* **170**:166-176. https://doi.org/10.1016/j.petrol.2018.06.045

Speight, J. 2016. *Introduction to Enhanced Recovery Methods for Heavy Oil and Tar Sands*, 2nd Edition. Cambridge, MA. Gulf Publishing Company. https://doi.org/https://doi.org/10.1016/C2014-0-01296-8

Sun, X., Dong, M., Zhang, Y. et al. 2015. Enhanced Heavy Oil Recovery in Thin Reservoirs Using Foamy Oil-Assisted Methane Huff-n-Puff Method. *Fuel* **159**: 962–973. https://doi.org/10.1016/j.fuel.2015.07.056

Wang, J., Yuan, Y., Zhang, L. et al. 2009. The Influence of Viscosity on Stability of Foamy Oil in the Process of Heavy Oil Solution Gas Drive. *Journal of Petroleum Science and Engineering* **66**(1–2): 69–74. https://doi.org/10.1016/j.petrol.2009.01.007

Zhou, X., Yuan, Q., Peng, X. et al. 2018. A Critical Review of the CO2 Huff-N-Puff Process for Enhanced Heavy Oil Recovery. *Fuel* **215**: 813–824. https://doi.org/10.1016/j.fuel.2017.11.092

Chapter 3

Abusahmin, B.S., Karri, R.R., and Maini, B.B. 2017. Influence of Fluid and Operating Parameters on the Recovery Factors and Gas Oil Ratio in High Viscous Reservoirs under Foamy Solution Gas Drive. *Fuel* **197**: 497–517. https://doi.org/10.1016/j.fuel.2017.02.037

Adil, I. and Maini, B. 2007. Role of Asphaltene in Foamy Oil Flow. *Journal of Canadian Petroleum Technology* **46**(4): 97-104. https://doi.org/10.2523/94786-MS

Akin, S. and Kovscek, A.R. 2002. Heavy Oil Solution Gas Drive: A Laboratory Study. *Journal of Petroleum Science and Engineering* **35**: 33–48. https://doi.org/10.1016/S0920-4105(02)00162-6

Albartamani, N.S., Ali, S.M.F., Lepski, B. et al. 1999. Investigation of Foamy Oil Phenomena in Heavy Oil Reservoirs. Presented at the SPE International Thermal Operations and Heavy Oil Symposium, Bakersfield, California, 17-19 March. https://doi.org/10.2118/54084-MS

Ali, S.M.F. 1976. Non-Thermal Heavy Oil Recovery Methods. Presented at the SPE Rocky Mountain Regional Meeting, Casper, Wyoming, 11-12 May. https://doi.org/10.2118/5893-MS

Alzahrani, M.S., Aramco, S., Tutuncu, A.N. et al. 2014. A High Field Solid-State Nuclear Magnetic Resonance Experimental Study for Clay and Shale Swelling. Presented at the International Petroleum Technology Conference, Doha, Qatar, 19-22 January. https://doi.org/10.2523/IPTC-17523-MS

Arora, P. and Kovscek, A.R. 2003. A Mechanistic Modeling and Experimental Study of Solution Gas Drive. *Transport in Porous Media* **51**(3): 237-265. https://doi.org/10.1023/A:1022353925107

Banerjee, D.K. 2012. *Oil sands, Heavy oil & Bitumen: From Recovery to Refinery*. Tulsa, OK. PenWell.

Basilio, E. and Babadagli, T. 2018. Use of Air with Different Solvents Mixtures for Improved Foam Stability and Cost-Effective Heavy Oil Recovery. Presented at the SPE International Heavy Oil Conference and Exhibition, Kuwait City, Kuwait, 10-12 December. https://doi.org/10.2118/193761-MS

Basilio, E. and Babadagli, T. 2019. Use of Air with Methane for Improved Foam Stability and Cost-Effective Heavy Oil Recovery. Under Review at *SPE Reservoir Evaluation & Engineering.*

Bertram, E.A. and Lacey, W.N. 1935. Rate of Solution of Methane in Oils Filling Spaces between Sand Grains. *Industrial & Engineering Chemistry* **28**(3): 316–318. https://doi.org/10.1021/ie50315a014

Bird, R.B., Stewart, W.E., and Lightfoot, E.N. 1924. *Transport Phenomena*, Second Edition. USA: John Wiley & Sons

Bjorndalen, N., Jossy, W.E., and Alvarez, J.M. 2012. Foamy Oil Behaviour in Solvent Based Production Processes. Presented at the SPE Heavy Oil Conference, Calgary, Alberta, 12-14 June. https://doi.org/10.2118/157905-MS

Bora, R., Maini, B.B., and Chakma, A. 2000. Flow Visualization Studies of Solution Gas Drive Process in Heavy Oil Reservoirs with a Glass Micromodel. *SPE Reservoir Evaluation & Engineering* **3**(3): 224–229. https://doi.org/10.2118/64226-PA

Brady, A.P. and Ross, S. 1944. The Measurement of Foam Stability. *Journal of the American Chemical Society* **66**(8): 1348–1356. https://doi.org/10.1021/ja01236a045

Busahmin, B., Maini, B.B., Karri, R.R., and Sabet M. 2017. Studies on the Stability of the Foamy Oil in Developing Heavy Oil Reservoirs. *Defect and Diffusion Forum* **371**: 111–116. https://doi.org/10.4028/www.scientific.net/DDF.371.111

Butler, R.M. and Mokrys, I.J. 1991. A New Process (VAPEX) For Recovering Heavy Oils Using Hot Water and Hydrocarbon Vapour. *Journal of Canadian Petroleum Technology* **30**(1). https://doi.org/10.2118/91-01-09

Bybee, K. 2008. Heavy Oil: Optimize Cyclic Steam Stimulation Though Experimental Design. *Journal of Petroleum Technology* **60**(3): 85–86. https://doi.org/10.2118/0308-0085-JPT

Chen, J.Z. and Maini, B. 2005. Numerical Simulation of Foamy Oil Depletion Tests. Presented at the Canadian International Petroleum Conference, Calgary, Alberta, 7-9 June. https://doi.org/10.2118/2005-073

Chen, Z., Sun, J., Wang, R. et al. 2015. A Pseudobubblepoint Model and its Simulation for Foamy Oil in Porous Media. *SPE Journal* **20**(2): 239–247. https://doi.org/10.2118/172345-PA

Claridge, E.L. 1994. A Proposed Model and Mechanism for Anomalous Foamy Heavy Oil Behavior. Presented at the International Heavy Oil Symposium, Calgary, Alberta, 19-21 June.

Creux, P., Meyer, V., Graciaa, A. et al. 2005. Diffusivity in Heavy Oils. SPE International Thermal Operations and Heavy Oil Symposium, Calgary, Alberta, 1-3 November. https://doi.org/10.2118/97798-MS

Das, S.K. and Butler, R.M. 1998. Mechanism of the Vapor Extraction Process for Heavy Oil and Bitumen. *Journal of Petroleum Science and Engineering* **21**(1–2): 43-59. https://doi.org/10.1016/S0920-4105(98)00002-3

Das, S.K. and Butler, R.M. 1996. Diffusion Coefficients of Propane and Butane in Peace River Bitumen. *Canadian Journal of Chemical Engineering* **74**(6): 985–992. https://doi.org/10.1002/cjce.5450740623

Denney, D. 1997. Steam-Assisted Gravity-Drainage and Vapex Process Reservoir Screening. *Journal of Petroleum Technology* **49**(10): 1122–1124. https://doi.org/10.2118/1097-1122-JPT

Do, H.D. and Pinczewski, W.V. 1993. Diffusion-Controlled Swelling of Reservoir Oil by Indirect Contact with Injection Gas. *Chemical Engineering Science* **48**(18): 3243–3252. https://doi.org/10.1016/0009-2509(93)80208-8

Dong, M., Huang, S.-S.S., and Hutchence, K. 2006. Methane Pressure-Cycling Process with Horizontal Wells for Thin Heavy-Oil Reservoirs. *SPE Reservoir Evaluation & Engineering* **9**(02): 154–164. https://doi.org/10.2118/88500-PA

Donnelly, J.K. 2000. The Best Process for Cold Lake: CSS vs. SAGD. *Journal of Canadian Petroleum Technology* **39**(8). https://doi.org/10.2118/00-08-TN

Du, Z., Zeng, F., and Chan, C. 2015. An Experimental Study of the Post-CHOPS Cyclic Solvent Injection Process. *Journal of Energy Resources Technology* **137**(4). https://doi.org/10.1115/1.4029972

Faruk, C. and Maurice, L.R. 2003. Analysis and Interpretation of Gas Diffusion in Quiescent Reservoir, Drilling, and Completion Fluids: Equilibrium vs. Non-equilibrium Models. Presented at the SPE Annual Technical Conference and Exhibition, Denver, Colorado, 5-8 October. https://doi.org/10.2118/84072-MS

Faruk, C. and Maurice, L.R. 2002. Improved Measurement of Gas Diffusivity for Miscible Gas Flooding Under Nonequilibrium vs. Equilibrium Conditions. Presented at the SPE/DOE Improved Oil Recovery Symposium, Tulsa, Oklahoma, 13-17 April. https://doi.org/10.2523/75135-MS

George, D.S., Hayat, O., and Kovscek, A.R. 2005. A Microvisual Study of Solution-Gas-Drive Mechanisms in Viscous Oils. *Journal of Petroleum Science and Engineering* **46**(1–2): 101-119. https://doi.org/10.1016/j.petrol.2004.08.003

Goodarzi, N.N. and Kantzas, A., 2008. Observations of Heavy Oil Primary Production Mechanisms from Long Core Depletion Experiments. *Journal of Canadian Petroleum Technology* **47**(4): 46–54. https://doi.org/10.2118/08-04-46

Grogan, A.T., Pinczewski, V.W., Ruskauff, G.J. et al. 1988. Diffusion of CO_2 at Reservoir Conditions: Models and Measurements. *SPE Reservoir Engineering* **3**(1): 93–102. https://doi.org/10.2118/14897-PA

Hama, M.Q., Wei, M., Saleh, L.D. et al. 2014. Updated Screening Criteria for Steam Flooding Based on Oil Field Projects Data. Presented at the SPE Heavy Oil Conference-Canada, Calgary, Alberta, 10-12 June. https://doi.org/10.2118/170031-MS

Hepler, L.G. and Hsi, C. 1989. *AOSTRA Technical Handbook on Oil Sands, Bitumens and Heavy Oils*. Edmonton, Alberta: Alberta Oil Sands Technology and Research Authority.

Hirasaki, G.J., Lo, S.W., and Zhang, Y. 2003. NMR Properties of Petroleum Reservoir Fluids. *Magnetic Resonance Imaging* **21**(3–4): 269-277. https://doi.org/10.1016/S0730-725X(03)00135-8

Hong, S.Y., Zeng, F., and Du, Z. 2017. Characterization of Gas-Oil Flow in Cyclic Solvent Injection (CSI) for Heavy Oil Recovery. *Journal of Petroleum Science and Engineering* **152**: 639–652. https://doi.org/10.1016/j.petrol.2017.01.029

Hongfu, F., Yongjian, L., Liying, Z. et al. 2002. The Study on Composition Changes of Heavy Oils during Steam Stimulation Processes. *Fuel* **81**(13): 1733–1738. https://doi.org/10.1016/S0016-2361(02)00100-X

Huber, C., Su, Y., Nguyen, C.T. et al. 2013. A New Bubble Dynamics Model to Study Bubble Growth, Deformation, and Coalescence. *Journal of Geophysical Research : Solid Earth* **119**(1): 216-239. https://doi.org/10.1002/2013JB010419

Huc, A.-Y. 2010. *Heavy Crude Oils - From Geology to Upgrading. An Overview*. Paris, France. Editions Technip.

Issever, K., Pamir, A.N., and Tirek, A. 1993. Performance of a Heavy-Oil Field under CO_2 Injection, Bati Raman, Turkey. *SPE Reservoir Engineering* **8**(4): 256–260. https://doi.org/10.2118/20883-PA

Ivory, J., Chang, J., Coates, R., et al. 2010. Investigation of Cyclic Solvent Injection Process for Heavy Oil Recovery. *Journal of Canadian Petroleum Technology* **49**(9): 22–33. https://doi.org/10.2118/140662-PA

Jamaloei, B. Y., Dong, M., Yang, P. et al. 2013. Impact of Solvent Type and Injection Sequence on Enhanced Cyclic Solvent Process (ECSP) for Thin Heavy Oil Reservoirs. *Journal of Petroleum Science and Engineering* **110**: 169-183. https://doi.org/10.1016/J.PETROL.2013.08.028

Jamialahmadi, M., Emadi, M., and Müller-Steinhagen, H. 2006. Diffusion Coefficients of Methane in Liquid Hydrocarbons at High Pressure and Temperature. *Journal of Petroleum Science and Engineering* **53**(1–2): 47-60. https://doi.org/10.1016/j.petrol.2006.01.011

Jha, K.N. 1986. A Laboratory Study of Heavy Oil Recovery with Carbon Dioxide. *Journal of Canadian Petroleum Technology* **25**(2): 54–63. https://doi.org/10.2118/86-02-03

Jia, X., Zeng, F., and Gu, Y. 2015. Gasflooding-Assisted Cyclic Solvent Injection (GA-CSI) for Enhancing Heavy Oil Recovery. *Fuel* **140**(15): 344–353. https://doi.org/10.1016/j.fuel.2014.09.066

Jiang, T., Zeng, F., Jia, X. et al. 2014. A New Solvent-Based Enhanced Heavy Oil Recovery Method: Cyclic Production with Continuous Solvent Injection. *Fuel* **115**: 426–433. https://doi.org/10.1016/J.FUEL.2013.07.043

Kraus, W.P., Mccaffrey, W.J., and Boyd, G.W. 1993. Pseudo-Bubble Point Model for Foamy Oils. Presented at the Annual Technical Conference, Calgary, Alberta, 9-12 May. https://doi.org/10.2118/93-45

Kumar, R. and Pooladi-Darvish, M. 2002. Solution-Gas Drive in Heavy Oil: Field Prediction and Sensitivity Studies Using Low Gas Relative Permeability. *Journal of Canadian Petroleum Technology* **41**(3): 26–32. https://doi.org/10.2118/02-03-01

Kumar, R. and Pooladi-Darvish, M. 2001. Effect of Viscosity and Diffusion Coefficient on the Kinetics of Bubble Growth in Solution-Gas Drive in Heavy Oil. *Journal of Canadian Petroleum Technology* **40**(3): 30–37. https://doi.org/10.2118/01-03-02

Li, S., Li, Z., Lu, T. et al. 2012. Experimental Study on Foamy Oil Flow in Porous Media with Orinoco Belt Heavy Oil. *Energy & Fuels* **26**(10): 6332–6342. https://doi.org/10.1021/ef301268u

Li, X. and Yortsos, Y.C. 1995. Theory of Multiple Bubble Growth in Porous Media by Solute Diffusion. *Chemical Engineering Science* **50**(8): 1247-1271. https://doi.org/10.1016/0009-2509(95)98839-7

Liu, P., Li, W., Hao, M. et al. 2016. Quantitative Evaluation of Factors Affecting Foamy Oil Recovery in the Development of Heavy Hydrocarbon Reservoirs. *International Journal of Hydrogen Energy* **41**(35): 15624-15631. https://doi.org/10.1016/j.ijhydene.2016.04.031

Luo, P., Yang, C., Tharanivasan, A.K. et al. 2007. In Situ Upgrading of Heavy Oil in a Solvent-Based Heavy Oil Recovery Process. *Journal of Canadian Petroleum Technology* **46**(9). https://doi.org/10.2118/07-09-03

Maini, B. 1996. Foamy Oil Flow in Heavy Oil Production. *Journal of Canadian Petroleum Technology* **35**(6): 5–6. https://doi.org/10.2118/96-06-01

Maini, B.B. 2001. Foamy-Oil Flow. *Journal of Petroleum Technology* **53**(10): 54–64. https://doi.org/10.2118/68885-JPT

Maini, B.B. 2003. Effect of Depletion Rate on Performance of Solution Gas Drive in Heavy Oil Systems. Presented at the SPE Latin American and Caribbean Petroleum Engineering Conference, Port-of-Spain, Trinidad 27-30 April. https://doi.org/10.2118/81114-MS

Maini, B.B. and Busahmin, B. 2010. Foamy Oil Flow and its Role in Heavy Oil Production. *AIP Conference Proceedings* **1254**(2010): 103–108. https://doi.org/10.1063/1.3453794

Maini, B.B., Sarma, H.K., and George, A.E. 1993. Significance of Foamy-oil Behaviour in Primary Production of Heavy Oils. *Journal of Canadian Petroleum Technology* **32**(9). https://doi.org/10.2118/93-09-07

Mayorquin-Ruiz, J. and Babadagli, T. 2016a. Optimal Design of Low-Temperature Air Injection with Propane for Efficient Recovery of Heavy Oil in Deep Naturally Fractured Reservoirs: Experimental and Numerical Approach. *Energy & Fuels* **30**(4): 2662–2673. https://doi.org/10.1021/acs.energyfuels.5b02864

Mayorquin-Ruiz, J. and Babadagli, T. 2016b. Low Temperature Air Injection with Solvents in Heavy-Oil Containing Naturally Fractured Reservoirs: Effects of Matrix/Fracture Properties and Temperature on Recovery. *Fuel* **179**: 376–390. https://doi.org/10.1016/j.fuel.2016.03.079

Nguyen, T.A. and Farouq Ali, S.M. 1998. Effect of Nitrogen On the Solubility And Diffusivity of Carbon Dioxide Into Oil And Oil Recovery By the Immiscible WAG Process. *Journal of Canadian Petroleum Technology* **37**(2): 24–31. https://doi.org/10.2118/98-02-02

Or, C., Sasaki, Y., Sugai, Y., Nakano M., Imai, M. 2014. Numerical Simulation of CO2 Gas Microbubble of Foamy Oil. *Energy Procedia* **63**(2014): 7821–7829. https://doi.org/10.1016/j.egypro.2014.11.816

Ostos, A.N. and Maini, B.B. 2005. An Integrated Experimental Study of Foamy Oil Flow during Solution Gas Drive. *Journal of Canadian Petroleum Technology* **44**(4): 43–50. https://doi.org/10.2118/05-04-05

Peng, J., Tang, G.Q., and Kovscek, A.R. 2009. Oil Chemistry and its Impact on Heavy Oil Solution Gas Drive. *Journal of Petroleum Science and Engineering* **66**(1–2): 47-59. https://doi.org/10.1016/j.petrol.2009.01.005

Pomeroy, R.D., Lacey, W.N., Scudder, N.F. et al. 1933. Rate of Solution of Methane in Quiescent Liquid Hydrocarbons. *Industrial & Engineering Chemistry* **25**(9): 1014–1019. https://doi.org/10.1021/ie50285a021

Qazvini Firouz, A. and Torabi, F. 2012. Feasibility Study of Solvent-Based Huff-n-Puff Method (Cyclic Solvent Injection) To Enhance Heavy Oil Recovery. Presented at the SPE Heavy Oil Conference, Calgary, Alberta, 12-14 June. https://doi.org/10.2118/157853-MS

Qazvini Firouz, A. and Torabi, F. 2014. Utilization of Carbon Dioxide and Methane in Huff-and-Puff Injection Scheme to Improve Heavy Oil Recovery. *Fuel* **117**: 966–973. https://doi.org/10.1016/j.fuel.2013.10.040

Rangriz Shokri, A. and Babadagli, T. 2017. Feasibility Assessment of Heavy-Oil Recovery by CO_2 Injection after Cold Production with Sands: Lab-to-Field Scale Modeling Considering Non-Equilibrium Foamy Oil Behavior. *Applied Energy* **205**: 615-625. https://doi.org/10.1016/j.apenergy.2017.08.029

Reamer, H.H., Opfell, J.B., and Sage, B.H. 1956. Diffusion Coefficients in Hydrocarbon Systems Methane-Decane-Methane in Liquid Phase. *Industrial & Engineering Chemistry* **48**(2): 275–282. https://doi.org/10.1021/ie50554a034

Riazi, M.R. 2005. *Applications: Estimation of Transport Properties, in: Characterization and Properties of Petroleum Fractions: (MNL 50)*, Chapter 8.

Riazi, M.R. 1996. A New Method for Experimental Measurement of Diffusion Coefficients in Reservoir Fluids. *Journal of Petroleum Science and Engineering* **14**(3–4): 235-250. https://doi.org/10.1016/0920-4105(95)00035-6

Riazi, M.R. and Whitson, C.H. 1993. Estimating Diffusion Coefficients of Dense Fluids. *Industrial & Engineering Chemistry* **32**(12): 3081–3088. https://doi.org/10.1021/ie00024a018

Sarma, H. and Maini, B. 1992. Role of Solution Gas in Primary Production of Heavy Oils. Presented at the SPE Latin American and Caribbean Petroleum Engineering Conference, Caracas, Venezuela, 8-11 March. https://doi.org/10.2118/23631-MS

Sayegh, S.G. and Maini, B.B. 1984. Laboratory Evaluation of the CO2 Huff-N-Puff Process for Heavy Oil Reservoirs. Journal of Canadian Petroleum Technology **23**(3): 29–36. https://doi.org/10.2118/84-03-02

Shayegi, S., Jin, Z., Schenewerk, P. et al. 1996. Improved Cyclic Stimulation Using Gas Mixtures. Presented at the SPE Annual Technical Conference and Exhibition, Denver, Colorado, 6-9 October. https://doi.org/10.2118/36687-MS

Sheikha, H., Pooladi-Darvish, M., and Mehrotra, A.K. 2005. Development of Graphical Methods for Estimating the Diffusivity Coefficient of Gases in Bitumen from Pressure-Decay Data. *Energy & Fuels* **19**(5): 2041–2049. https://doi.org/10.1021/ef050057c

Sheng, J.J. 1997. *Foamy Oil Flow in Porous Media*. Thesis, University of Alberta, Edmonton, Alberta.

Sheng, J.J. 2013. *Cold Production of Heavy Oil, in: Enhanced Oil Recovery - Field Case Studies*. Lubbock, TX: Gulf Professional Publishing. https://doi.org/10.1016/C2010-0-67974-0

Sheng, J.J., Hayes, R.E., Maini, B.B. et al. 1995. A Proposed Dynamic Model for Foamy Oil Properties. Presented at the SPE International Heavy Oil Symposium, Calgary, Alberta, 19-21 June. https://doi.org/10.2118/30253-MS

Sheng, J.J., Maini, B.B., Hayes, R.E. et al. 1999. Critical Review of Foamy Oil Flow. *Transport in Porous Media* **35**(2): 157–187. https://doi.org/10.1023/A:1006575510872

Sheng, J.J., Maini, B.B., Hayes, R.E. et al. 1997. Experimental Study of Foamy Oil Stability. *Journal of Canadian Petroleum Technology* **36**(4): 31–37. https://doi.org/10.2118/97-04-02

Shi, R. and Kantzas, A. 2008. Enhanced Heavy Oil Recovery on Depleted Long Core System by CH4 and CO2. Presented at the SPE International Thermal Operations and Heavy Oil Symposium, Calgary, Alberta, 20-23 October. https://doi.org/10.2118/117610-MS

Sigmund, P.M. 1976. Prediction of Molecular Diffusion at Reservoir Conditions. *Journal of Canadian Petroleum Technology* **15**(02): 48–57. https://doi.org/10.2118/76-02-05

Singhal, A.K., Ito, Y., and Kasraie, M. 1998. Screening and Design Criteria for Steam Assisted Gravity Drainage (SAGD) Projects. Presented at the SPE International Conference on Horizontal Well Technology, Calgary, Alberta, 1-4 November. https://doi.org/10.2118/50410-MS

Smith, G.E. 1988. Fluid Flow and Sand Production in Heavy-Oil Reservoirs under Solution-Gas Drive. *SPE Production Engineering* **3**(2): 169–180. https://doi.org/10.2118/15094-PA

Soh, Y. and Babadagli, T. 2017. Cost Effective EOR in Heavy-Oil Containing Sands by Gas Injection: Improvement of the Efficiency of Foamy Flow and Pressurization. Presented at the SPE/IATMI Asia Pacific Oil & Gas Conference and Exhibition, Jakarta, Indonesia, 17-19 October. https://doi.org/10.2118/186196-MS

Soh, Y., Rangriz-Shokri, A., and Babadagli, T. 2018. Optimization of Methane Use in Cyclic Solvent Injection for Heavy-Oil Recovery after Primary Production through Experimental and Numerical Studies. *Fuel* **214**: 457–470. https://doi.org/10.1016/j.fuel.2017.11.064

Soh, Y.J., Rangriz-shokri, A., and Babadagli, T. 2016. A New Modeling Approach to Optimize Methane-Propane Injection in a Field after CHOPS. Presented at the SPE Annual Technical Conference and Exhibition, Dubai, UAE, 26-28 September. https://doi.org/10.2118/181322-MS

Speight, J. 2016. *Introduction to Enhanced Recovery Methods for Heavy Oil and Tar Sands*, 2nd Edition. Cambridge, MA. Gulf Publishing Company. https://doi.org/https://doi.org/10.1016/C2014-0-01296-8

Srivastava, R.K., Huang, S.S., and Dong, M. 1999. Comparative Effectiveness of CO2, Produced Gas, and Flue Gas for Enhanced Heavy-Oil Recovery. *SPE Reservoir Evaluation & Engineering* **2**(3). https://doi.org/10.2118/56857-PA

Sun, X., Dong, M., Zhang, Y. et al. 2016. A New Foamy Oil-Assisted Methane Huff-N-Puff Method for Enhanced Heavy Oil Recovery in Thin Reservoirs. Presented at the SPE Canada Heavy Oil Technical Conference, Calgary, Alberta, 7-9 June. https://doi.org/10.2118/180742-MS

Sun, X., Dong, M., Zhang, Y. et al. 2015. Enhanced Heavy Oil Recovery in Thin Reservoirs Using Foamy Oil-Assisted Methane Huff-n-Puff Method. *Fuel* **159**: 962–973. https://doi.org/10.1016/j.fuel.2015.07.056

Tang, G.Q., Leung, T., Castanier, L.M. et al. 2006. An Investigation of the Effect of Oil Composition on Heavy Oil Solution-Gas Drive. *SPE Journal* **11**(1): 1265–1281. https://doi.org/10.2118/84197-PA

Temizel, C., Energy, A., Balaji, K. et al. 2017. Optimization of Foamy Oil Production in Horizontal Wells. Presented at the SPE Latin America and Caribbean Mature Fields Symposium, Salvador, Bahia, 15-16 March. https://doi.org/10.2118/184904-MS

Tharanivasan, A.K., Yang, C., and Gu, Y. 2006. Measurements of Molecular Diffusion Coefficients of Carbon Dioxide, Methane, and Propane in Heavy Oil under Reservoir Conditions. *Energy & Fuels* **20**(6): 2509–2517. https://doi.org/10.1021/ef060080d

Tharanivasan, A.K., Yang, C., and Gu, Y. 2004. Comparison of Three Different Interface Mass Transfer Models Used in the Experimental Measurement of Solvent Diffusivity in Heavy Oil. *Journal of Petroleum Science and Engineering* **44**(3–4): 269–282. https://doi.org/10.1016/j.petrol.2004.03.003

Torabi, F., Yadali Jamaloei, B., Stengler, B.M. et al. 2012. The Evaluation of CO2-Based Vapour Extraction (VAPEX) Process for Heavy-Oil Recovery. *Journal of Petroleum Exploration and Production Technology* **2**(2): 93–105. https://doi.org/10.1007/s13202-012-0025-y

Turta, A.T., Maimi, B.B., and Jackson, C. 2003. Mobility of Gas-in-Oil Dispersions in Enhanced Solution Gas Drive (Foamy Oil) Exploitation of Heavy Oil Reservoirs. *Journal of Canadian Petroleum Technology* **42**(3): 48–55. https://doi.org/10.2118/03-03-05

Upreti, S.R., Lohi, A., Kapadia, R.A. et al. 2007. Vapor Extraction of Heavy Oil and Bitumen: A Review. *Energy and Fuels* **21**(3): 1562–1574. https://doi.org/10.1021/ef060341j

Upreti, S.R. and Mehrotra, A.K. 2002. Diffusivity of CO2, CH4, C2H6 and N2 in Athabasca Bitumen. *Canadian Journal of Chemical Engineering* **80**(1): 116–125. https://doi.org/10.1002/cjce.5450800112

Wang, J., Yuan, Y., Zhang, L. et al. 2009. The Influence of Viscosity on Stability of Foamy Oil in the Process of Heavy Oil Solution Gas Drive. *Journal of Petroleum Science and Engineering* **66**(1–2): 69–74. https://doi.org/10.1016/j.petrol.2009.01.007

Warner, H.R. 2007. *Petroleum Engineering Handbook, Volume VI: Emerging and Peripheral Technologies*. Richardson, TX: Society of Petroleum Engineers.

Wen, Y.W. and Kantzas, A. 2005. Monitoring Bitumen−Solvent Interactions with Low-Field Nuclear Magnetic Resonance and X-ray Computer-Assisted Tomography. *Energy and Fuels* **19**(4): 1319–1326. https://doi.org/10.1021/ef049764g

Wenlong, G., Shuhong, W., Jian, Z. et al. 2008. Utilizing Natural Gas Huff and Puff to Enhance Production in Heavy Oil Reservoir. Presented at the International Thermal Operations and Heavy Oil Symposium, Calgary, Alberta, 20-23 October. https://doi.org/10.2118/117335-MS

Wong, R.C.K. and Maini, B.B. 2007. Gas Bubble Growth in Heavy Oil-Filled Sand Packs under undrained Unloading. *Journal of Petroleum Science and Engineering* **55**(3–4): 259-270. https://doi.org/10.1016/j.petrol.2006.08.006

Yang, C. and Gu, Y. 2006. Diffusion Coefficients and Oil Swelling Factors of Carbon Dioxide, Methane, Ethane, Propane, and their Mixtures in Heavy Oil. *Fluid Phase Equilibria* **243**(1–2): 64-73. https://doi.org/10.1016/j.fluid.2006.02.020

Yen, T.F., Erdman, J.G., and Pollack, S.S. 1961. Investigation of the Structure of Petroleum Asphaltenes by X-Ray Diffraction. *Analytical Chemistry* **33**(11): 1587–1594. https://doi.org/10.1021/ac60179a039

Zekri, A.Y. and Jerbi, K.K. 2002. Economic Evaluation of Enhanced Oil Recovery. *Oil & Gas Science and Technology – Rev. IFP* **57**(3): 259-267

Zhang, Y., Chakma, A., and Maini, B.B. 1999. Effects of Temperature on Foamy Oil Flow in Solution Gas-drive in Cold Lake Field. Presented at the SPE Annual Technical Meeting. https://doi.org/10.2118/99-41

Zhang, Y.P., Hyndman, C.L., and Maini, B.B. 2000. Measurement of Gas Diffusivity in Heavy Oils. *Journal of Petroleum Science and Engineering* **25**(1–2): 37–47. https://doi.org/10.1016/S0920-4105(99)00031-5

Zhou, X. 2015. *Experimental Study on Foamy Oil Flow by Using Different Heavy Oil-Solvent*. Thesis, University of Regina.

Zhou, X., Yuan, Q., Peng, X. et al. 2018. A Critical Review of the CO2 Huff-N-Puff Process for Enhanced Heavy Oil Recovery. *Fuel* **215**: 813–824. https://doi.org/10.1016/j.fuel.2017.11.092

Zhou, X., Yuan, Q., Zeng, F. et al. 2017. Experimental Study on Foamy Oil Behaviour Using a Heavy Oil-Methane System in the Bulk Phase. *Journal of Petroleum Science and Engineering* **158**: 309-321. https://doi.org/10.1016/j.petrol.2017.07.070

Zhou, X., Zeng, F., Zhang, L. et al. 2016. Foamy Oil Flow in Heavy Oil-Solvent Systems Tested by Pressure Depletion in a Sandpack. *Fuel* **171**: 210–223. https://doi.org/10.1016/j.fuel.2015.12.070

Chapter 4

Abusahmin, B.S., Karri, R.R., and Maini, B.B. 2017. Influence of Fluid and Operating Parameters on the Recovery Factors and Gas Oil Ratio in High Viscous Reservoirs under Foamy Solution Gas Drive. *Fuel* **197**: 497–517. https://doi.org/10.1016/j.fuel.2017.02.037

Basilio, E. and Babadagli, T. 2018. Use of Air with Different Solvents Mixtures for Improved Foam Stability and Cost-Effective Heavy Oil Recovery. Presented at the SPE International Heavy Oil Conference and Exhibition, Kuwait City, Kuwait, 10-12 December. https://doi.org/10.2118/193761-MS

Basilio, E. and Babadagli, T. 2019a. Use of Air with Methane for Improved Foam Stability and Cost-Effective Heavy Oil Recovery. Under Review at *SPE Reservoir Evaluation & Engineering.*

Basilio, E. and Babadagli, T. 2019b. Mechanics of Foamy Oil during Primary and Secondary Recovery of Heavy Oil: A Comprehensive Review. Under Review at *SPE Reservoir Evaluation & Engineering.*

Bondino, I., McDougall, S.R., Hamon, G., 2009. A Pore-Scale Modelling Approach to the Interpretation of Heavy Oil Pressure Depletion Experiments. *Journal of Petroleum Science and Engineering* **65**: 14–22. https://doi.org/10.1016/J.PETROL.2008.12.010

Bora, R., Maini, B.B., and Chakma, A. 2000. Flow Visualization Studies of Solution Gas Drive Process in Heavy Oil Reservoirs with a Glass Micromodel. *SPE Reservoir Evaluation & Engineering* **3**(3): 224–229. https://doi.org/10.2118/64226-PA

Chakma, A., & Jha, K. N. 1992. Heavy-Oil Recovery From Thin Pay Zones by Electromagnetic Heating. Presented at the SPE Annual Technical Conference and Exhibition, Washington, D.C., 4-7 October. https://doi.org/10.2118/24817-MS

Chen, J.Z. and Maini, B. 2005. Numerical Simulation of Foamy Oil Depletion Tests. Presented at the Canadian International Petroleum Conference, Calgary, Alberta, 7-9 June. https://doi.org/10.2118/2005-073

Chen, X., 2006. *Heavy Oils, Part 1*. SIAM News, Society of Industrial and Applied Mathematics, Philadelphia, Pennsylvania. **39**(3).

Du, Z., Zeng, F., and Chan, C. 2015. An Experimental Study of the Post-CHOPS Cyclic Solvent Injection Process. *Journal of Energy Resources Technology* **137**(4). https://doi.org/10.1115/1.4029972

Firoozabadi, A., 2001. Mechanisms of Solution Gas Drive in Heavy Oil Reservoirs. *Journal of Canadian Petroleum Technology* **40**(3). https://doi.org/10.2118/01-03-DAS

Gharbi, Ridha & Alajmi, Abdullah & Algharaib, Meshal. 2012. The Potential of a Surfactant/Polymer Flood in a Middle Eastern Reservoir. Energies. *Energies* **2012**(5): 58-70. https://www.mdpi.com/1996-1073/5/1/58

Goodarzi, N.N. and Kantzas, A., 2008. Observations of Heavy Oil Primary Production Mechanisms from Long Core Depletion Experiments. *Journal of Canadian Petroleum Technology* **47**(4): 46–54. https://doi.org/10.2118/08-04-46

Joseph, D.D., 2002. Modeling Foamy Oil Flow in Porous Media. *International Journal of Multiphase Flow* **28**(10): 1659-1686. https://doi.org/10.1016/S0301-9322(02)00051-4

Kumar, R. and Pooladi-Darvish, M. 2002. Solution-Gas Drive in Heavy Oil: Field Prediction and Sensitivity Studies Using Low Gas Relative Permeability. *Journal of Canadian Petroleum Technology* **41**(3): 26–32. https://doi.org/10.2118/02-03-01

Kumar, M. 2006. Heavy Oil Recovery—Recent Developments and Challenges. Los Angeles Monthly Petroleum Technology Forum. L.A. Basin Section, SPE. http://www.laspe.org/petrotech/petrooct10906.html

Li, S., Li, Z., Lu, T. et al. 2012. Experimental Study on Foamy Oil Flow in Porous Media with Orinoco Belt Heavy Oil. *Energy & Fuels* **26**(10): 6332–6342. https://doi.org/10.1021/ef301268u

Liu, P., Li, W., Hao, M. et al. 2016. Quantitative Evaluation of Factors Affecting Foamy Oil Recovery in the Development of Heavy Hydrocarbon Reservoirs. *International Journal of Hydrogen Energy* **41**(35): 15624-15631. https://doi.org/10.1016/j.ijhydene.2016.04.031

Maini, B. 1996. Foamy Oil Flow in Heavy Oil Production. *Journal of Canadian Petroleum Technology* **35**(6): 5–6. https://doi.org/10.2118/96-06-01

Maini, B.B. 2003. Effect of Depletion Rate on Performance of Solution Gas Drive in Heavy Oil Systems. Presented at the SPE Latin American and Caribbean Petroleum Engineering Conference, Port-of-Spain, Trinidad 27-30 April. https://doi.org/10.2118/81114-MS

Maini, B.B. and Busahmin, B. 2010. Foamy Oil Flow and its Role in Heavy Oil Production. *AIP Conference Proceedings* 1254(2010): 103–108. https://doi.org/10.1063/1.3453794

Morrison, I. D. 1996. Ross's Rule: Sydney Ross and the Phase Diagram. *Colloids and Surfaces A: Physicochemical and Engineering Aspects* **118**(3): 257-261. https://doi.org/10.1016/S0927-7757(96)03690-4

Ostos, A.N., 2003. *Effect of Capillary Number on Performance of Solution Gas Drive in Heavy Oil Reservoirs*. Thesis, University of Calgary, Calgary, Alberta.

Ostos, A.N. and Maini, B.B. 2005. An Integrated Experimental Study of Foamy Oil Flow during Solution Gas Drive. *Journal of Canadian Petroleum Technology* **44**(4): 43–50. https://doi.org/10.2118/05-04-05

Qazvini Firouz, A. and Torabi, F. 2012. Feasibility Study of Solvent-Based Huff-n-Puff Method (Cyclic Solvent Injection) To Enhance Heavy Oil Recovery. Presented at the SPE Heavy Oil Conference, Calgary, Alberta, 12-14 June. https://doi.org/10.2118/157853-MS

Rangriz Shokri, A. and Babadagli, T. 2014. Modeling of CHOPS (Cold Heavy Oil Production with Sand) for Subsequent Thermal/Solvent Injection Applications. *Journal of Canadian Petroleum Technology* **53**(2): 95-108. https://doi.org/10.2118/158934-PA

Sarma, H. and Maini, B. 1992. Role of Solution Gas in Primary Production of Heavy Oils. Presented at the SPE Latin American and Caribbean Petroleum Engineering Conference, Caracas, Venezuela, 8-11 March. https://doi.org/10.2118/23631-MS

Sheng, J.J. 2013. *Cold Production of Heavy Oil, in: Enhanced Oil Recovery - Field Case Studies*. Lubbock, TX: Gulf Professional Publishing. https://doi.org/10.1016/C2010-0-67974-0

Shi, R. and Kantzas, A. 2008. Enhanced Heavy Oil Recovery on Depleted Long Core System by CH4 and CO2. Presented at the SPE International Thermal Operations and Heavy Oil Symposium, Calgary, Alberta, 20-23 October. https://doi.org/10.2118/117610-MS

Smith, G.E. 1988. Fluid Flow and Sand Production in Heavy-Oil Reservoirs under Solution-Gas Drive. *SPE Production Engineering* **3**(2): 169–180. https://doi.org/10.2118/15094-PA

Soh, Y., Rangriz-Shokri, A., and Babadagli, T. 2018. Optimization of Methane Use in Cyclic Solvent Injection for Heavy-Oil Recovery after Primary Production through Experimental and Numerical Studies. *Fuel* **214**: 457–470. https://doi.org/10.1016/j.fuel.2017.11.064

Soh, Y., and Babadagli, T. 2018. Use of Air to Improve the Efficiency of Foamy Flow and Reservoir Pressurization in Heavy Oil Recovery. *Journal of Petroleum Science and Engineering* **170**: 166-176. https://doi.org/10.1016/j.petrol.2018.06.045

Speight, J. 2016. *Introduction to Enhanced Recovery Methods for Heavy Oil and Tar Sands*, 2nd Edition. Cambridge, MA. Gulf Publishing Company. https://doi.org/https://doi.org/10.1016/C2014-0-01296-8

Srivastava, R.K., Huang, S.S., and Dong, M. 1999. Comparative Effectiveness of CO2, Produced Gas, and Flue Gas for Enhanced Heavy-Oil Recovery. *SPE Reservoir Evaluation & Engineering* **2**(3). https://doi.org/10.2118/56857-PA

Sun, X., Zhang, Y., Song, Z., Huang, L., Chen, G., 2017. Study on Equilibrium and Non-Equilibrium PVT Behavior of Foamy Oil Using Experiments and PVT Correlations. *Journal of Petroleum Science and Engineering* **156**: 927-944. https://doi.org/10.1016/j.petrol.2017.06.041

Vesna, K. M., Branko L., and Dušan D. 2014. Factors Influencing Successful Implementation of Enhanced Oil Recovery Projects. *Underground Mining Engineering* **25**(2014): 41-50.

Zhang, Y., Chakma, A., Maini, B.B., 1999. Effects of Temperature on Foamy Oil Flow in Solution Gas-drive In Cold Lake Field. Presented at the Annual Technical Conference and Exhibition, Calgary, Alberta, 14-18 June. https://doi.org/10.2118/99-41

Zhou, X., Zeng, F., Zhang, L. et al. 2016. Foamy Oil Flow in Heavy Oil-Solvent Systems Tested by Pressure Depletion in a Sandpack. *Fuel* **171**: 210–223. https://doi.org/10.1016/j.fuel.2015.12.070